

On some basic results by application of the CZF method.

Elio Conte^(1,2), Maria Pieralice⁽¹⁾, Vincenza Laterza⁽¹⁾, Antonella Losurdo⁽¹⁾, Nunzia Santacroce⁽¹⁾, Sergio Conte⁽¹⁾, Antonio Federici⁽²⁾
and
Alessandro Giuliani⁽³⁾

(1) School of Advanced International Studies for Applied Theoretical and non Linear Methodologies in Physics. Bari-Italy

(2) Department of Pharmacology and Human Physiology, TIRES-Center for Innovative Technologies for Signal Detection and Processing, University of Bari, Italy;

(3) Istituto Superiore di Sanità, Viale Regina Elena 299, 0016, Rome, Italy

Corresponding author

Name: Elio Conte

Address: *School of Advanced International Studies for Applied Theoretical and non Linear Methodologies in Physics. Bari-Italy- Department of Pharmacology and Human Physiology, TIRES-Center for Innovative Technologies for Signal Detection and Processing, University of Bari, Italy*

E-Mail Address:: elio.conte@fastwebnet.it

Key words : Heart Rate Variability, CZF method, ANS contribution analysis of R-R intervals.

Abstract :

The aim of the present contribution is to give an educational support on a new methodology that we may use when we are employed in the analysis of one of the most fundamental signals that we encounter in electrophysiology.the R-R intervals in analysis of the ECG.

Introduction.

The aim of the present contribution is to give an educational support on a new methodology that we may use when we are employed in the analysis of one of the most fundamental signals that we encounter in electrophysiology. As it is well known, we are concerned with the R-R intervals in analysis of the ECG.

The autonomic nervous system (ANS) regulates internal organs and circulation dynamics. The term 'autonomic' is related to the fact that we retain that such regulation happens without any consciousness advent so that the body reaches an homeostatic (or better homeorhetic as proposed by Conrad Waddington to put the accent to the dynamic character of equilibrium) balance following 'its own rules' and so contrasting the influences arising from a mainly stochastic environment. Heart Rate Variability (HRV) must be considered to represent the most privileged observatory of ANS given the crucial role of having a blood flux consistent with the body needs, this regulation of blood flux entity is achieved by the variation in the periods of subsequent contraction/relaxation acts of heart muscle.

The concept of sympathovagal balance in HRV refers to the autonomic state resulting from sympathetic and parasympathetic influences, *i.e.* 'mainly activating' and 'mainly inactivating' drives. During the last three decades, numerous studies have shown that abnormalities in the sympathovagal balance are related to different diseases (33)

Experimental studies have shown significant relations between ANS and cardiovascular diseases (33, 2). It has been observed that there is a relation between the risk of developing a lethal cardiac arrhythmia and signs of either increased sympathetic activity or decreased parasympathetic activity (33,32). Predominance of sympathetic activity and reduced parasympathetic cardiac control have been seen in patients with acute myocardial infarction (27). Moreover, congestive heart failure patients show alterations of the sympathovagal balance.

The general approach points to a sympathetic overdrive rather than a parasympathetic withdrawal in such patients. An altered sympathovagal balance is also identified in patients after cardiovascular surgery and it has been related to myocardial ischemic episodes in patients who have undergone coronary artery bypass grafting (33). As a complication of diabetes mellitus, autonomic neuropathy occurs and this often affects the cardiac autonomic function as well. Diabetic neuropathy is characterized by early and widespread neuronal degeneration of small sympathetic and parasympathetic nerve fibres (42, 27). Patients with cervical and high thoracic spinal cord lesions also have autonomic abnormalities that affect the heart. In these patients some autonomic pathways are severed, but baroreceptor afferents and parasympathetic efferents of the ANS are intact. This causes a reduced ability to regulate the cardiac activity (21).

In the last few years, HRV analysis has shown increasing interest also in psychophysiology.

Higher HRV is linked with better physical and emotional health overall and has been shown to reduce risk for stress-related illness, such as cardiac problems. Moreover a decrease in HRV was observed to be strictly related to aging even in normal subjects (7,15)

Studies have shown that training HRV can improve physical, mental, and emotional stability. Positive outcomes include improved cognitive abilities and mental clarity, greater emotional balance, enhanced creativity.

HRV values are in turn influenced by the psychophysiological state of the individual (see as example J.F. Thayer et al.). In general, each subject shows a baseline (average) value of heart rate variability and sympathetic activation. These baseline values undergo relevant (around 30%) changes in response to routine psychological environmental solicitations along the day. It is also possible to modify the HRV by means of suitable psychological techniques. This modifications *can be stabilized with* learning.

There are *two* main ways for such externally induced HRV changes: the first is based on somatic techniques (breathing, massage, relaxation, movement) and brings the patient towards an (at least subjectively) increased wellbeing state. The second way is based on psychological techniques and consists in a work on the deep consciousness and on the personality of the patient.

Growing evidence suggests that alterations in autonomic function contribute to the pathophysiology of panic disorder (PD). The risk of adverse clinical cardiac events is increased in patients with panic disorder (PD). Autonomic nervous system (ANS) dysfunction and reduced heart rate variability (HRV) have been reported in a wide variety of psychiatric disorders. Some authors recorded cardiac activity and assessed HRV in acutely hospitalized manic bipolar (BD) and schizophrenia (SCZ) patients. Autonomic dysregulation is associated with more severe psychiatric symptoms, suggesting HRV dysfunction, (17, 38).

It is known that autonomic nervous activities change in correspondence with sleep stages. The characteristics of continuous fluctuations in nocturnal autonomic nerve tone have been studied in some different experimental conditions (44).

Autonomic dysfunction has been the target of numerous other investigations and, as previously said, has been linked to generalized anxiety disorder, panic disorder, and depression. Symptoms of depression often are accompanied by ANS abnormalities, including reductions in HRV, vagus nerve activity, and baroreflex sensitivity. Animal studies exploring the specific ANS mechanisms of depression by using the chronic mild stress rodent model of depression found that exposure to chronic stress decreased HRV and elevated sympathetic tone to the heart. It is of great interest also the application in HRV Biofeedback Training for Depression

In conclusion: HRV is a very important marker of autonomic activity and thus a privileged observatory for a lot of disease conditions. Some of these conditions are very elusive and practically impossible to detect with reliable diagnosis methods. This justifies the interest in the development of analysis methods of HRV that could increase the sensitivity of diagnosis methods in different pathology fields.

The methodology for HRV

During the last decades different methods have been applied to assess the autonomic activity; these include for example cardiovascular reflex tests and biochemical tests (28). In recent years, noninvasive techniques based on electrocardiographic recordings have been used as markers of cardiac autonomic tone; Among these, heart rate variability (HRV) is the most widely used and evaluated (33).

The ANS regulates the heart rate; increased sympathetic activity causes acceleration whereas increased parasympathetic activity causes deceleration of the heart rate (16), which is the reason why HRV is used as a marker of autonomic activity. The increasing diffusion of HRV as a method to measure autonomic activity since the 70's and a lack of method standardization combined with a continuous introduction of new HRV measures lead to the formation of a task force of the European Society of Cardiology and The North American Society of Pacing and Electrophysiology in 1996. The task force established standards of measurement, physiological interpretation, and clinical use of HRV (33).

In order to quantify HRV, the intervals between consecutive beats originating in the SA node, also called normal to normal intervals (NN intervals), must be found in the electrocardiogram (ECG). The analysis of HRV must satisfy four conditions:

- 1) a satisfactory signal-to-noise ratio of the ECG is necessary to identify the each beat properly.
- 2) the digital sampling must be regular and robust to identify a fiducial point for each beat,.
- 3) morphology and rhythm characteristics for each beat must be classified to distinguish between beats originating in the sinus node and ectopic beats.
- 4) only beats originating in the sinus node should be considered for the HRV analysis (42).

Two main approaches have been used to measure the HRV; time domain analysis and frequency domain analysis. Besides these, nonlinear analysis is an emerging field within the analysis of HRV.

Frequency Domain Analysis

The frequency domain measures are based on a transform of the series of subsequent registered RR intervals into the frequency domain. The series can be represented in two ways; as the RR intervals versus the beat number, as a discrete event series where the $R_i - R_{i-1}$ interval is plotted versus the time of occurrence of R_i . *While Frequency Domain Analyses have a time honoured tradition in the study of time series in any scientific fields, nevertheless they show some evident limitations as the particular case of HRV.*

RR series can be considered as irregularly sampled signal: it is the system itself, by giving rise to a 'beat', that decides the sampling interval, but Fourier Transform (the classical frequency domain analysis method) requires an equidistant sampled signal. Therefore, an interpolation and a re-sampling of the signal is required prior to a Fourier transform (33). This is of course a forced procedure introducing some undesirable modifications affecting the outcome of the analysis.

Basically Fourier analysis considers any time series (in this case the length of subsequent RR intervals) as coming from the superposition of n sinusoids, i.e. of n functions of the form $Y(t) = a \sin(bt)$ where b points to the different frequencies and a is the amplitude, that is to say...the "relative relevance" of the frequency b to explain the observed series. This gives rise to a power spectrum in which frequencies are on the X axis and on the Y axis we have the relative squared amplitude in the analysed series.

When a power spectral density analysis is made on the series, following this procedure, it provides information about the distribution of power as a function of frequency (14). In short terms, recordings (5-6 minutes), three main frequency bands have been identified: a very low frequency (≤ 0.04 Hz), a low frequency (0.04-0.15 Hz), and a high frequency (0.15-0.4 Hz) component. In addition, an ultra low frequency component (≤ 0.03 Hz) has been identified in long term recordings (24 hours) (33).

The frequency domain parameters for short term and long term analysis of HRV are listed in table 1.

Efferent vagal activity has been shown to be a major contributor to the high frequency component in clinical and experimental observations of autonomic manoeuvres e.g. electrical vagal stimulation, muscarinic receptor blockade and vagotomy. Some researchers consider the low frequency component as a marker of sympathetic modulation whereas others consider it as a parameter that is under both sympathetic and parasympathetic influences (33).

The physiological correlate of the very low and ultra low frequency component is still an area under investigation (2), but has been related to circadian, neuroendocrine rhythms and thermo regulation (32). As table 1 also indicates, a general consensus about the physiological correlates of the different frequency measures has not been fully established (2).

The derivation of information about HRV requires a precise detection of R peaks in the recording, because imprecise location affects the outcome of the different measures. Furthermore, the fact that HRV is based on the NN intervals limits its use of HRV measures to individuals with a sinus rhythm and a limited number of ectopic beats (1, 24). Both the statistical time domain and frequency domain measures are highly sensitive to artifacts, ectopic beats and missing beats. Thus, an optimal HRV analysis demands recordings without ectopic beats. For the analysis to be reliable, different criteria have been proposed, e.g. the number of beats originating in the SA node must be at least 70 % (some even demand 99 % of the beats) to originate in the SA node. The most strict criteria demands that the recording must not contain more than 10 ectopic beats per hour. These criteria excludes many patients from HRV analysis, e.g. 20-30 % of all high-risk patients in post acute myocardial infarct groups are excluded from HRV analysis due to frequent ectopic beats, artifacts, or arrhythmia episodes (18).

It is interesting to report here a statement coming from (33);

"when evaluating results of the HRV measures, it should be noted that it is totally inappropriate to compare measures calculated on ECG of different duration".

Many researchers continue to commit such basic error.

As previously said, the HF component of the power spectrum is related to vagal activity, whereas the meaning of the LF component is more controversial; some consider it as a measure of sympathetic modulations when expressed in normalised units, others interpret it as a combination of sympathetic and parasympathetic activity. The prevalent consensus about the LF component is that both sympathetic and parasympathetic inputs contribute to it (25). The HF component can be significantly influenced by respiratory patterns (2).

Let us also repeat a severe limitation recurring in frequency analysis. The translation of the NN interval series from the time domain to the frequency domain presupposes that there is an underlying periodicity in the signal. This is a technical limitation, since the heart rate signal is a nonstationary signal. This stationarity issue is a frequently questioned feature that, in addition to missing periodicity and linearity, will be considered seriously by taking in consideration the CZF method. Here we give only preliminary evaluations outlining that a signal can be considered stationary if the modulations of a certain frequency remain unchanged during the recording. If the modulations change, the interpretation of the results are not well defined. The heart rate signal can be considered as a non stationary signal, and this feature does not justifies the indiscriminate use of transform into the frequency domain (33).

Non linearity has been discussed in detail by a very large number of authors. Moreover it is important to stress the fact that the translation between observed spectral components and physiological control drivers is not without problems. There has been a lot of confusion regarding the meaning of the different measures, especially in the frequency domain. In the early studies the spectral components were regarded as a reflection of the autonomic tone (25), i.e the balance between the activity in the sympathetic and parasympathetic division (22). Studies comparing the firing rates of vagal and sympathetic cardiac fibres with the sino-atrial response have started to evidence that the heart rate variations not necessarily correspond to variations in the mean firing rate, but also and rather to the sino-atrial responsiveness to the changes in the autonomic tone (25).

Generation of the Electrocardiogram

For brevity we resume some basic notions taking directly from an excellent thesis that is available on line and reported in (6).

ECG reflects the electrical activity of the heart. When the electrical impulse propagates through the myocardium a small portion of this electrical activity reaches the body surface, where it can be recorded by placing surface electrodes on specified places on the skin. It is the cardiac electrical system of the heart that is responsible for generating and conduction the electrical activity.

The electrical system of the heart contains two types of cells; specialised cells of the conducting system and cardiac contractile cells. The former generate and conduct electrical current, while the latter respond to the electrical current and produce the contraction that propels blood into the circulatory systems (31, 16).

The components of the conduction system of the heart can be seen on figure 1.

The generation of the action potential leading to a contraction of the heart's chambers is initiated by a spontaneous generation of an action potential in the sinoatrial node (SA node), which is located in the posterior wall of the right atrium. The action potential is conducted through both atria to the atrioventricular node (AV node) by the internodal pathways. The propagation of the action potential through both atria excites the contractile cells of the atria and ensures their full contraction of these. The AV node conducts the impulse from the atria into the ventricles through the bundle of His, bundle branches, and the Purkinje fibers, which finally spreads the stimulus to the ventricular myocardium and causes it to contract .

The action potentials generated in the different structures are somewhat different. Figure 2. illustrates the action potentials from different structures of the heart.

The convolution of these action potentials, each characterized by a somewhat different shape, gives rise to the peculiar ECG shape as depicted in Fig.2.

Two main types of cells are found in the heart; pacemaker cells and contractile cells. Cardiac pacemaker cells depolarise spontaneously without any external stimulation, whereas the cardiac contractile cells only contract when stimulated (31). The SA node and AV node exhibit similar shapes of the action potential and the AV bundle, bundle branches, Purkinje fibres, and myocardium exhibit similar shapes of the action potential (8). The two action potentials' shapes and the flux of ions responsible for the shapes are illustrated in figure 2a and 2b.

Figure 2.a shows the action potential for a pacemaker cell. The action potential for a pacemaker cell can be divided into three phases; a prepotential phase (phase 4), a depolarisation phase (phase 0), and a repolarisation phase (phase 3). Pacemaker cells do not have a constant resting potential, instead they slowly depolarise again immediately after a repolarisation. At a maximum diastolic potential (MDP) of about -70 mV, Na⁺/K⁺ channels open and causes a large influx of Na⁺ ions and a small efflux of K⁺ ions. This initiates the prepotential phase (phase 4). When the membrane potential reaches about -55 mV the transient Ca²⁺ channels (also called T-type Ca²⁺ channels) open and cause an influx of Ca²⁺ ions. As Ca²⁺ ions enter the cell, the membrane potential is further increased and reaches the threshold potential (TP) at about -40 mV. At this stage another type of calcium channels opens; the longer lasting Ca²⁺ channels (also called L-type Ca²⁺ channels). Opening of these channels increases influx of Ca²⁺ ions and depolarizes the cell (phase 0). At approximately 0 mV, the L-type Ca²⁺ channels close and at the same time K⁺ channels open, which causes an efflux of K⁺ ions. This initiates the repolarisation phase of the action potential (phase 3), which makes the membrane potential return to -70 mV (31, 35).

As seen on figure 2,a and b, the influx and efflux of different ions are responsible for the appearance of the action potentials. Changes in the slope of prepotential, the amplitude of the TP, and the amplitude of the MDP determine the rate of impulse generation in the SA node and thereby the heart rate. The duration of myocardial action potentials are dependent on the heart rate; the higher the frequency is, the shorter will the action potential be (8).

The contractile cells in the heart are connected by gap junctions, which makes them function as a syncytium i.e. as a joint unit where processes in a single cell quickly spreads to the adjacent cells, almost as if it was a single large cell. Thus, the atrial myocardium functions as a syncytium and the ventricular myocardium function as a syncytium (16). Also the specialised cells of the conducting system are connected by gap junctions (10). Gap junctional coupling between the cells are responsible for the propagation of an action potential from its initial point in the SA node along the specialised conduction pathways to the contractile cells of the ventricles (29).

Elements of the Electrocardiogram

As mentioned, it is the impulse propagation through the myocardium that is reflected in an ECG. As a basic notion, we remember here that a normal ECG exhibits three different waveforms; the P wave, the QRS complex, and the T wave. The QRS complex is made of three distinct waves; the Q wave, R wave, and the S wave (16). An illustration of a normal ECG is given in figure 3.

Immediately after the SA node has generated an impulse, the depolarisation of both atria occurs. This is reflected as the P wave in the ECG. The isoelectric line between the P wave and the Q wave corresponds to the conduction of the impulse through the AV node.

The Q wave represents the depolarisation of the septum. The left part of the septum is depolarised before the right side, this causes the negativity of the Q wave. The R wave is caused by the propagation of the depolarisation wave in the septum towards the apex and afterwards depolarisation of the apex to the base of the heart. The S wave reflects the depolarisation of the posterior portion of the base of the left ventricle. Altogether, the Q, R, and S waves constitute the

QRS complex, which represents the depolarisation of the ventricles (22, 16). The QRS complex is a relative strong electrical signal because the ventricular muscle is much more massive than the atrial muscle (16, 22).

The atrial repolarisation wave also called *Ta* is directly opposite in polarity to the P wave (14). The isoelectric line between the QRS complex and the T wave is the period where the entire ventricular myocardium is depolarised and repolarisation of the ventricles has not yet begun (16, 22).

The T wave is the last wave appearing in a normal ECG and represents the repolarisation of the ventricular muscle.

The positivity of the T wave is due to the propagation of the repolarisation wave, which spreads in reversed direction of the depolarisation wave (22, 16).

The appearance of the ECG is determined by the transmission of impulses through the heart, because, any changes in the transmission pattern and velocity will affect the current flow around the heart and consequently affect the shape of the waves in the ECG. This can be understood by considering a vectorcardiographic representation of a depolarising muscle. During the propagation of the depolarisation wave a part of the muscle will be depolarised while the remaining part is still polarised. This causes a voltage difference between the two parts. The voltage difference is determined by the amount of depolarised and polarised muscle respectively; the largest difference is seen when half of the muscle mass is depolarised and the other half is not. The direction and magnitude of the current generated in the heart at a given instant can be depicted as a vector that points in the direction of the current flow and with length proportional to the voltage difference between depolarised and polarised muscle (16).

A representation of the magnitude and direction of the instantaneous mean electrical vector of the ventricles during the depolarisation is shown in figure 4.

By projecting the mean electrical vector onto the three bipolar leads (i.e. I, II, and III) a picture of the electrical activity measured by each lead is obtained (30, 16). The first step in figure 4 shows a short mean electrical vector because only small portion of septum is depolarised, thus all electrocardiographic voltages are low in the three bipolar leads. Next, the mean electrical vector is long because much of the ventricular muscle is depolarised, this is also shown as the shaded areas in figure 4. The voltage at lead II is greater comparing to the rest of the leads because the mean electrical vector extends almost in the same direction as the axis of lead II. Next, the depolarisation wave reaches the epicardium and the apex of the heart, the mean electrical vector becomes shorter and the electrocardiographic voltages becomes lower. The direction of the mean electrical vector is changing slowly toward the left side, due to the greater amount of ventricular muscle mass in the left side, thus slower depolarisation.

Afterwards, the mean vector becomes shorter because only small portion of the ventricular muscle is still polarised.

Furthermore the direction of the vector is toward the base of the left ventricle. In this case only lead I has positive electrical voltage.

Finally, the entire ventricular muscle is depolarised and no current flows around the heart. Therefore, the mean electrical vector becomes zero and consequently the voltages measured in all leads become zero, as shown in figure 4.

From the above, it can be seen that the ECG is determined by the pattern, amplitude, and velocity of the impulse propagation during cardiac activity. The ANS effects on these variables is therefore crucial to clarify whether the ANS has an effect on the morphology of the ECG or not.

Autonomic Innervation and Regulation of the Heart

The autonomic innervation of the heart is rich. Parasympathetic innervation is particularly rich to the SA node, sinoatrial conducting pathways, and the AV node, whereas the parasympathetic

innervations to the ventricles are sparse (37, 21, 5, 16). The sympathetic nervous system innervates all parts of the heart but is dominating in the ventricles (37, 16).

Figure 5 illustrates the sympathetic and parasympathetic innervations of the heart.

The parasympathetic innervation is dominating in the SA node, atrial myocardium, and the AV node compared to the ventricles. In contrast, sympathetic innervation dominates in the ventricles. (16)

The two divisions have opposite effects on the heart; the sympathetic division causes excitation, whereas the parasympathetic causes inhibition. The parasympathetic division predominates in resting conditions whereas the sympathetic division dominates in more demanding situations (22).

Parasympathetic Effects on Cardiac Cells

The parasympathetic nervous system releases acetylcholin at the postganglionic nerve endings. Acetylcholin binds to one or more subtypes of muscarinic (M) receptors in the human heart. Five different muscarinic receptor subtypes (M1-M5) have been identified. M2 is the predominating muscarinic receptor type in the heart (5). An inhibitory G protein (*Gi*) is attached to the M2 receptor on the membrane of the cell. When acetylcholine binds to the M2 receptor, the *Gi* protein is activated, which causes an inhibition of adenylate cyclase. The inhibition of adenylate cyclase inhibits the formation of cyclic adenosine monophosphate (cAMP) from adenosine triphosphate (ATP) (16, 8). cAMP would have activated type A protein kinase (PKA) which is capable of phosphorylating proteins. The absence of PKA causes a reduction of Ca²⁺ influx, due to inactivation of L-type Ca²⁺ channels. Furthermore, the activation of the *Gi* protein opens potassium channels which causes an efflux of K⁺ from the cell leading to hyperpolarisation (5).

Sympathetic Effects on Cardiac Cells

The sympathetic nervous system uses epinephrine and norepinephrine as primary transmitter substances. There are two adrenergic receptor types.. When epinephrine or norepinephrine binds to the adrenoceptor it activates a G protein in a manner similar to that of acetylcholine binding to M2 receptors.

Instead of activating an inhibitory G protein, adrenoceptors activates a stimulatory G (*Gs*) protein. The activation of the *Gs* protein activates cAMP which in turn activates PKA (31). PKA phosphorylates Ltype Ca²⁺ channels which activates them, and consequently increases the intracellular Ca²⁺ concentration (18). This causes a positive chronotropic effect on the SA node and positive dromotropic effect on the AV node.

Autonomic Innervation and Regulation of the Heart

The increased concentration of cytosolic Ca²⁺ activates ryanodine receptors (RyR) in the sarcoplasmic reticulum (SR). This causes a release of a large amount of Ca²⁺ from the SR to the cytosol. In the membrane of the SR, there is a Ca²⁺ pump called sarcoplasmic reticulum Ca²⁺-ATPase (SERCA2), which pumps the cytosolic Ca²⁺ back into the SR. In humans, the activity of SERCA determines the rate of removal of more than 80% of cytosolic Ca²⁺ (13). SERCA2 pumps are regulated by a protein called phospholamban (PLB). Normally, PLB inhibits SERCA2, but under adrenergic stimulation PKA phosphorylates PLB and thereby reduces the inhibitory effect of PLB on SERCA2. This causes an increase of the rate of intracellular Ca²⁺ removal from the cytosol into the SR.

The result of the described process is a rapid increase in intracellular Ca^{2+} concentration due to the RyR receptor but of short duration due to the Ca^{2+} removal mediated by SERCA2 (14, 3). This produces positive inotropic effects on the myocardium. The high concentration of the intracellular Ca^{2+} increase the amplitude and decrease the duration of the action potential of the cardiac contractile cells (26).

From the above discussion, it becomes obvious that the ANS has great influence on the cardiac activity. In general, the parasympathetic division causes negative chronotropic, dromotropic, and inotropic effects to occur. In contrast, the sympathetic division causes positive chronotropic, dromotropic, and inotropic effects to occur. *The intermingled picture presented, where systemic effects go hand-in-hand with cellular level features need to be supplemented by another very important element: the ANS also regulates the conductance of the gap junctions which connect adjacent cells in the heart. This implies a direct involvement of ANS in the structure of the conduction tissue that has very important consequences on its conductive properties and thus on the general ECG shape.*

As mentioned before, gap junctions are responsible for the impulse propagation in the heart (29). Gap junctions are regulated by different substances, among these are cAMP, PKA, and Ca^{2+} (10). The concentration of these substances changes in the intracellular environment due to autonomic innervation.

An increase in intracellular cAMP leads to increased coupling between adjacent cells (10). PKA enhances the conductance of the most abundant type of gap junction found in the heart. The change is very rapid and may last for several minutes. A large increase in intracellular Ca^{2+} causes reduction in conductance of the gap junctions.

Under normal conditions the Ca^{2+} concentration does not reach sufficient levels to cause a reduction in gap junctional conductivity (9).

If the changes, in the mentioned substances mediated by the autonomic nervous system are high enough to cause a regulation of the cardiac gap junctions then, sympathetic innervation would cause an increase in gap junctional conductance, whereas the parasympathetic innervation would cause a decrease in gap junctional conductance.

Going back to the initial problem of the effect of ANS on ECG shape and consequently on the HRV in terms of systemic variations of RR intervals) we can state that changes in the ECG are mediated by changes in the pattern of impulse propagation, the velocity of impulse propagation through the heart, and the amplitude of the voltage differences generated by the impulse.

This allows us to make the subsequent general statements:

- 1) *There has been a lot of confusion regarding the meaning of the different measures, especially in the frequency domain. In the early studies the spectral components were regarded as a reflection of the autonomic tone (25), i.e the balance between the activity in the sympathetic and parasympathetic division (22), but studies comparing the firing rates of vagal and sympathetic cardiac fibres with the sino-atrial response shows that the heart rate variations not necessarily correspond to variations in the mean firing rate, but also rather to the sino-atrial responsiveness to the changes in the autonomic tone (25).*
- 2) *ANS has great influence on the cardiac activity. In general, the parasympathetic division causes negative chronotropic, dromotropic, and inotropic effects to occur. In contrast, the sympathetic division causes positive effects to occur.*

Interestingly, the analysis showed that sympathetic stimulation of the heart causes an increase in heart rate, an increase in conduction velocity through the AV node and myocardium, and an increased amplitude of the action potentials of cardiac contractile cells. The parasympathetic division inhibits the processes which causes these changes, thus, the parasympathetic division has

the opposite effect. This encourages to believe that the morphology of the QRS complex changes with variation in ANS balance.

Following such long and detailed discussion we have to pose a specific question.

Have we to day a marker of the ANS activity that may be considered really suitable to take in accurate consideration the complex mechanisms that we have so far taken into consideration?

The Methodology of Analysis

We may now pass to introduce our methodology.

The emerging indication from the previous studies is that we are in presence of a very complex system regulated from linear and non linear interrelationships and couplings. The most important feature is that such system exhibits an ANS balance that we must attempt to correctly evaluate.

The answer to our previous posed question is that we need to introduce a new methodological treatment that is able to account for chronotropic, dromotropic, and inotropic effects to occur.

The use of spectral analysis implies that the event series can be represented by a sum of sinusoidal components, of different amplitude, frequency and phase values. Well defined fluctuations can be identified in distinct frequency bands, which have been attributed to the influence of vagal and/or sympathetic outflows. Various spectral methods for the calculation of power spectra density have been applied since the 1960's; they may be generally classified as non-parametric and parametric. The non-parametric approach mainly used is the Fast Fourier Transform (FFT) just to avoid statistical uncertainty related to the choice of the model order, which is inherent to the parametric PSD estimates.

Traditional spectral analysis of heart rate variability (HRV) and blood pressure variability (BPV) results in a spectrum with three major components, defined as very low-frequency (VLF: 0.003 – 0.04 Hz), low-frequency (LF: 0.04 – 0.15 Hz) and highfrequency (HF: 0.15 – 0.4 Hz) .

Note the essential feature of the method. We speak here only of power.

The distribution of the power and the central frequency of these components are not fixed but vary in relation to changes in autonomic modulation of heart rate and blood pressure.

Note some further limitations of the method. It is important to observe that a large proportion of the VLF component is due to nonharmonic noise (direct current - DC), rendering VLF assessment from short-term recordings a very dubious measure that should be avoided. *Nevertheless this is the by-far most important power spectrum component, so reaching the conundrum that the most relevant component in terms of explained variability of the HRV is in the same time the less reliable as for their quantitative estimation for the simple fact, at least in the short-term recordings setting it cannot be considered as being an oscillatory component at all.*

The LF and HF components are evaluated in terms of frequency (Hz) and power. This power is assessed by the area of each component and, therefore, squared units are used for its absolute value. In addition, an appraisal of the fractional distribution of power, independent of the absolute values of variance, can be obtained with computation of normalized units (nu). They are obtained by dividing the power of a given component by the total power from which the VLF has been subtracted. This procedure focuses on the possible reciprocal link between LF and HF components but remains somewhat controversial.

In the framework of a correct methodological approach it remains thus to introduce a correct marker of ANS. In our opinion we may reach this objective starting from the conclusion that was reached from Zbiliut, Giuliani, *i.e. that the main dynamical feature of heartbeat dynamics can be explained by a quantum-like model in which the system undergoes a jumping between adjacent states (adjacent in terms of RR length classes) in response to changes in the internal state (15). This 'jumps' point to an intrinsically discrete kind of dynamics that happens at all the time scales (the*

fractal, scale invariant, nature of these state changes is described in (15) so asking for a less demanding (in terms of continuity and stationarity constraints) technique as Fourier Transform for adopting a frankly discrete and model independent analysis method.

Linked to such conclusion is the notion of Recurrence that Zbilut and Webber were able to quantify by the well known methodology called RQA, Recurrence Quantification Analysis. *Recurrence and Variability are two tightly related concepts. It is important to stress the functional meaning of the concept of variability in the realm of ANS regulation of HRV. At odds with the great majority of man-made tools in which the increase in variability is the signature of malfunctioning, in the case of heartbeat regulation the situation (at least when variability is confined in a given physiological range) is just the opposite: given HRV is the image in light of the fine-tuning of blood flux to the ever changing needs of the internal 'milieu' (as Claude Bernard defined the whole organism state) with the resulting heartbeat length as a sort of 'majority vote' or 'integration' of the various signals impinging on the heart from ANS, an high variability in time corresponds to an efficient sensing of the environment by the autonomic nervous system, while a low variability goes hand-in-hand with a less efficient control (as in the extreme case of heart transplanted patients where ANS control is practically abolished and the HRV is severely decreased). This is the main biological reason for focusing on the concept of Variability for the phenomenological estimation of chronotropic, dromotropic, and inotropic effects.*

Let us explain the matter in more detail. Let us observe that we are in presence of non linear processes. They are the anteroom of arising very complex dynamics crossing of the frontier of the chaotic processes. From the conceptual point of view there is only one variable that is able to account for such complex biological behaviours and it is that one of Recurrence. It was introduced by Eckmann and subsequently developed by Zbilut and Webber in the well established methodology of analysis that is actually provided with reference as RQA (Recurrence Quantification Analysis) (36).

While the basic idea of Recurrence is immediately intuitive 'The periodic character of a series can be quantified by the number of times the same pattern (letter, number, symbol..) recurs in the series' and this immediacy and freedom from mathematical assumptions makes RQA apt to model complex nonlinear systems, it is worth noting to go more in depth into the subtleties of the concept of Recurrence. In doing so we will rely upon explanation that was furnished rather recently by Norbert Marwan, in his excellent paper (23).

We adopt here his introduction to this basic concept:

If we observe the sky on a hot and humid day in summer, we often "feel" that a thunderstorm is brewing. When children play, mothers often know instinctively when a situation is going to turn out dangerous. Each time we throw a stone, we can approximately predict where it is going to hit the ground. Elephants are able to find food and water during times of drought. These predictions are not based on the evaluation of long and complicated sets of mathematical equations, but rather on two facts which are crucial for our daily life:

- (1) similar situations often evolve in a similar way;***
- (2) some situations occur over and over again.***

The first fact is linked to a certain determinism in many real world systems. Systems of very different kinds, from very large to very small time-space scales can be modelled by (deterministic) differential equations. On very large scales we might think of the motions of planets or even galaxies, on intermediate scales of a falling stone and on small scales of the firing of neurons. All of these systems can be described by the same mathematical tool of differential equations.

They behave deterministically in the sense that in principle we can predict the state of such a system to any precision and forever once the initial conditions are exactly known. Chaos theory has taught us that some systems—even though deterministic—are very sensitive to fluctuations

and even the smallest perturbations of the initial conditions can make a precise prediction on long time scales impossible. Nevertheless, even for these chaotic systems short-term prediction is practicable.

The second fact is fundamental to many systems and is probably one of the reasons why life has developed memory.

Experience allows remembering similar situations, making predictions and, hence, helps to survive. But remembering similar situations, e.g., the hot and humid air in summer which might eventually lead to a thunderstorm, is only helpful if a system (such as the atmospheric system) returns or recurs to former states. Such a recurrence is a fundamental characteristic of many dynamical systems.

They can indeed be used to study the properties of many systems, from astrophysics (where recurrences have actually been introduced) over engineering, electronics, financial markets, population dynamics, epidemics and medicine to brain dynamics. The methods described in this review are therefore of interest to scientists working in very different areas of research. The formal concept of recurrences was introduced by Henri Poincaré in his seminal work from 1890 for which he won a prize sponsored by King Oscar II of Sweden and Norway on the occasion of his majesty's 60th birthday. Therein, Poincaré did not only discover the "homoclinic tangle" which lies at the root of the chaotic behaviour of orbits, but he also introduced (as a by-product) the concept of recurrences in conservative systems. When speaking about the restricted three body problem he mentioned: "In this case, neglecting some exceptional trajectories, the occurrence of which is infinitely improbable, it can be shown, that the system recurs infinitely many times as close as one wishes to its initial state." Even though much mathematical work was carried out in the following years, Poincaré's pioneering work and his discovery of recurrence had to wait for more than 70 years for the development of fast and efficient computers to be exploited numerically. The use of powerful computers boosted chaos theory and allowed to study new and exciting systems. Some of the tedious computations needed to use the concept of recurrence for more practical purposes could only be made with this digital tool.

In 1987, Eckmann et al. introduced the method of recurrence plots (RP) to visualise the recurrences of dynamical systems. Suppose we have a trajectory $[\vec{x}_i]_{i=1}^N$ of a system in its phase space (23). The components of these vectors could be, e.g., the position and velocity of a pendulum or quantities such as temperature, air pressure, humidity and many others for the atmosphere. The development of the systems is then described by a series of these vectors, representing a trajectory in an abstract mathematical space. Then, the corresponding RP is based on the following recurrence matrix:

$$R_{i,j} = \begin{cases} 1 & \text{if } x_i \approx x_j \\ 0 & \text{if } x_i \neq x_j \end{cases}$$

where N is the number of considered states and $x_i \approx x_j$ means equality up to an error (or distance) ε . Note that this ε is essential as systems often do not recur exactly to a formerly visited state but just approximately. Roughly speaking, the matrix compares the states of a system at times i and j . If the states are similar, this is indicated by a one in the matrix, i.e. $R_{i,j}=1$. If on the other hand the states are rather different, the corresponding entry in the matrix is $R_{i,j}=0$. So the matrix tells us when similar states of the underlying system occur.

In conclusion, if we consider a given time series, as example, a time series made by R-R intervals. Recurrence, as example for the point $R - R_i$ and $R - R_{i+5}$, means that we have $R - R_i$ -value $\approx R - R_{i+5}$ -value in the limit of a prefixed convergence value ε .

The concept of Variability is in itself the exact conceptual counterpart of the concept of Recurrence. Given a time series of N intervals $R - R$, points realizing the greatest recurrence will give correspondingly the minimum variability. On the other hand, points giving the minimum recurrence will correspondingly exhibit maximum variability. When we speak of counterpart we do not intend

Recurrence is NOT the simple 'opposite' of Variability, if this would be the case we obviously had no need of another parameter given we should simply use variability and look at it in the two directions of increase/decrease. The point is that Recurrence catches the 'order dependent' portion of variability while variability as such (i.e. standard deviation of RR intervals) is totally independent from order, i.r. from the actual dynamics of the studied series. Let's imagine a series like this 1, 2, 3, 1, 2, 3, 1, 2, 3 (series A) and a series A' : 3, 2, 1, 2, 2, 1, 3, 3, 1 they have the same standard deviation (SD=1), both while the first shows a highly recurrent behavior in time the second is totally random. If we measure the recurrence of A by taking an embedding dimension of three (i.e. considering atomic elements made up of three consecutive values we obtain a Recurrence = 100%, while the second does not show any Recurrence). This different consideration of what Variability (and thus the nature of ANS control exerted on heart) is, allows us to discover periodic endogenous 'cycles' in which the system gets entrapped (and thus implying a decoupling from the continuous adaptation to a stochastic environment) nor simple variability, nor FFT can put into light.

This is the essence of the CZF method that is based on Recurrence Quantification.

The details of the method have been exposed by us elsewhere (see as example the section devoted to selected publications in this site) but we may mention here again some essential feature.

Let us take as reference a given time series of N , $R - R$ intervals.

In the current analysis of HRV we just use a concept of 'order dependent' variability that, in the case of Poincaré plot is only limited to adjacent beats .

In fact, by using such technique we plot $(R - R_{i+1} - R - R_i)$ and thus just we estimate the correlation between two adjacent points. In our case we need a more far reaching method encompassing different periods variability . In particular, we need to estimate, as ANS marker, the variability for each pair of $R - R$ points, the first time considering adjacent points, the next time considering variability between $R - R_i$ and $R - R_{i+2}$, the third time between $R - R_i$ and $R - R_{i+3}$, and, in general, between $R - R_i$ and $R - R_{i+\tau}$. Calling τ the lag, and varying at each step the Lag τ from 1 to $(N - 3)$, we will estimate the variability for each pair of points in the given $R - R$ time series, and covering this time the exploration of the whole series for any possible time interval. Take the Lag $\tau = 1$, we will estimate the total variability induced from the ANS for all the adjacent points of the given series of intervals. Take the Lag $\tau = 2$, we will estimate this time the total variability, induced from the ANS, for all the point shifted by one. Take the Lag $\tau = 3$, we will estimate the total variability induced from the ANS between points shifted by 3 and so on. In this manner we reconstruct the variability that is induced from ANS starting from adjacent $R - R$ values and advancing, step by step, each time of a shift given by one Lag. We characterize in this manner the variability as new marker of the ANS on the given recorded $R - R$ time series.

We may now mention the particular algorithm that we use for the calculation of the *order-dependent* variability. It is called the **Variogram**. We do not repeat here the formulas just to unburden the treatment from mathematical formulas but the details of the mathematical treatment have been given by us elsewhere.

Finally, we arrive to estimate the final variogram and a plot in which in abscissa we have the values of the Lags that we have considered, and in ordinate we have the value of the new ANS marker, that is to say, the values of the calculated total variability in correspondence of each Lag.

The next and final step is now easy to reach. We may pass from the domain of the time (the Lags) to the domain of the Frequency by a proper transformation so that we have finally the values of the total variability this time corresponding to the given frequency. This is quite similar to what is realized by FFT. In abscissa we have the values of the frequencies. In ordinate, this time we have the true values of the variability and not the PSD. Also in the case of the CZF method we will consider, as in FFT, three basic frequency bands, the VLF, the LF, and the HF and for each band we

will have the value of the total variability. In this manner we will proceed to calculate standard indexes as LF/HF (balance) (it will indicate in this case the ratio between the total variability in the LF and HF bands), we still will calculate the VLF%, the LF%, the HF%, the VLF, LF, and HF in n.u. and still the value of the ratios VLF/LF+HF or LF/(LF+HF) or HF/(LF+HF)). In conclusion, the visual inspection will give results as in the FFT case with the basic difference that in the case of the FFT we are expressing the power of the modulation. In the case of the CZF method we are estimating instead the variability. We will have also new quantitative markers that obviously will account this time for *chronotropic, dromotropic, and inotropic effects to occur*.

The Limitations of the FFT.

We had various possibilities to outline some insufficiencies in application of FFT in analysis of R-R intervals. We would add here still some further comments.

We first remind ourselves of three basic properties of the **FFT (Fast Fourier Transform)** process.

Generally speaking:

- First, information in signal must be preserved during transformation. That is, the variable measured on time signal must equal the variable measured on the frequency representation of that signal.
- Second, an FFT converts the signal representation between time and frequency domains. The time domain representation shows when something happens and the frequency domain representation shows how often something happens.
- Finally, an FFT assumes that the signal is repetitive and continuous. Other strong requirements are discussed by us elsewhere [see the section selected publications of this site]

Let us take a standard example as well discussed and available on line (New Version of DATS software, <http://blog.prosig.com/2009/07/20/data-windows-what-why-and-when/>).

Let us take the case of a 10 Hz sinusoid (Figure 6). This signal is periodic within the time record used to calculate the spectrum.

If we perform an FFT (Figure 6a), the result, shown below, will consist of a single line in the spectrum with an amplitude that represents, as example, the rms in relation to the time series amplitude.

Now, let us consider a second example. In this case (Figure 7) we have a 9.5 Hz sinusoid.

If we perform an FFT operation on this signal, it yields the multi-line spectrum shown in Figure 8.

The important thing to consider is that we no more obtain a single line spectrum. It is still a sinusoid but its spectrum is a multi-line spectrum as erroneously seen by the FFT process. It assumes the signal to be periodic (not only within a single record) and on-going or continuous. The 9.5 Hz signal (Figure 7), seen in analog form, is on-going and continuous, but when viewing it from a digital perspective (discrete number of samples in a specified time block), this signal is not a sinusoid (see Figure 9).

This is the reason because the FFT produces the multi-line spectrum in figure 4 with no less than 20 visible lines. A totally deformed result.

At this point, in R-R FFT analysis a problem becomes of crucial importance.

How may we minimize the effects of such discontinuities? Note that we speak about the methodological manner to minimize, not to cancel such undesired effects. The possibility is that we use something called a “window”. Typically, the window used for most general purpose data is the “Hanning” or “Von Hann”.

The “Von Hann” or “Hanning” window is named after Julius Von Hann (1839-1921). Von Hann was an Austrian meteorologist and is seen as the father of modern meteorology. He was the director of the Central Institute for Meteorology in Vienna (1887-1897), professor of meteorology at the University of Graz (1897-1890) and professor of cosmic physics at the University of Vienna (1890-1910). In signal processing the Hann function was named after him (4). Multiplying the window function (Figure 10) by the original time signal forces the signal to zero at the beginning and end of each time record (Figure 11). Placing multiple time records shown end to end shows the signal is now forced to be periodic when the time records are placed end to end. One problem solved, but the signal now in each of the time records is not a sinusoid any longer. This modification to the sinusoid is represented in the frequency domain by 4 dominant lines in the frequency representation of the signal plus also other.

The spectrum which was 20 lines before applying the Hanning Window function has now been reduced to a spectrum of only 4 lines plus other lines of reduced values but however present. The result is thus not extremely accurate, but reaches a much closer representation respect to the single line spectrum one would expect for the single frequency time signal. Obviously, one must remember here that, calculating HRV in VLF, LF, and HF bands, we integrate into some previously prefixed bands of frequency and thus the presence in such bands of such, also if reduced, undesired peaks, may alter totally the goodness of the estimated so called variabilities in PSD. In addition, let us see what happens to the single line spectrum from the 10 Hz single frequency time signal. Instead of a single line spectrum, the modified single frequency signal now is represented by a 3 line spectrum (Figure 13). There is no loss in amplitude read out accuracy, but a loss in frequency resolution is evident and particularly affecting negatively the estimations that we perform.

We should have to discuss here what it happens about the data that are being missed at the beginning and end of each record. Data are being reduced and/or set to zero over one half the time record. To assume events happening in the region of reduced amplitude areas, a processing technique exists called “overlap” processing. By applying this technique, the events occurring at or near the beginning and ending of the time records are enhanced by using overlap processing. Figure 14 represents records being processed “end-to-end” or 0% overlap. Figure 15 shows overlap of 50%.

Typically 67% overlap (Figure 16) is considered sufficient to weight the events near the beginning/end of the time record, however 75% overlap (Figure 17) is somewhat better. Today, with the high processing capabilities of computers, there is little reason not to utilize overlap processing.

Different shapes of the windowing function dictate what the spectrum shaping looks like. The table below lists a few window function types. All Window functions that operate on the time domain signals typically zero out the beginning and end of time record. The obvious exceptions to this are the “force” and “exponential decay” windows used in hammer/modal applications. Let us use the following suggestions:

Type	When to use
Rectangular	Only when signal is known to be periodic within time record
Hanning	Most often used for general purpose
Flat top	When absolute amplitude accuracy is required – calibration/sensitivity check
Kaiser-Bessel	When relatively high amplitude accuracy and frequency resolution are important

Results.

In order to evaluate the possibilities of the FFT as marker of ANS, we studied a number of normal subjects using a sampling frequency of 250 Hz in ECG recording and thus selecting each time a piece of R-R intervals and comparing obviously each time HRV calculated on the same epoch lengths.

The aim was to compare the results that may be obtained using some different windows.

Let us inspect the results for the different normal subjects that we examined (Figures 18).

We advise the reader that the abbreviations FE, GM, SM..... in the figures indicate the reference to the examined subjects.

By inspection of the results, we deduce that they are strongly dependent from the choice of the selected window and we have not so robust indications about the most appropriate window to be selected. Consequently, it is rather adventurous to consider the FFT as a definite and accurate marker for ANS in analysis of R-R intervals. The second indication arising from the results is that we never must compare set of data relating different number of epochs or different time intervals recording.

We have selected three basic time intervals for short term analysis of HRV: one corresponding to about 8.30-11 minutes, the second corresponding to about 7 minutes and finally the third about 5-6 minutes.

The reasons for such recommendations, relating the first and the second inspection of data, is rather evident.

R-R is a non linear and non stationary, highly complex signal. We have spent all the previous section of the present paper to delineate in some detail how it is realized physiologically the ANS control of beat to beat heart dynamics.

The conclusion of the previously reported set of data is that FFT evidences so profound limits if we aim to consider it as an actual Marker of the ANS. It may give only phenomenological indications.

Now, it is very clear to us that it is well difficult to eradicate a consolidated prejudice, and, still harder, to accept to submit to a pressing criticism a methodological approach that has been consolidated by years of its application, but the clinicians must strongly take in their mind some important features. We repeat here:

R-R is a non linear and non stationary, an highly complex signal.

We must understand that the calculated spectrum obtained by FFT arises by fitting a continuous function to discrete data. Systematically it introduces alterations as cutting off, arbitrary interpolations, average operations on the whole explored system so that the final results by FFT cannot be considered as definite and accurate marker of ANS in analysis of R-R intervals.

This is the reason because why we introduced the CZF method whose conceptual foundations were previously exposed. They were outlined with accuracy in the Added Note of explication

of the Nevrokard software, and still discussed in detail in the paper that we published on Chaos, Solitons, and Fractals (see selected publications).

We reassume in brief here the reasons to place side by side the CZF with the FFT.

The CZF, due to the simplicity of its mathematical foundations (it is a count of similarities and does not impose any predefined functional form to the data) does not suffer of the basic methodological limits of FFT. The central feature is that by the CZF the statistics is originally performed on the primary observable that is the wait between a heart beat and the other so not imposing any model to the data.

How to perform analysis by the CZF method.

The nevrokard software is arranged to perform CZF analysis automatically.

First of all one has to select the time interval in which the clinician decided to perform his experimentation. We outlined previously that we selected three possible time intervals (8.30-11 minutes), 7 or (5-6) minutes. This is for short time HRV analysis.

The nevrokard software downloads the recorded ECG, usually sampled at 250 Hz, as second step by means of a HRV file preparation-software it performs the calculation of the R-R intervals that in turn saves automatically in .rri extension in the HRV analysis software. Running this software it is possible to automatically perform the elaboration of the CZF and to obtain the results in an appropriate window. Therefore, the operations to perform CZF analysis are very simple so that the clinician cannot expect difficulties of any kind in performing such methodological approach.

The analysis gives the following results. The total variability in the VLF range. This is to say that the CZF has calculated the total variability of the input R-R signal in the range 0.01- 0.04 Hz. It calculates also the total variability in the LF band, that is to say .. such variability in the ranging frequencies between 0.04-.0.15 Hz, and finally CZF calculates the total variability in the HF range, that is to say from 0.15 to 0.4 Hz Soon after the CZF calculates the Total Variability that is to say the variability of VLF+LF+HF. *It is worth noting to remind that CZF works directly on periods (the inverse of frequencies) and that we report the results in terms of frequency only with the goal to make them comparable with traditional FFT.*

The Nevrokard software performs soon after the calculation of the %VLF , of %LF, of %HF and thus the LF, and the HF in n.u. (normalized unities), and the ratios LF/HF, LF/LF+HF), and finally of HF/(LF+HF). We may say that it follows in some manner that same scheme that it is obtained usually by employing the FFT analysis with the basic conceptual difference that we explained previously. In the case of the FFT we measure a “power” in PSD (Power Spectral Density). In CZF we are instead evaluating Variability *in both its aspects of order-independent (the equivalent of the Total Power of Fourier) and order-dependent (the equivalent of different bands) variability.*

Our primary attention must be reserved to the values of total variability in VLF, LF, and HF bands and to the Total Variability. These represent for us the markers to look at with great consideration in our CZF analysis.

Let us give an example on the manner in which we must read such CZF results

Let us consider that we have examined by the Nevrokard software an R-R input signal, and let us admit that we have obtained the following values of total Variability by using CZF:

VLF=55.000 msec² , LF=160000 msec² , HF=260000 msec² , and

Total Variability =475000 msec²

We read the results in the following manner:

VLF gives a total variability of 234.5 msec in the range of frequency from 0.01 to 0.04 Hz and this is to say ... VLF gives a total variability of 234.5 msec with a periodicity ranging from 25 to 100 sec.

LF gives a total variability of 400 msec in the frequency range from 0.04 to 0.15 Hz and this is to say that we have a total variability of 400 msec with a periodicity ranging from 6.66 to 25 sec.

Finally HF gives a total variability of 509.9 msec in the frequency ranging from 0.15 to 0.4 Hz and this is to say that we have a total variability of 509.9 msec with periodicities ranging from 6.66 sec to 2.5 sec.

Finally, the Total Variability must be estimated to be about of 689. msec.

We must carefully consider as markers such arising values of variability for LF and HF. These are the fundamental values that one must compare in the different experimental situations, i.e among normal subjects or in control subjects respects to other subjects with pathologies.

Obviously we may also take in consideration, as previously said, other indexes as the %VLF, of %LF, of %HF and thus the LF, and the HF in n.u. (normalized unities), and the ratios LF/HF, LF/(LF+HF), and finally of HF/(LF+HF). However, the first indexes that we must take in consideration as markers are those previously explained. It is the Variability among normal subjects and that one in normal respect to pathological conditions that give detailed signature of the action of the ANS on heart rate variability.

Let us add a further example in order to explain in detail. The results that we have just given for variability relate a normal subject. It is seen that the total variability in LF gives 400 msec while that one in HF is 509.9 msec. These two are values that differ about 22% with prevalence for a greater variability for HF respect to LF. From a physiological view point a difference of about 22% it is not so large. Of course we must expect that, in contradiction with the so different predictions of FFT, a large situation of compensation and of balancing, directly due also to the constant coupling existing between sympathetic and parasympathetic components, must always exist in ANS activity on heart rate variability. Such compensation reveals that we must expect not so large difference in normal subjects in balance between sympathetic and parasympathetic components. This is to say that we must attribute a so extended meaning to the parameter LF/HF . It is very indicative but of course we cannot expect to perform so accurate estimations using directly only such ratio.

Let us express now

In order to quantify HRV, the intervals between consecutive beats originating in the SA node, also called normal to normal intervals (NN intervals), must be found in the electrocardiogram (ECG).

The digital sampling must be regular and robust to identify a fiducial point for each beat

- 5) morphology and rhythm characteristics for each beat must be classified to distinguish between beats originating in the sinus node and ectopic beats.
- 6) only beats originating in the sinus node should be considered for the HRV analysis (42).

Furthermore, the fact that HRV is based on the NN intervals limits its use of HRV measures to individuals with a sinus rhythm and a limited number of ectopic beats

For the analysis to be reliable, different criteria have been proposed, e.g. the number of beats originating in the SA node must be at least 70 % (some even demand 99 % of the beats to originate in the SA node). The most strict criteria demands that the recording must not contain more than 10 ectopic beats per hour. These criteria excludes many patients from HRV analysis, e.g. 20-30 % of all highrisk patients in post acute myocardial infarct groups are excluded from HRV analysis due to frequent ectopic beats, artifacts, or arrythmia episodes

Let us add now a final explanation.

In Nevrokard software we have from one hand the possibility to estimate the variability by the CZF method. On the other hand we have also the possibility to perform the FFT using a very articulated set of windows. Selected a given window, we may calculate the spectrum and thus the Power Spectral Density in the previous mentioned regions of interest that are the VLF, the LF, the HF.

We repeat: CZF estimates Variability. FFT estimates Powers. Also with the basic insufficiencies that we previously acknowledged to the FFT, we may in any case compare the ratios that arise, for a given R-R interval, between the Power and the Variability in any selected band, VLF, LF and, HF, using the FFT from one hand and the CZF from the other. We obtain an important index informing us about the balance between the power of the sympathetic and parasympathetic modulations, and the corresponding influences that are induced on the Variability of the given R-R signals in the three bands of interest.

Nevrokard software calculates also such ratios. As example, in the previous mentioned example using the Hanning window, we obtained the ratios

$$\frac{VLF_{FFT}}{VLF_{CZF}} \text{ resulted to be } 345.45$$

The ratio

$$\frac{LF_{FFT}}{LF_{CZF}} \text{ resulted to be } 606.25$$

and, finally, the ratio

$$\frac{HF_{FFT}}{HF_{CZF}} \text{ resulted to be } 46.15$$

We have here other three important estimation indexes of balancing of ANS on HRV.

We must add still another comment.

The Nevrokard software in the CZF window also gives a final graph in which in abscissa we have the frequency with its three basic ranges VLF, LF, HF and in ordinate we have the values of variability in msec². We may say that we have a global graph that moves in analogy with the standard and traditional PSD in FFT. However, we must account for some profound conceptual differences. Peaks in the CZF graph corresponds now to greatest variability, instead the down sinking correspond to periodicities or more recurrent points in the R-R input series. The situation is

inverted respect to a traditional FFT where peaks corresponds to frequencies giving highest power in periodic components. The CZF, on the contrary and respect to FFT, is able to identify the frequencies in which variability reaches its maximum values and frequencies in which variability reaches its minimum ... that is to say .. by CZF we acquire detailed knowledge of the frequencies at which the R-R signal gives its greatest periodicities or very near periodicities, and those in which it gives the greatest variability.. The figures 21, 22, 23 are explaining to this regard.

In Figures 21, 22, 23 we discuss the case of two normal subjects, subjected to controlled respiration. In Fig.21 we appreciate the frequencies at which a great variability is induced. Of course, we also appreciate the cases in which it induces a lower variability .. that is to say a periodicity or a recurrent behaviour in points of the R-R intervals. In conclusion, by this graph we reconstruct, step by step, the dynamic modalities in which the ANS control is realized. Obviously, the corresponding values give a quantitative estimation as markers of the ANS activity. Of course, the corresponding FFT graph in Fig. 22 only enables to estimate that the subject is forced to a controlled respiration happening at about 0.2 Hz and the relative power in the PSD.

Of course, it is also of interest the Fig. 23, still corresponding to a normal subject forced to controlled respiration. The graph is obviously very similar to that one given in Fig.21 with the exception that in this case we may also appreciate the very oscillating behaviour (sinusoid-like) that the forced respiration is inducing. Finally note that, in the cases of the CZF we are still in the condition to appreciate the dynamics of variability that the forced respiration induces in the LF and VLF bands, (in addition to the HF band) while instead, by the FFT, the corresponding spectrum coarsely reproduces what is also happening in the corresponding VLF and LF regions.

Let us express now a final comment that relates one of the most important novel features of using the CZF method.

In order to be clear let us reconsider here some of the phrases that we introduced in our previous exposition:

- 1) **In order to quantify HRV, the intervals between consecutive beats originating in the SA node, also called normal to normal intervals (NN intervals), must be found in the electrocardiogram (ECG).**
- 2) **The digital sampling must be regular and robust to identify a fiducial point for each beat**
- 3) **Morphology and rhythm characteristics for each beat must be classified to distinguish between beats originating in the sinus node and ectopic beats.**
- 4) **Only beats originating in the sinus node should be considered for the HRV analysis**
Furthermore, the fact that HRV is based on the NN intervals limits its use of HRV measures to individuals with a sinus rhythm and a limited number of ectopic beats
- 5) **For the analysis to be reliable, different criteria have been proposed, e.g. the number of beats originating in the SA node must be at least 70 % (some even demand 99 % of the beats to originate in the SA node). The most strict criteria demands that the recording must not contain more than 10 ectopic beats per hour. These criteria excludes many patients from HRV analysis, e.g. 20-30 % of all high risk patients in post acute myocardial infarct groups are excluded from HRV analysis due to frequent ectopic beats, artifacts, or arrhythmia episodes**

The CZF methods does not suffer of the previously mentioned limitations. It may applied in all the different cases of clinical interest so that we have for the first time a marker of the ANS that enables us to explore the whole set of hearth and cardiovascular pathologies.

An analysis of young normal subjects by the CZF.

We may now go to expose some other results obtained by the CZF method.

We examined 14 young subjects, between 20 and 25 years old. According to our protocol, ECG recordings in all subjects took place at 8:30 AM at rest, in a quiet and comfortable environment. The electrocardiographic signals were digitized (sampled at a rate of 250 Hz), and stored on hard disk. We selected three time intervals of time recording, (8.30-11 minutes), (7 minutes), and (5-6.30 minutes).

The ECG traces were analysed by the Nevrokard software and the obtained R-R intervals were subsequently analysed by the CZF method.

We report here the obtained results.

As first we tried and reproduce the results obtained by Giuliani et al (15). These authors demonstrated the possibility of a straightforward representation of cardiac dynamics in terms of a first-order Markov model. According to this model, heartbeat dynamics may be considered a random walk, where the system at each beat is presented with three alternatives:

- a) To remain in the same state (i.e., having a beat of a length very similar to the previous one)
- b) To shift to the higher class of beat duration,
- c) To shift to the lower class of beat duration

So displaying a sort of quantum-like behaviour. This paradigm is particularly suited for CZF. By the above sketched model gives birth to a fractal structure of the R-R signal, given the above sketched Markov model holds at every scale (e.g. focusing on class a) intervals we will see a microscopic version of the same dynamics).

Two observables must be taken always in consideration in order to give an interpretation of the CZF graph. They are:

- a) The values exhibited from the variability (in the three bands VLF, LF, HF);
- b) the behaviour of the variogram against the frequency.

For R-R time series relating an ECG recording of about 7 minutes there are acceptable values of Variability in HF ranging from 1200 to 3500 msec² as maximum value and in the range 400-700 msec² as minimum values. For R-R time series relating 5-6 minutes also lower values may be accepted for the minimum values until 200 msec². Note that Variability of 1200-3500 msec² means calculated Variability about 35-60 msec., while calculated values about 400-700 msec² means Calculated Variability about 20-27 msec that result still acceptable as marker of variability.

We previously mentioned that we examined subjects at rest, in a quiet and comfortable environment according to the standard well known protocol. It must be clear that we are speaking here of a pure abstract theorization. The so called subject at rest is a pure abstraction. When recording an ECG, as minimum, the subjects are thinking to some thing. Also with all its rough approximations we may verify by the FFT that the shown peaks indicate a different height in such cases. Generally speaking, we must always be aware that the condition of each subject vary rather continuously in time respect to himself and respect to the other subjects also when they are normal subjects in resting conditions. It is certainly true that we have indicated previously some values of Variability obtained by the CZF method. However, we must always expect possible fluctuations about such values about 20% in order to be sure to enlarge the possible ranges with more realistic features. On the other hand, we have to outline here a particular characteristic of the CZF. As repeatedly outlined, this method calculates variability extended along the whole given R-R time series and for the valuable Lags. Variabilities are calculated as squared difference between R-R values shifted each time by a prefixed Lag, and thus we estimate that fluctuations valued in excess about the 20% should be rather sufficient to account for the possible deviations respect to the values that we previously introduced in the case of young normal subjects.

The other important feature that we take in consideration is the behaviour of the variogram vs the frequency. It is evident that it must be rather uniform showing values of increased variability followed from values of decreased variability. Sudden changes in such uniform behaviour or, in any case, a non uniform distribution about such estimated values of variability induces to suspect some sudden modification of the heart rhythm and thus the presence of some abnormal rhythmic. Also a rather constant behaviour of the variogram not

evidencing its characteristic decreasing behaviour at the increasing values of the frequency, should induce the suspect of some acting anomaly in rhythmic, failing in this case the evidence of the due variability in the analyzed R-R time series

Let us look now to the results obtained from the examination of the previously mentioned young subjects.

Note that we report here only the results obtained for 7 minute and for 5-6.30 minutes, indicating the first by 7 and the second by 6. We exclude the results corresponding to (8.30-11) minutes for brevity but soon after we give such results by histograms.

An optimum subject under the profile of the exhibited values of variability and behaviour vs frequency is TA, VDA gives an optimum profile in the investigation of 7 minutes but it manifests a sudden change in the behaviour in the exploration on 6 minutes.

We suggest that in such cases a more accurate investigation is required on subjects of such kind. MA may be considered very satisfactory in 7 minutes but a quite satisfactory behaviour in 6 minutes. VDB is very satisfactory. AM is satisfactory also if it manifests a too reduced variability about 0.4 HZ in the investigation about 6 minutes. SC is satisfactory. DCP is satisfactory also if with some insufficiency in the variability behaviour in CZF-6 minutes graph. RR, AT, CP, SCI are satisfactory as well as still also PF while GE and RS evidence a rather low Variability in the range 0.3-0.4 Hz.

For the LF evaluation the criterium must be that Variability must remain rather constant in the explored frequency band 1500-3000

$msec^2$ (39-55 $msec$) suspecting in particular for those behaviours that present a too accentuated decay respect to the frequency values in the LF band.

Let us give also a look at the consequent histograms. Fig.25

Comments:

- 1) The examined subjects are the same that we analysed previously by the FFT.
- 2) First of all, let us appreciate the uniformity of the results that we obtained with relation to the calculated variabilities. We have now a graph and quantitative estimations of the marker of ANS activity. We have furnished also some general criteria to read and to interpret the CZF graphs Variability against frequency. Actually we have to conclude that by the CZF we have now a reliable marker for ANS
- 3) It is of particular interest also the inspection of the ratio LF/HF. It remained rather constant among all the examined subjects with the rather obvious difference about the mean value of 0.73 ± 0.16 for 7 minutes recording and 0.86 ± 0.17 for recording of 5-6.30 minutes. 0.57 ± 0.04 was obtained in the case of examined recording of 8.30-11 minutes, that in fact represents a rather long interval of measurement for short time HRV analysis. In any case the CZF show an evident novel feature. There is a rather constant balance between Variability In LF and HF respectively, and we retain that this is of course the correct physiological interpretation since we must account that there is continuous balance, interference and thus coupling between the two modulating components of the ANS system. We observe of course that this is a feature that improbably arise by using the FFT analysis.
- 4) In conclusion: the results that we obtained by using the CZF result to be excellent when considered as markers of the ANS.

There is still a novel feature that we may estimate by using the CZF method. We may appreciate, as previously explained, the ratio between the Power of the modulating components of the ANS and the correspondent Variability that is induced. This a very important new parameter that we may appreciate for the first time. Obviously we must always take in consideration the limits that enter in the R-R time series analysis by using the FFT.

Just so, let us examine now the ratio of VLF_{FFT}/VLF_{CZF} , LF_{FFT}/LF_{CZF} and HF_{FFT}/HF_{CZF} . We have the histograms of Figures 26.

Also with all the limitations arising from using FFT, we consider decidedly important to estimate how it is the ratio between the Power (estimated by PSD of FFT) of the ANS modulating components and the corresponding Variability that they induce, and that we estimate by the CZF method. By inspection of the previous histograms, such ratio remains rather constant among the different normal young subjects that we examined.

For VLF we had a mean value of such ratio of 18.62 ± 4.12 for 8.30-11 minutes, 12.40 ± 3.29 for 7 minutes and 12.31 ± 3.00 . for 5-6 minutes.

For LF we had a value of such ratio of 22.67 ± 6.07 for 8.30-11 minutes, 16.30 ± 4.83 for 7 minutes and 16.02 ± 4.76 for 5-6 minutes

For HF we had instead very fluctuating values with a mean value of 33.06 ± 12.93 for 8.30-11 minutes, of 22.12 ± 11.42 for 7 minutes and of 19.96 ± 10.60 for 5-6 minutes.

In brief, the estimation of such parameter seems to realize a satisfactory agreement for VLF and LF but not for HF.

In order to confirm such result, we proceeded to estimate the correlation coefficient between the Power estimated by the FFT and the Variability estimated by the CZF. We obtained a very satisfactory value of the correlation coefficient for the VLF and for the LF, but such statistical parameter indicated that we have not correlation between the calculated value of Power in FFT and Variability in CZF for the HF. Assuming that the CZF is the correct marker of ANS, we must conclude that the FFT gives its greater worse estimation just in the frequency band ranging from 0.15 – 0.4 Hz, that is to say ...in the periodicities included in the interval going from 2.5 to 6.6 seconds.

This concludes our approach on application of the CZF method on normal young subjects.

Let us take now a step on. We examined four subjects in condition of spontaneous and controlled respiration. Time interval of 5-6 minutes.

We report here the obtained graphs and histograms in Figg. 27 and 28.

Let us discuss the results obtained by the FFT.

We used the Hanning window being the most frequent used in standard studies of HRV.

As expected, the FFT did not give homogeneous results, implying the practical impossibility to use this technique as marker of the ANS status.

Let us give a look at the results on a subject by subject basis.

BS gave peaked results on both the frequency bands of interest, LF and HF in condition at rest and spontaneous respiration. The spectrum in condition of controlled respiration gave a peak band only in the HF region at about 0.2 Hz.

FE strangely evidenced well only the HF band in condition of spontaneous respiration and it became dominant in condition of controlled respiration always centred about 0.2 Hz.

Another unexpected behaviour was highlighted by GC who gave a peaked band only in the LF region with some minor evidence in the HF band. The previous results refer to spontaneous respiration conditions, while the same subject shows two well defined peaks at LF and HF when in controlled respiration conditions.

Again, SM evidenced a dominant HF and a rather evident activity in the LF band when in condition of spontaneous respiration (0.2 Hz).

These qualitative results (quantified by the resulting histograms) make evident the presence of some inconsistencies in the analysis by FFT.

Let us examine now the results that we obtained by the CZF method.

First consider BS. It has a proper graph on the basis of the interpretative criteria that we exposed previously and is reflected by the entire set of the relevant spectral bands. This was true for both spontaneous and controlled respiration conditions. For the Variability we obtained in brief rather equivalent results. In the controlled respiration we had the expected sinusoidal-like behaviour differentiating such variability in controlled respiration respect to spontaneous respiration.

Let us now examine FE. Remember that by FFT we were only able to evidence the peaked region in HF. By the CZF we had an optimum behaviour both for LF and HF with the characteristic sinusoidal-like behaviour. Nothing to add. In condition of controlled respiration we had evidence of the most important effect expected by such procedure of respiration control. The graph always exhibited a very regular behaviour but (the most expected result) the values of the variability enhanced largely. The results are very clear also by inspection of the corresponding histograms. We had here a clear indication of the effect that is induced by the controlled respiration: generally speaking it is to induce a strong increasing in the Variability.

The histogram gives us the manner to quantify accurately the induced effect. Again, the CZF method reveals its intrinsic ability to be used as marker of ANS. Note the other important feature: the increase variability is induced simultaneously on both the HF and the LF bands. This is important to conclude, on the physiological basic, that the two basic modulating components of the ANS, the sympathetic and parasympathetic efferent actions, operate so that a systematic and balanced coupling is established between such two components.

Let us now examine GC. As we remember the FFT gave only evidence of one band in the LF in spontaneous respiration. We should examine such subject with greater consideration. The basic feature is that He has the tendency to exhibit a rather low variability both in the LF and HF bands and also with free failures in some regions in condition of spontaneous respiration. He recovers in condition of controlled respiration but only for the behaviour, not under the profile of the values relating the Variability. Let us look at the histograms relating GC. The results obtained by inspection of the graphs is immediately confirmed, and this time with a precise quantitative estimation.

Let us inspect now GM. By FFT he gave two well evidenced bands in LF and HF.

The examination by CZF evidences an excellent profile in condition of spontaneous respiration. In condition of controlled respiration such very good profile is highly confirmed and we inspect again the very excellent profile, and in addition we have also the expected effect of the controlled respiration. This is to say: strong increased values of the Variability. Still, also note the balance that is realized between LF and HF regimes. Look at the corresponding histograms to have a quantitative accurate estimation.

Finally, let us inspect SM. With the greatest contradiction respect to the real dynamics, the FFT spectrum showed only an evidenced band in the LF region. This is a very serious error in such analysis. Instead it is still a very interesting case. Really, by inspection with the CZF method one discovers that he has an excellent profile under spontaneous respiration but, however, it fails under the condition of controlled respiration. A look at the histograms also confirms that we had a net reduction of variability in passing from spontaneous to controlled respiration. The situation results inverted respect to the expected behaviour in such kind of experimentation. An inspection of the story of such subject finally cleared the Arcanum. SM is actually an athlete. Therefore, the condition of controlled respiration revealed itself as a condition of stress for such subject as promptly the CZF method revealed. The results may be inspected in figures 29 and 30 for the different subjects.

As final step we discuss now the case of some subjects affected by hypertension. We performed the analysis for seven minutes. In the following both the classical Hanning-window Fourier Analysis and CZF method will be presented for the same subjects. The results are given in Figures 31, 32, 33, 34

Final Comments.

The inspection by the FFT suggests that the subject BMG has a low LF and an high HF.

The subject CA instead has an high LF and a low HF.

The subject CO-A results rather equilibrated in both the components LF and HF. The same happens for subject GV.

The subject DM-S has an high HF/ moderate LF pattern analogously to CA.

The subject GV gives again an equilibrated spectrum.

IS shows an high LF, and the subject MA-AD eventually, is characterized by a very high LF.

In conclusion, even in this case, we observe a marked heterogeneity as for patients we know in advance to share the same general condition (in this case hypertension).

Let us comment now the results obtained by the CZF method. Looking at the graphs, BMG, CA, CO-A, DM-S, and GV subjects display a marked homogeneity and a general similarity to the 'normal' condition. The effects induced from the hypertension are instead clearly observable in IS and MA-AD subjects. Looking at such graphs we highlight two different physiological kind of effects. Hypertension induces a net lowering of the variability in the IS subject, and a very interesting novel feature is observed for the subject MA-AD. He evidences so a large increase in the variability reaching for the first time of 12000-13000 $msec^2$ that is about ten times greater the value of a normal subject. This is a very interesting case under the physiological and clinical profile that deserves carefully investigation (see Table 2).

As last point, let us give a look to the ratios FFT/CZF. Comparing such values with those that we estimated previously for normal subjects, it is clearly seen that only BMG seems indicate some non normal value for the LF(FFT)/LF(CZF), but all the other values remain in the range of normality that we calculated for normal subjects. Obviously we obtain instead rather large deviations for the two subjects IS and MA-AD as we confirmed also previously by the results obtained directly by using only the CZF

Under the physiopathological profile, it seems that we may conclude that there are stages of hypertension that still has not produced a profound alteration of heart R-R Variability (in this case of all the subjects

with the exception of IS and MA-AD), while instead there are stages in which such alteration has become evident and undoubtedly very severe.

References

1. **Acar, B., Savelieva, I., Hemingway, H. & Malik, M.**, Autonomic ectopic beat elimination in short-term heart rate variability measurement, *Computer Methods and Programs in Biomedicine* 63 (2): 123–131, 2000.
2. **Acharya, U.R., Joseph, K.P., Kannathal, N., Lim, C.M. & Suri, J.S.**, Heart rate variability: a review, *Medical & biological engineering & computing* 44 (12): 1031–1051, 2006.
3. **Bers, D.M.**, Calcium and cardiac rhythms: Physiological and pathophysiological, *Cardiovascular Research*, 90 (1): 14–17, 2002.
4. **Blackman, R.B. and Tukey, J.**, in “Particular Pairs of Windows.” published in *The Measurement of Power Spectra, From the Point of View of Communications Engineering*, New York: Dover, 1959, pp. 98-99.
5. **Brodde, O.E. & Michel, M.C.**, Adrenergic and muscarinic receptors in the human heart, *The American Society for Pharmacology and Experimental Therapeutics*, 51 (4): 651–690, 1999.
6. **Chreiteh, S.S. & Fisker, K.B.**, Master Thesis, Morphological Changes of the QRS Complex as a Marker of Autonomic Modulation of the Heart Rate; Biomedical Engineering and Informatics - Medical Systems Department of Health Science and Technology Aalborg University Spring, available on line (projekter.aau.dk/projekter/files/17645943/Rapport1085a.pdf); Prosig Noise and Vibration Measurement Blog, DATS software, available on line (<http://blog.prosig.com/2009/07/20/data-windows-what-why-and-when/>), [2009].
7. **Colosimo, A., Giuliani, A., Mancini, M., Piccirillo, G. and Marigliano V.**, Estimating a cardiac age by means of heart rate variability, *Am. J. Physiol.* 273 (Heart Circ. Physiol. 42): H1841–H1847, 1997.
8. **Despopoulos, A. & Silbernagl, S.**, Color Atlas of Physiology, 5 th edn, Thieme. ISBN 7-5046-4220-7, 2003.
9. **Dhein, S.**, *Cardiac Gap Junctions*, S. Karger. ISBN 3-8055-6567-4, 1998a.
10. **Dhein, S.**, Gap junction channels in the cardiovascular system: pharmacological and physiological modulation, *Trends in Pharmacological Sciences* 19 (6): 229–241, 1998b.
11. **Eckmann, J.P., Kamphorst, S.O., Ruelle D.**, Recurrence Plots of dynamical systems, *Europhys. Letters*, 4 (9): 973-977, 1987.
12. **Elliot, A. J., Payen, V., Brisswalter, J., Cury, F. and Thayer, J. F.**, A subtle threat cue, heart rate variability, and cognitive performance. *Psychophysiology*, 48: no. doi: 10.1111/j.1469- 8986.2011.01216.x, 2011.
13. **Frank, K.F., Bolck, B., Erdmann, E. & Schwinger, R.H.**, Sarcoplasmic reticulum ca^{2+} - atpase modulates cardiac contraction and relaxation, *Cardiovascular Research* 57 (2): 20–27, 2003.
14. **Fuster, V., Alexander, R. W. & O'Rourke, R.A.**, Hurst's the heart, 11 t h edn, McGraw-Hill. ISBN 0-07-14226-1, 2004.
15. **Giuliani, A., Lo Giudice, P., Mancini, A.M., Quatrini, G., Pacifici, L., Webber, C.L., Zak, M. and Zbilut, J.P.**, A Markovian formalization of heart rate dynamics evinces a quantum-like hypothesis. *Biol. Cybern.* 74: 181–187, 1996.
16. **Guyton, A.C. & Hall, J.E.**, *Textbook of Medical Physiology*, 11th edn, Elsevier. ISBN 0-7216-0240-1, 2006.
17. **Henry, B.L., Minassian, A., Paulus, M.P., Geyer, M.A., Perry, W.**, Heart rate variability in bipolar mania and schizophrenia, *Journal of Psychiatric Research*, 44: 328-346, 2009.

18. **Huikuri, H.V., Mäkikallio, T., Airaksinen, K.E.J., Mitrani, R., Castellanos, A. & Myerburg, R.J.**, Measurement of heart rate variability: a clinical tool or a research toy?, *Journal of the American College of Cardiology*, 34 (7): 1878–1883, 1999.
19. **Kamp, T.J. & Hell, J.W.**, Regulation of cardiac l-type calcium channels by protein kinase a and protein kinase c, *Circulation Research*, 87 (12): 1095–1102, 2000.
20. **Koelsch, S.A. Remppis, A., Sammler, D., Jentschke, S., Mietchen, D., Fritz, T., Bonnemeier, H., Siebel, W.A.**, A cardiac signature of emotionality, *European Journal of Neuroscience*, 26: 3328–3338, 2007.
21. **Malik, M.**, *Clinical Guide to Cardiac Autonomic Tests*, Kluwer Academic Publishers. ISBN 0-7923-5178-9, 1998.
22. **Martini, F.H.**, *Fundamentals of Human Anatomy and Physiology*, 6th edn, Pearson Education Int. ISBN 0-13-061568-4, 2004.
23. **Marwan, N., Romano, M.C., Thiel, M., Kurths, J.**, Recurrence plots for the analysis of complex systems, *Physics Reports*, 438: 237 – 329, 2007
24. **Mateo, J. & Laguna, P.**, Analysis of heart rate variability in the presence of ectopic beats using the heart timing signal, *IEEE Transactions on Biomedical Engineering*, 50 (3): 334–343, 2003.
25. **Notarius, C. F. & Floras, J. S.**, Limitations of the use of spectral analysis of heart rate variability for the estimation of cardiac sympathetic activity in heart failure, *Europace* 3 (1): 29–38, 2001.
26. **Parilak, L.D., Taylor, D.G., Song, Y., Burkart, T., Shryock, J.C., Curtis, A.B. & Knota, H.J.**, Contribution of frequency-augmented inward Ca^{2+} current to myocardial contractility, *Canadian Journal of Physiology and Pharmacology*, 87 (1): 69–75, 2009.
27. **Ravenswaaj-Arts, C.M.A.V., Kollée, L.A.A., Hopman, J.C.W., Stoeltinga, G.B.A. & van Geijn, H.P.**, Heart rate variability, *Annals of Internal Medicine* 118 (6): 436–447, 1993.
28. **Ravits, J.M.**, Autonomic nervous system testing, *Muscle & Nerve*, 20 (8): 919–937, 1997.
29. **Rohr, S.**, Role of gap junctions in the propagation of the cardiac action potential, *Cardiovascular Research*, 62 (2): 309–321, 2004.
30. **Sand, O., Øystein V. Sjaastad & Haug, E.**, *Fysiologi, en grundbog*, Munksgaard. ISBN 978-87-628-0401-2, 2004.
31. **Sherwood, L.**, *Human Physiology - From Cells to Systems*, 5th edn, Thomson Learning, Inc. ISBN 0-534-39536-8, 2004.
32. **Stein, P.K., Bosner, M.S., Kleiger, R.E. & Conger, B.M.**, Heart rate variability: A measure of cardiac autonomic tone, *American Heart Journal* 127 (5): 1376–1381, 1994.
33. **TaskForce**, Heart rate variability - standards of measurement, physiological interpretation, and clinical use, *European Heart Journal* 17 (3): 354–381. The North American Heart Association & The European Society of Cardiology, 1996.
34. **Thayer, J.F., Smith, M., Rossy, L.A., Sollers, J.J. Friedman, B.H.**, Heart Period Variability and Depressive Symptoms: Gender Differences, *Biol Psychiatry*, 44:304–306, 1998.
35. **Walker, C.A. & Spinale, F.G.**, The structure and function of the cardiac myocyte: A review of fundamental concepts, *The Journal of Thoracic and Cardiovascular Surgery* 118 (2): 375–382, 1999.
36. **Webber, C.L., Zbilut, J.P.**, Dynamical assessment of physiological systems and states using recurrence plot strategies, *J. Appl. Physiol.*, 76: 965-973, 1994.
37. **Wei-Jin, Z., Li-Na, C. & Xiao-Jiang, Y.**, Progress in the study of vagal control of cardiac ventricles, *Acta Physiologica Sinica*, 57 (6): 659–672, 2005.
38. **Yeragani, V.K., Ramesh, C., Glitz, D.A.**, Heart rate variability in patients with depression, *Psychiatry Res* 37: 35– 46, 1991.
39. **Zak, M., Zbilut, J.P., Meyers, R.E.**, From instability to intelligence, *Lecture Notes in Physics*, M49, Springer, Heidelberg, 1997.
40. **Zbilut, J.P., Zak, M., Meyers, R.**, A terminal dynamics of heartbeat, *Biol. Cybern.*, (75): 277-280, 1996.
41. **Zemaityte, D., Varoneckas, G., Sokolov, E.** Heart Rhythm control during sleep, *Psychophysiology*, 21 (3): 290-298, 1984.

Figure legend page

Table 1: The frequency domain parameters for short term and long term analysis of HRV

Figure 1: The conducting system of the heart. Edited from Guyton and Hall [2006].

Figure 2: The different action potentials for each of the specialized cells in the heart. Edited from Malmivuo and Plonsey [1995].

Figures 2a: Action potential in pacemaker cells (see ref. 6).

Figures 2b: Action potential in cardiac contractile cells (see ref. 6)..

Figure 3: Scheme of R-R interval.

Figure 4: Vectorcardiographic representation during the depolarisation of the ventricular muscle mass. I, II, and III corresponds to Einthoven's bipolar leads. Edited from Guyton and Hall [2006].

Figure 5: The sympathetic and parasympathetic innervation of the heart (see ref. 6).

Figure 6: A 10 Hz sinusoidal time series.

Figure 6a: FFT of the previous 10 Hz sinusoid

Figure 7: A 9.5 Hz sinusoidal time series.

Figure 8: Multi-line spectrum (FFT of 9.5 Hz sinusoid)

Figure 9: 9.5 Hz sinusoid (End-to-end)

Figure 10: The "Hanning" window

Figure 11: Sinusoid multiplied by window

Figure 12: Spectrum of 9.5Hz sinusoid (after windowing)

Figure 13: Spectrum of 10Hz sinusoid (after windowing)

Figure 14: End-to-end (0% overlap)

Figure 15: 50% overlap

Figure 16: 67% overlap

Figure 17: 75% overlap

Figures 18: FFT HRV analysis in normal subjects.

Figures 19: Fourier analysis of normal subjects

Figures 20: Fourier analysis of normal subjects

Figure 21: Explanation of CZF behaviour in subjects during controlled respiration

Figure 22: Explanation of CZF behaviour in subjects during controlled respiration

Figure 23: Explanation of CZF behaviour in subjects during controlled respiration

Figures 24: CZF behaviour in normal subjects for different minutes of recording.

Figures 25: Analysis of variability in normal subjects

Figures 26 : Analysis of ratio Fourier/ CZF

Figures 27 : A:Fourier analysis - Hanning - spontaneous respiration
B: Fourier analysis - Hanning - controlled respiration

Figures 28 : Fourier analysis - Hanning spontaneous respiration Hanning controlled respiration

Figures 29 : A: CZF analysis of spontaneous respiration,
B: CZF analysis controlled respiration

Figures 30 : Histograms of ratios Fourier/CZF Comparison of spontaneous vs controlled respiration

Figures 31 : Fourier analysis of subjects with hypertension

Figures 32 : Fourier analysis – Hanning – histograms of subjects with hypertension

Figures 33 : CZF analysis of subjects with hypertension

Figures 34: CZF analysis – histograms of subjects with hypertension

Table 2: ratio values Fourier/CZF

Table 1

Short term recordings (5 min)			
Variable	Units	Description	Remarks
Total power	ms ²	The variance of the NN intervals.	An estimate of overall variance.
VLF	ms ²	Power in the very low frequency range (≤ 0.04 Hz).	Its physiologic correlates are not fully understood, but it is assumed to reflect the influence of e.g. thermo regulation, circadian, and neuro-endocrine rhythms.
LF	ms ²	Power in the low frequency range (0.04-0.15 Hz).	Is assumed to reflect both sympathetic and parasympathetic modulations of the heart rate.
LF norm	n.u.	Power in the low frequency range (0.04-0.15 Hz) in normalised units (LF/(LF+HF)).	By some, it is assumed to be a quantitative marker for sympathetic modulations.
HF	ms ²	Power in the high frequency range (0.15-0.4 Hz).	Is assumed to reflect parasympathetic modulations of the heart rate. The respiratory rhythm contributes to the HF component.
HF norm	n.u.	Power in the high frequency range (0.15-0.4 Hz) in normalised units. (HF/(LF+HF)).	The same as above.
LF/HF ratio		The ratio between low and high frequency power.	By some, it is assumed to reflect the sympathovagal balance, by others the sympathetic modulations of the heart rate.

Long term recordings (24 hours)			
Variable	Units	Description	Remarks
Total power	ms ²	The variance of the NN intervals.	An estimate of overall variance.
ULF	ms ²	Power in the ultra low frequency range (≤ 0.003 Hz).	Its physiologic correlates are not fully understood, but it is assumed to reflect the influence of e.g. thermo regulation, circadian, and neuro-endocrine rhythms.
VLF	ms ²	Power in the very low frequency range (0.003-0.04 Hz).	The same as above.
LF	ms ²	Power in the low frequency range (0.04-0.15 Hz).	Is assumed to reflect both sympathetic and parasympathetic modulations of the heart rate.
HF	ms ²	Power in the high frequency range (0.15-0.4 Hz).	Is assumed to reflect parasympathetic modulations of the heart rate. The respiratory rhythm contributes to the HF component.

Figure 1

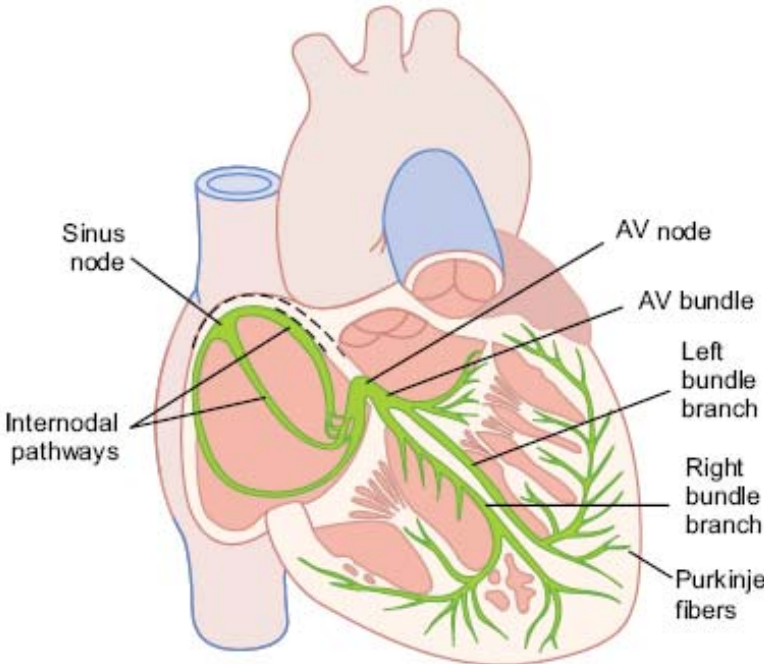
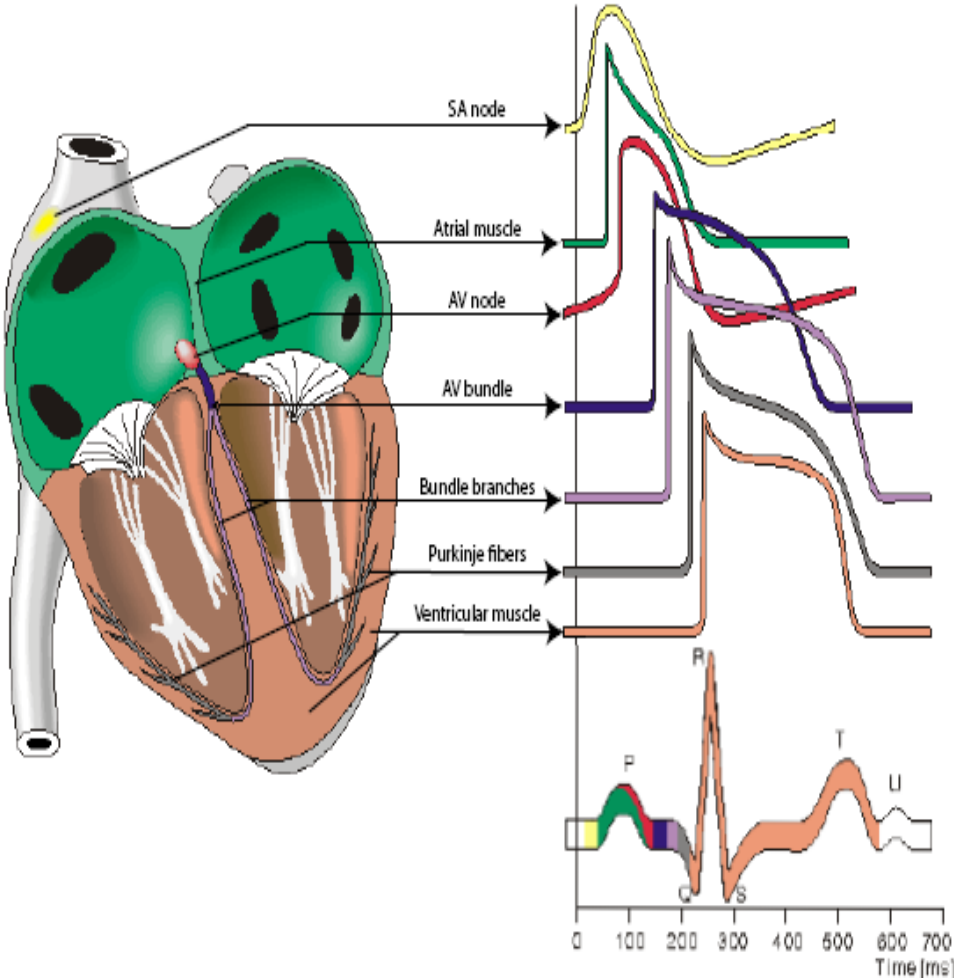
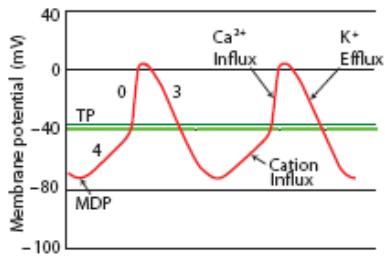


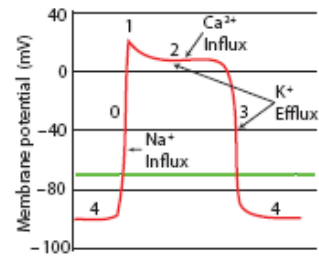
Figure 2



Figures 2a and 2b



(a) Action potential in pacemaker cells.



(b) Action potential in cardiac contractile cells.

Figure 3

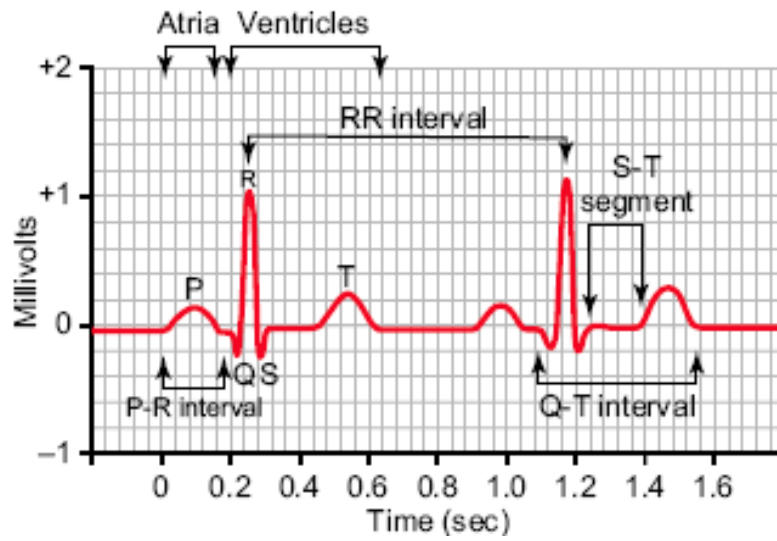


Figure 4

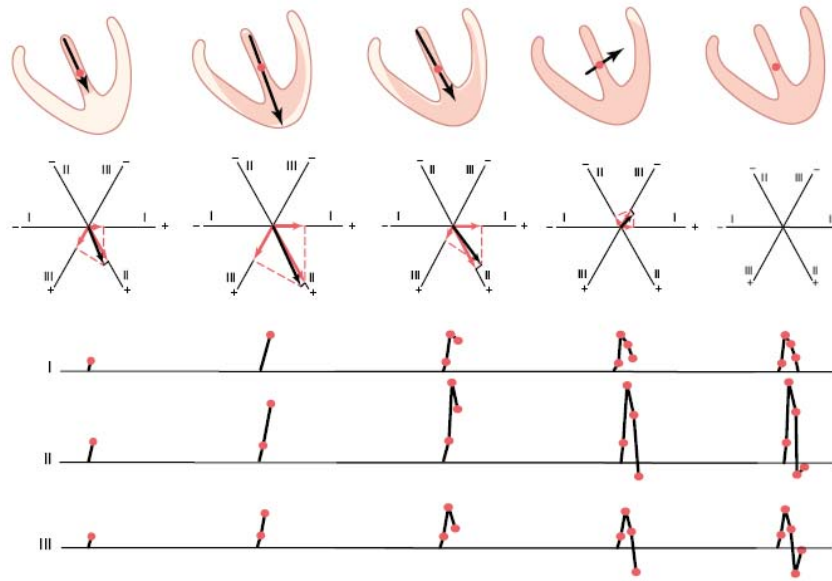


Figure 5

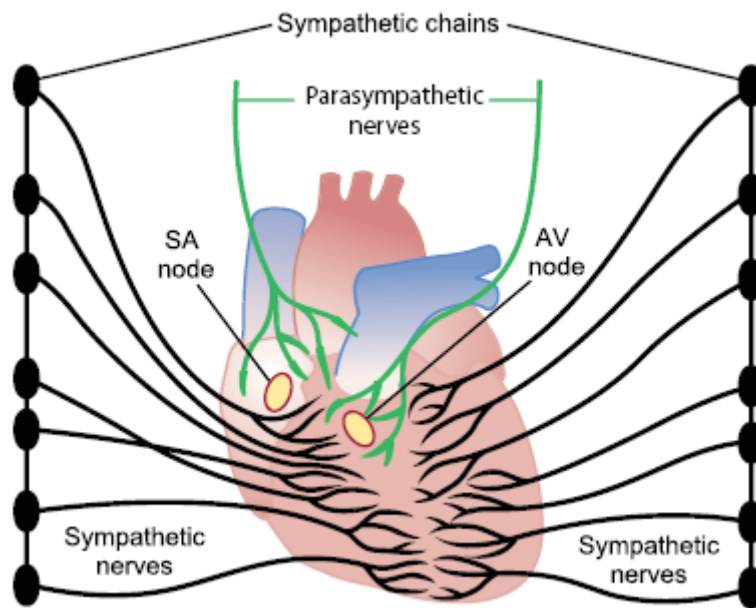


Figure 6

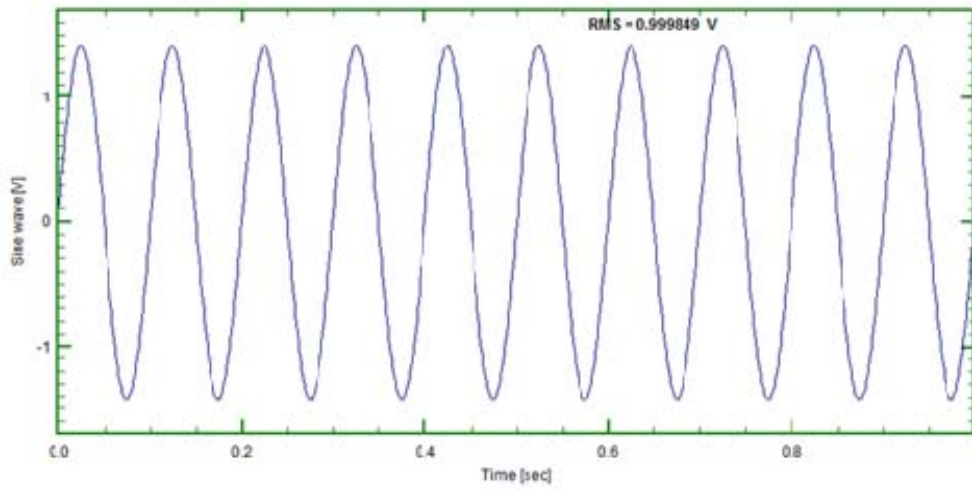


Figure 6?????

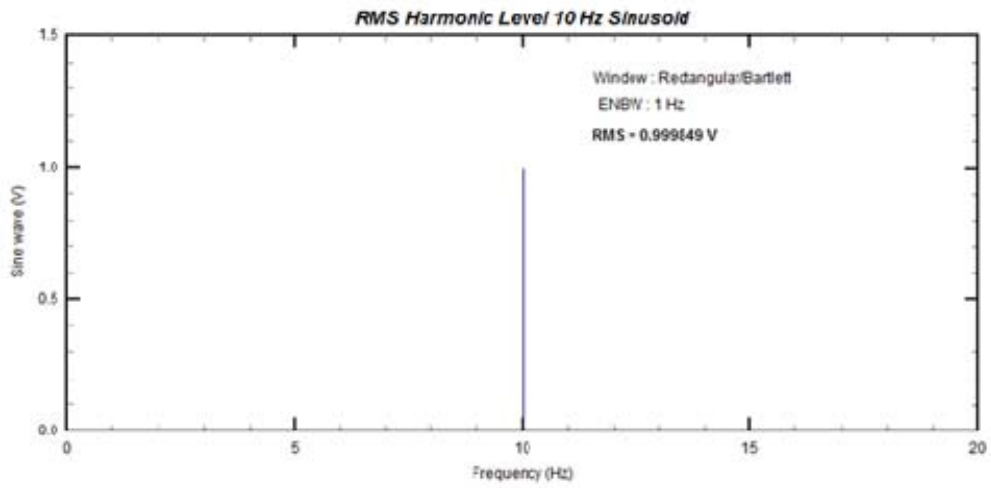


Figure 7

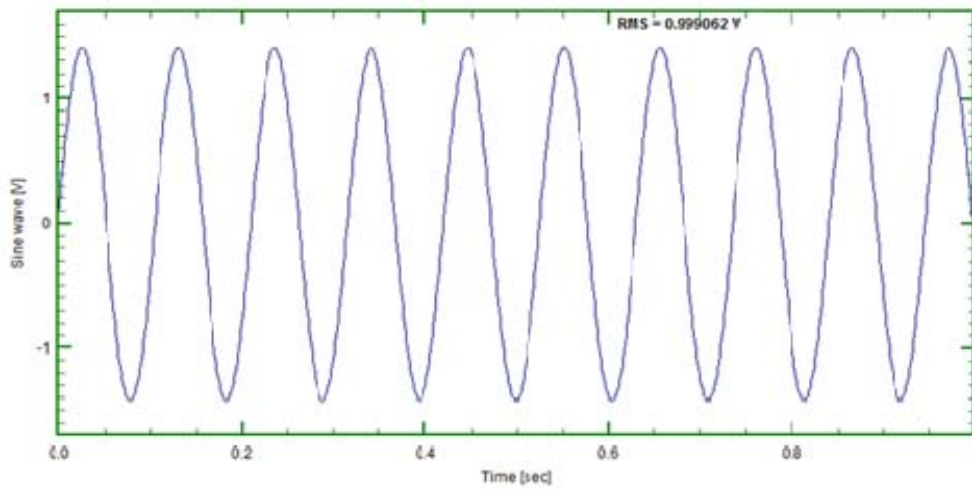


Figure 8

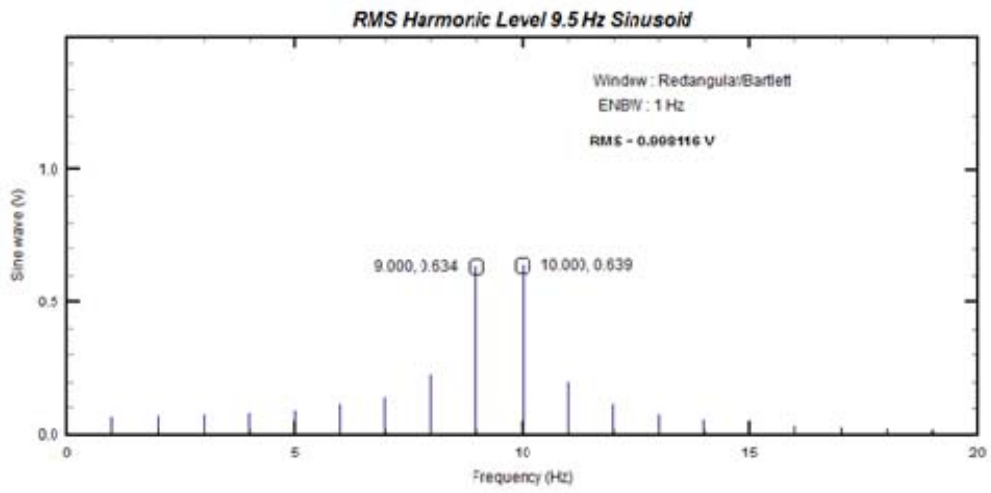


Figure 9

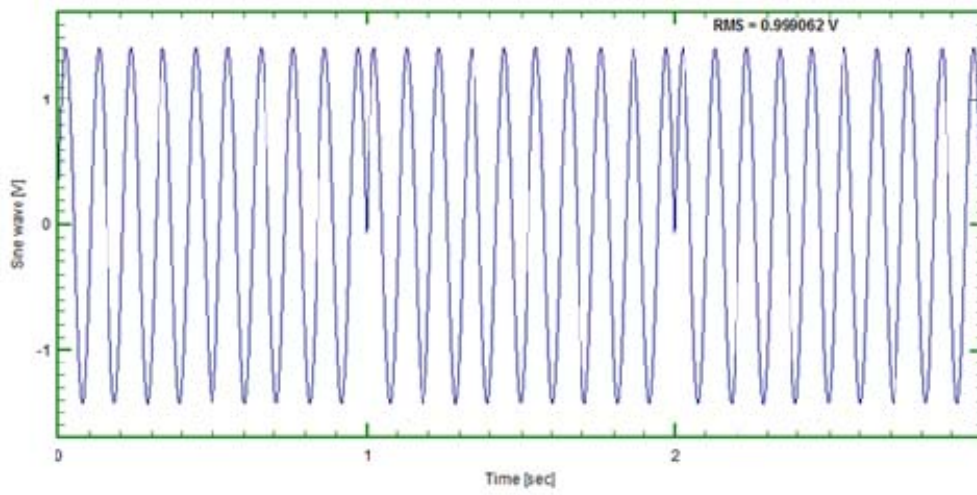


Figure 10

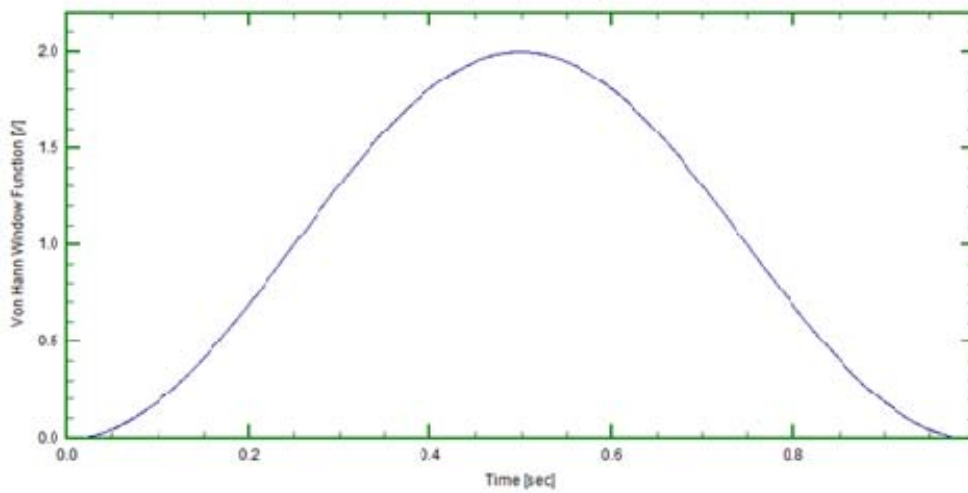


Figure 11

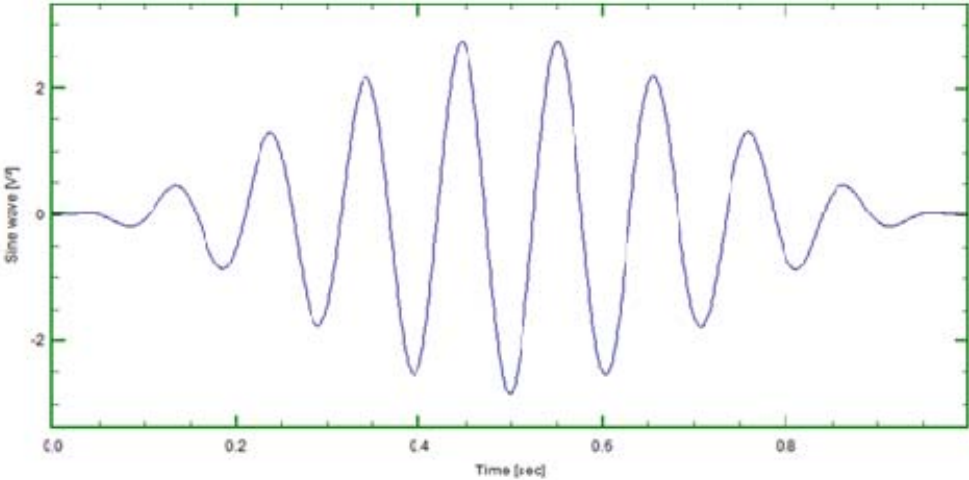


Figure 12

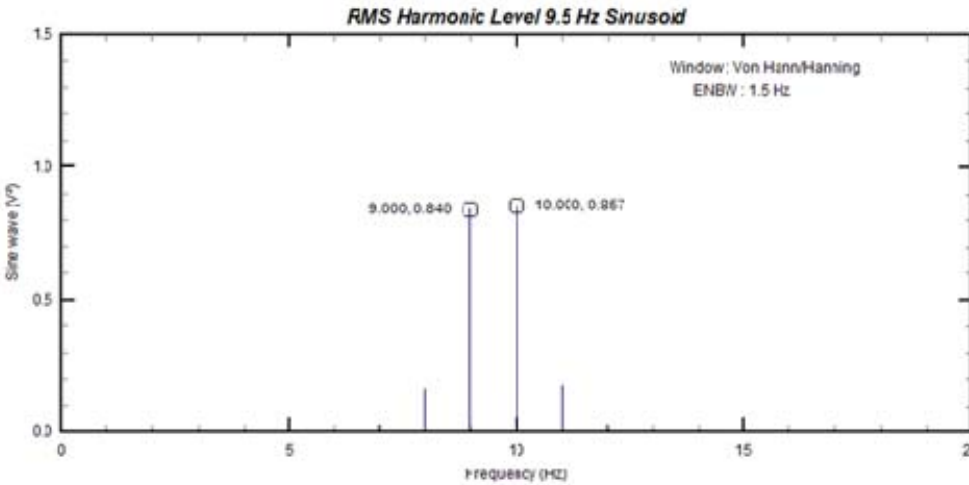


Figure 13

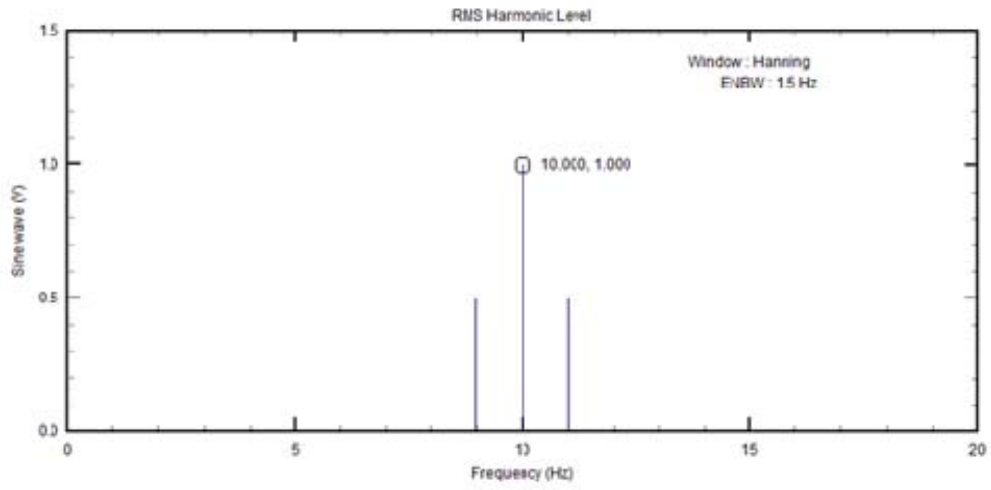


Figure 14

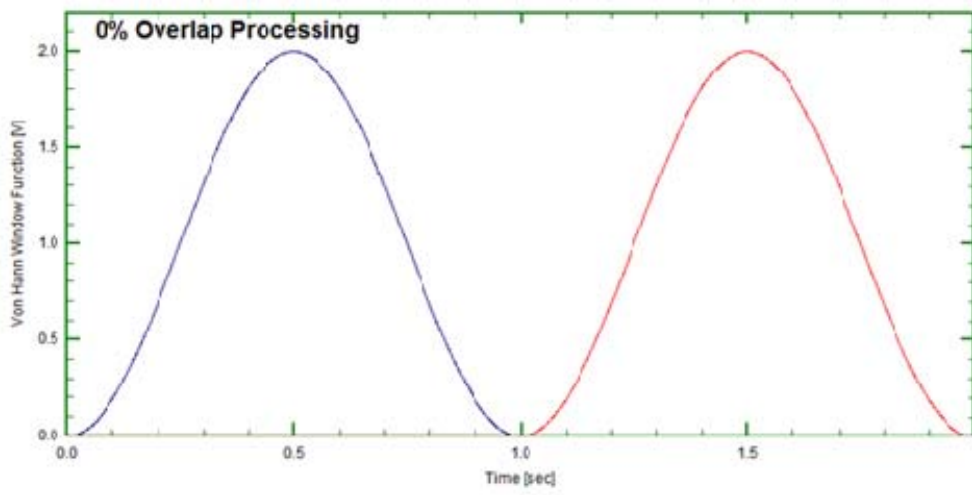


Figure 15

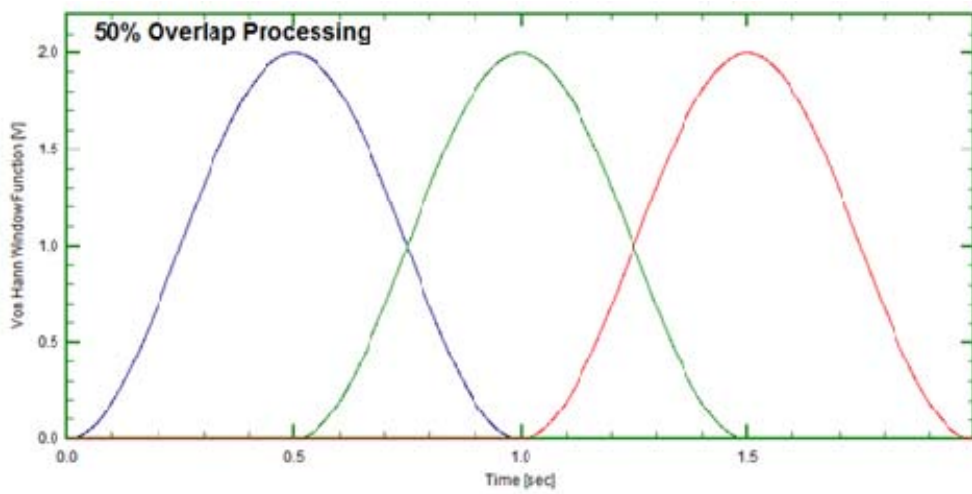


Figure 16

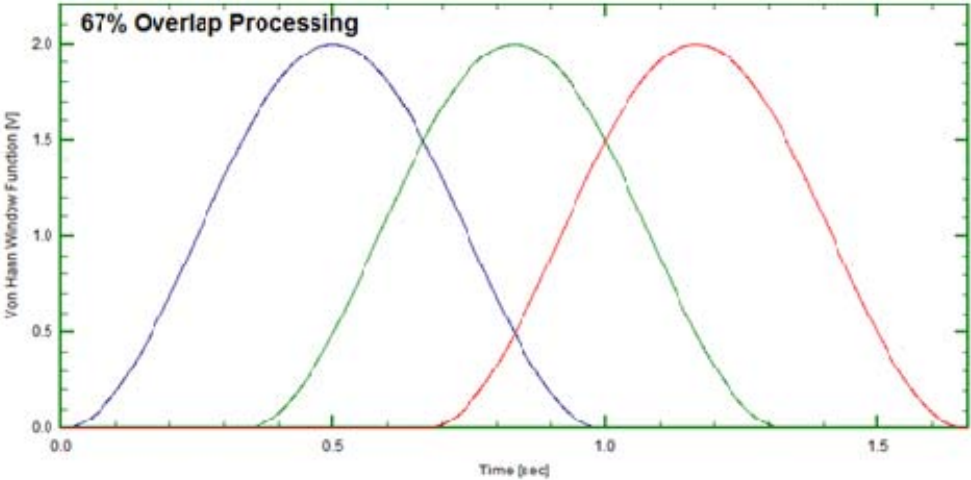
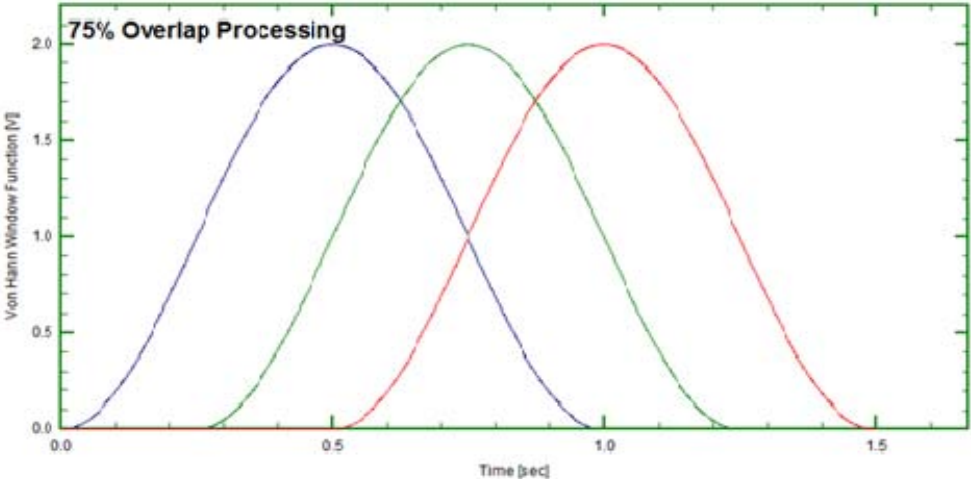
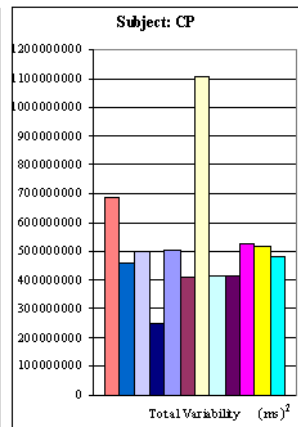
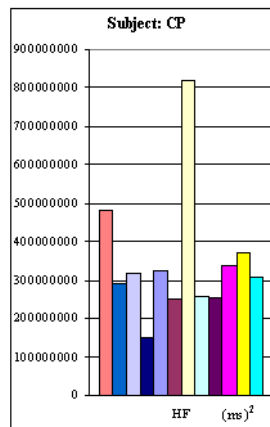
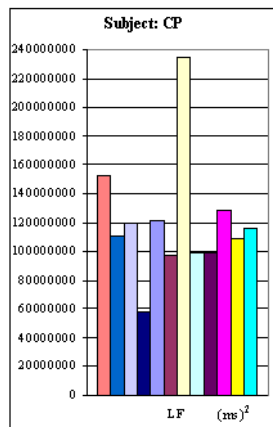
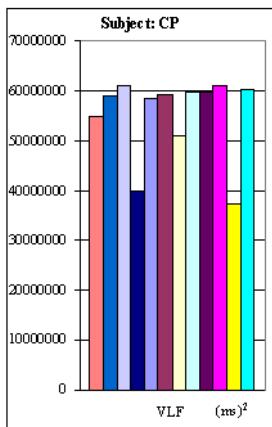
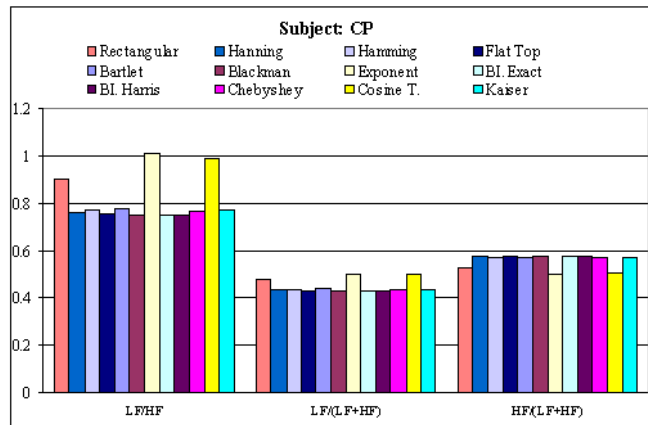
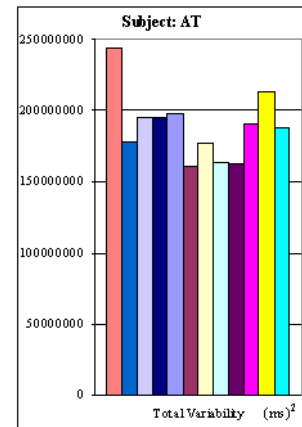
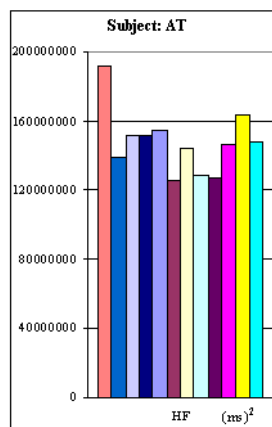
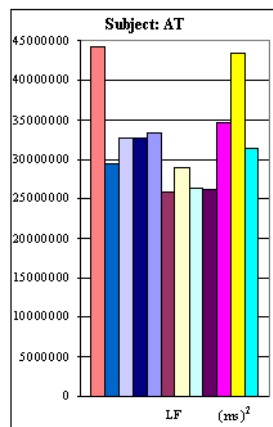
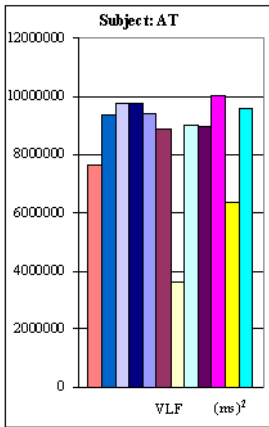
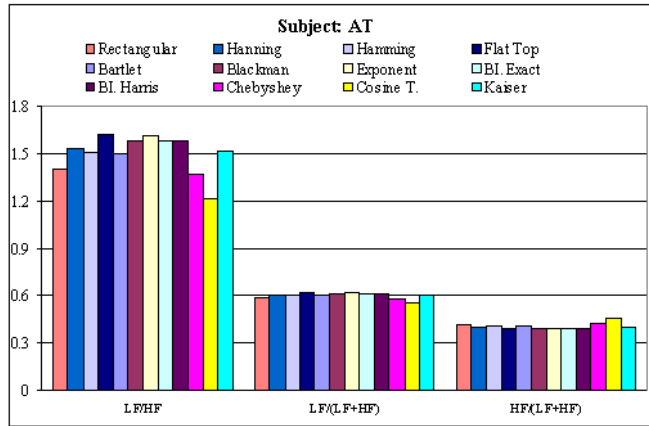
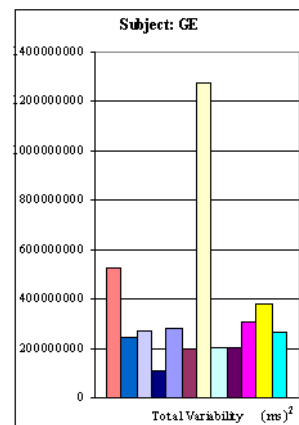
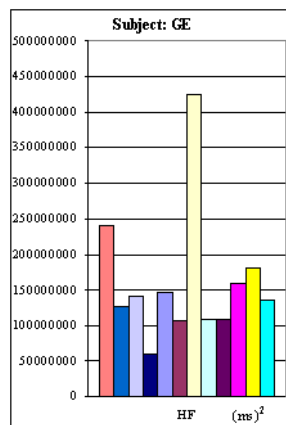
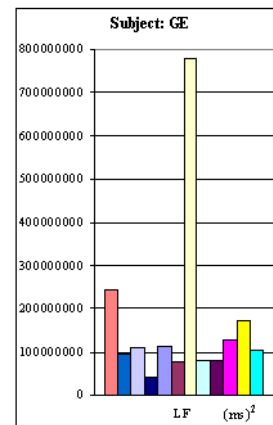
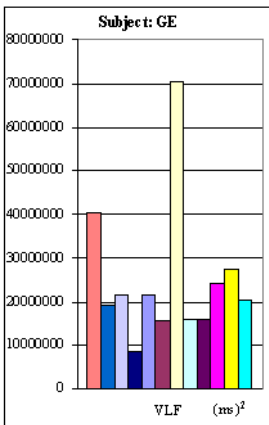
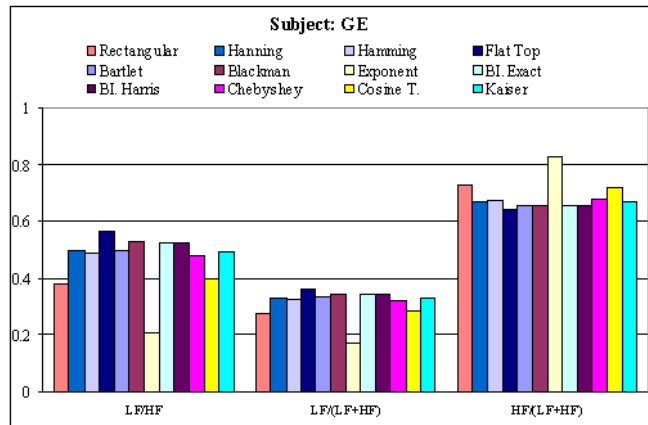
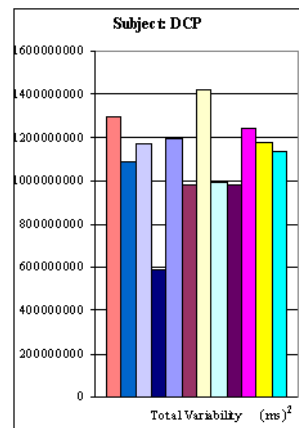
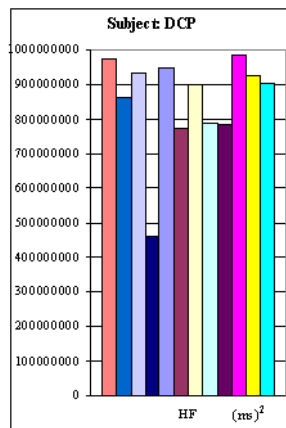
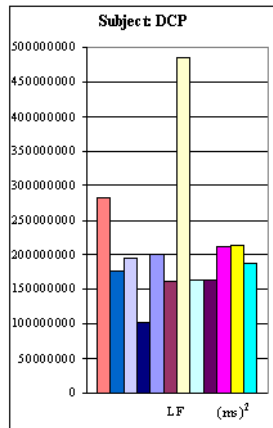
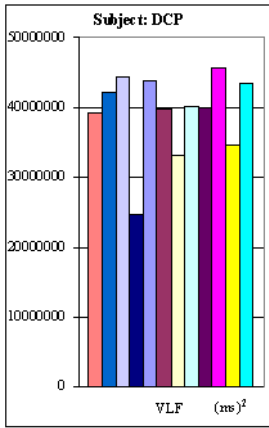
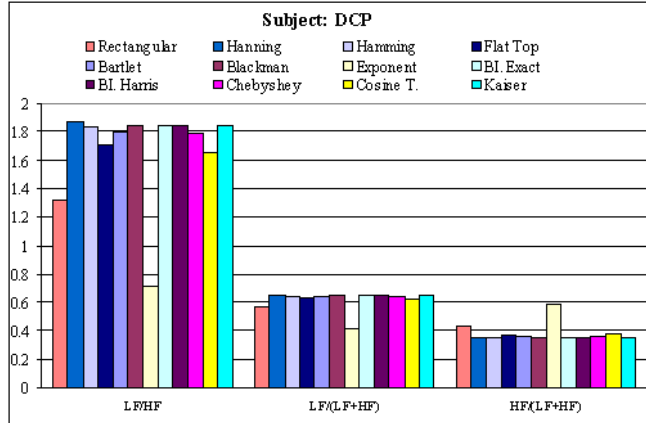


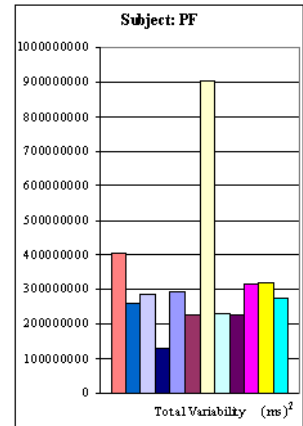
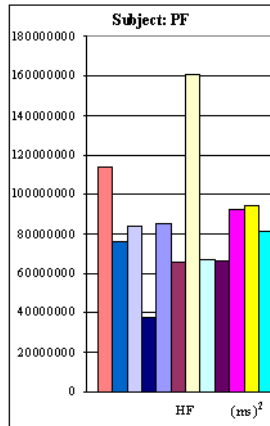
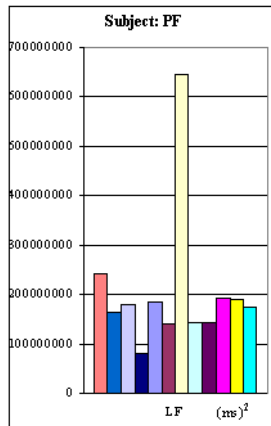
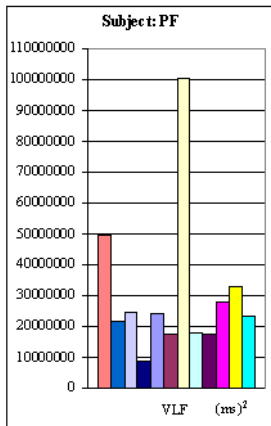
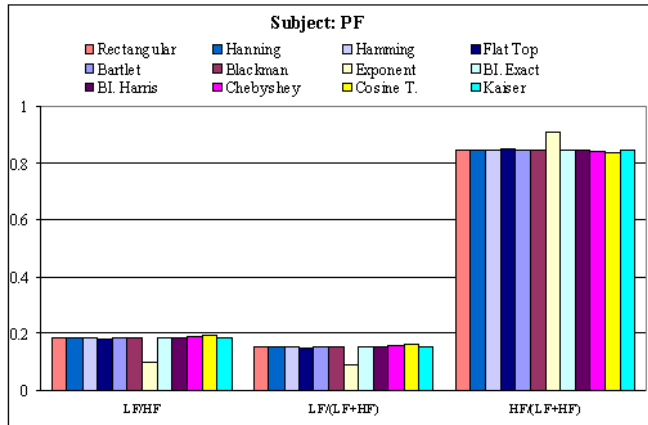
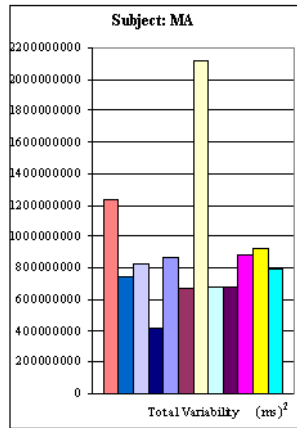
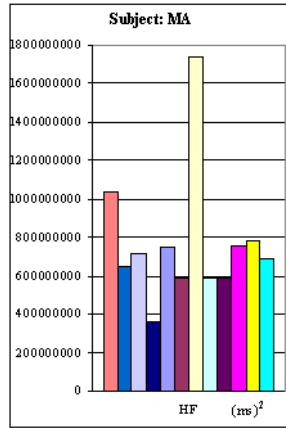
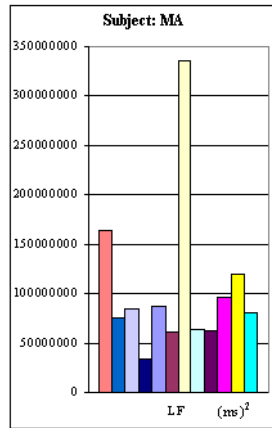
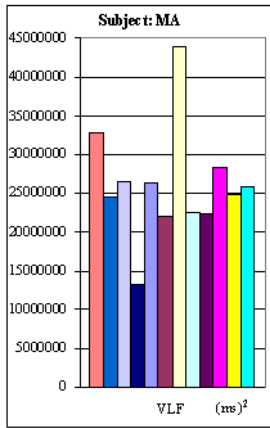
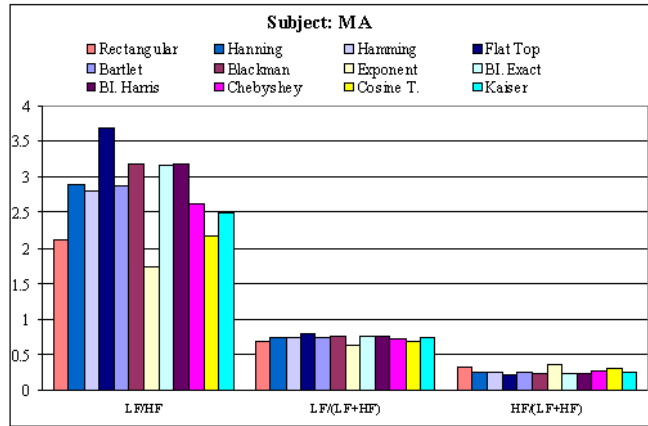
Figure 17

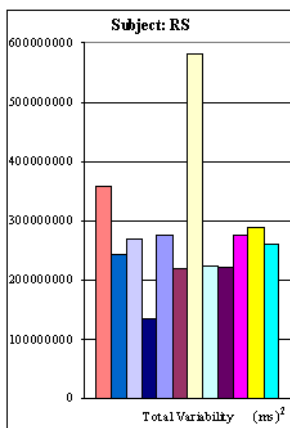
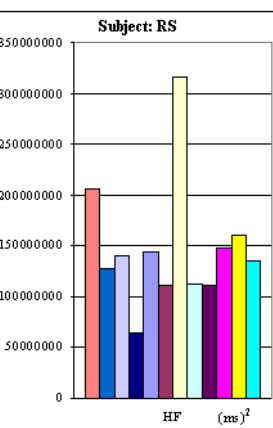
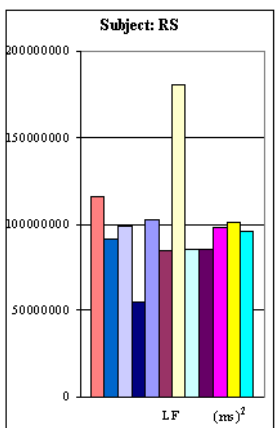
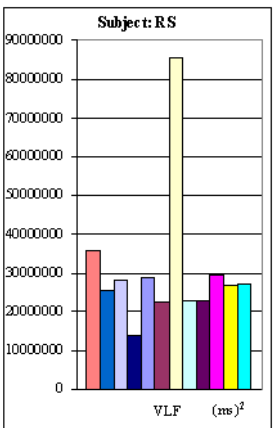
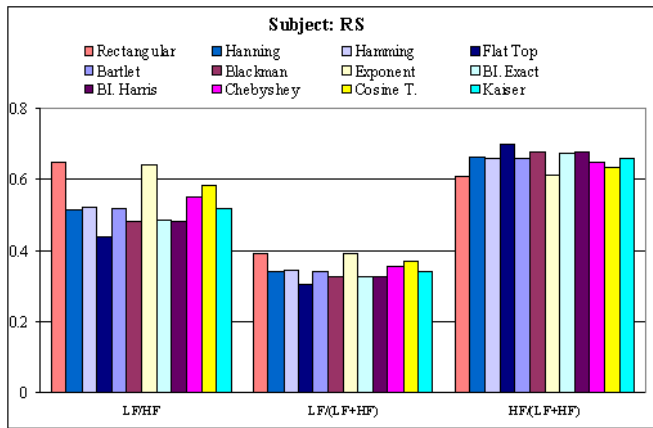
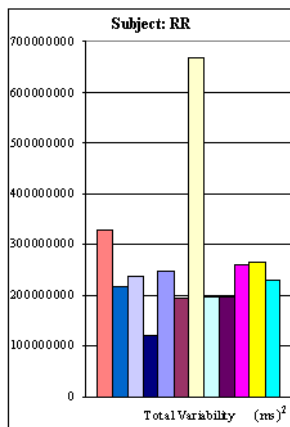
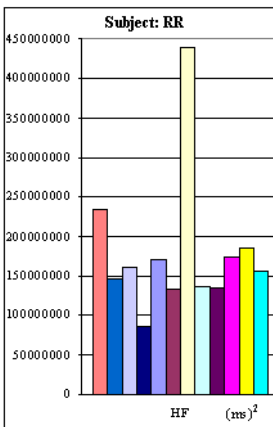
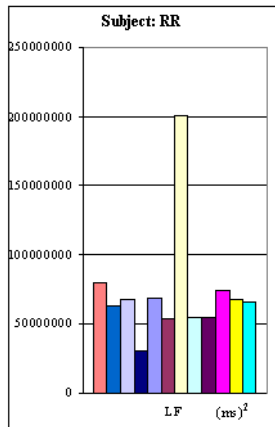
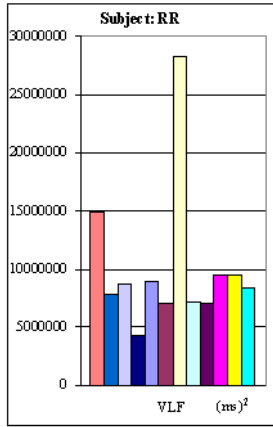
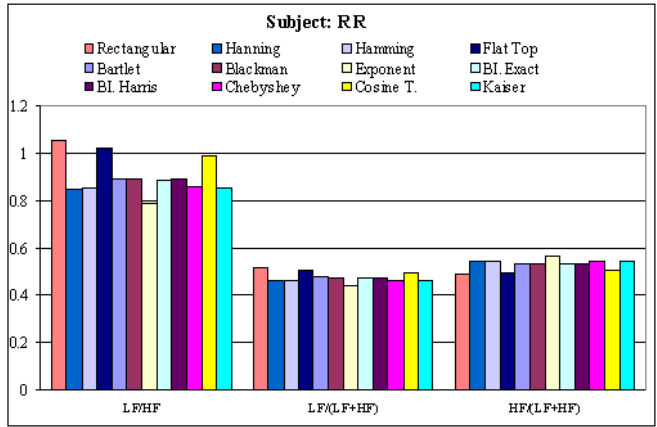


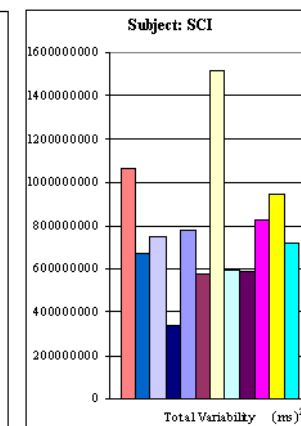
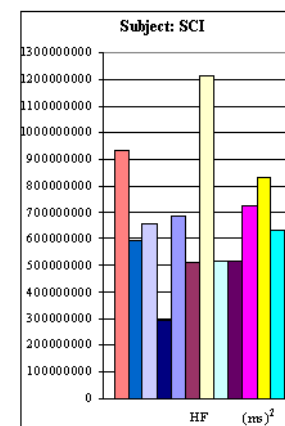
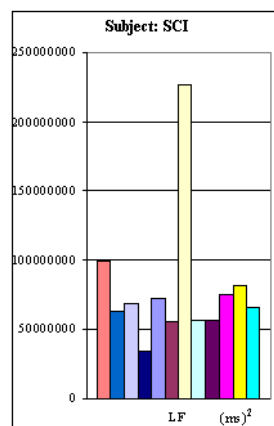
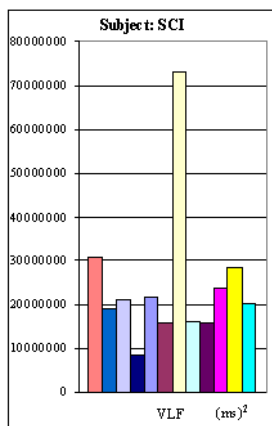
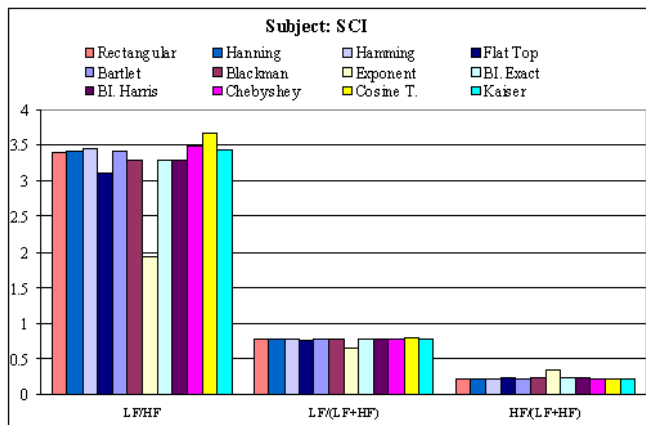
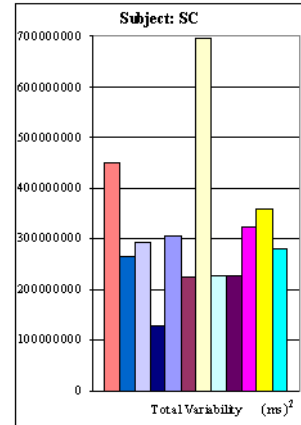
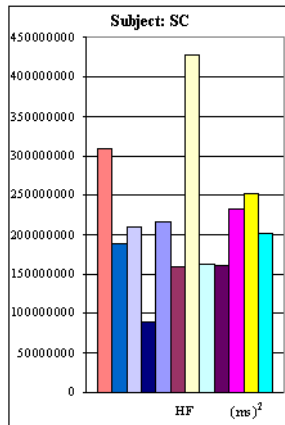
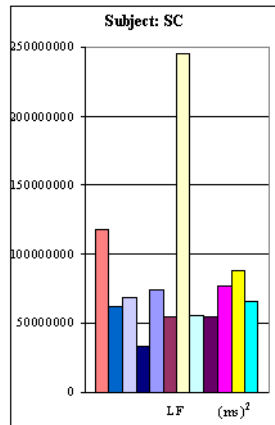
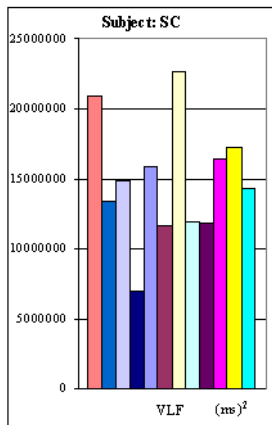
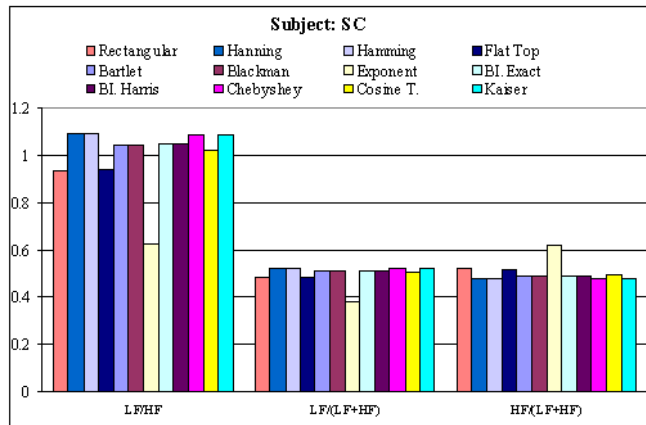
Figures 18

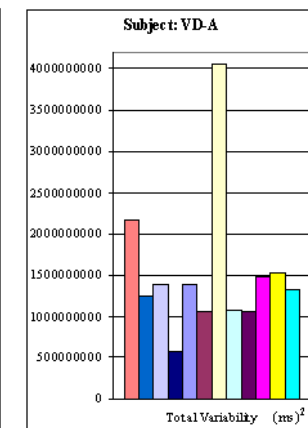
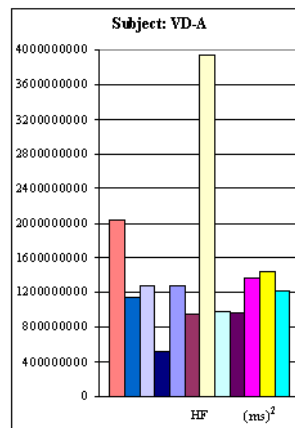
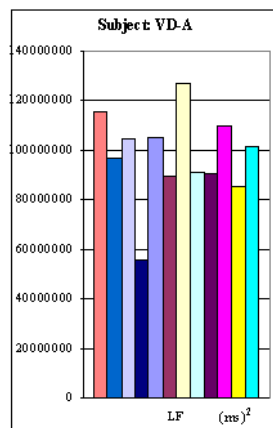
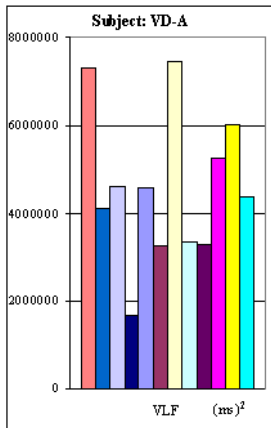
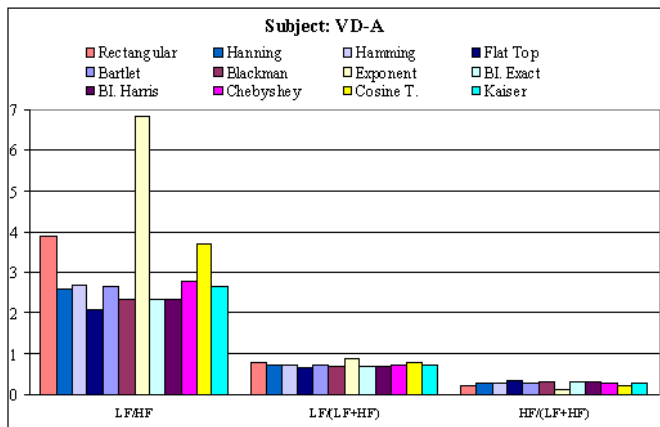
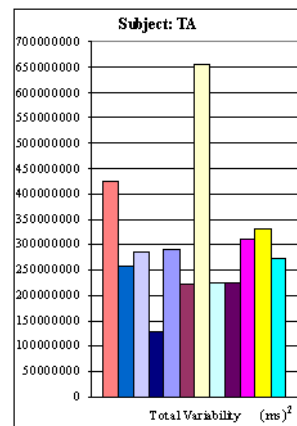
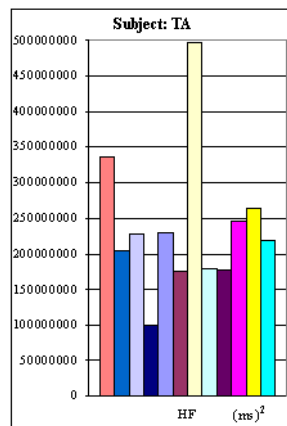
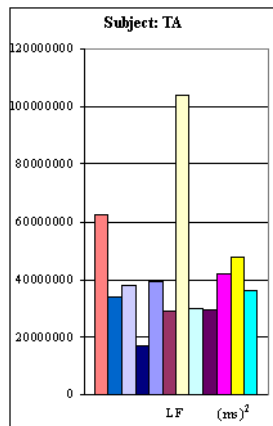
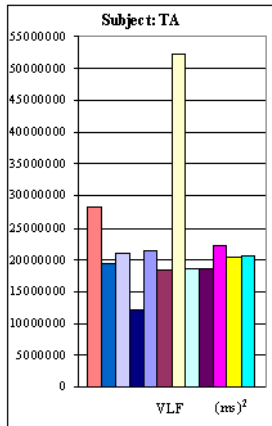
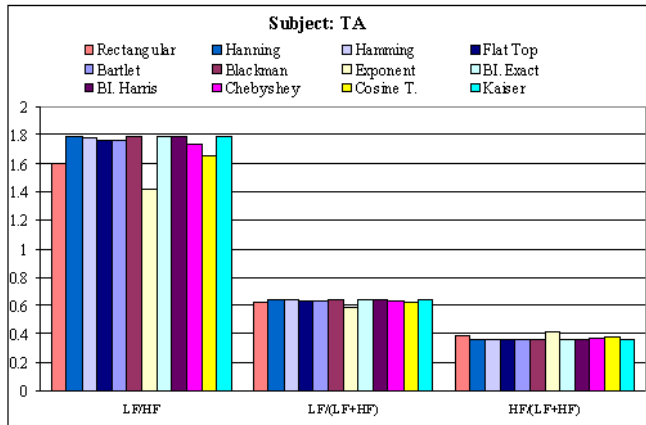


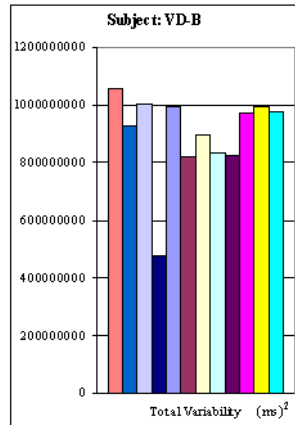
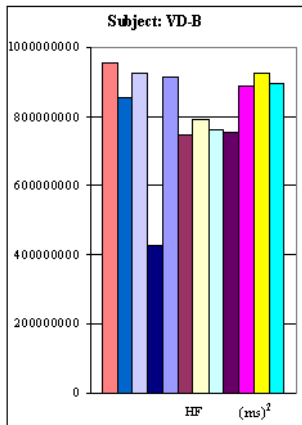
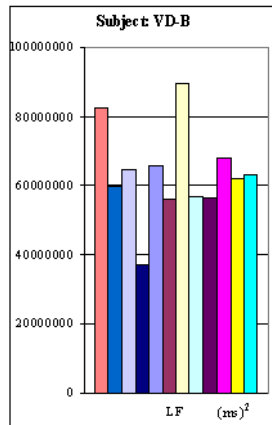
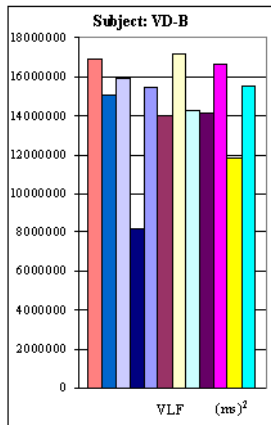
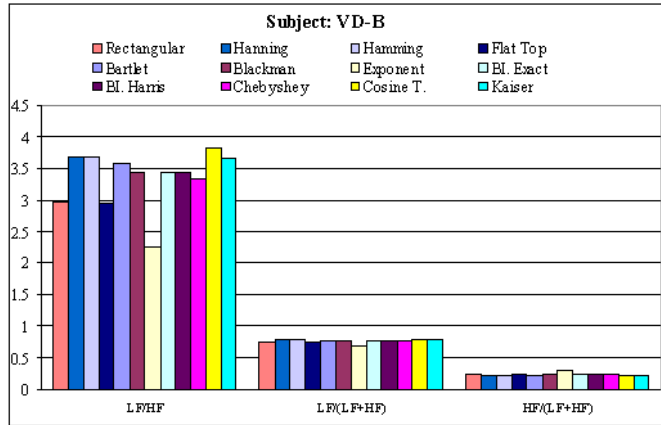




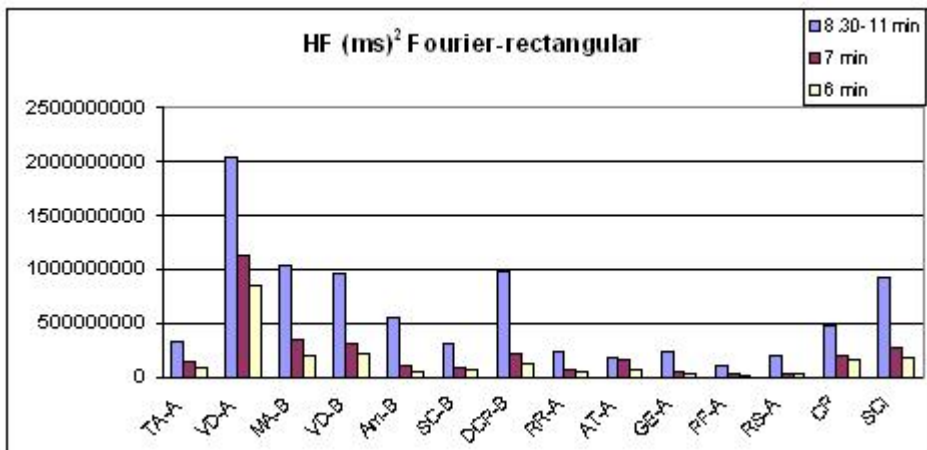
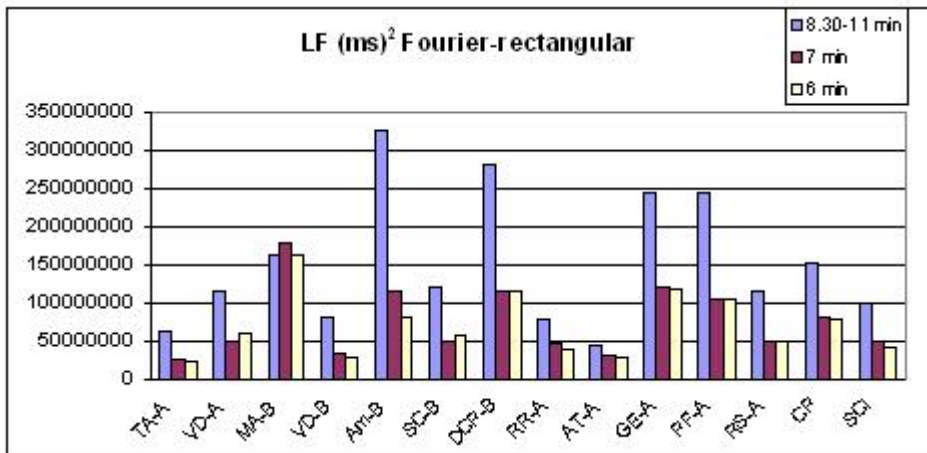
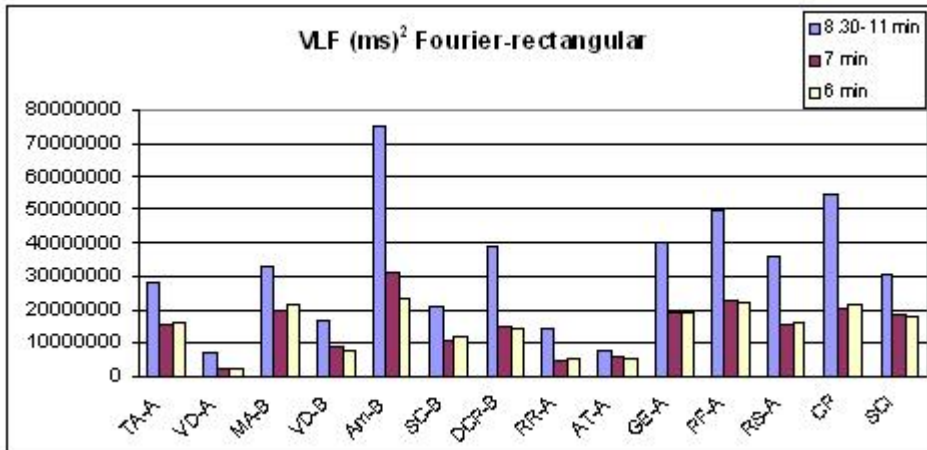


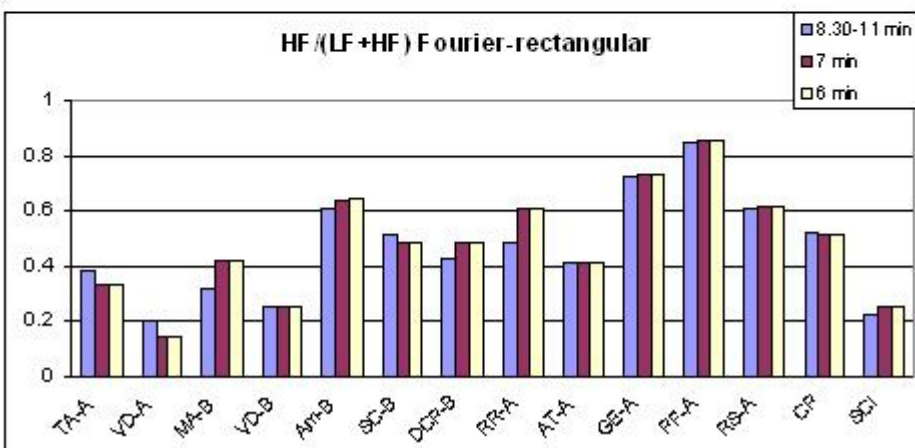
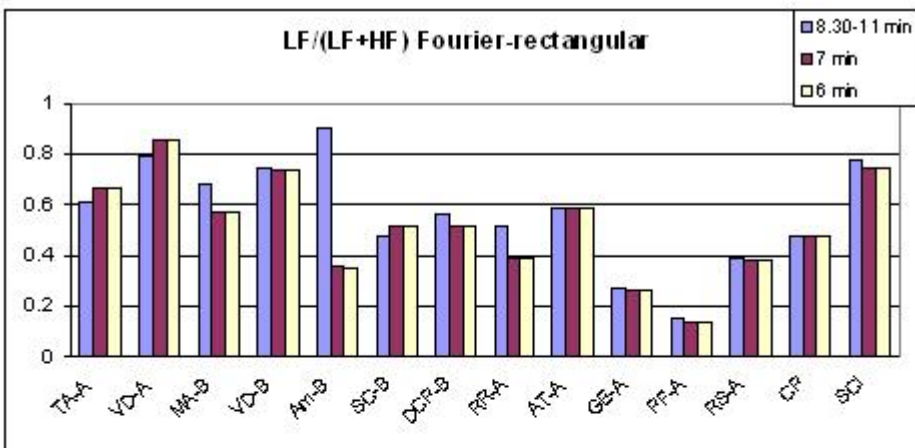
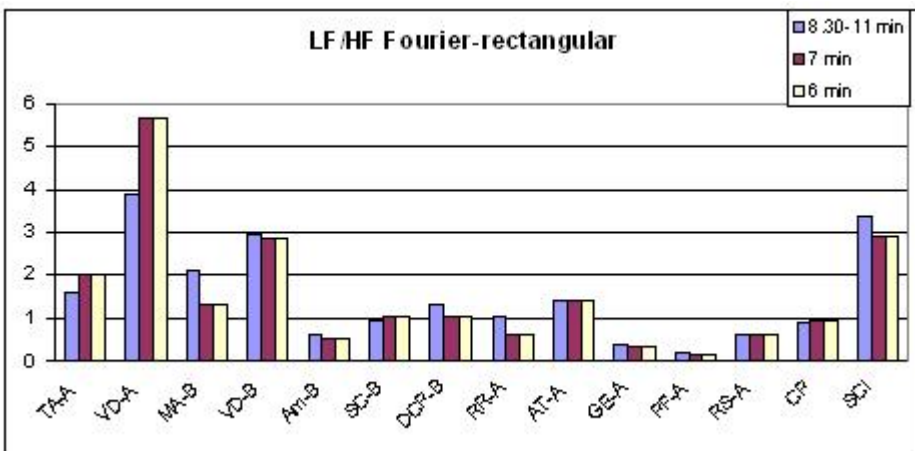
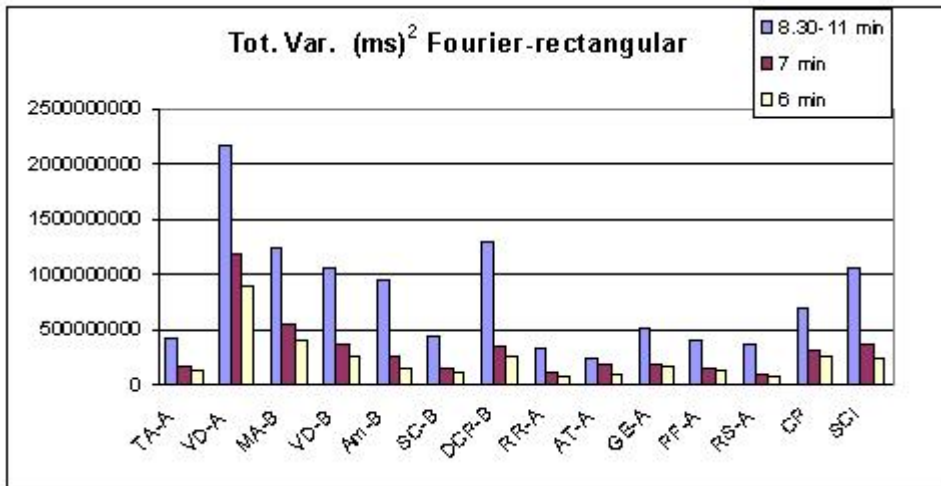


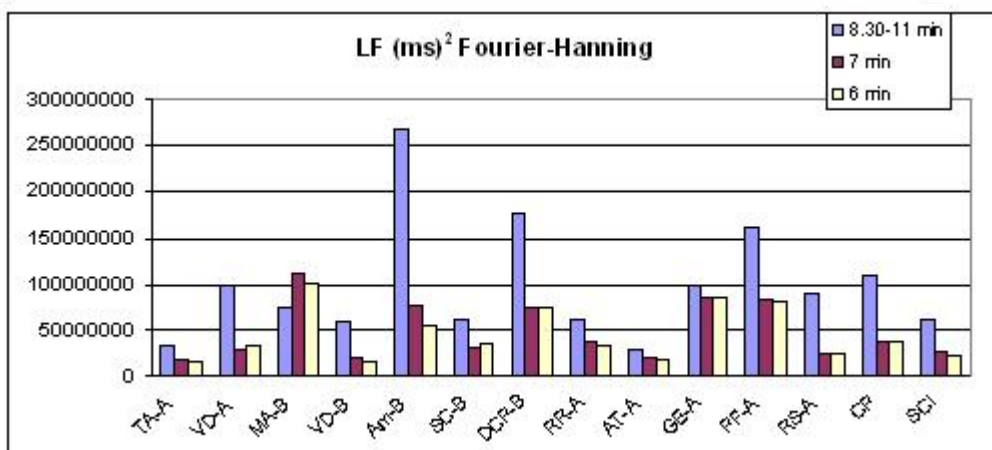
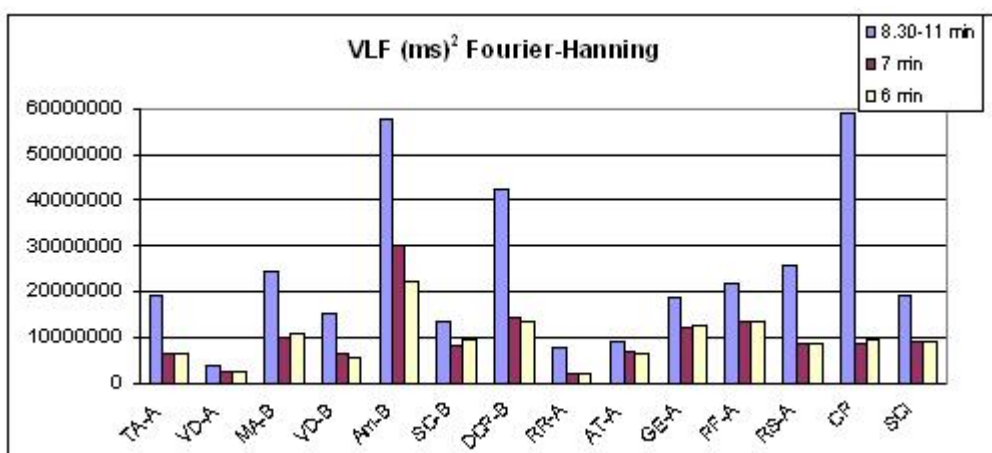


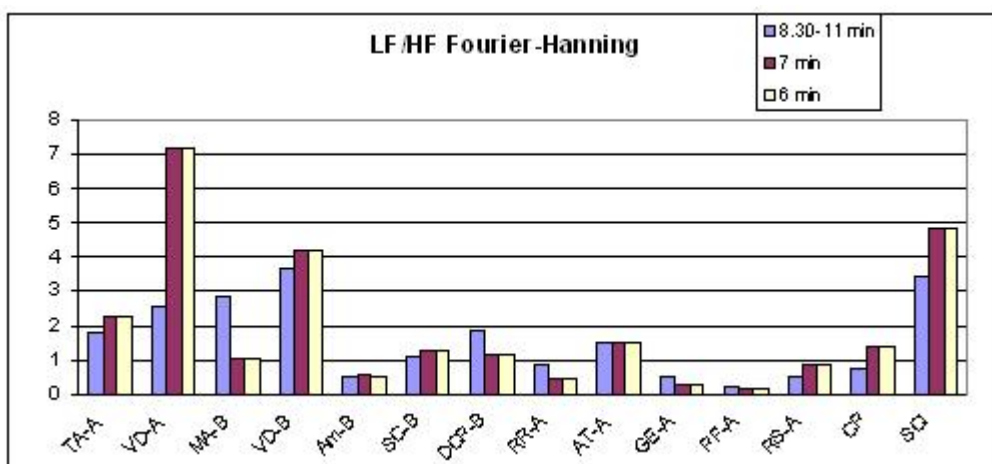
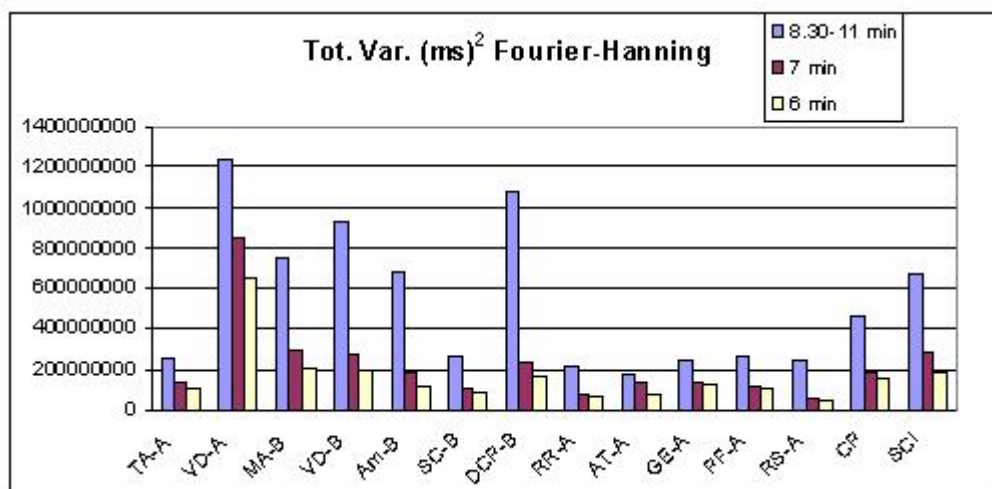
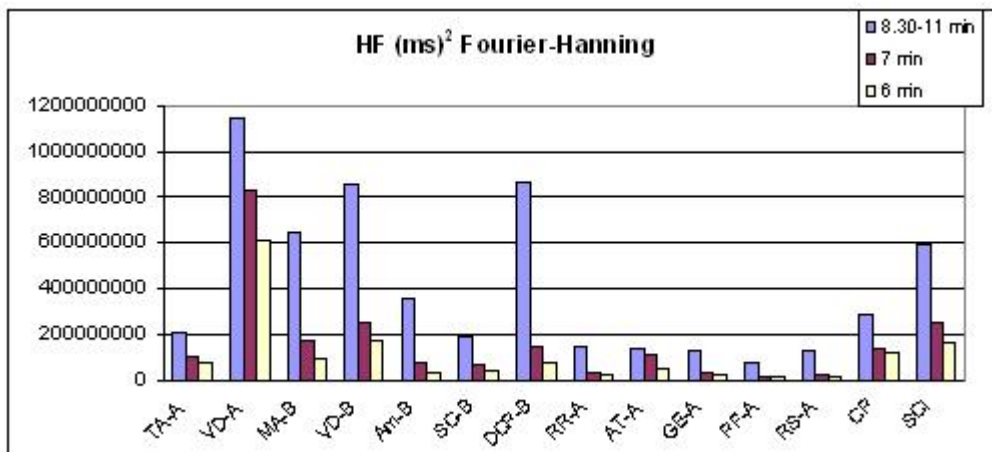


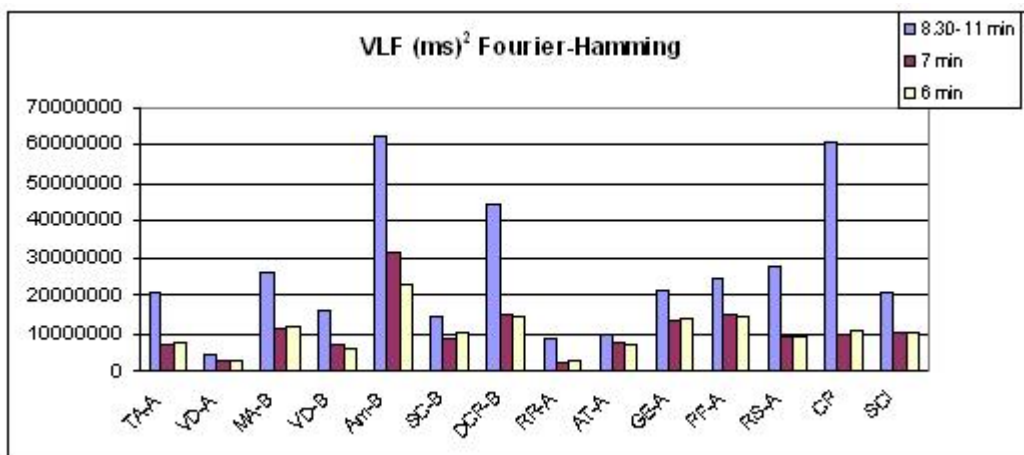
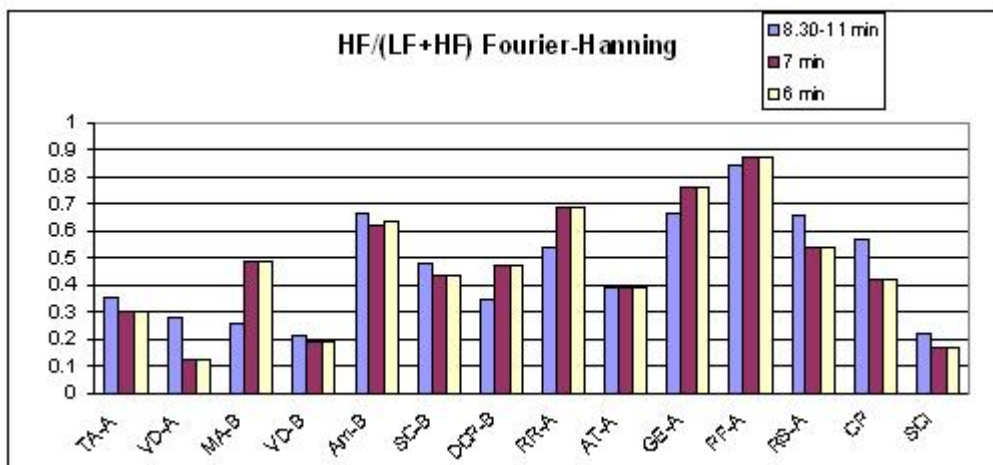
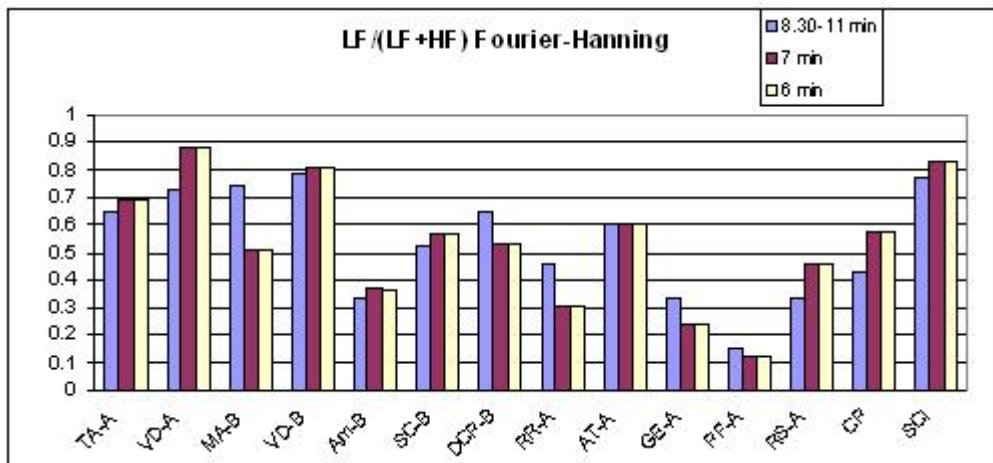
Figures 19

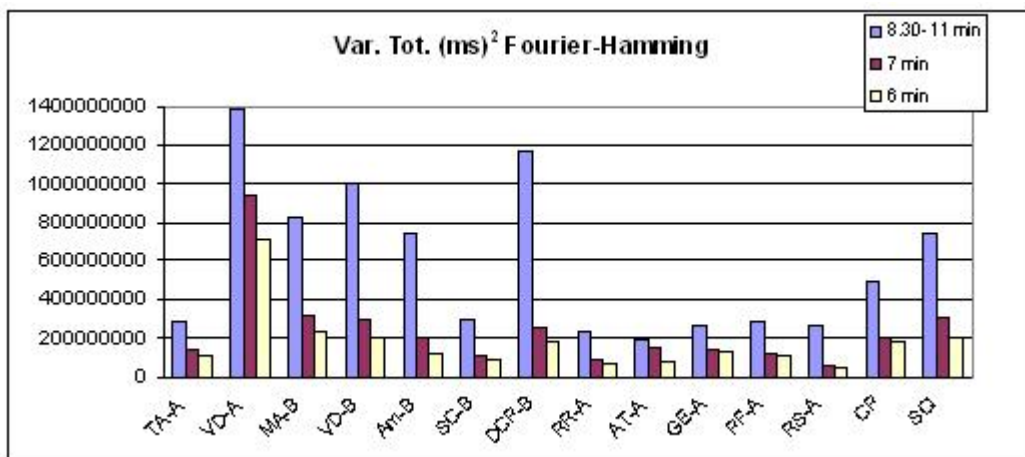
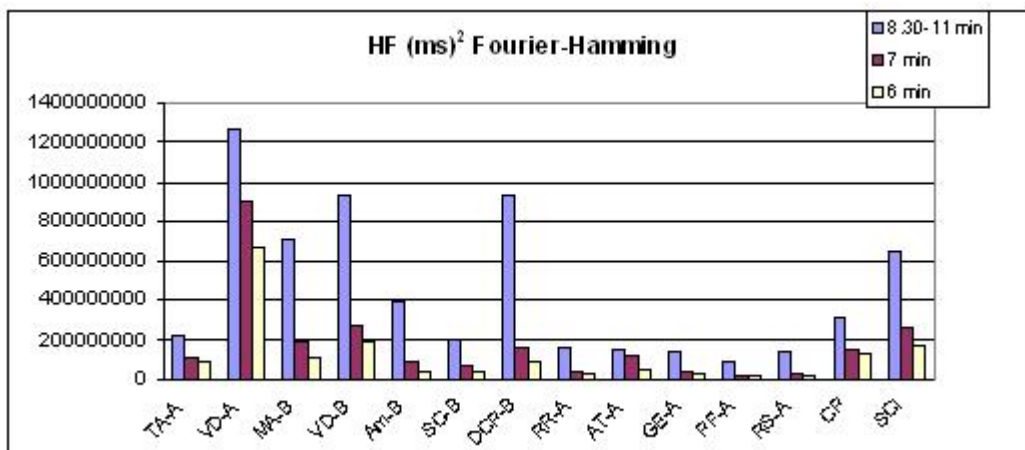
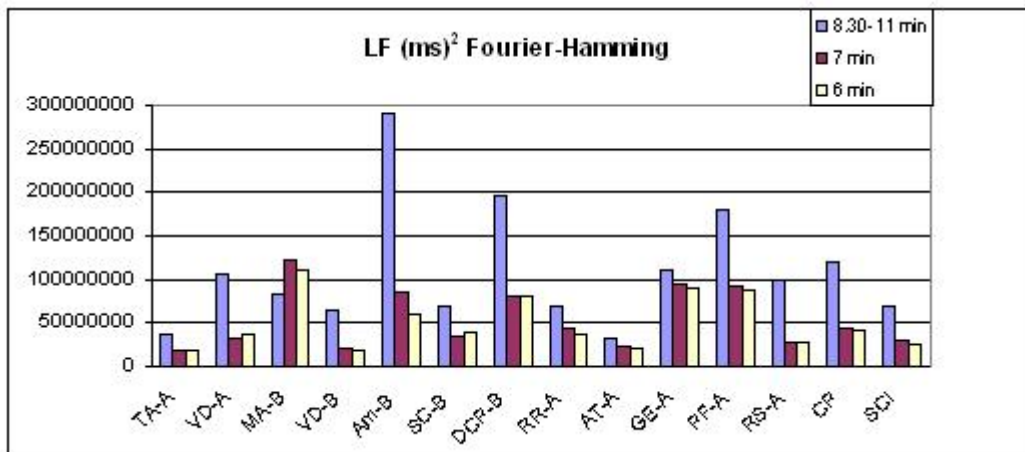


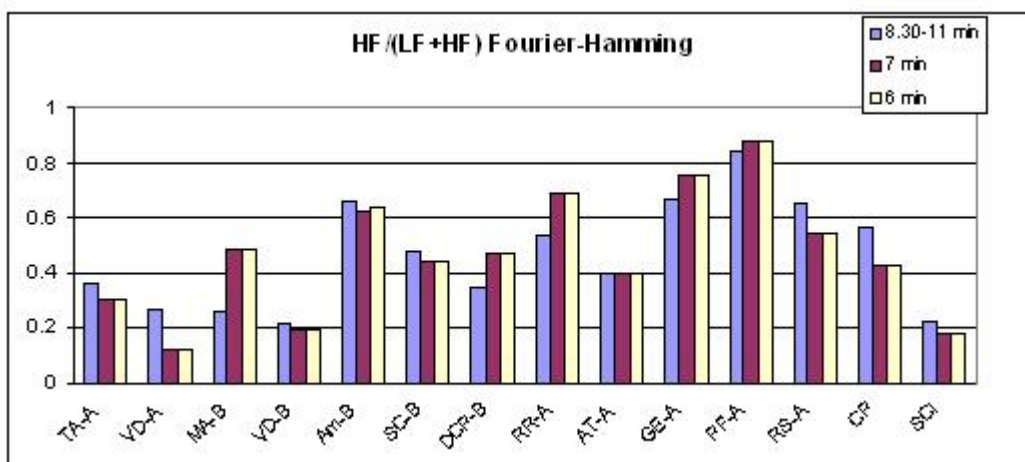
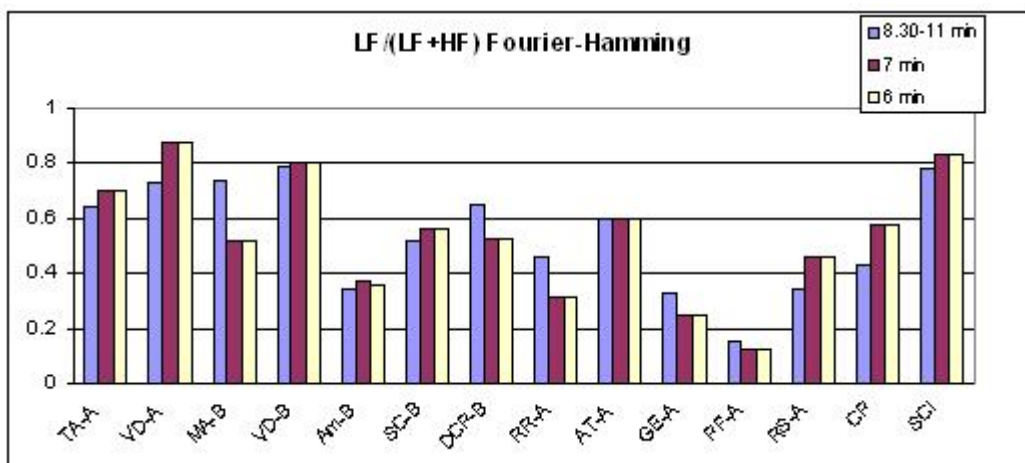
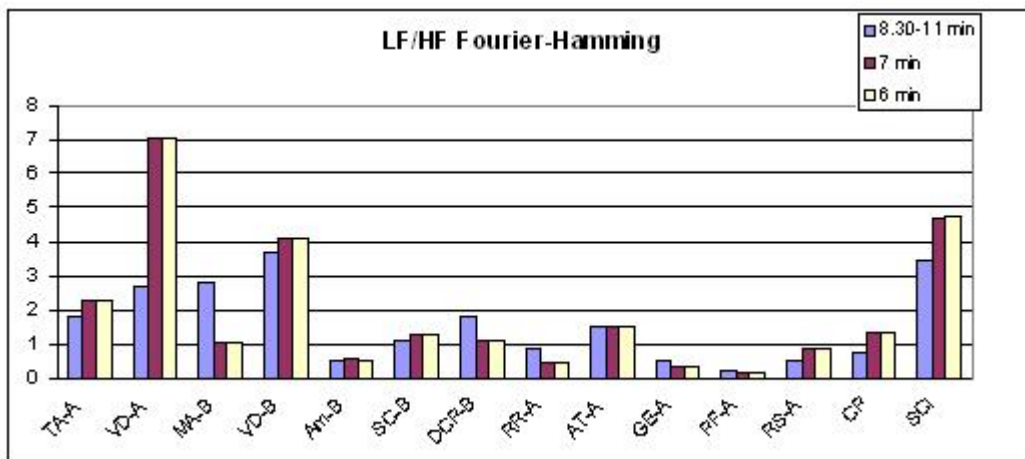


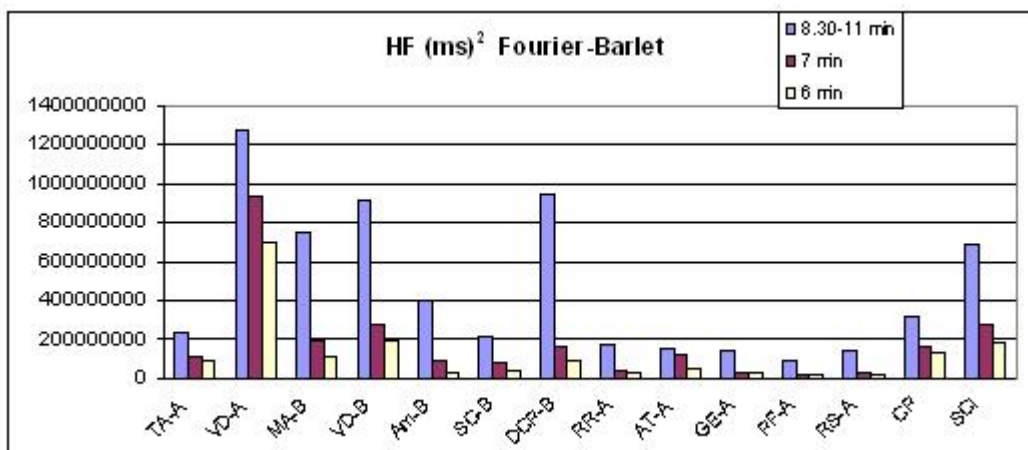
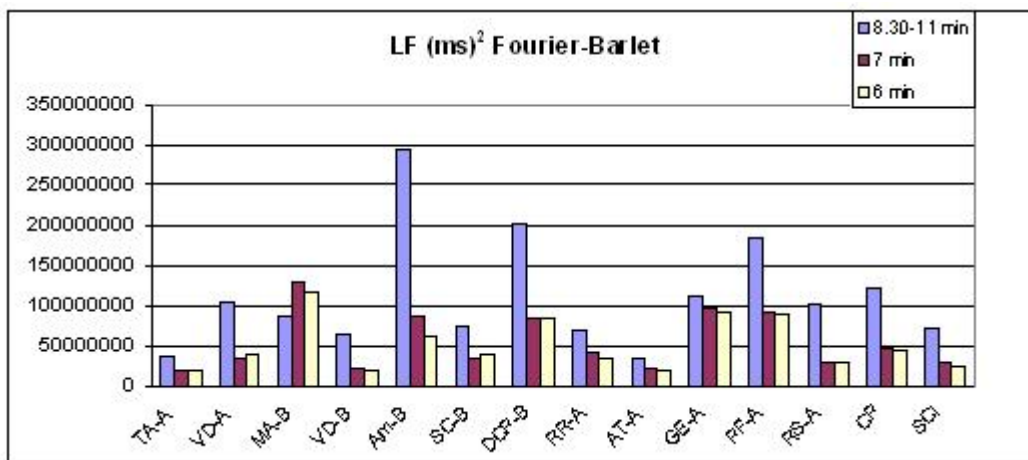
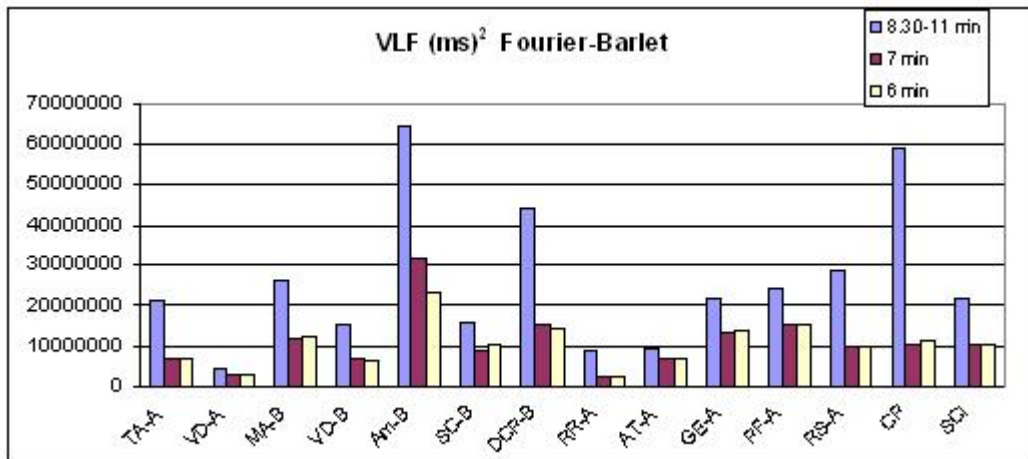


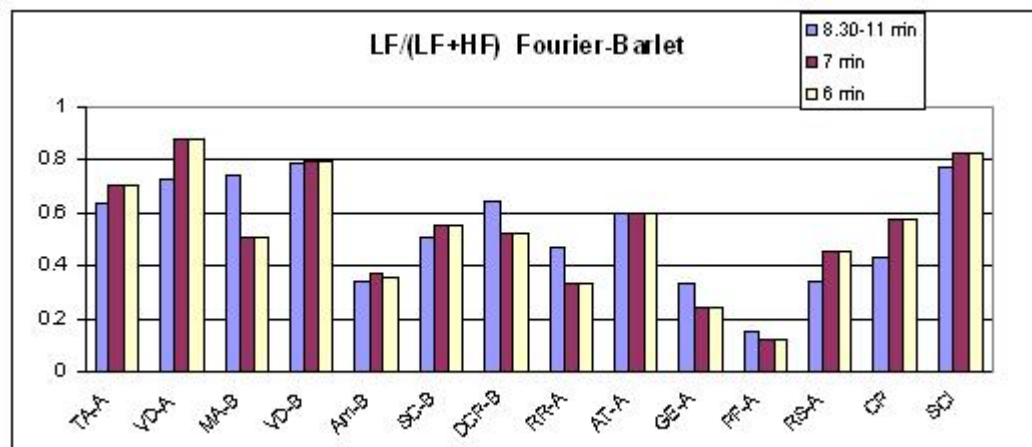
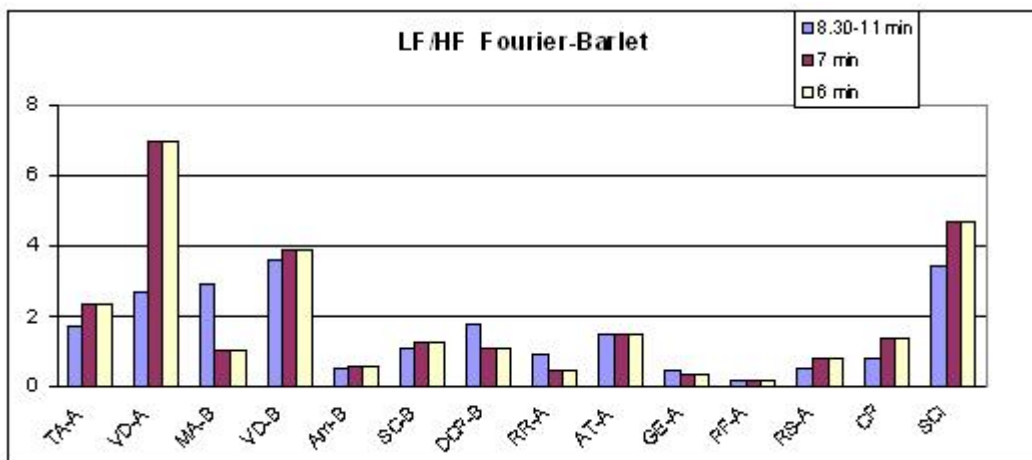
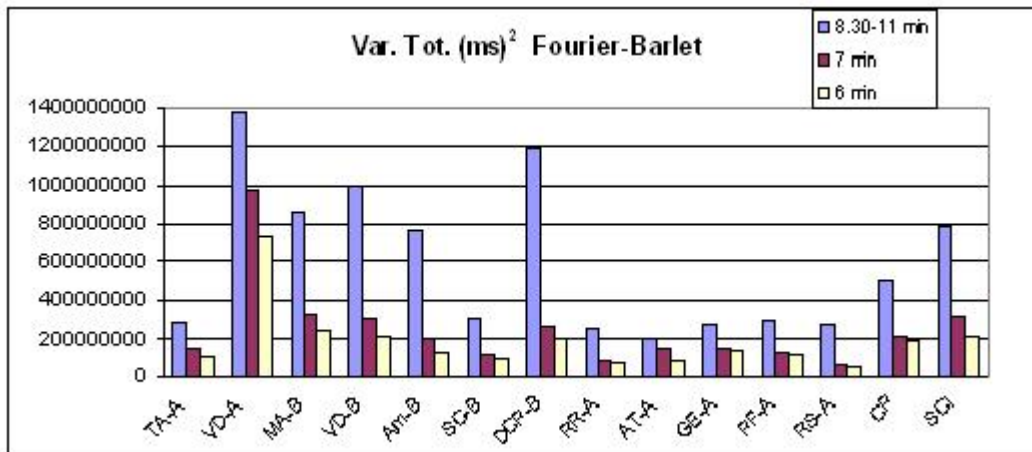


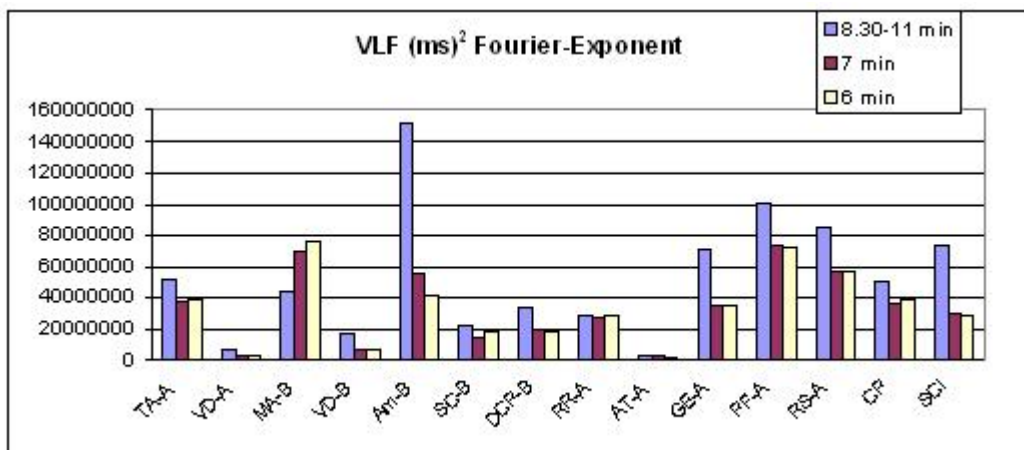
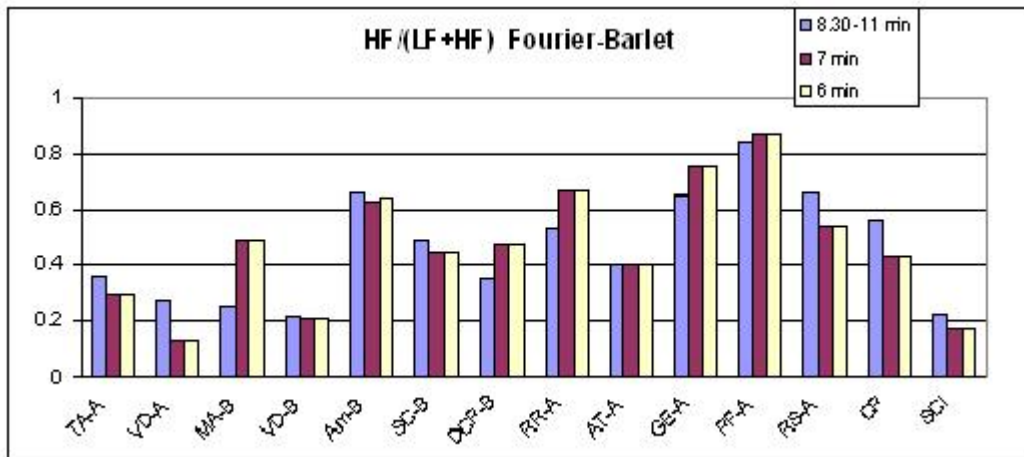


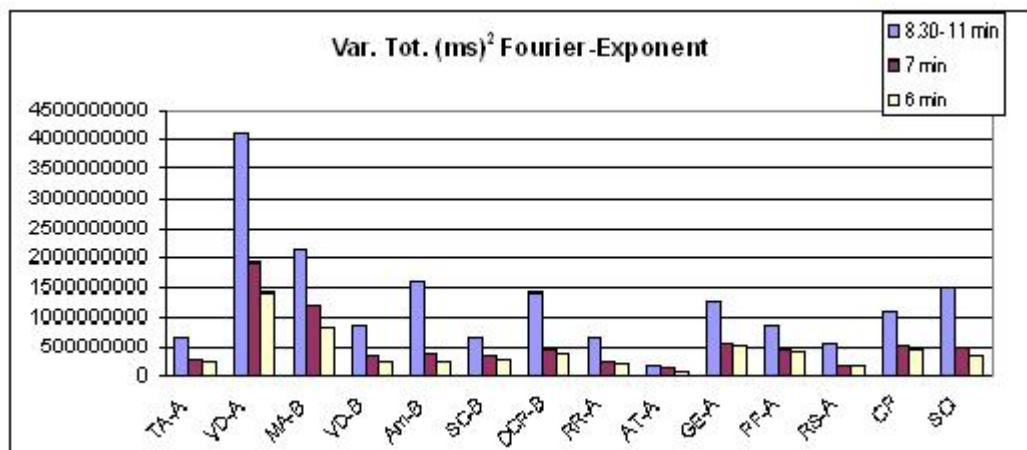
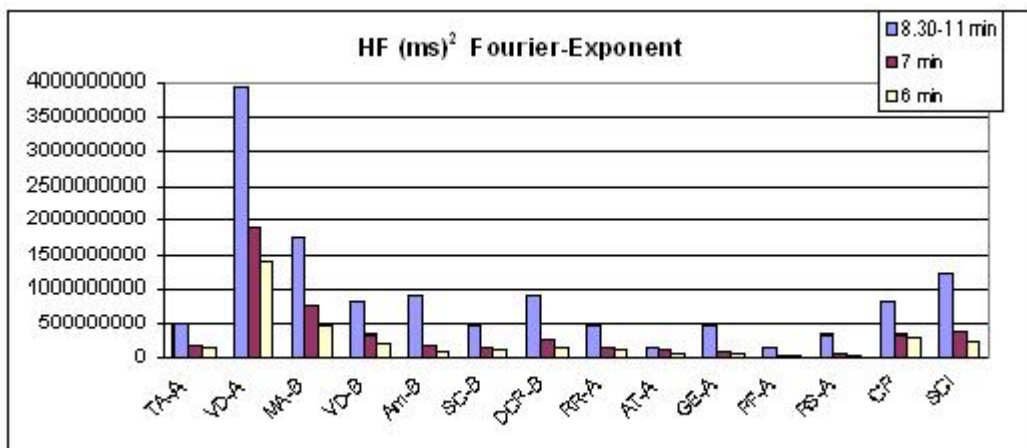
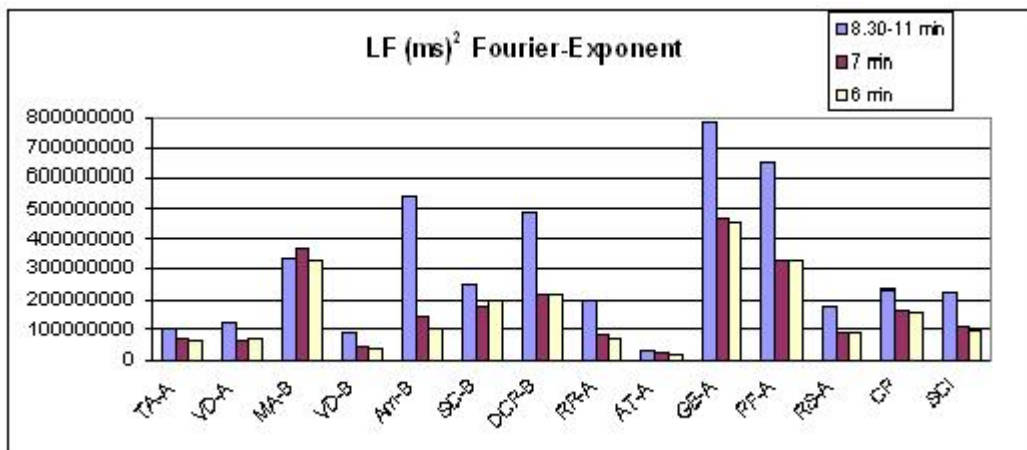












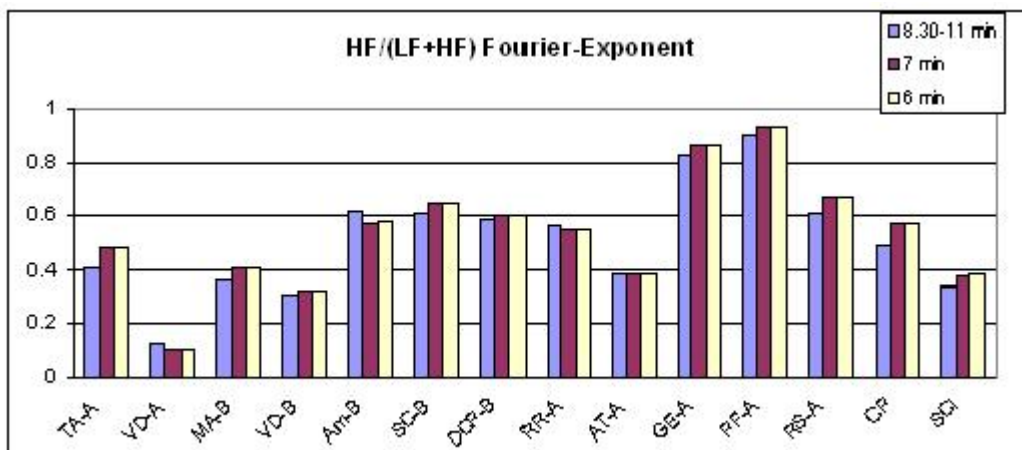
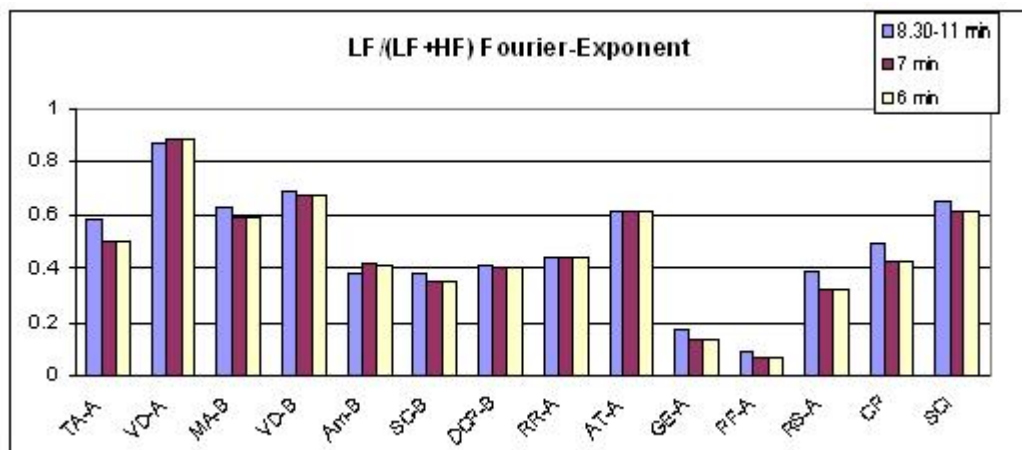
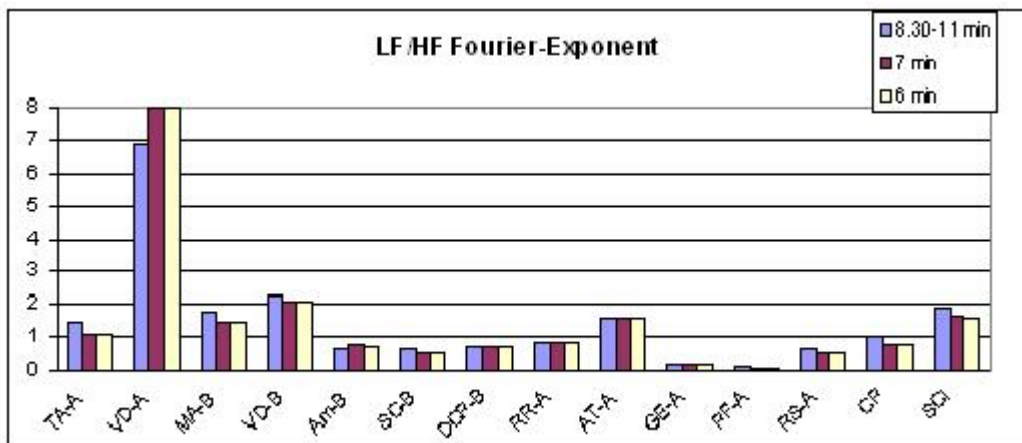


Figure 21

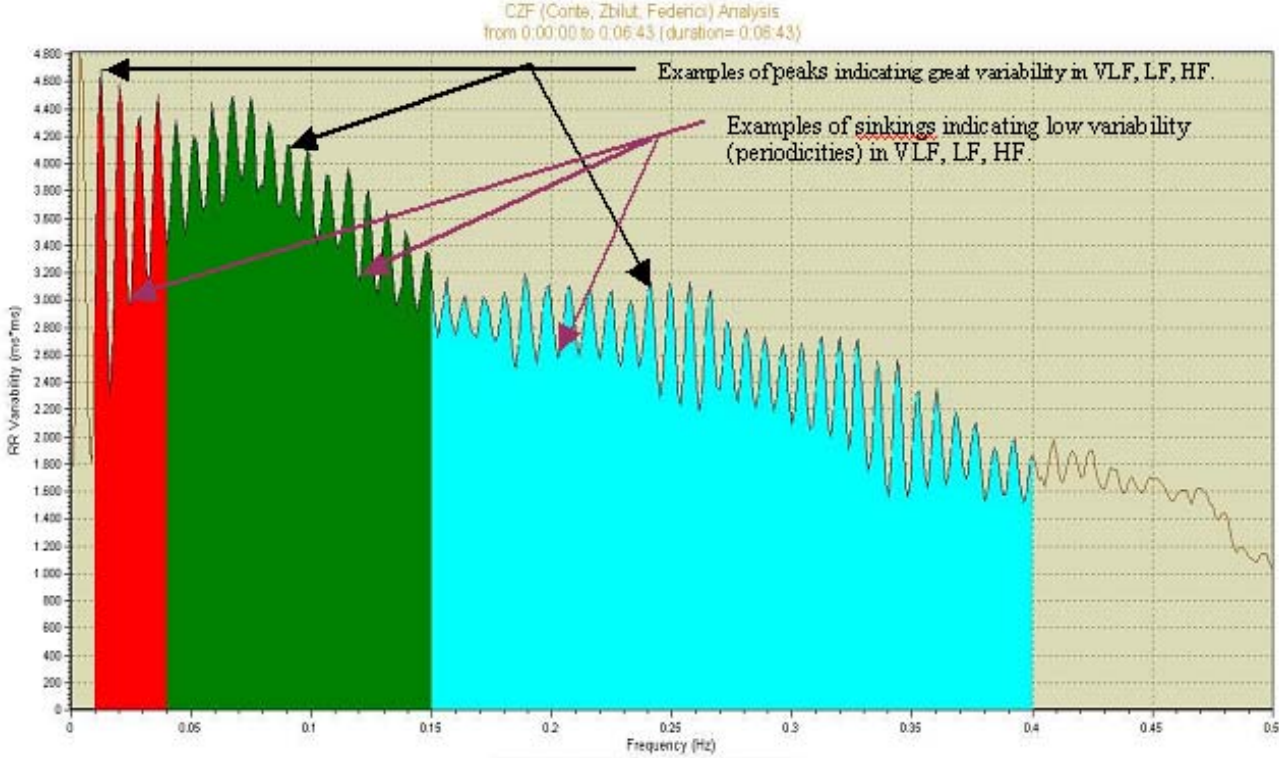


Figure 22

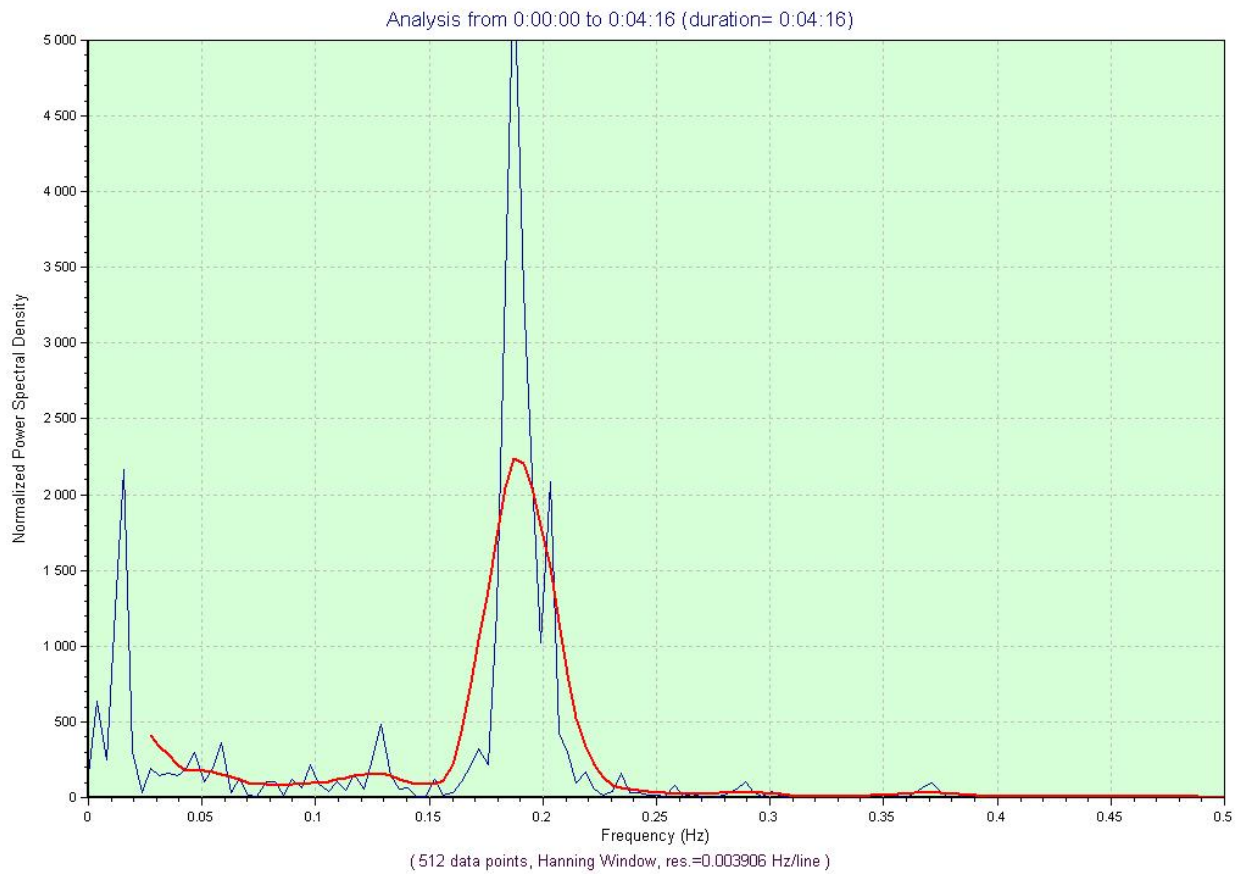
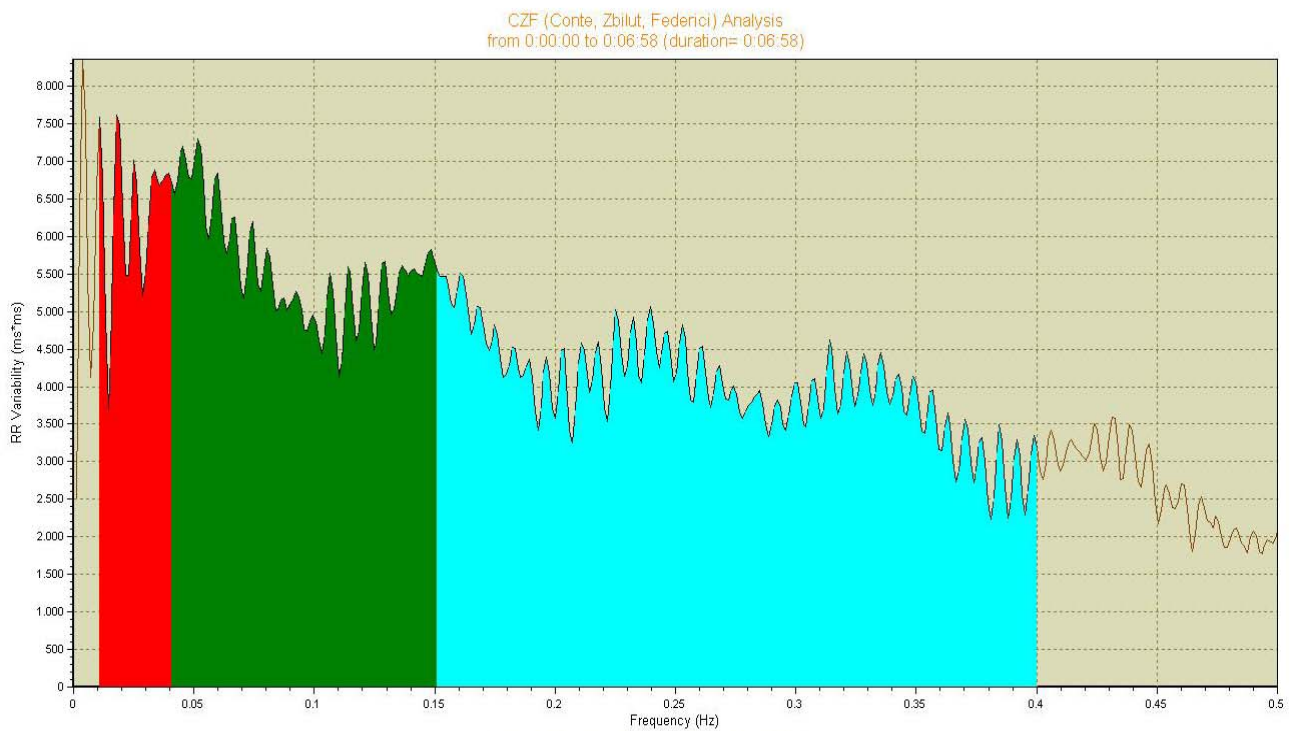
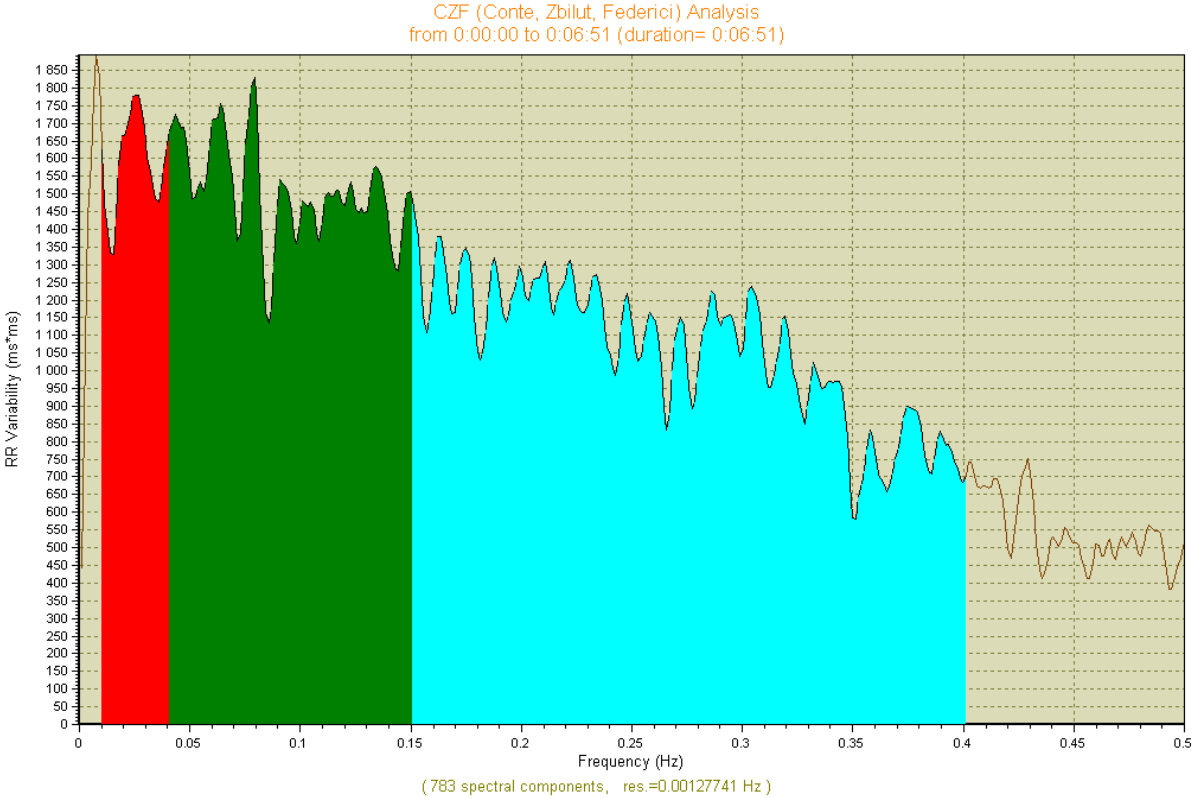


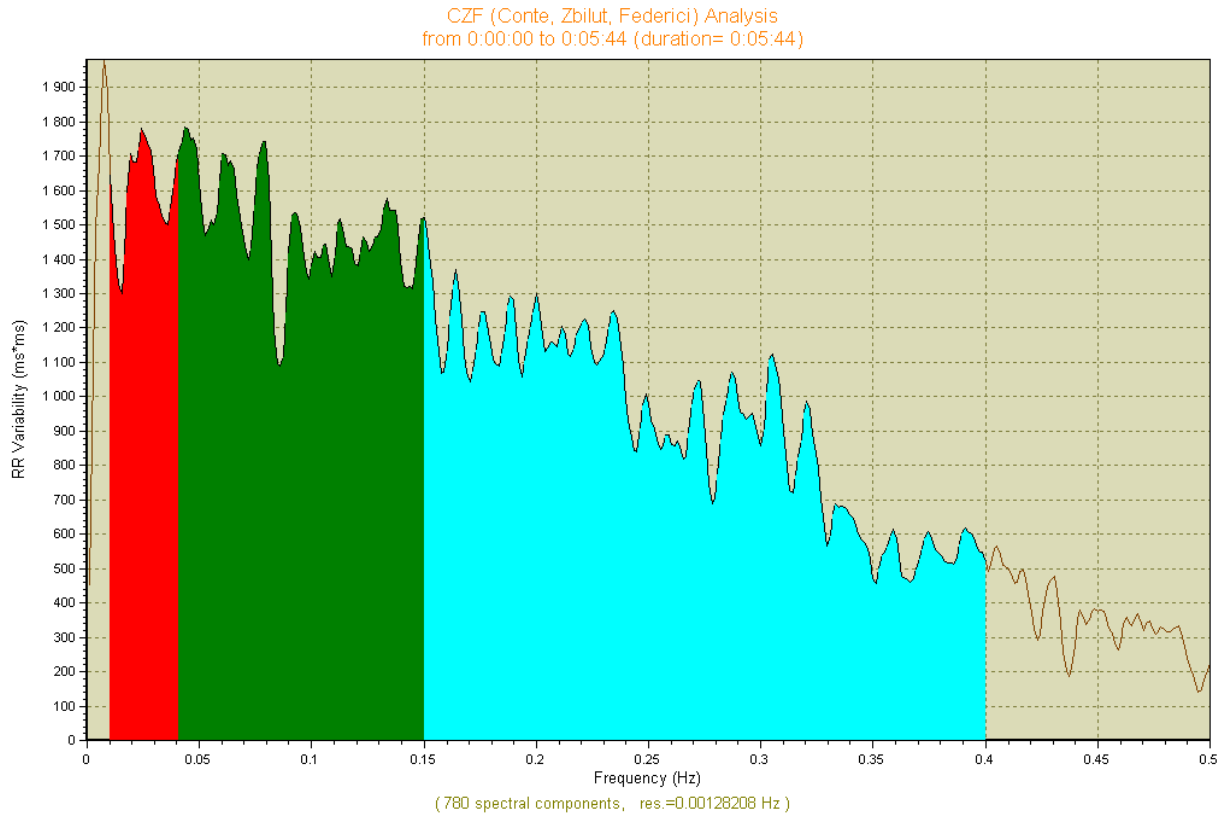
Figure 23



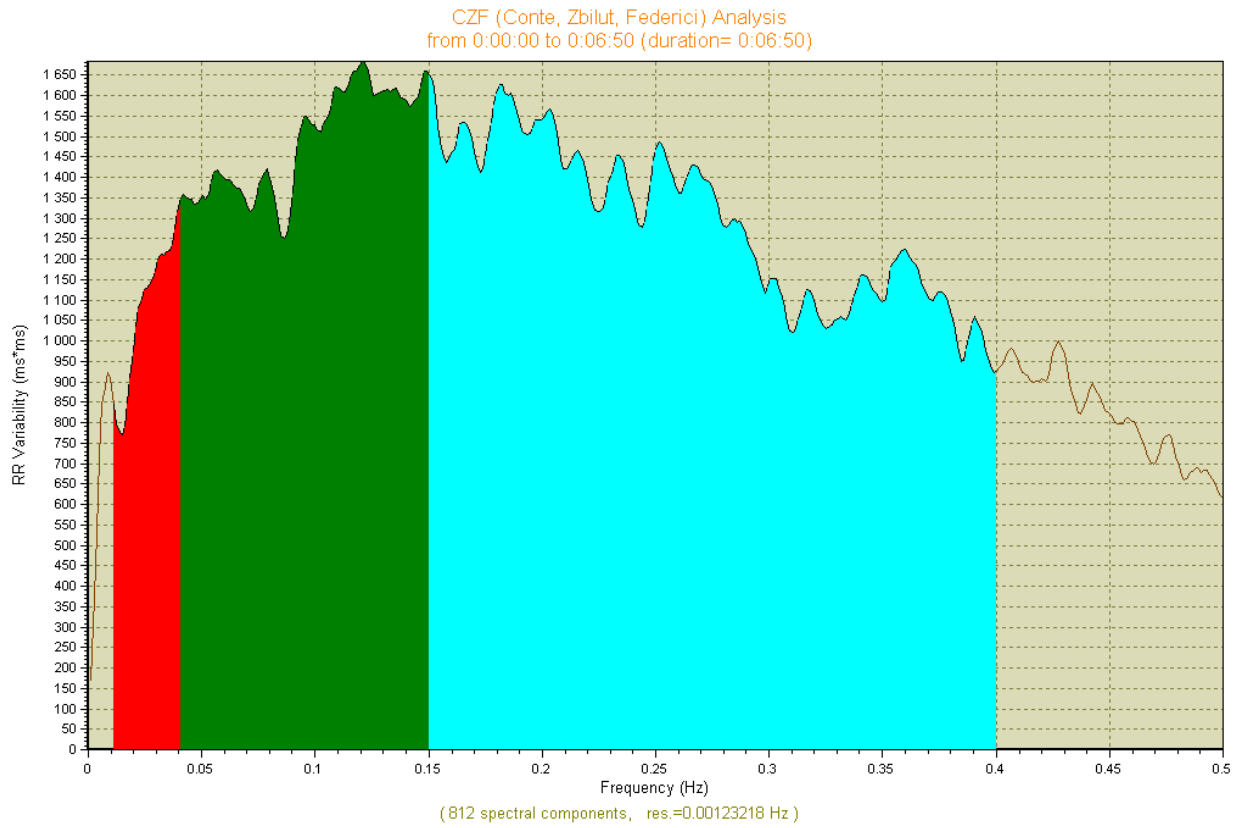
Figures 24
TA 7



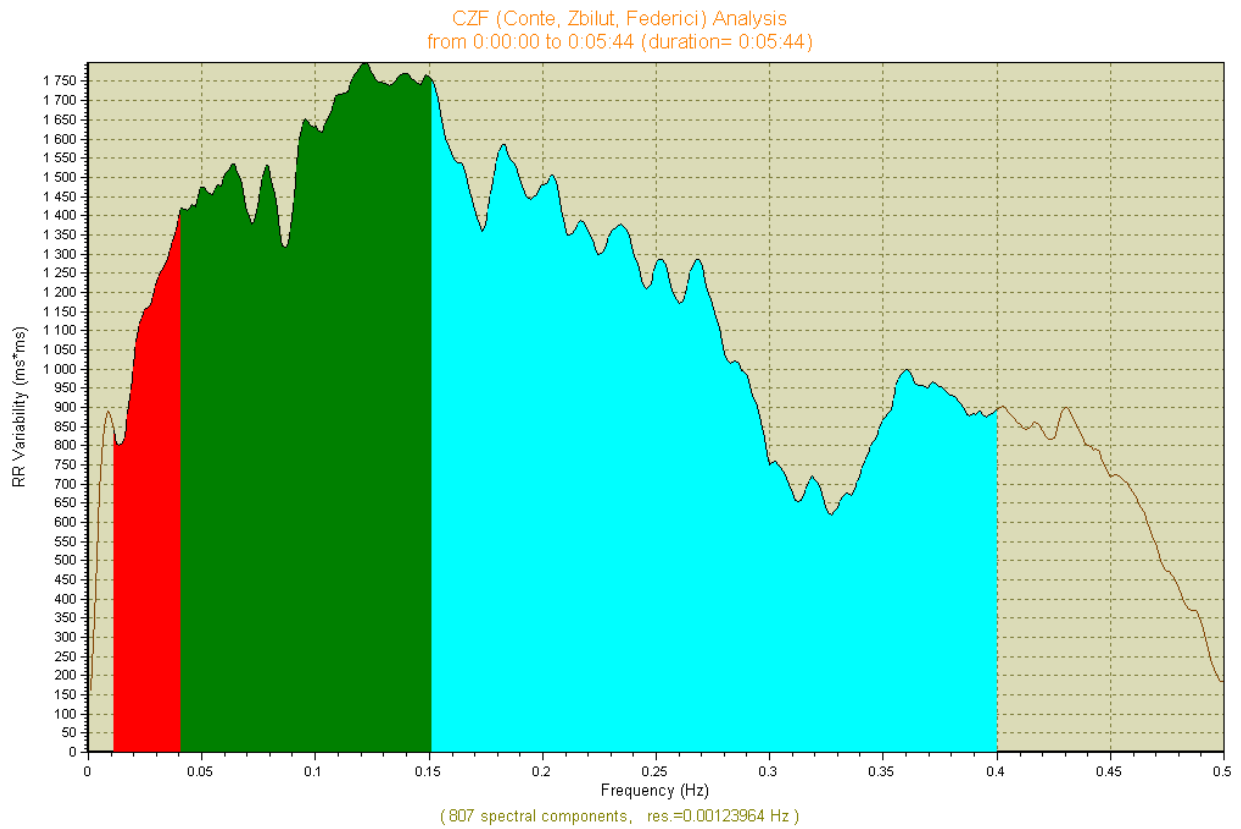
TA 6



VD-A 7

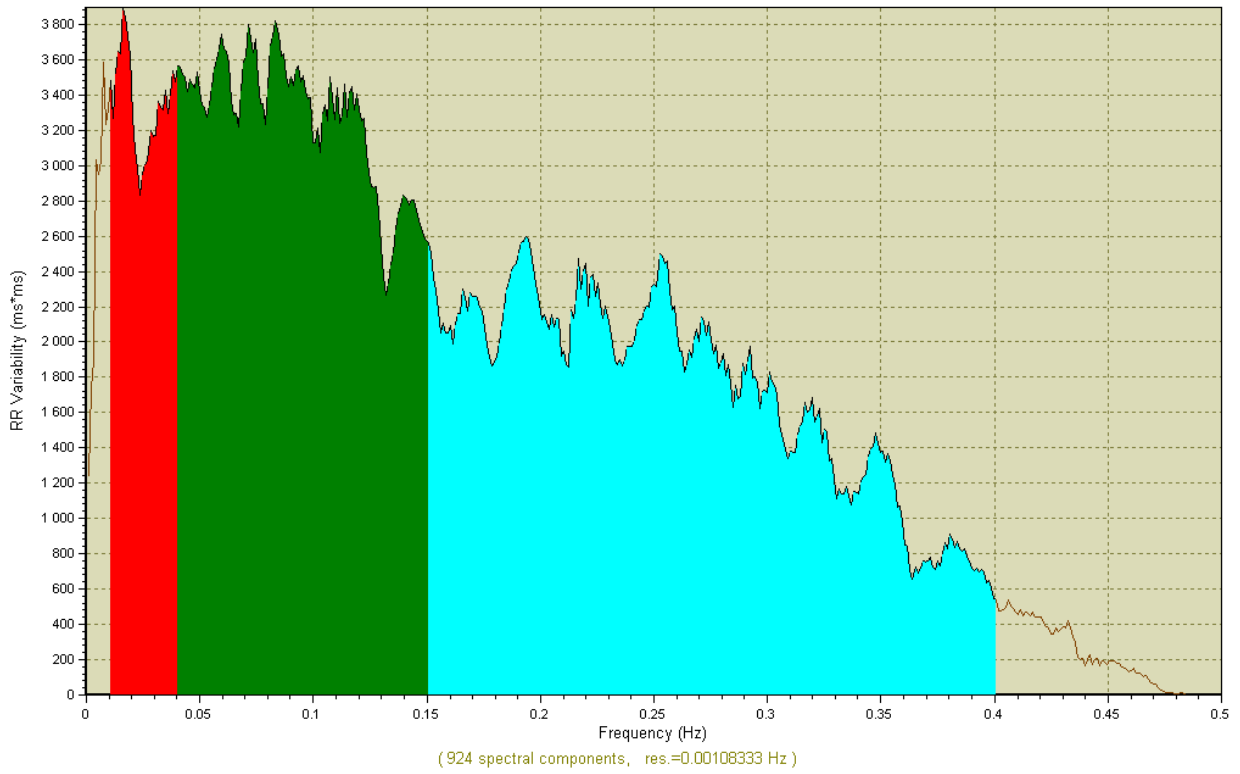


VD-A 6



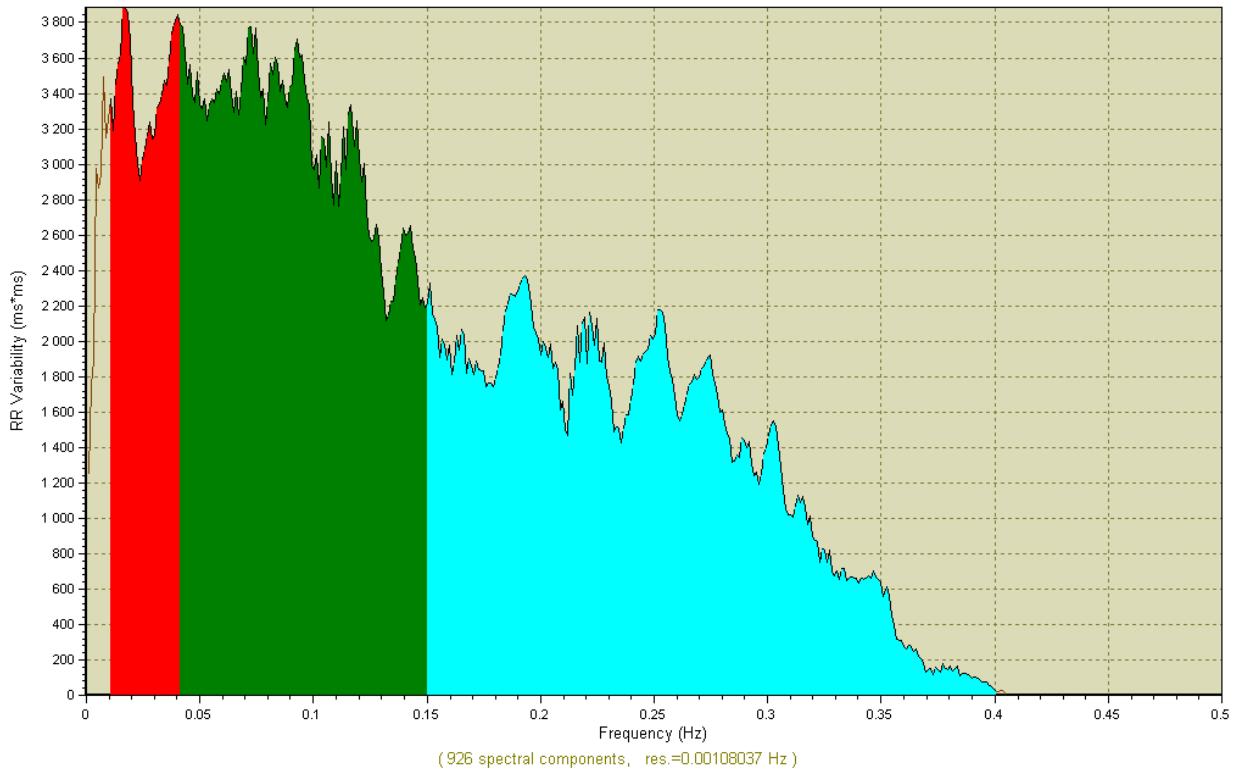
MA 7

CZF (Conte, Zbilut, Federici) Analysis
from 0:00:00 to 0:06:51 (duration= 0:06:51)

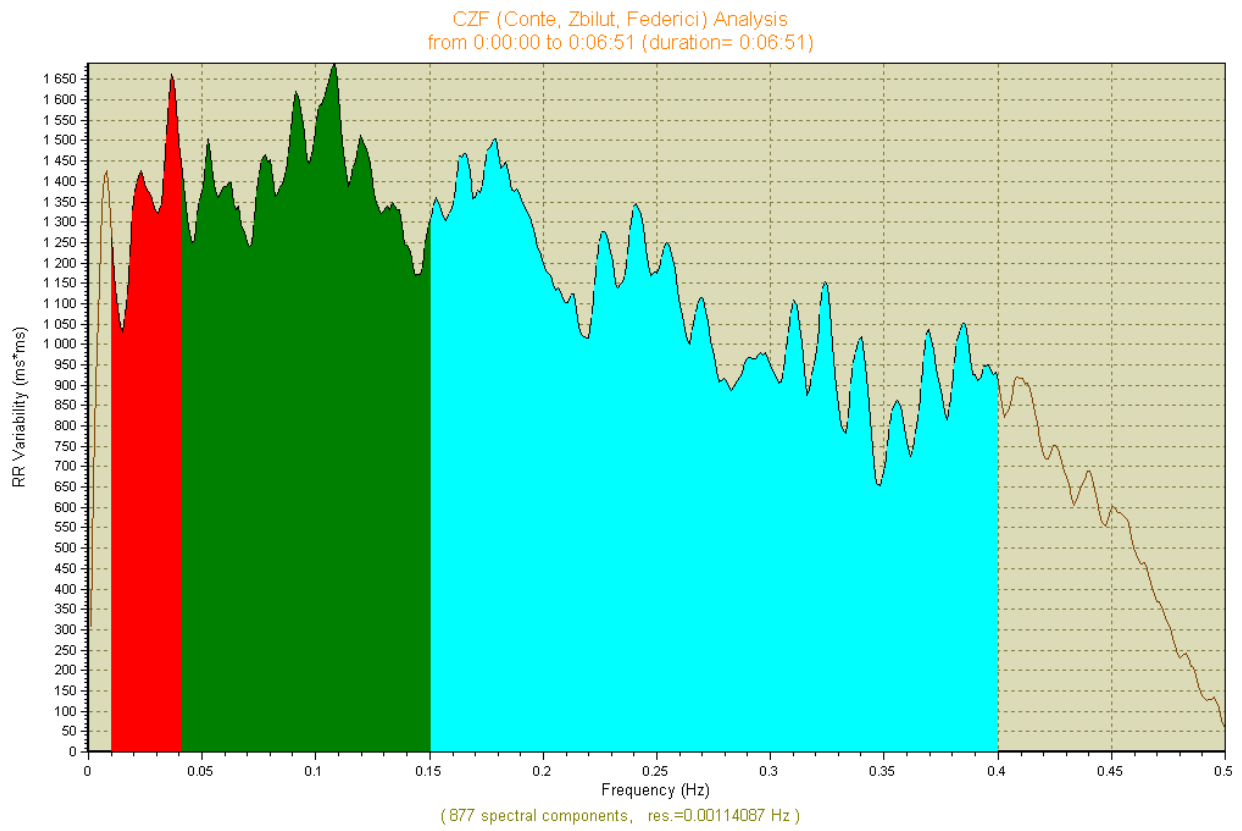


MA 6

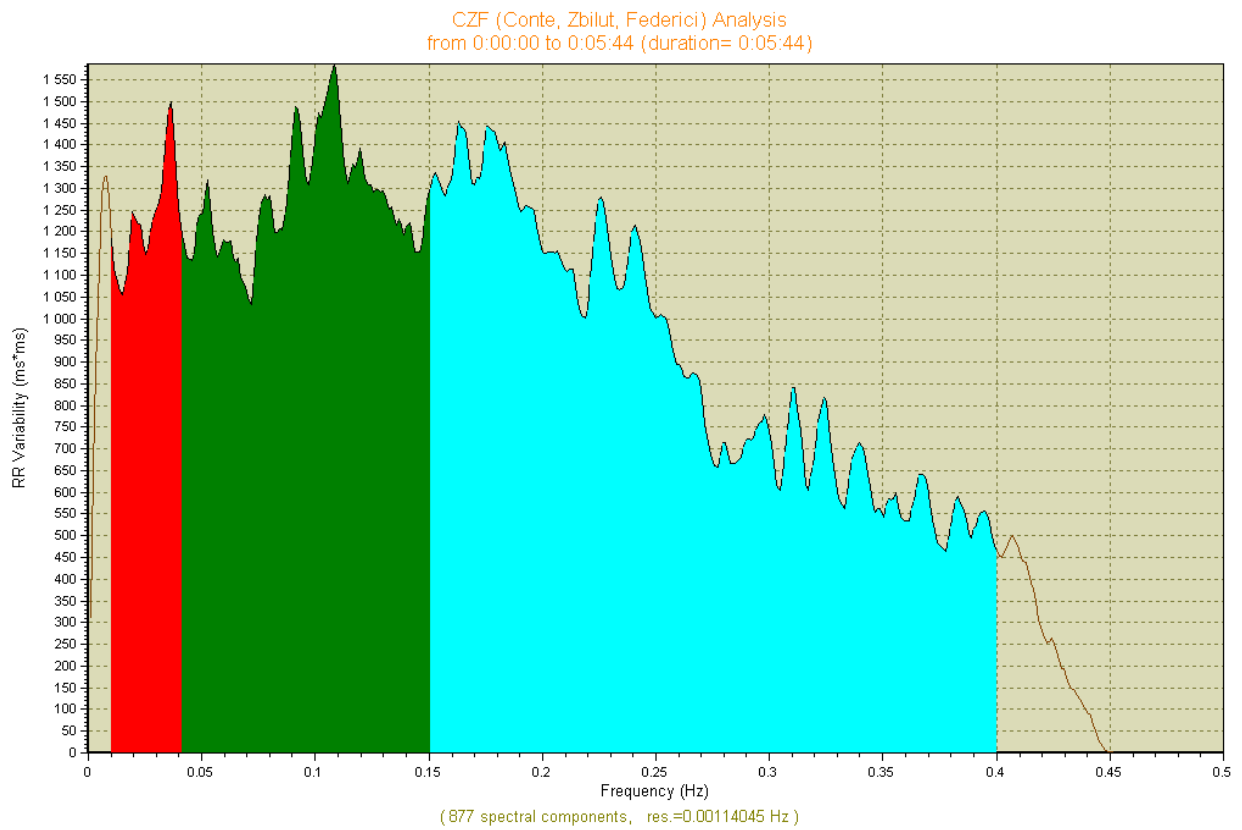
CZF (Conte, Zbilut, Federici) Analysis
from 0:00:00 to 0:05:44 (duration= 0:05:44)



VD-B 7

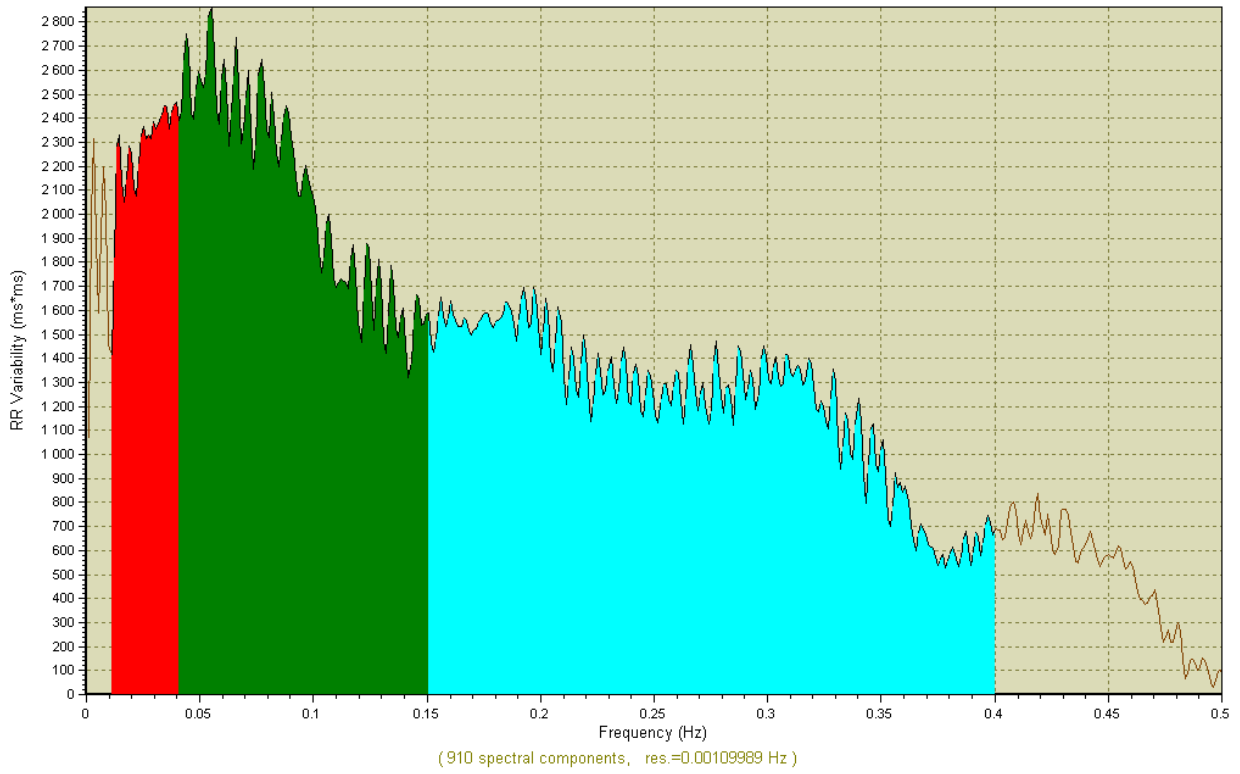


VD-B 6



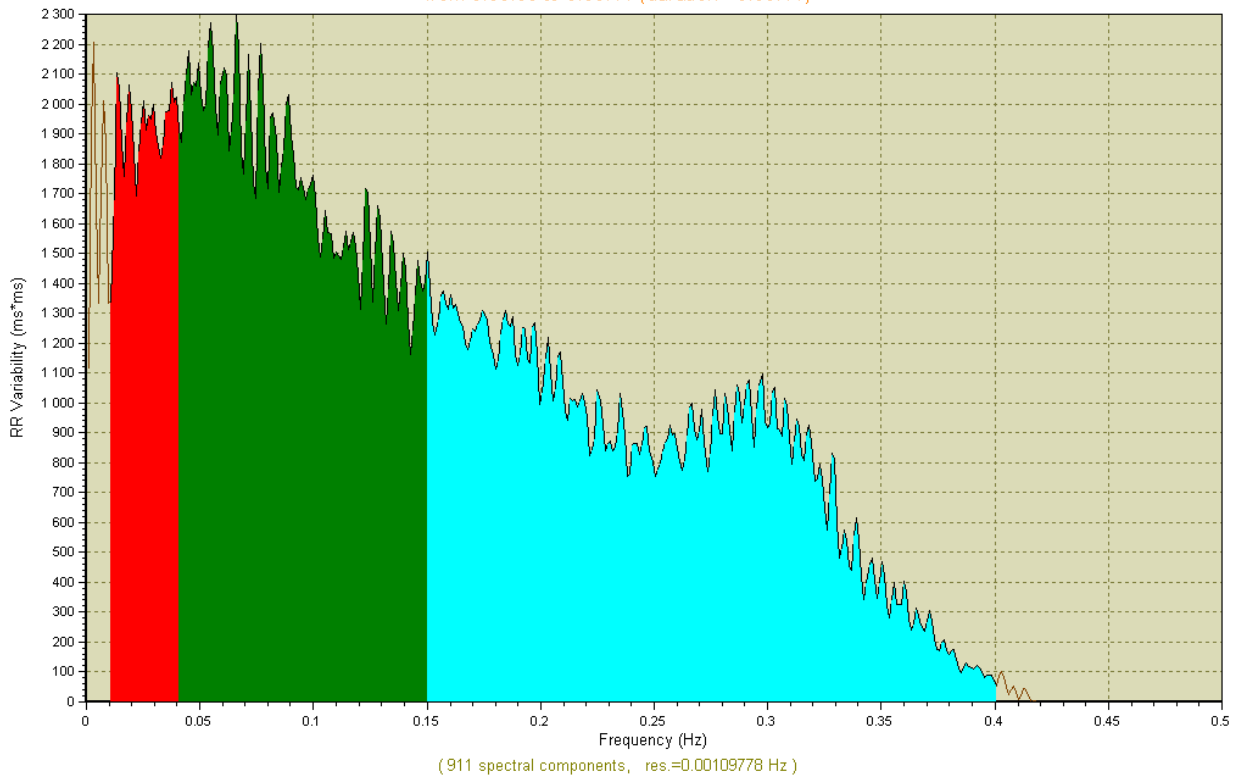
AM 7

CZF (Conte, Zbilut, Federici) Analysis
from 0:00:00 to 0:07:04 (duration= 0:07:04)



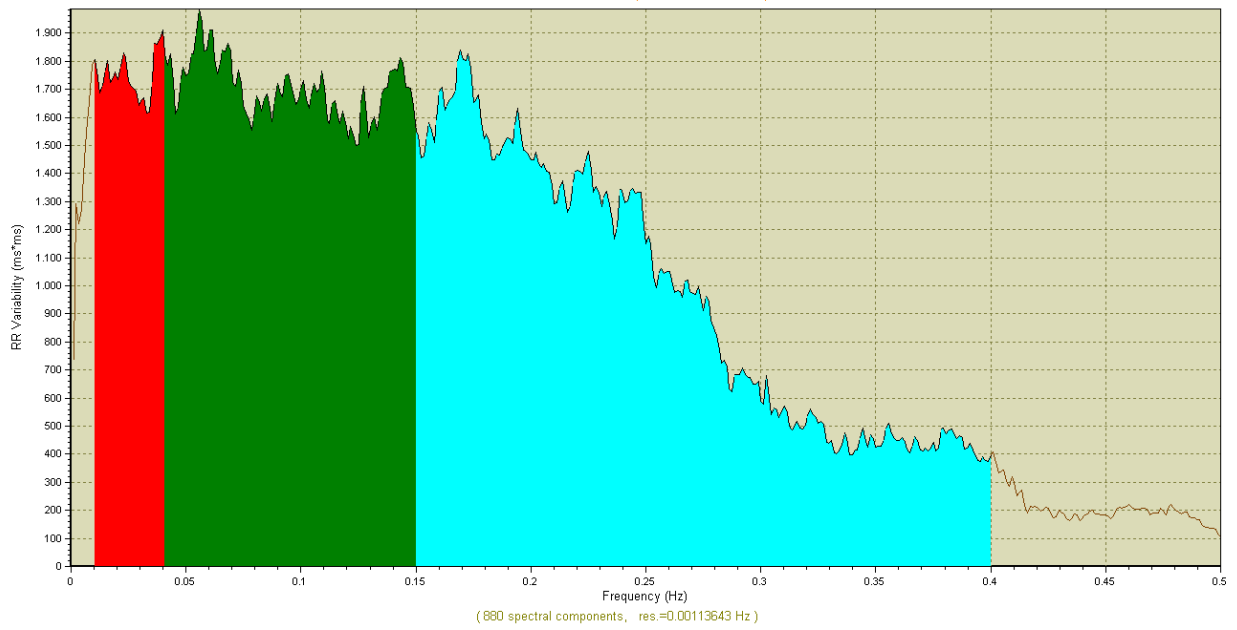
AM 6

CZF (Conte, Zbilut, Federici) Analysis
from 0:00:00 to 0:05:44 (duration= 0:05:44)

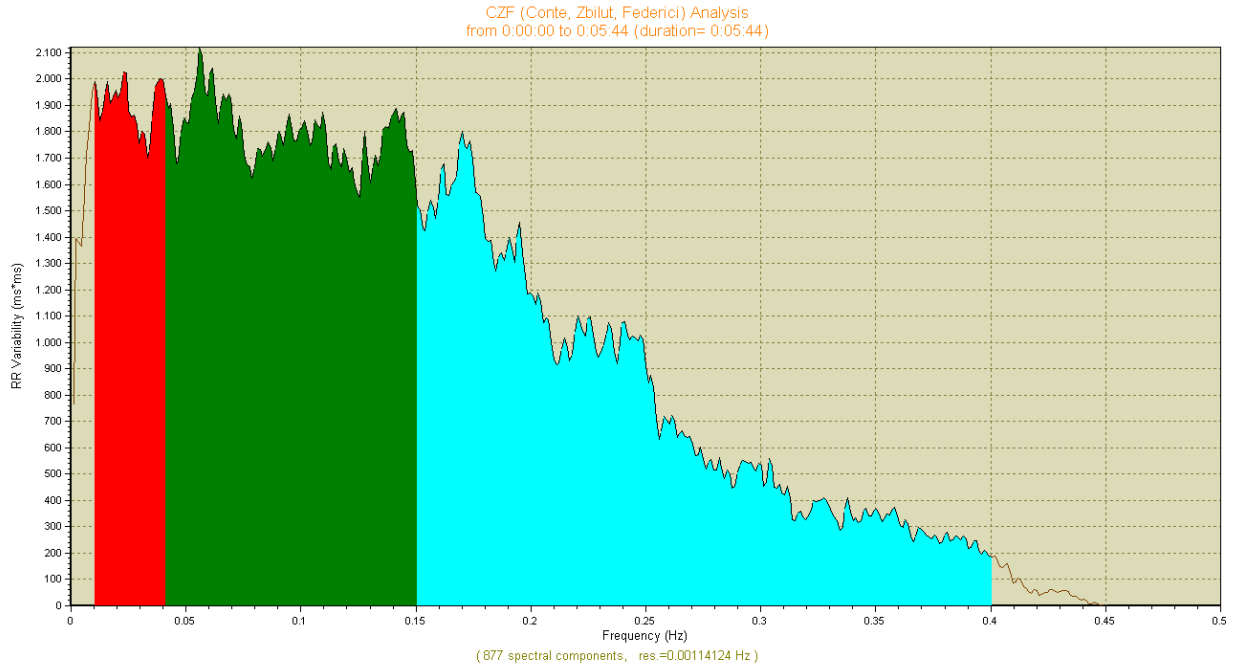


SC 7

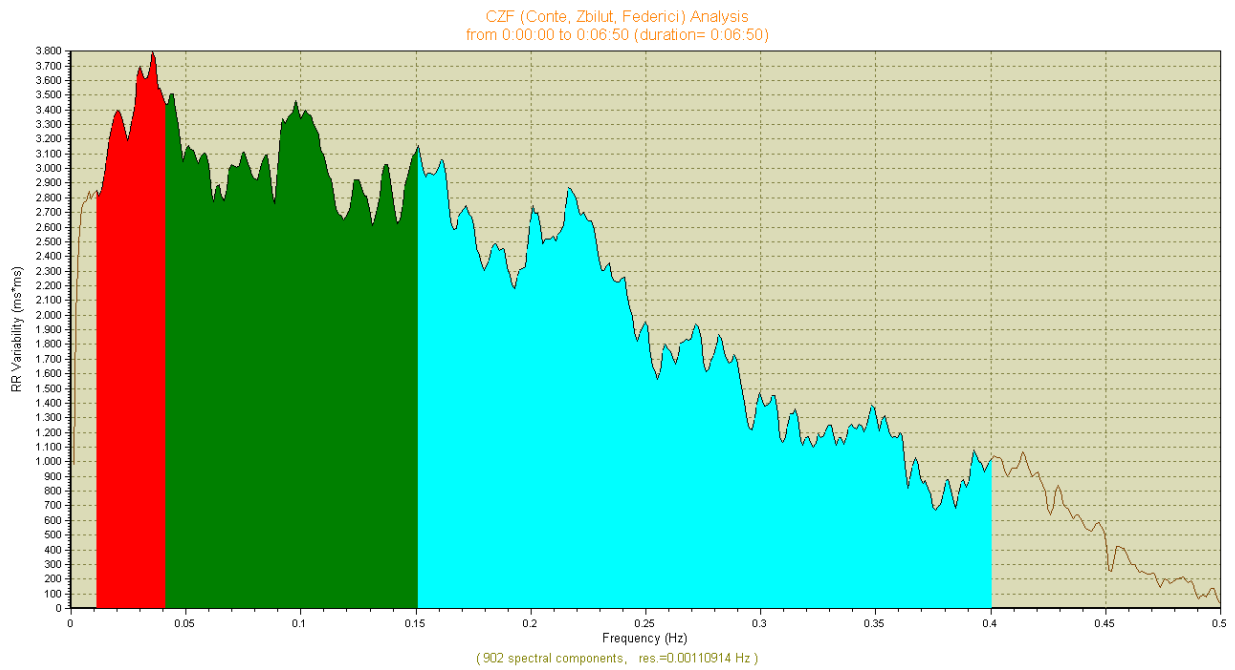
CZF (Conte, Zbilut, Federici) Analysis
from 0:00:00 to 0:06:50 (duration= 0:06:50)



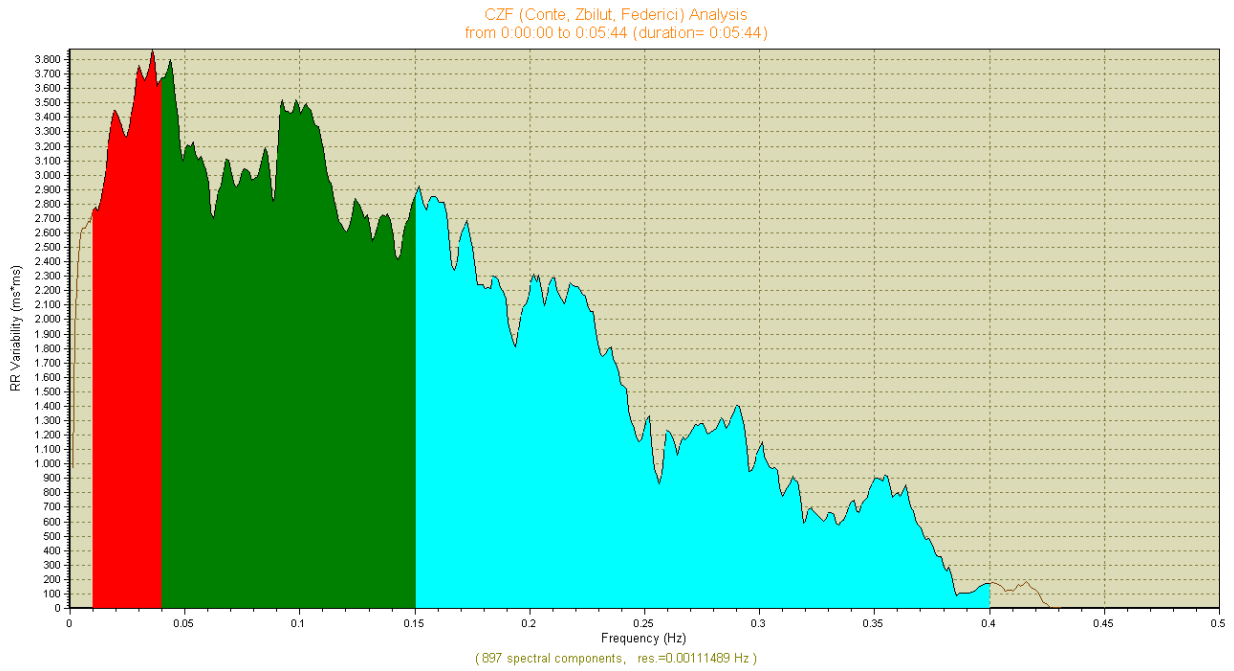
SC 6



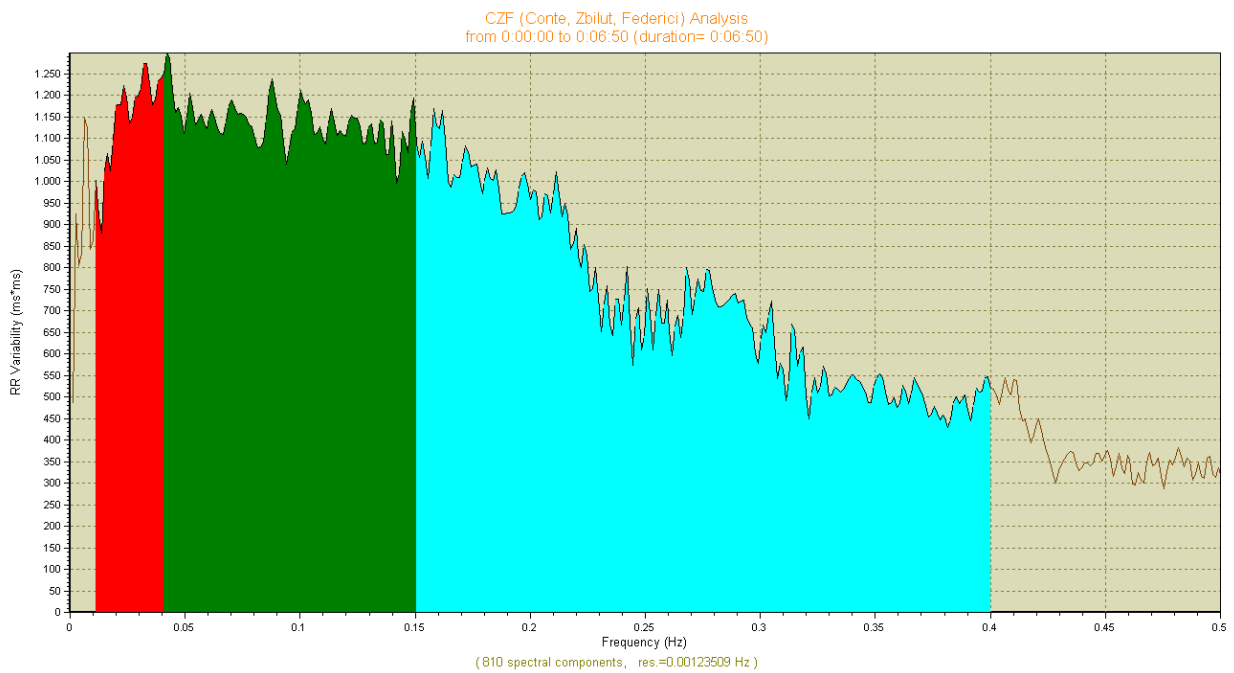
DCP 7



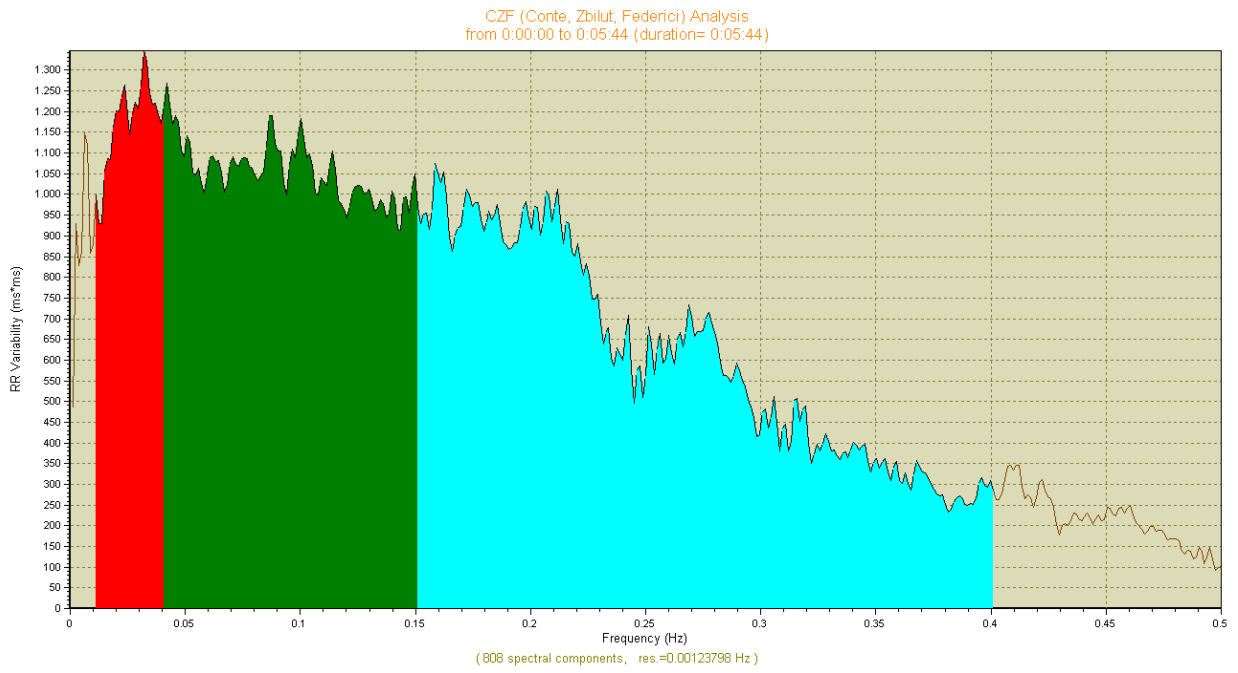
DCP 6



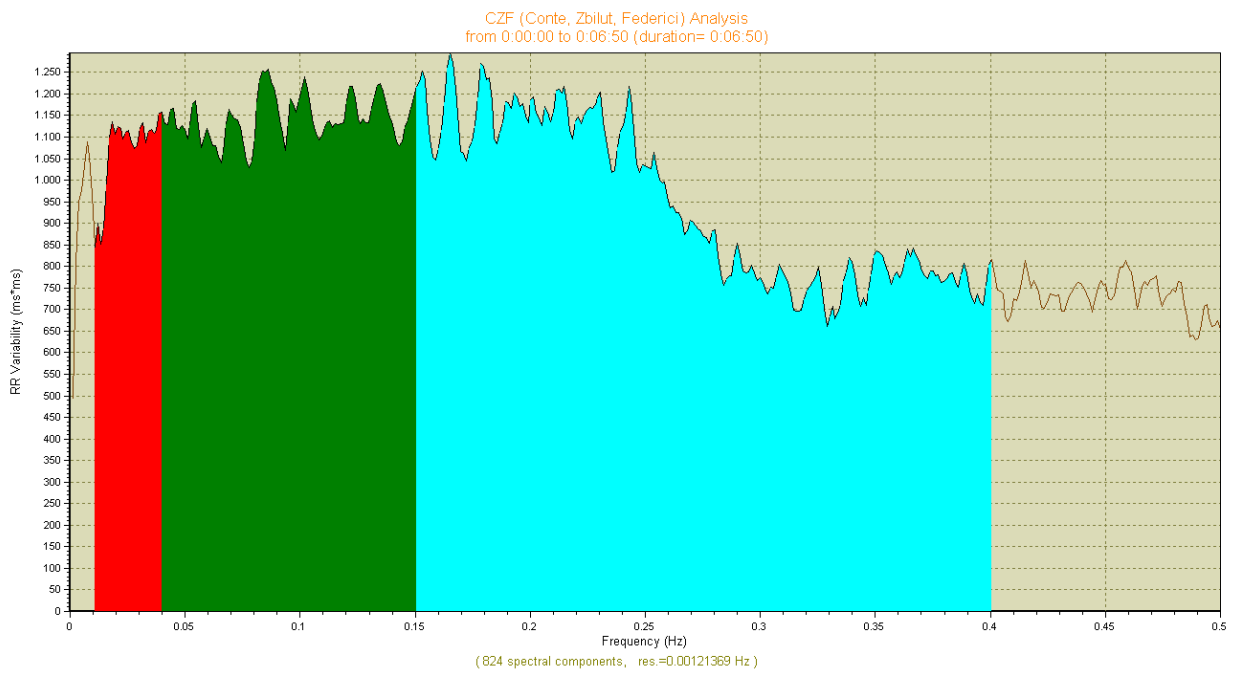
RR7



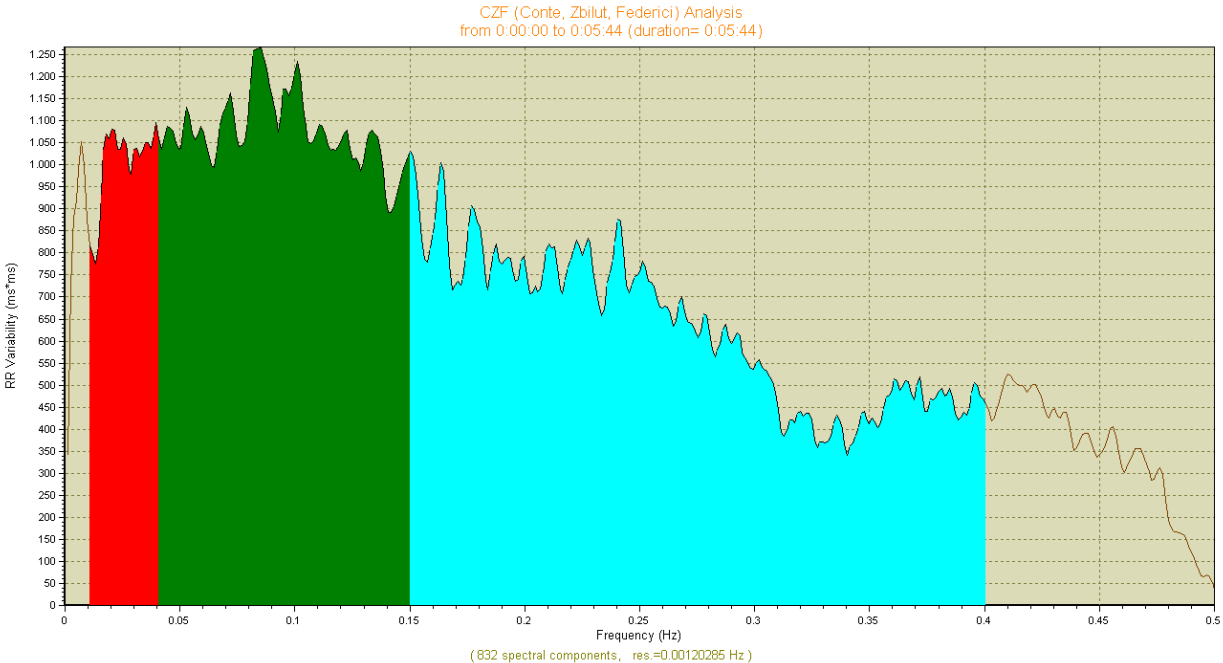
RR 6



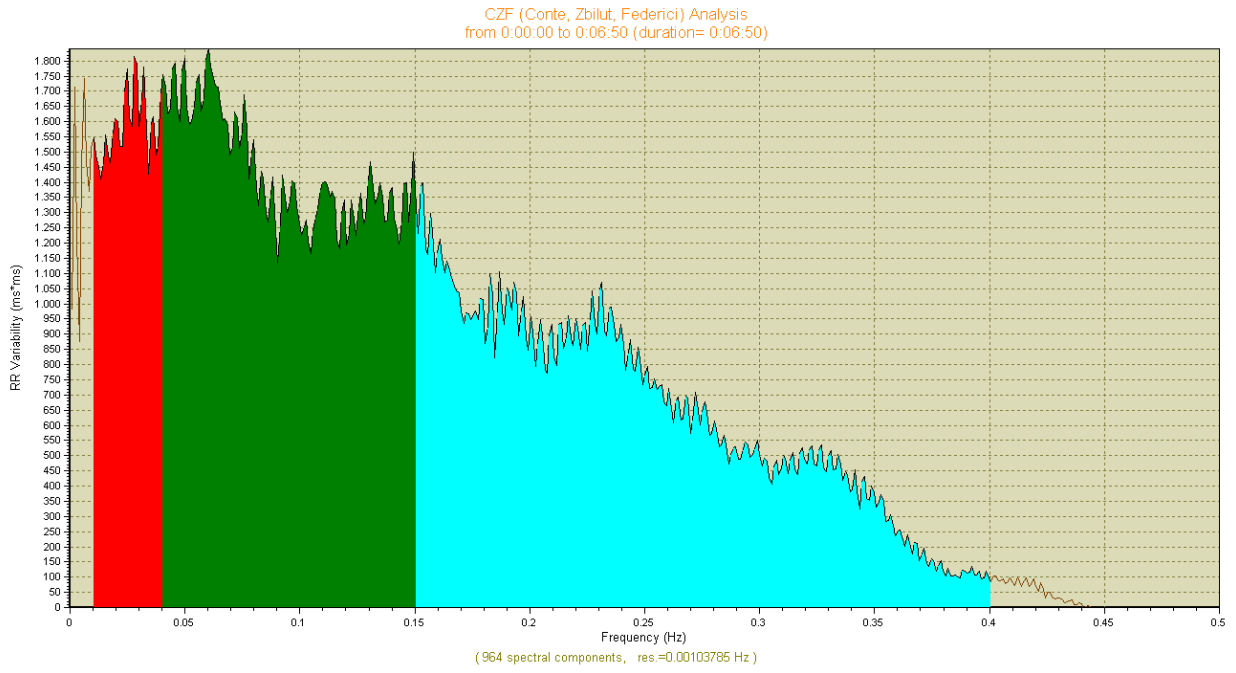
AT 7



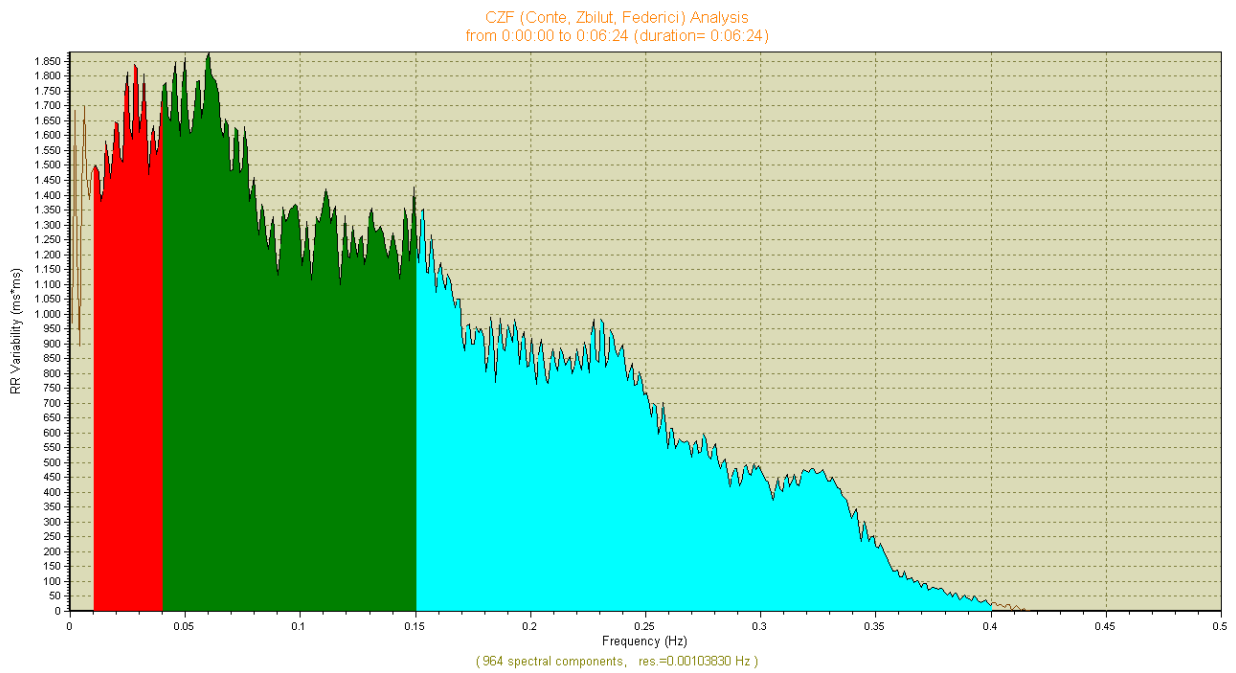
AT 6



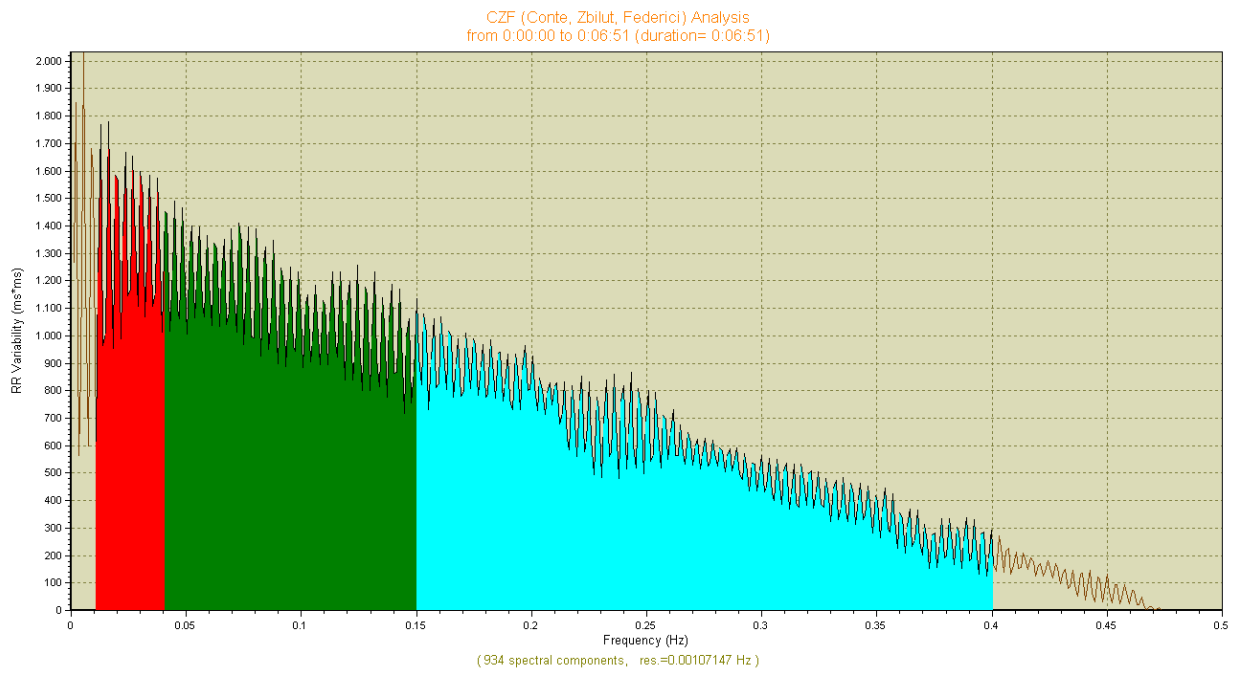
GE 7



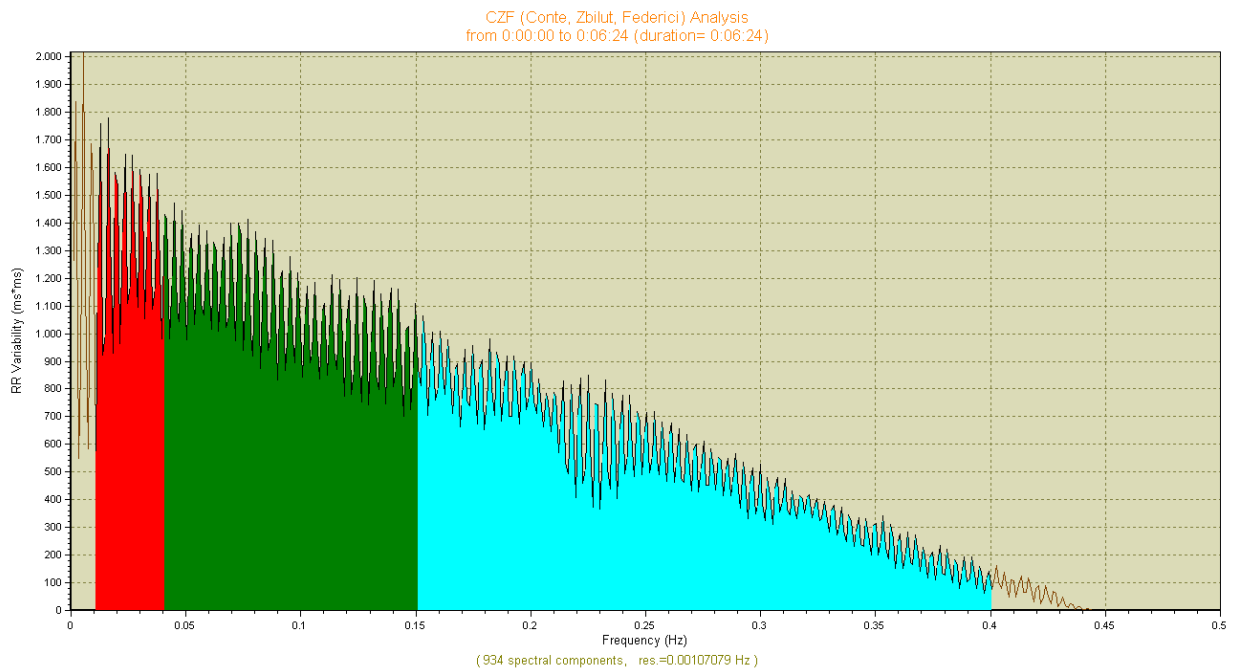
GE 6



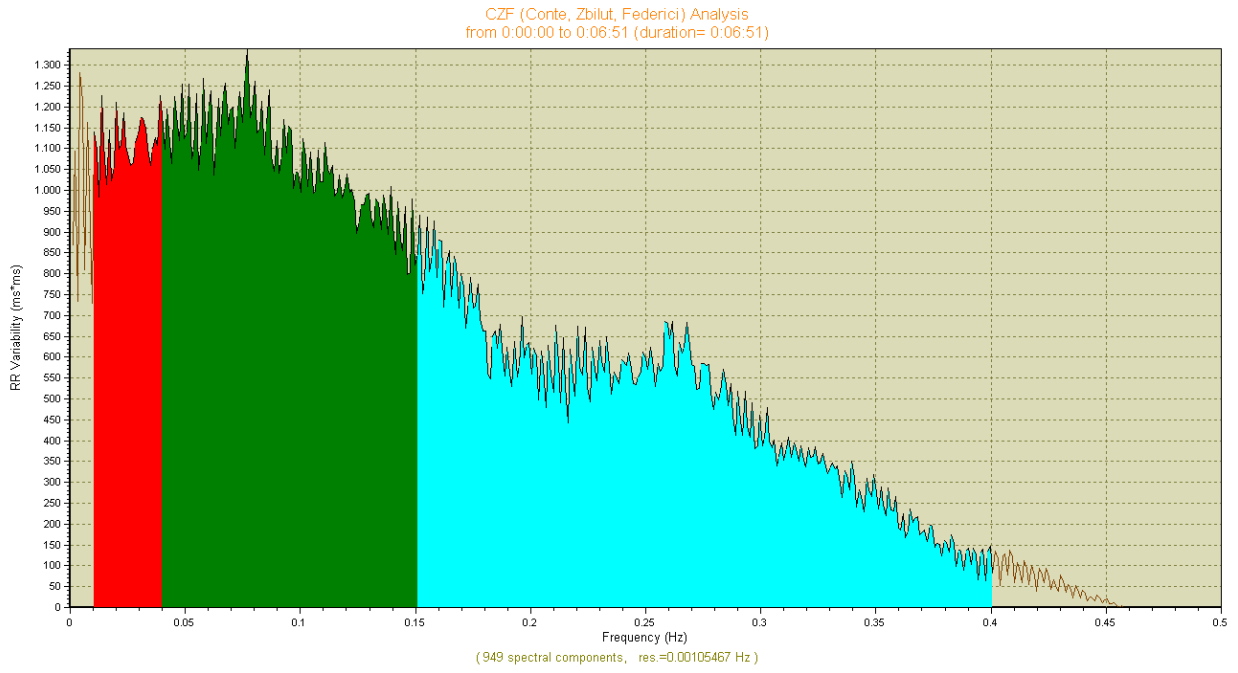
PF 7



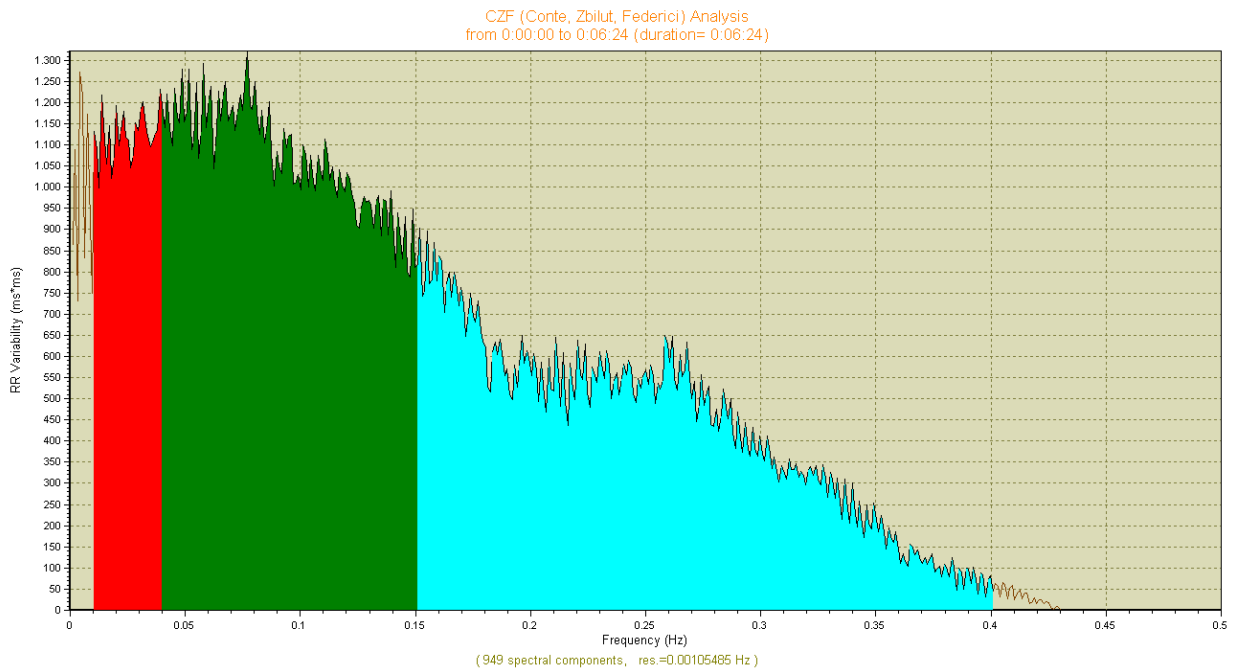
PF 6



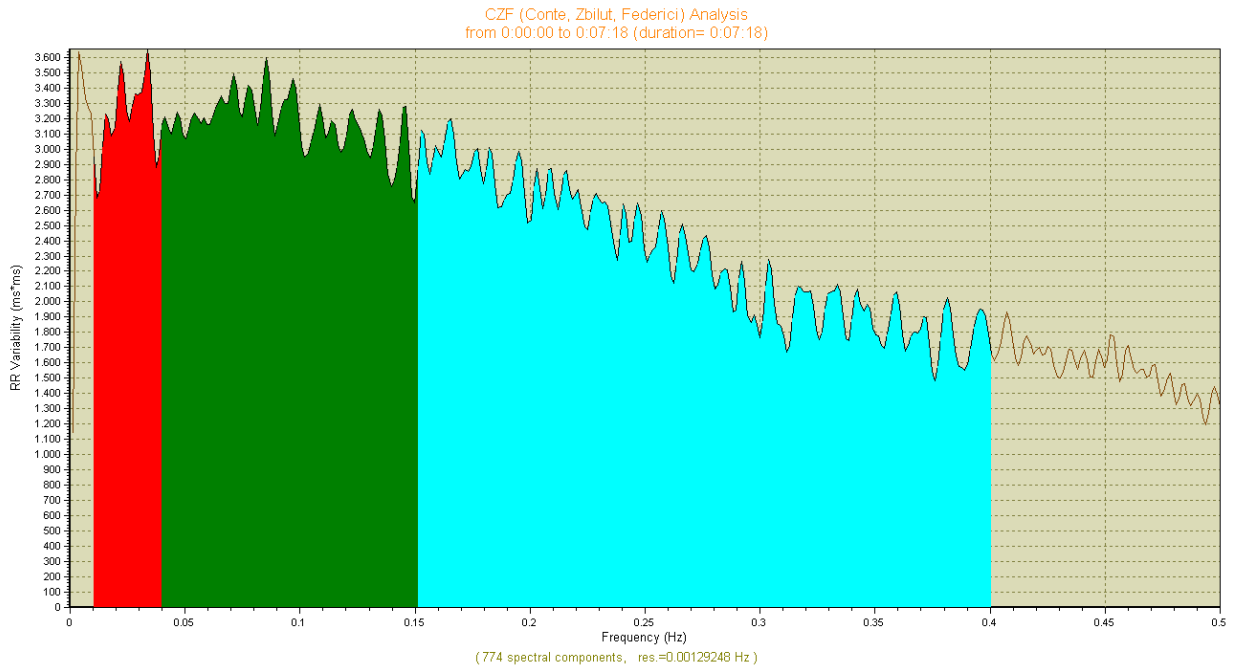
RS 7



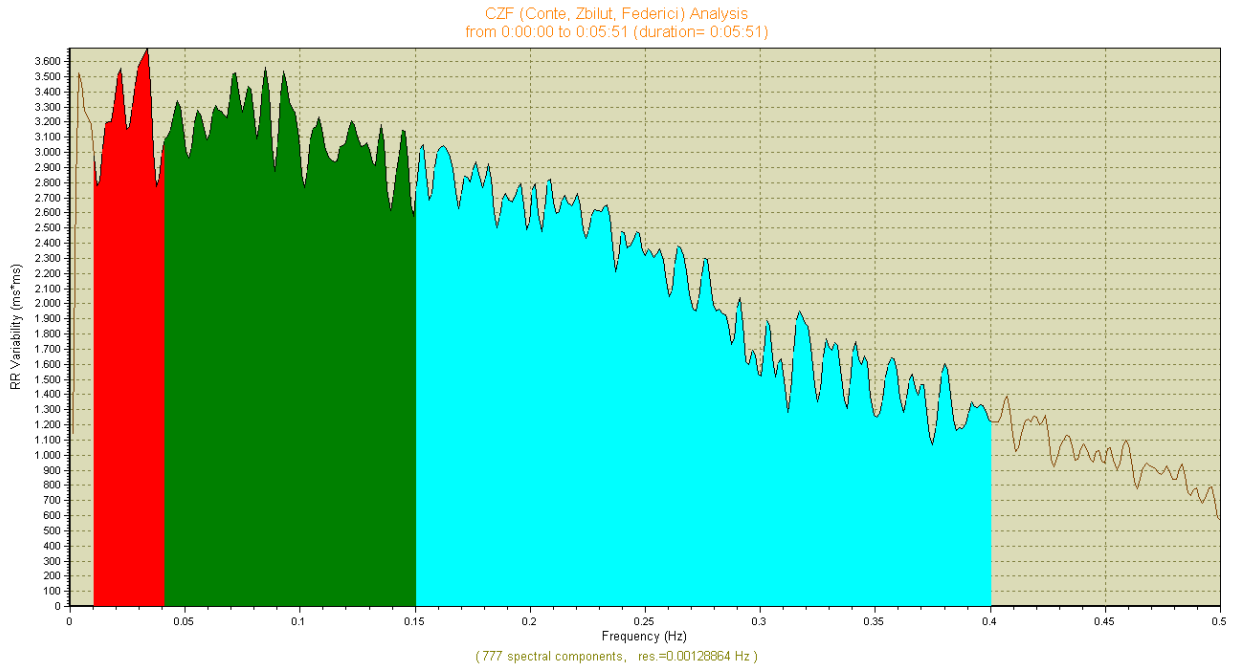
RS 6



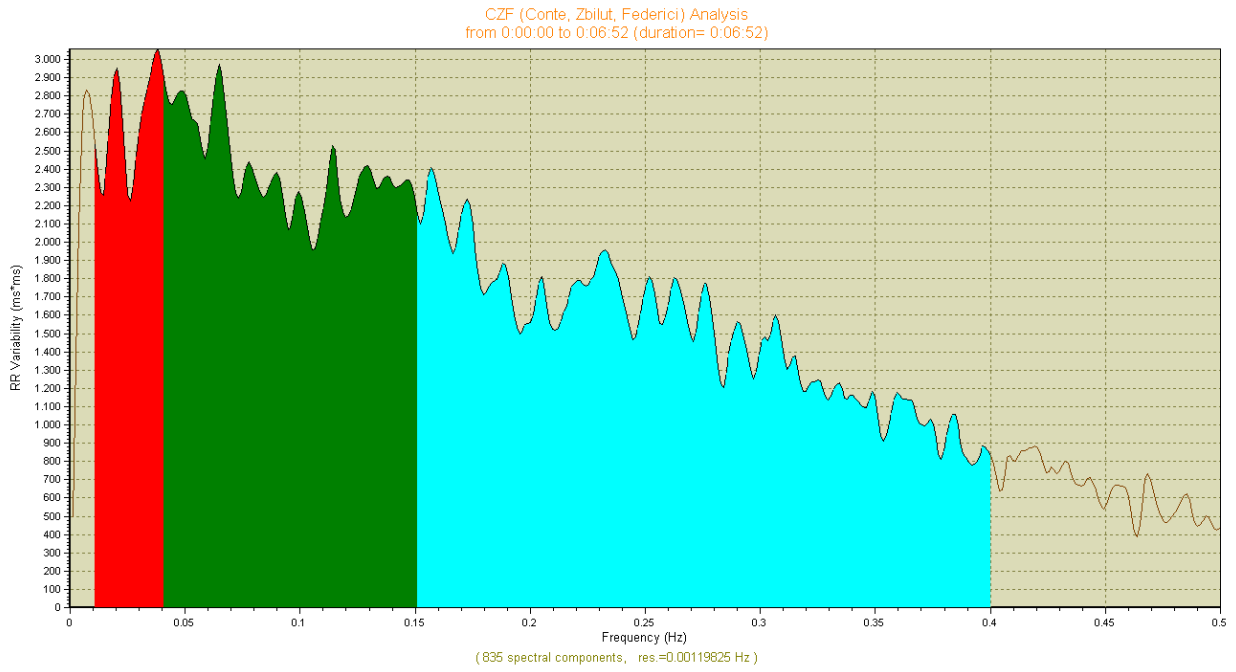
CP 7



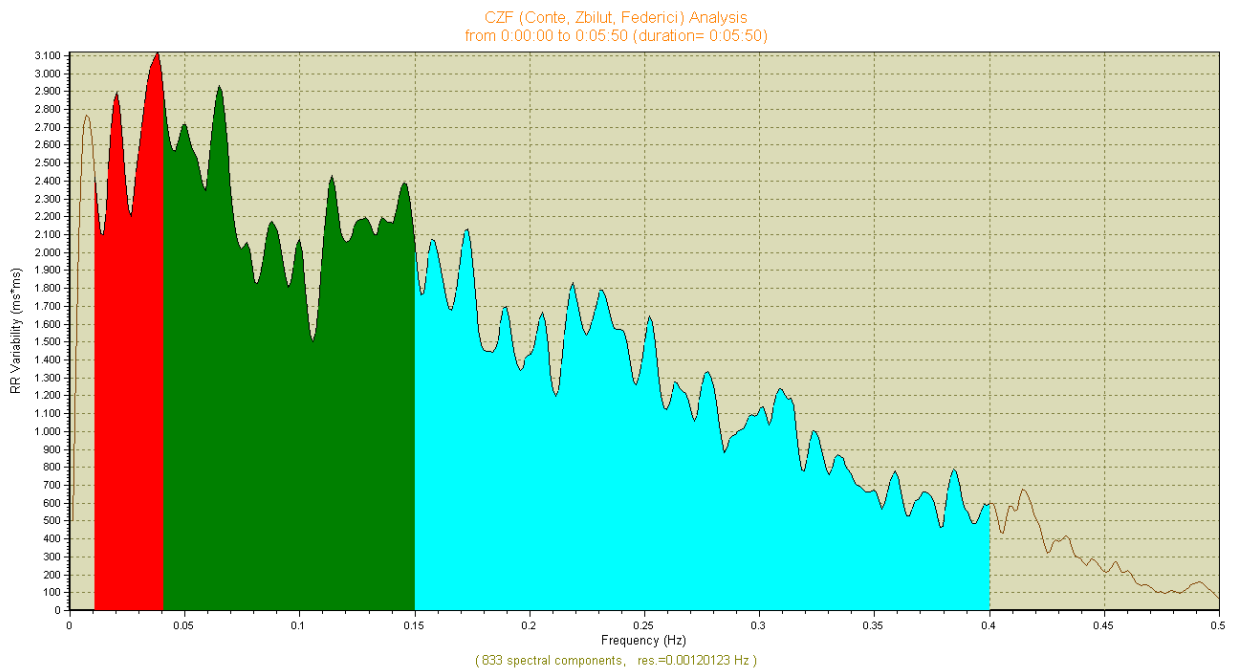
CP 6



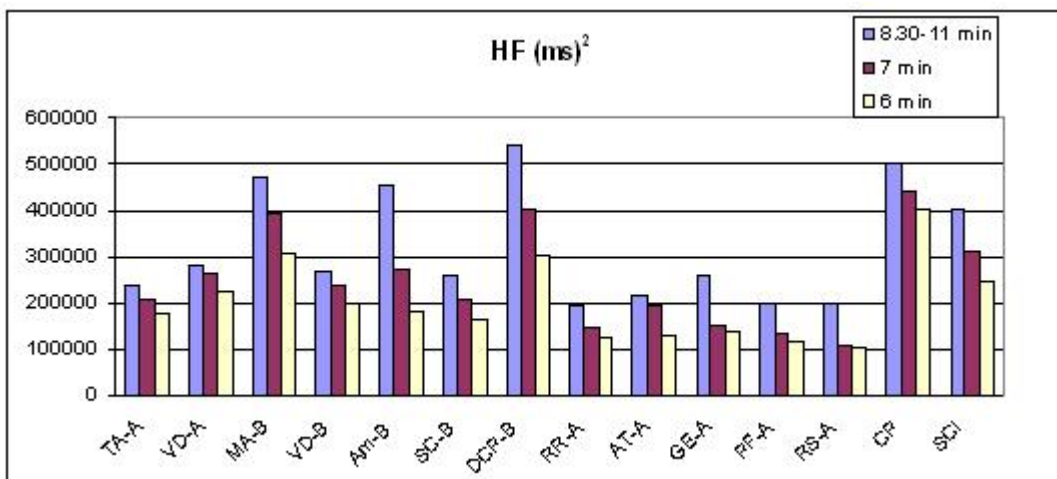
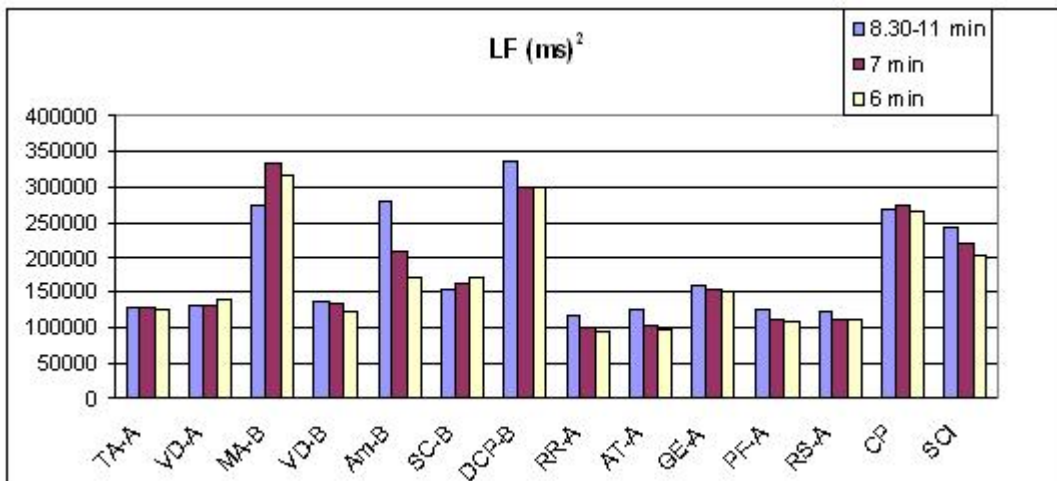
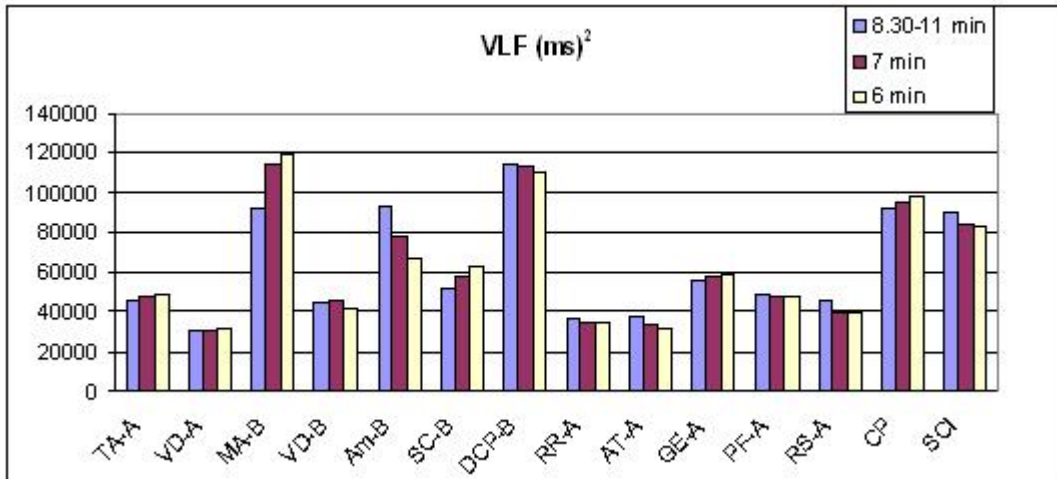
SCI 7

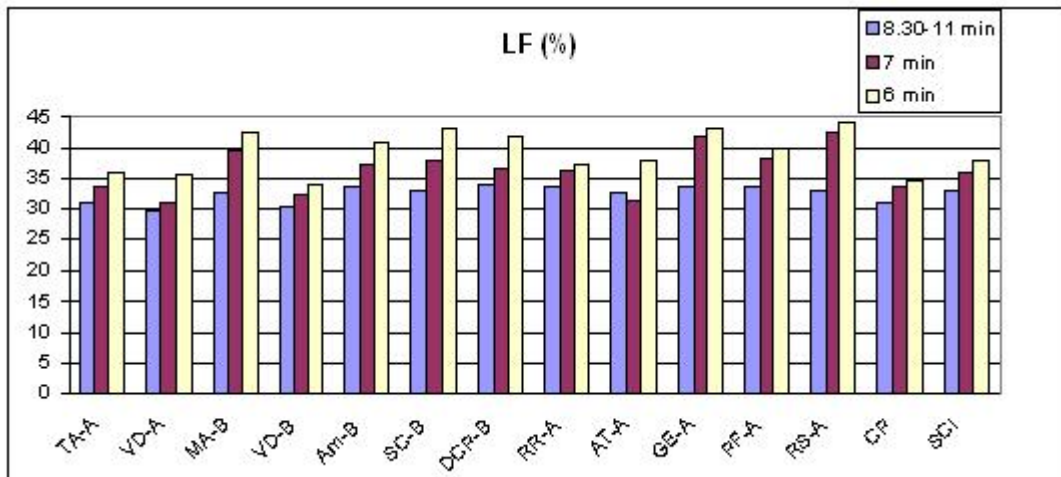
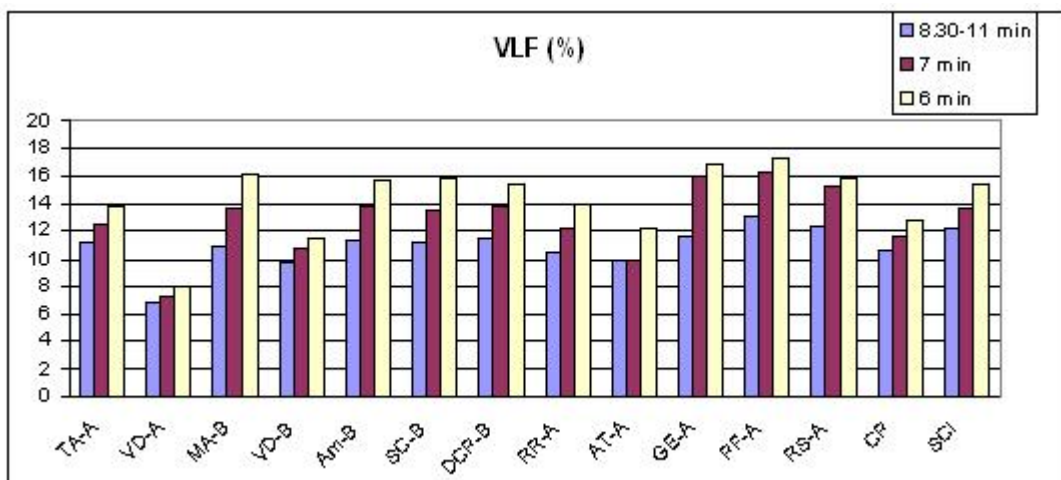
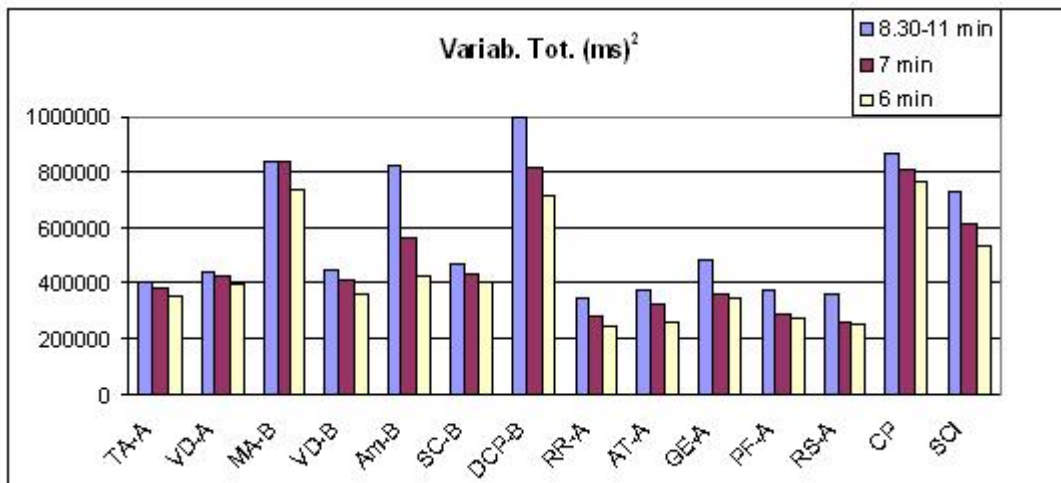


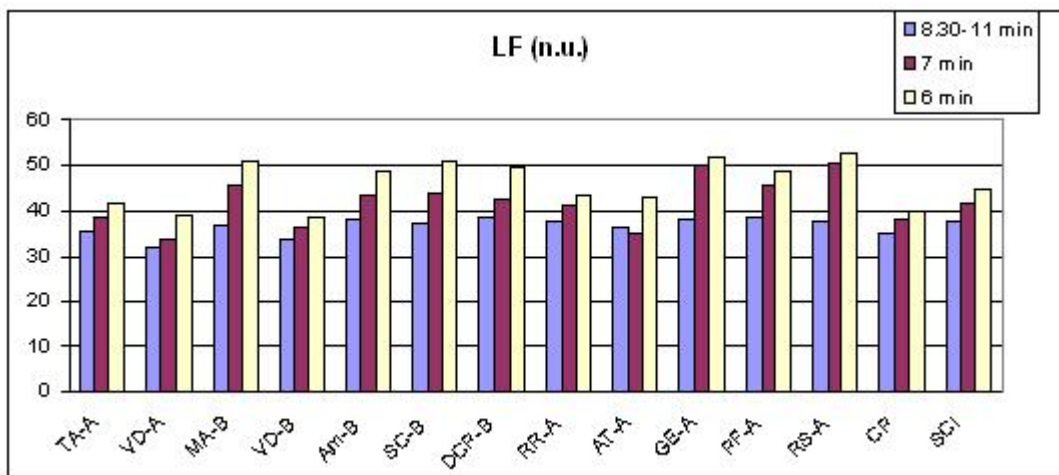
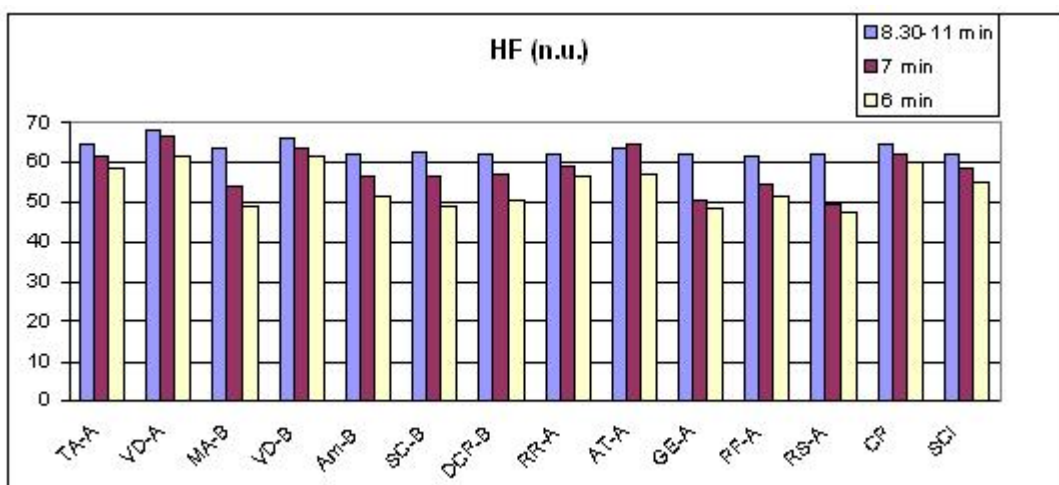
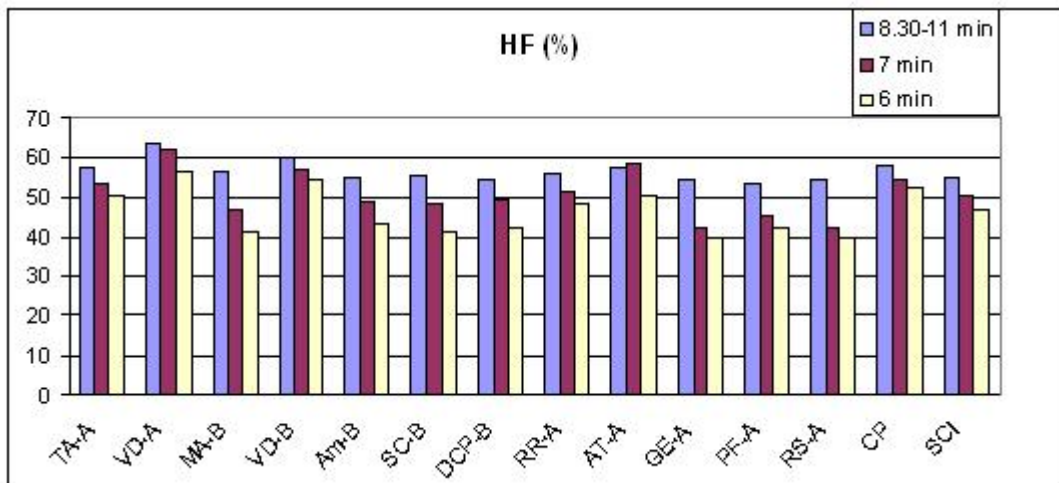
SCI 6

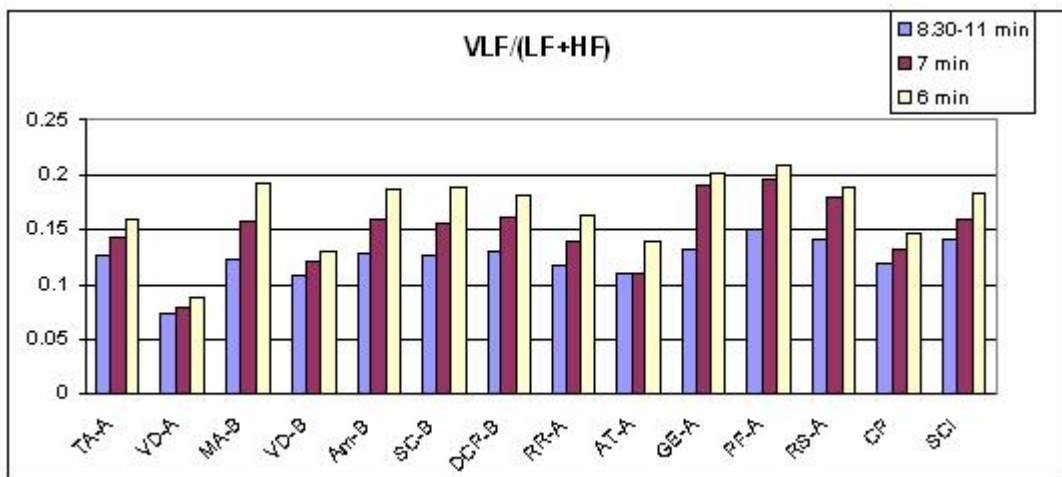
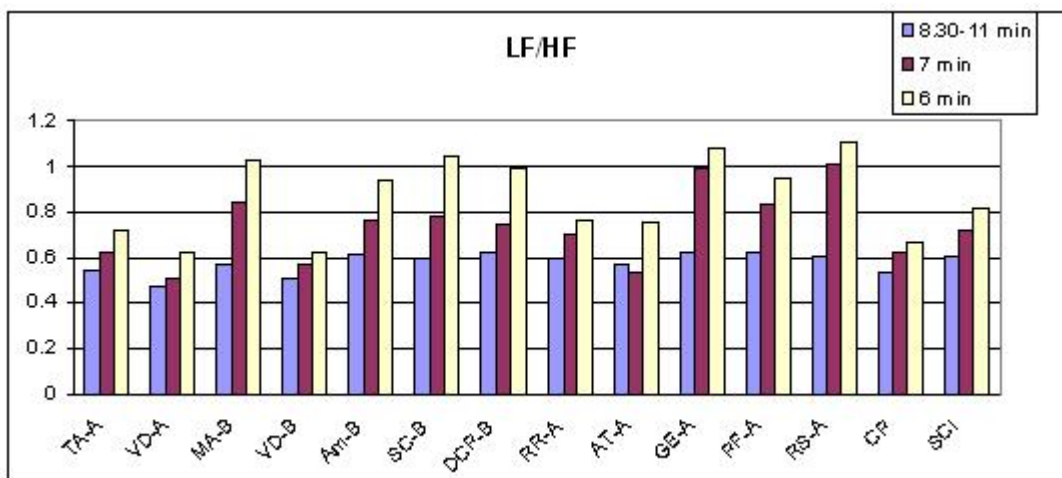
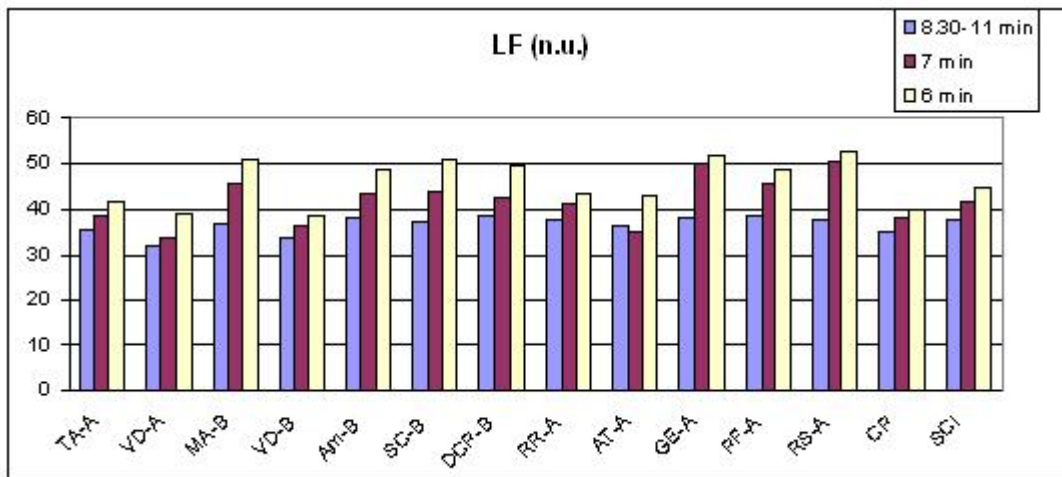


Figures 25

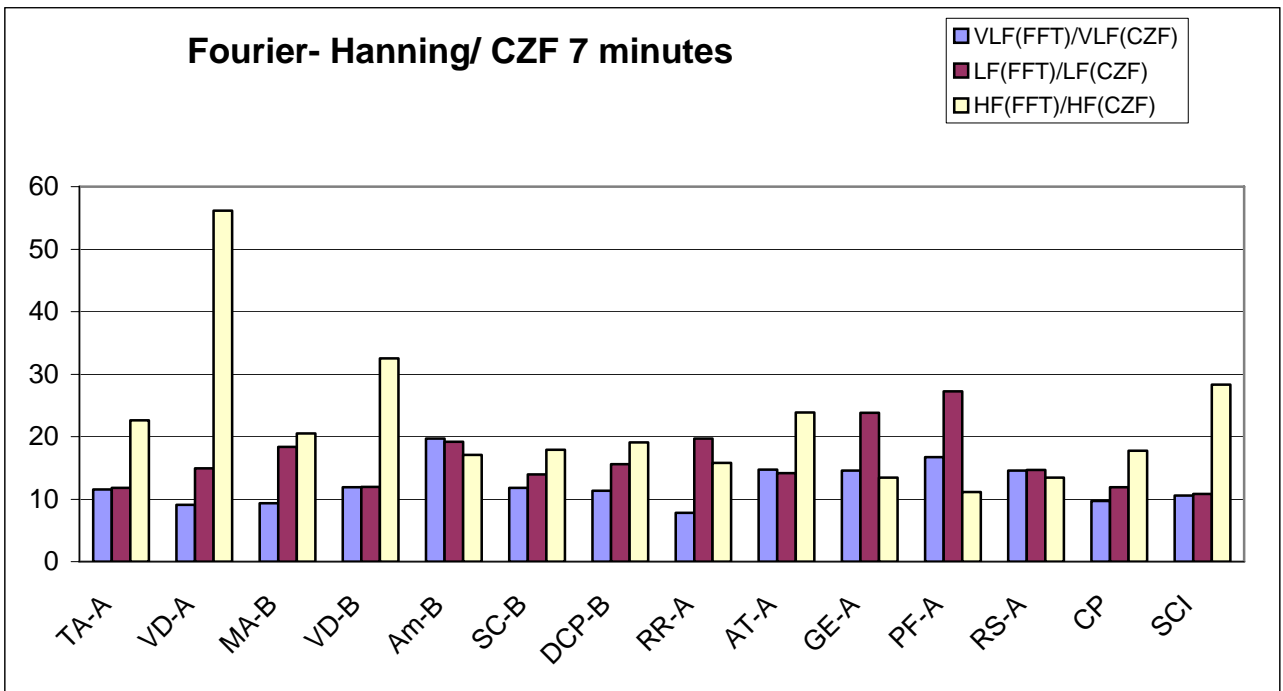
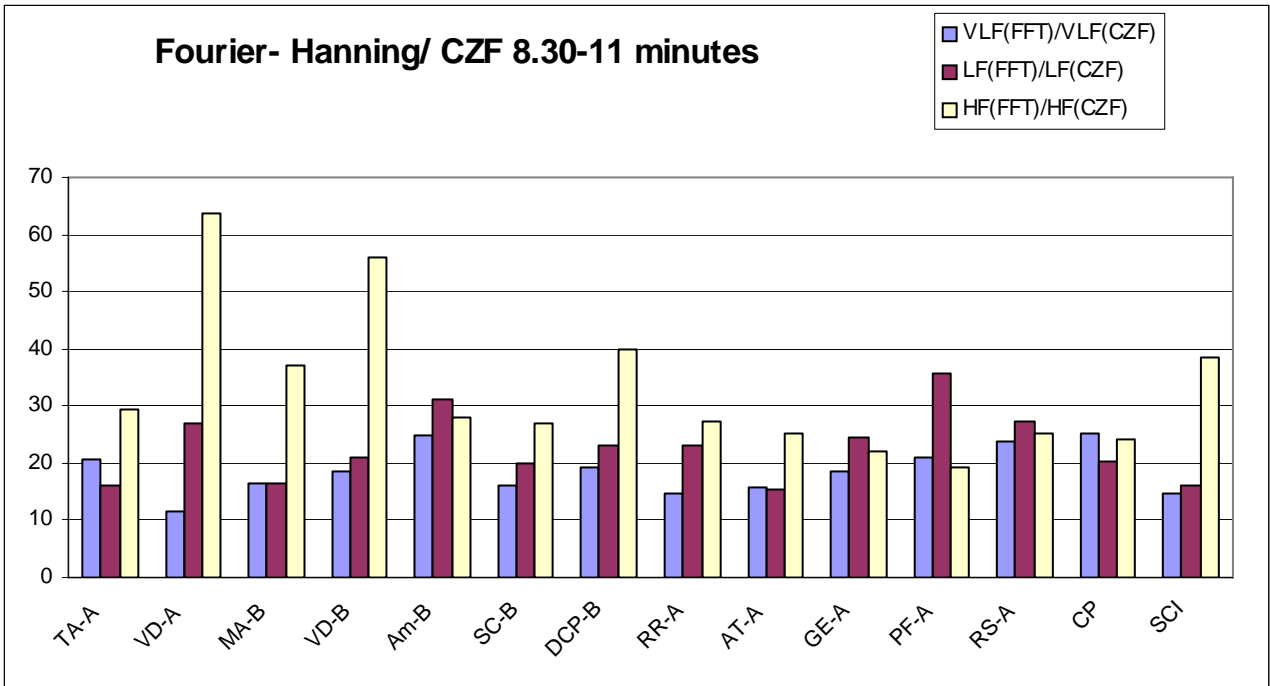


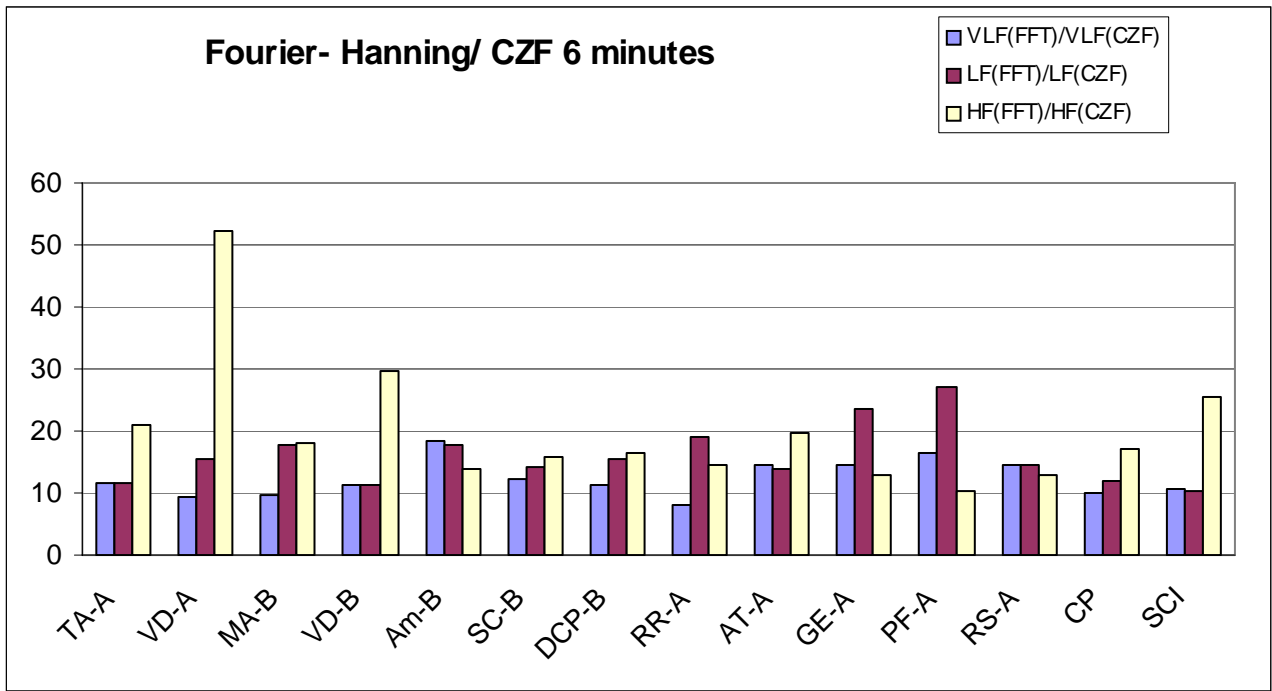






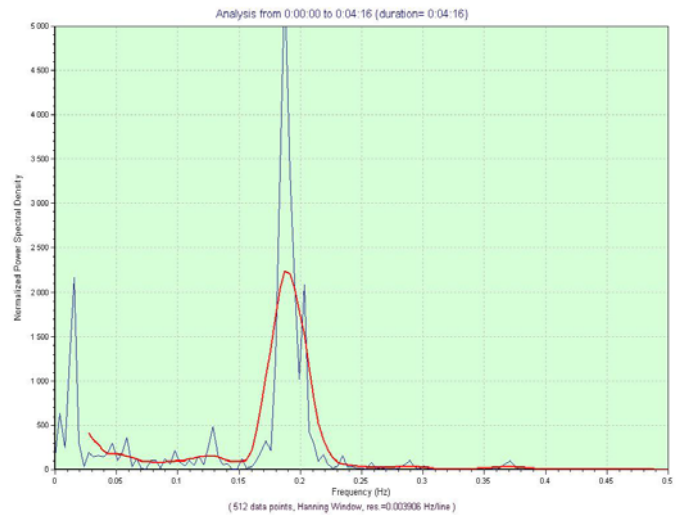
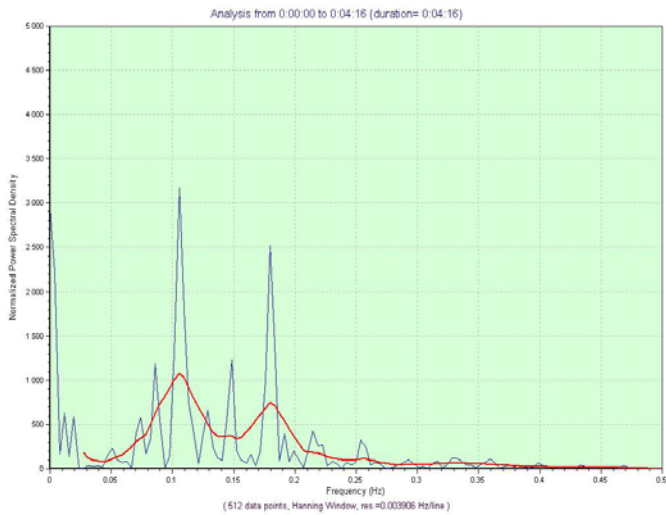
Figures 26



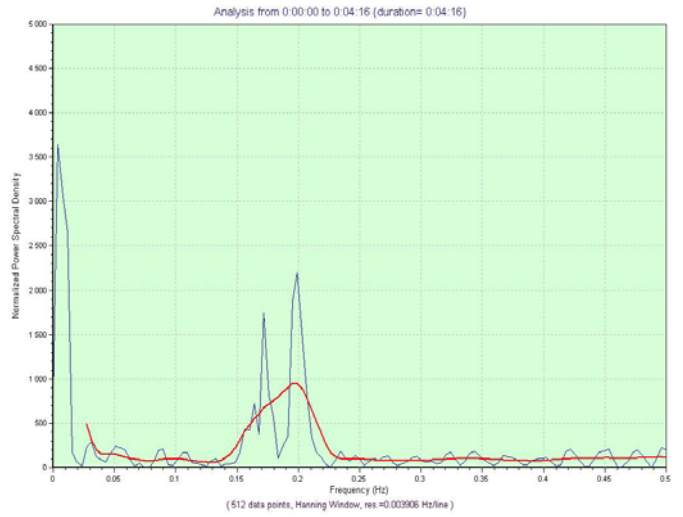
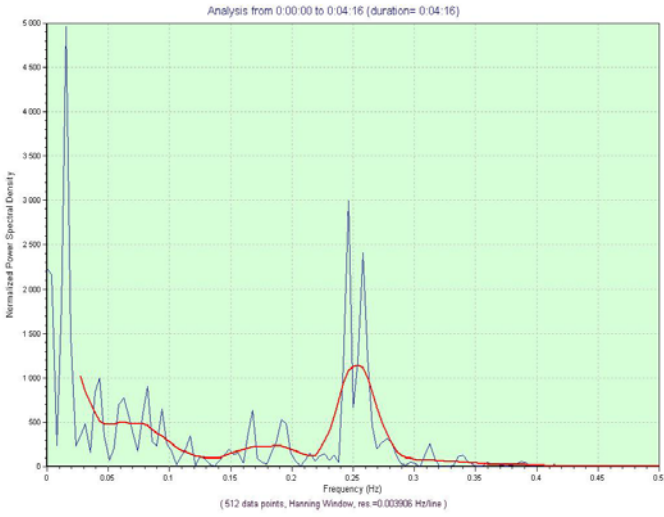


Figures 27

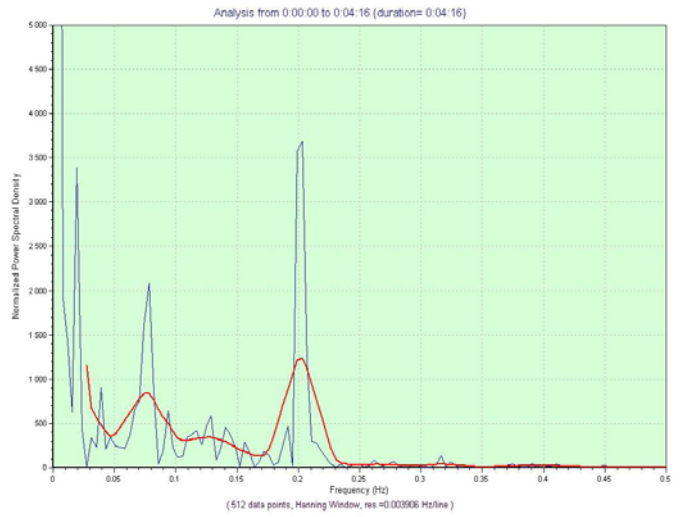
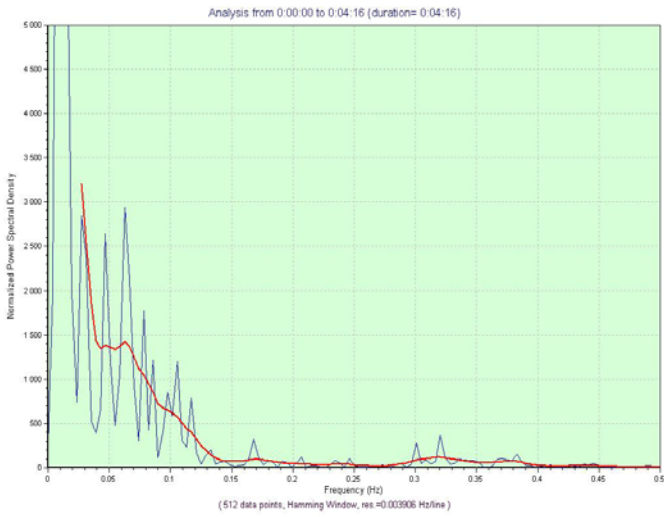
Fourier - Hanning spontaneous respiration BS Fourier - Hanning controlled respiration



Fourier - Hanning spontaneous respiration FE Fourier - Hanning controlled respiration

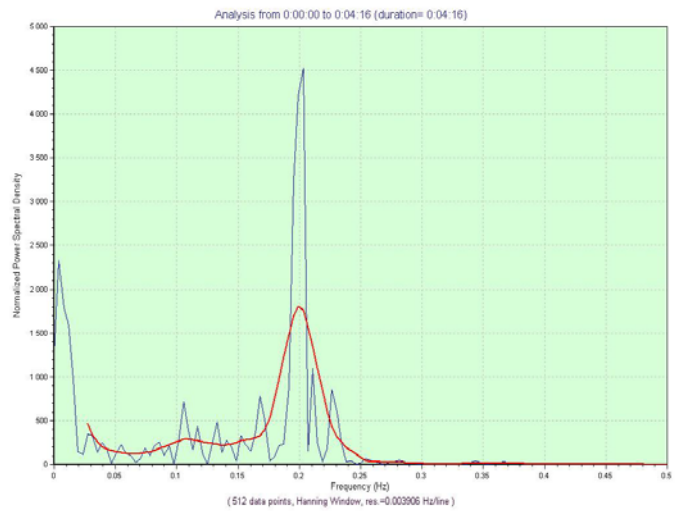
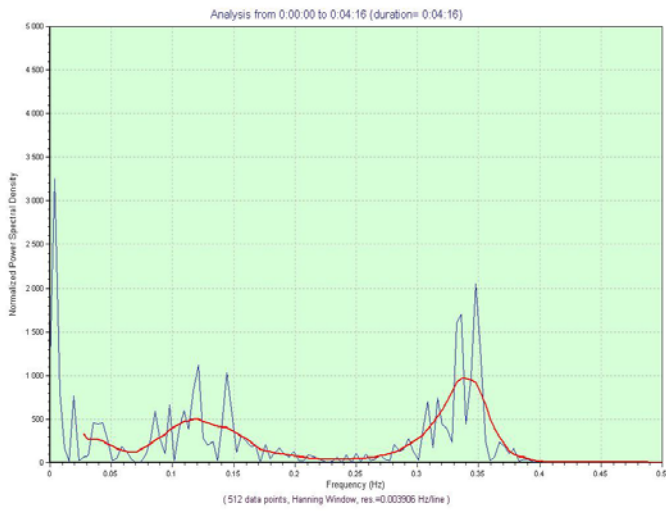


Fourier - Hanning spontaneous respiration GC Fourier - Hanning controlled respiration



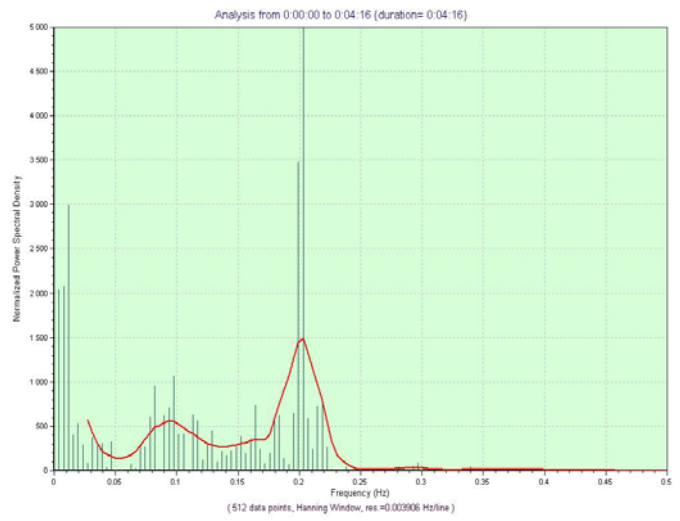
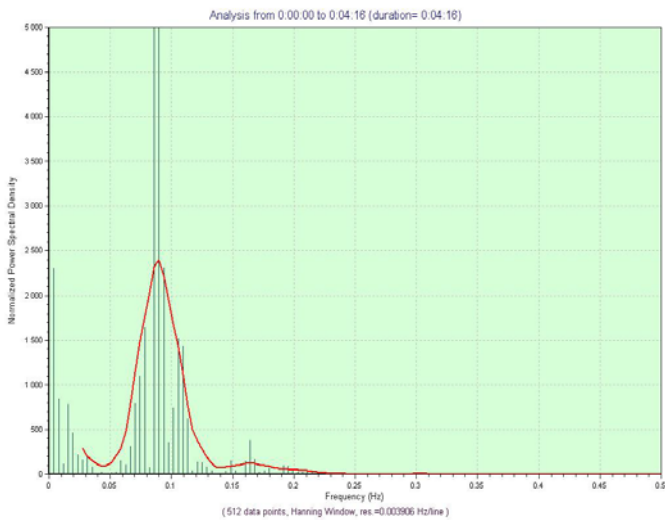
Fourier - Hanning spontaneous respiration

GM Fourier - Hanning controlled respiration

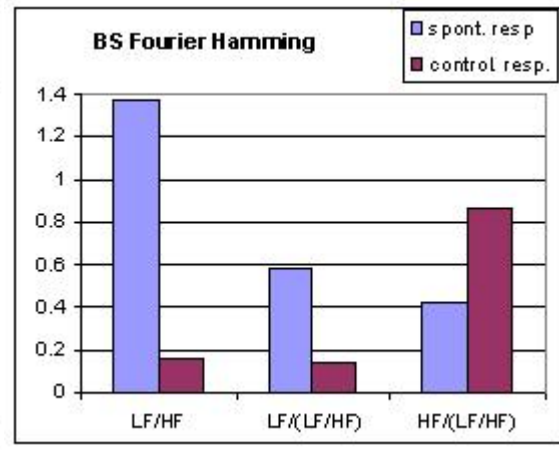
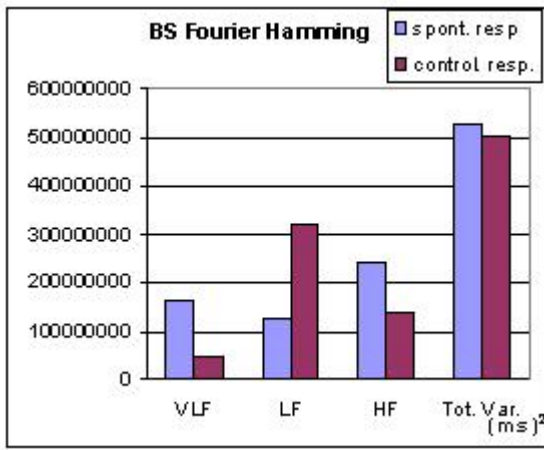
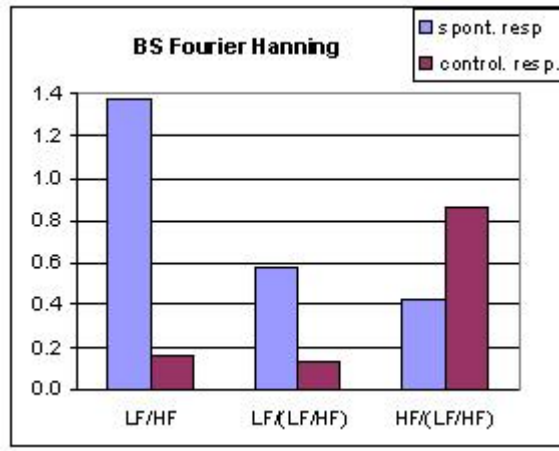
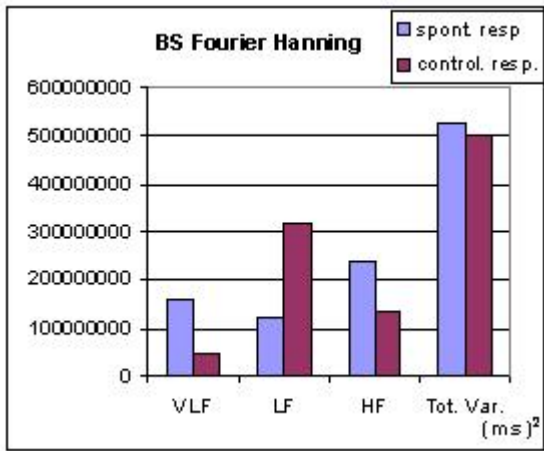


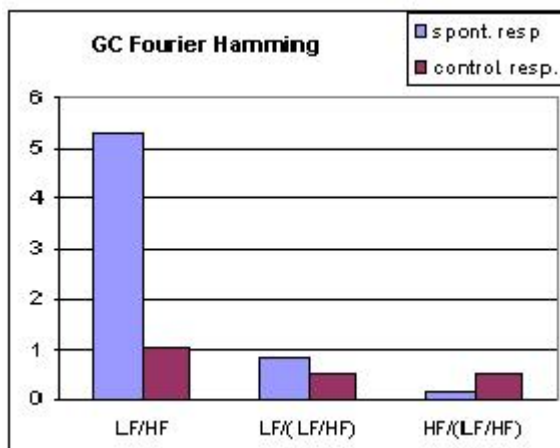
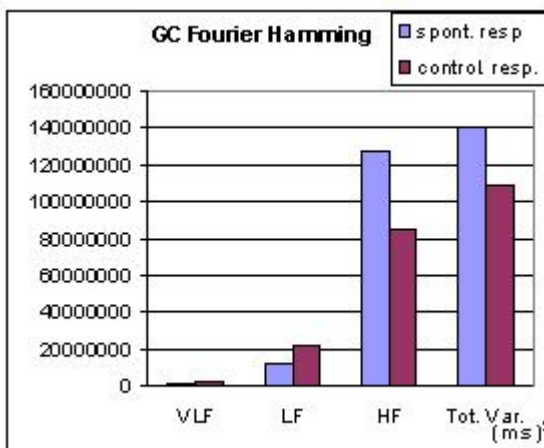
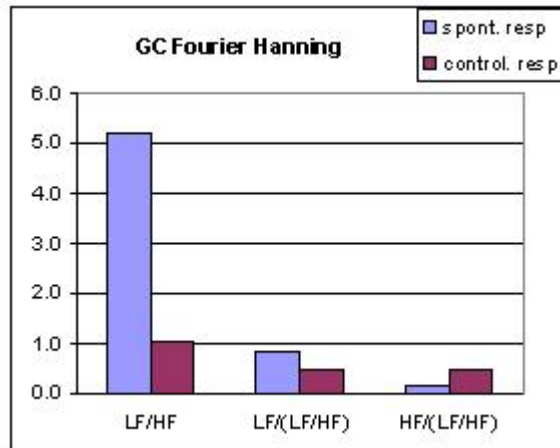
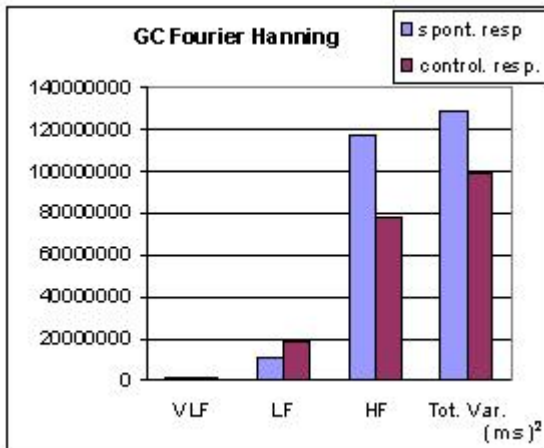
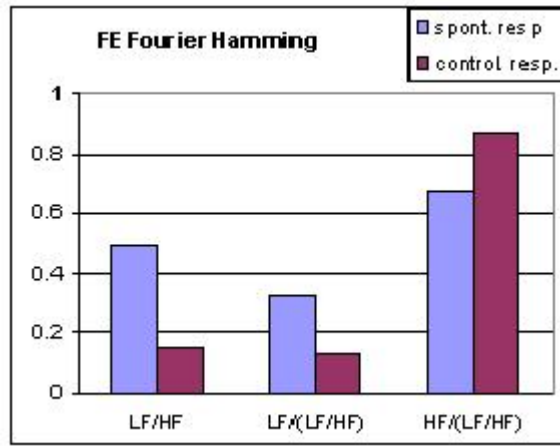
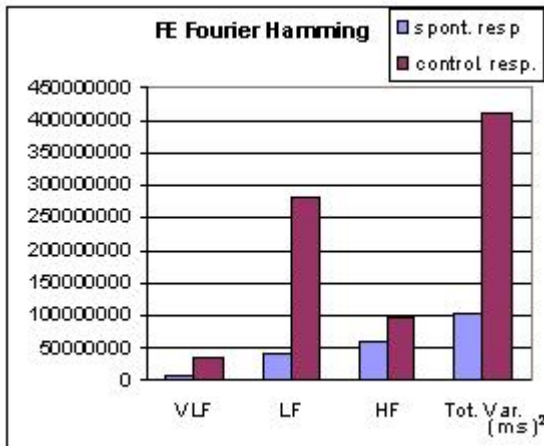
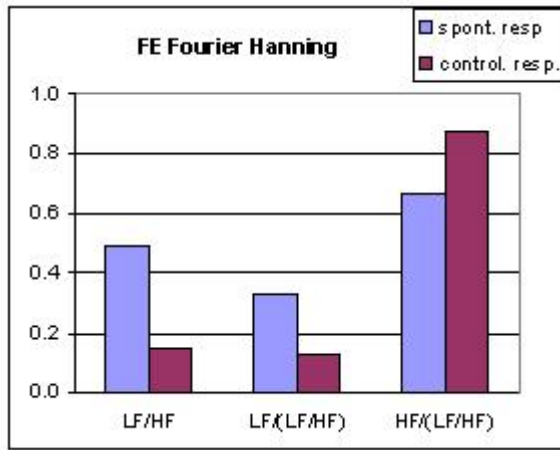
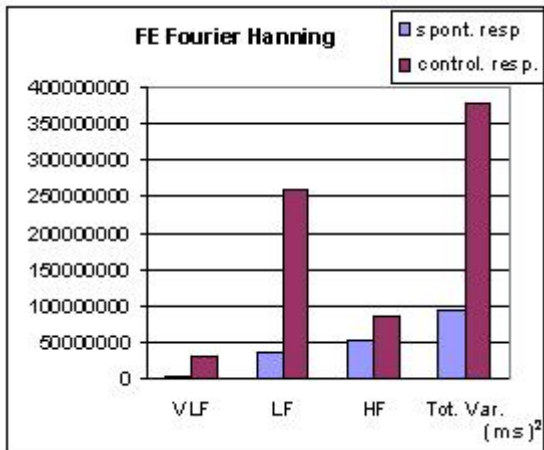
Fourier - Hanning spontaneous respiration

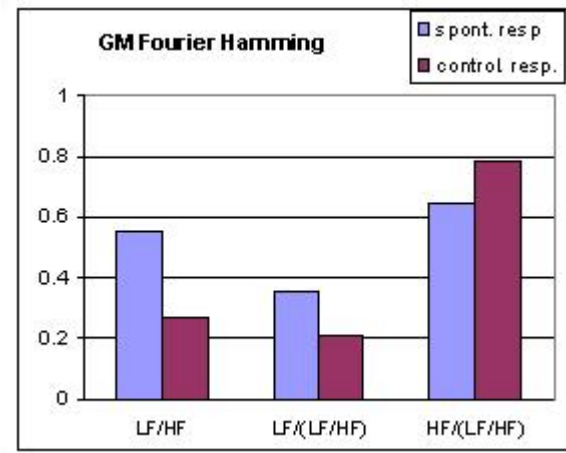
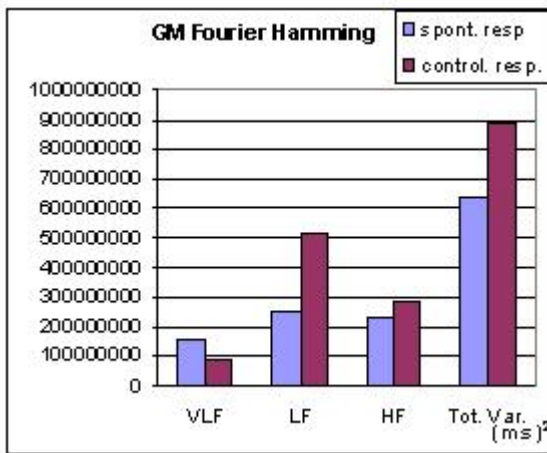
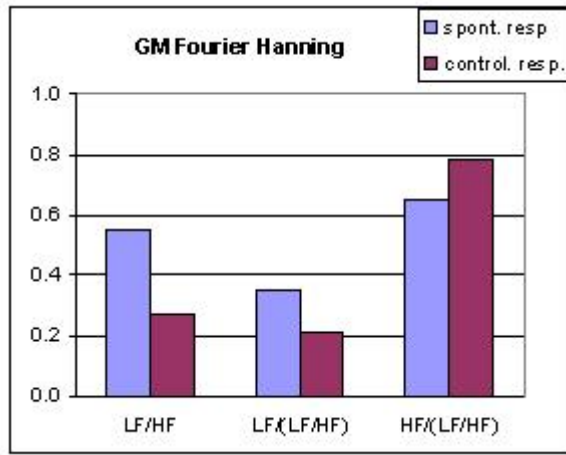
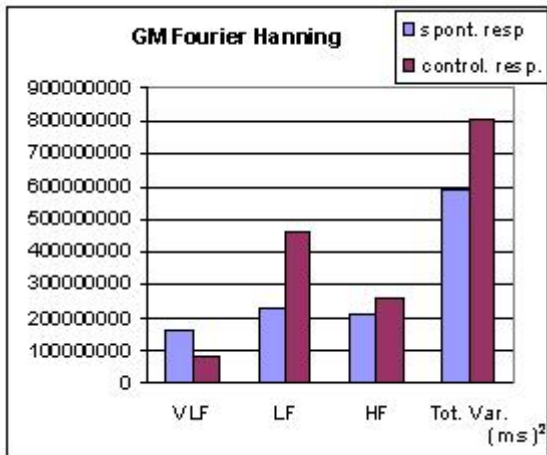
SM Fourier - Hanning controlled respiration

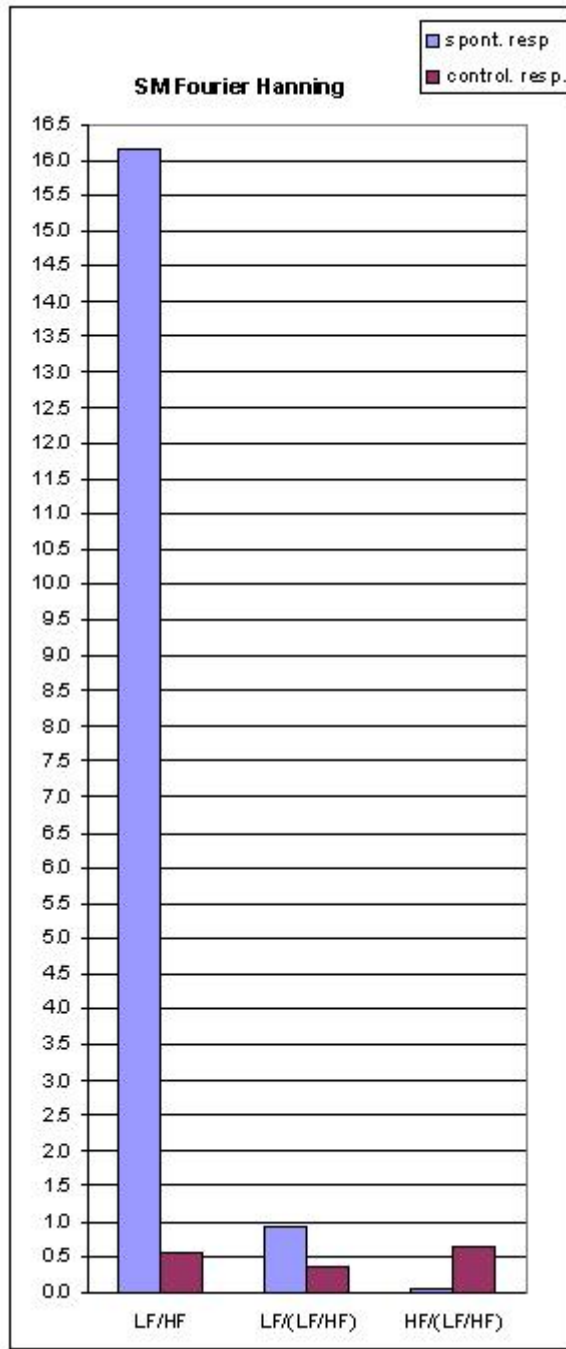
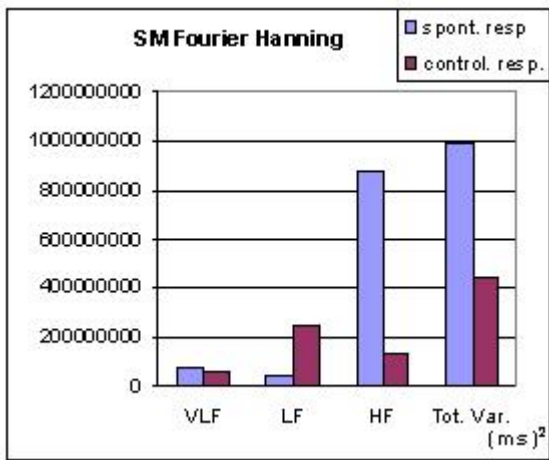


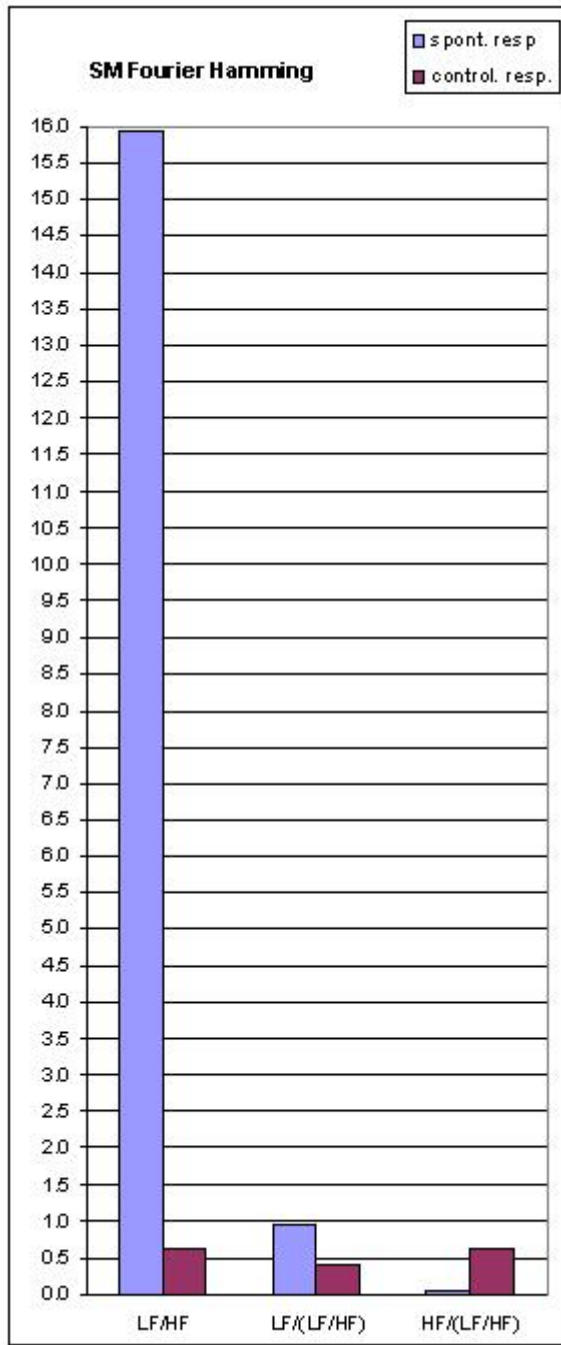
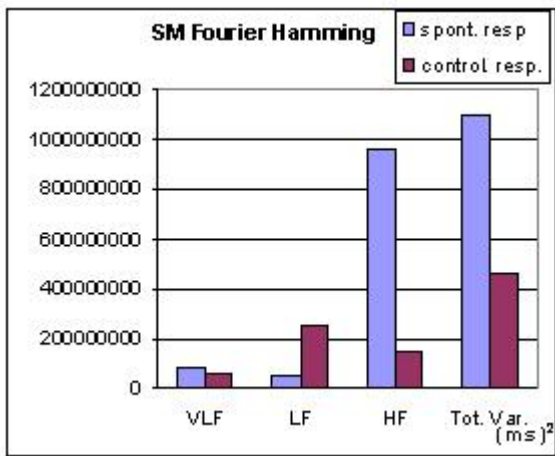
Figures 28





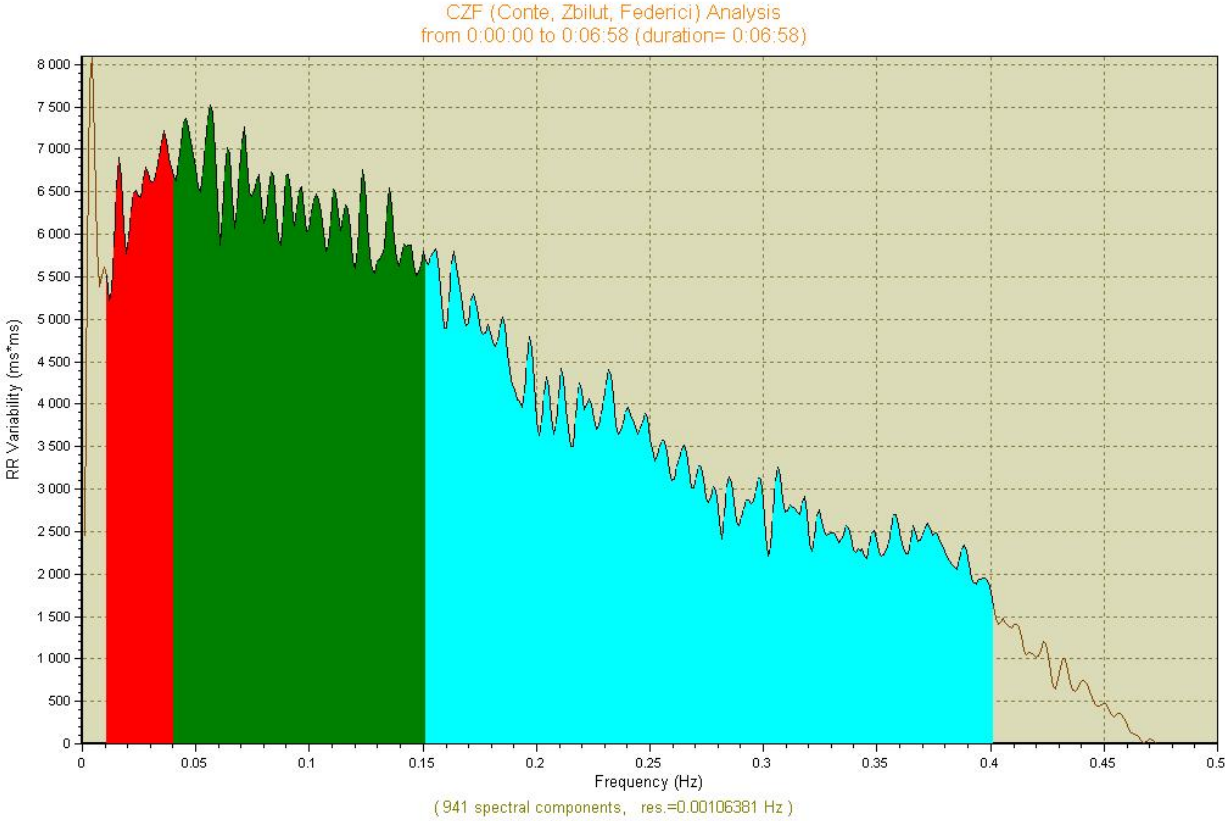






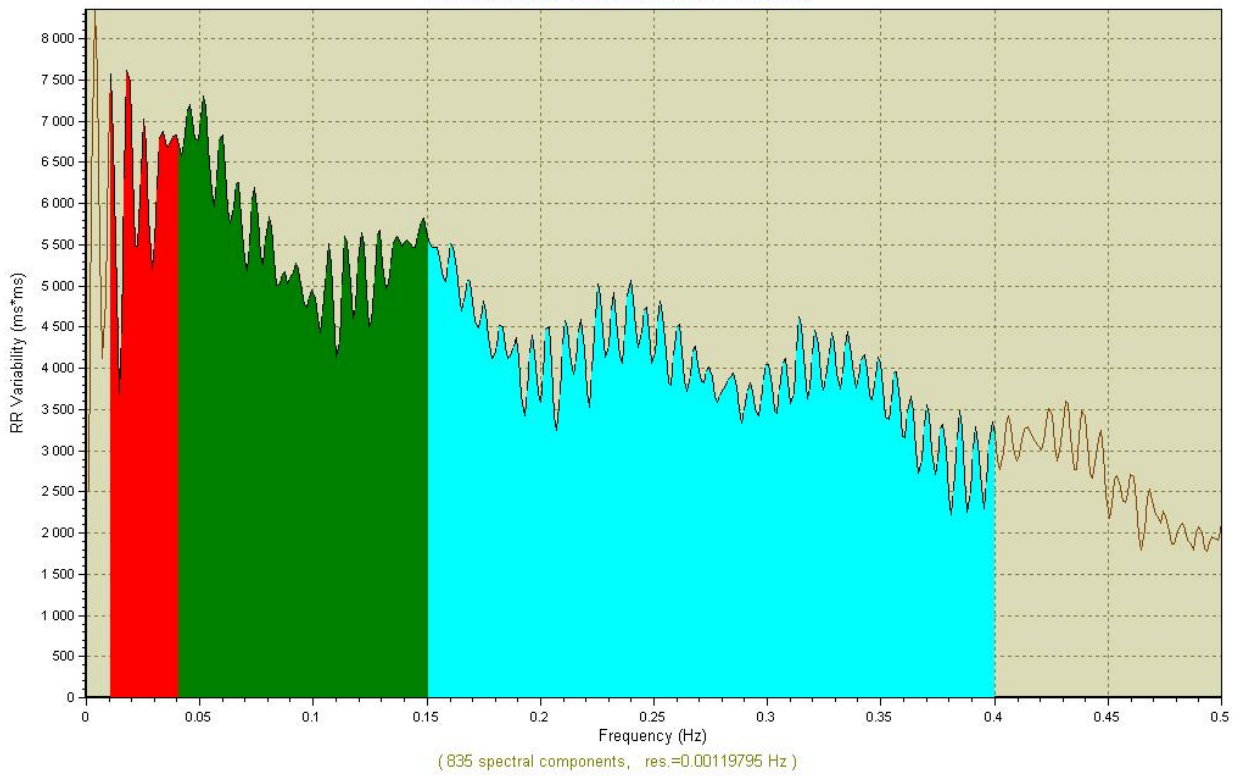
Figures 29

BS : CZF - spontaneous respiration



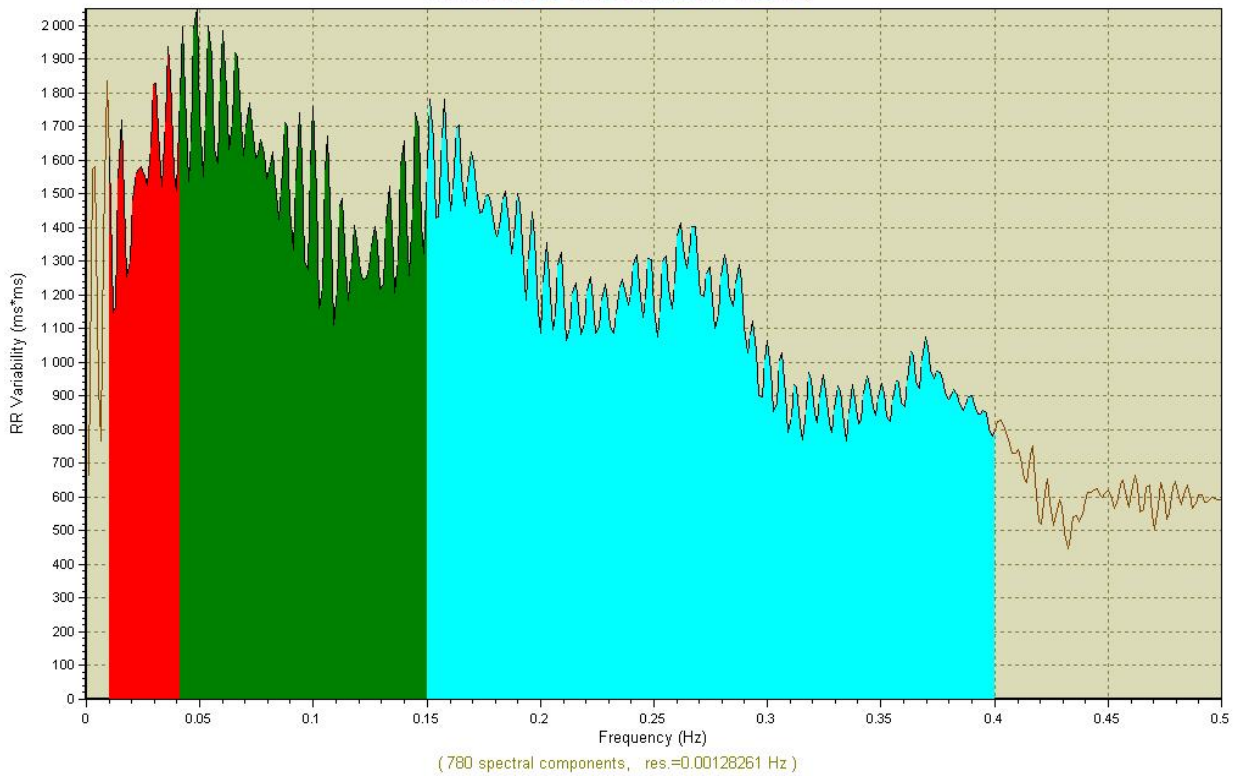
BS : CZF - controlled respiration

CZF (Conte, Zbilut, Federici) Analysis
from 0:00:00 to 0:06:58 (duration= 0:06:58)

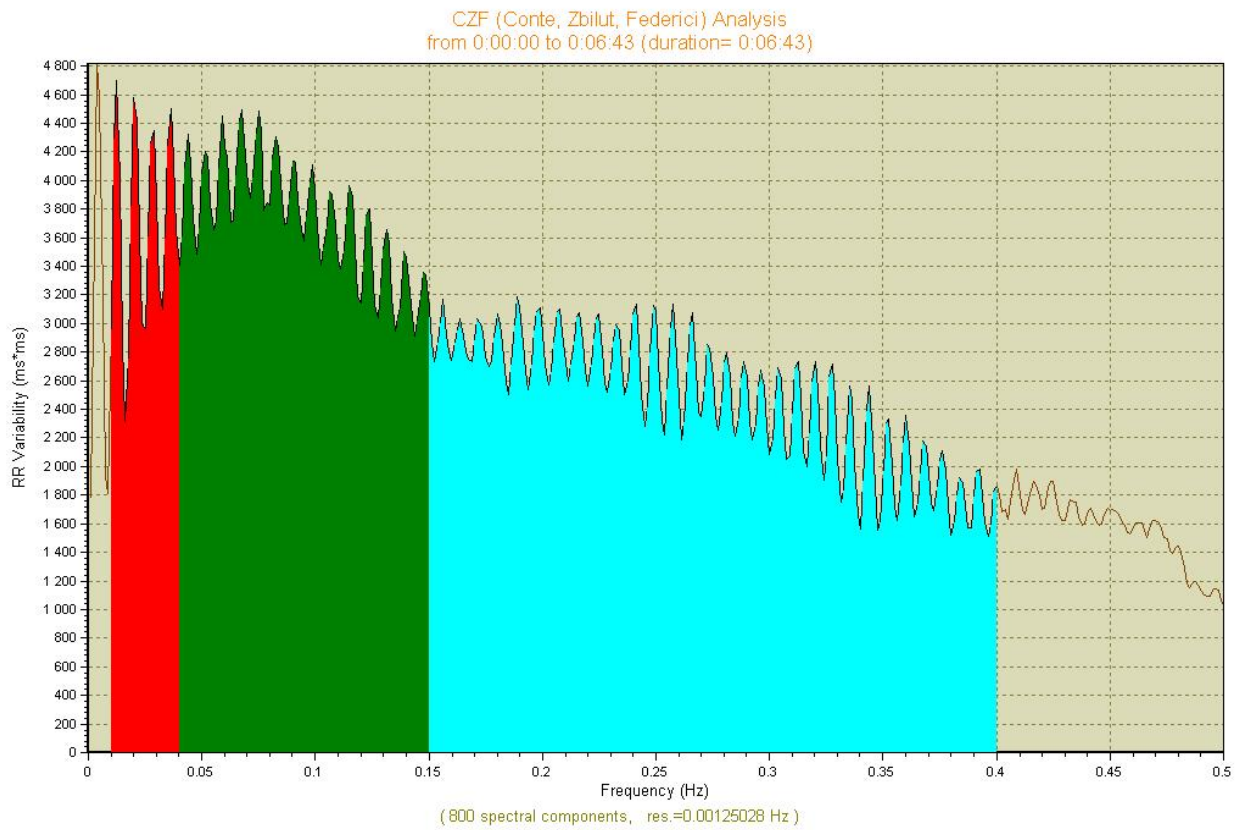


FE : CZF - spontaneous respiration

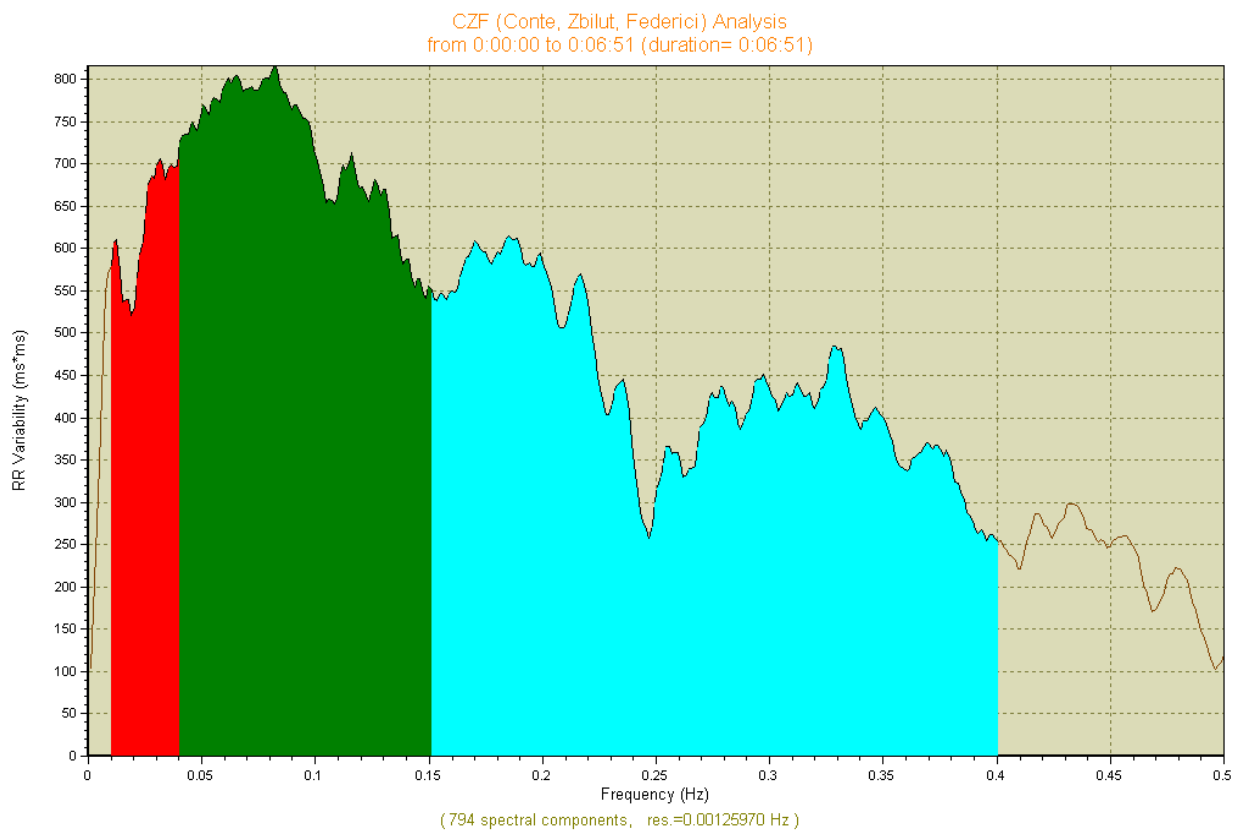
CZF (Conte, Zbilut, Federici) Analysis
from 0:00:00 to 0:06:59 (duration= 0:06:59)



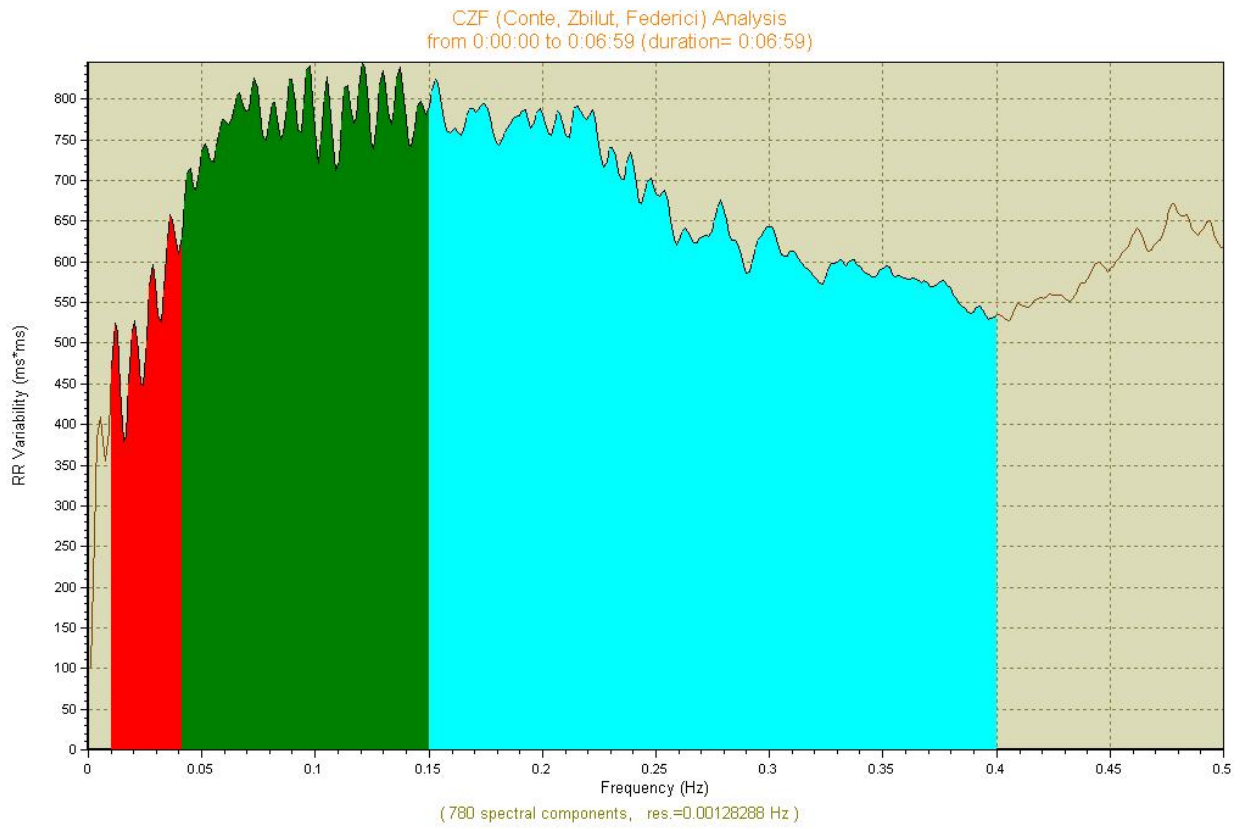
FE : CZF - controlled respiration



GC : CZF - spontaneous respiration

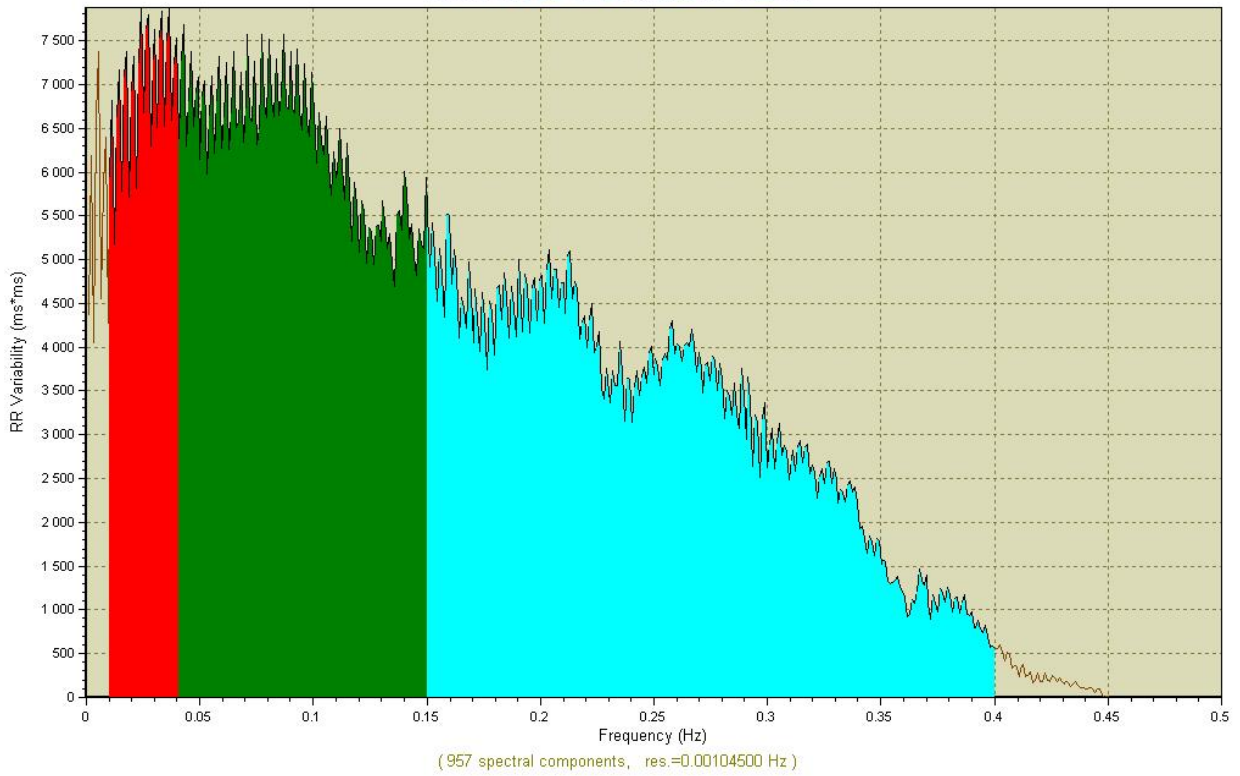


GC : CZF - controlled respiration



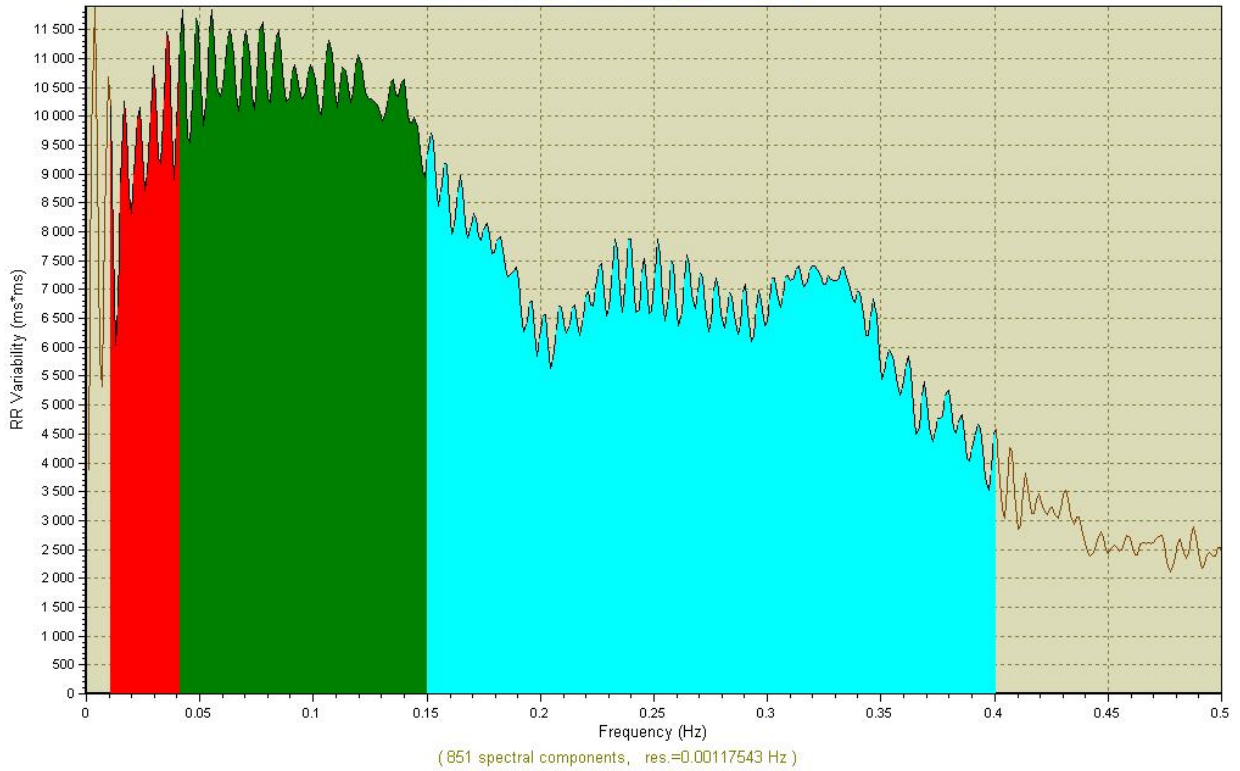
GM : CZF - spontaneous respiration

CZF (Conte, Zbilut, Federici) Analysis
from 0:00:00 to 0:06:50 (duration= 0:06:50)

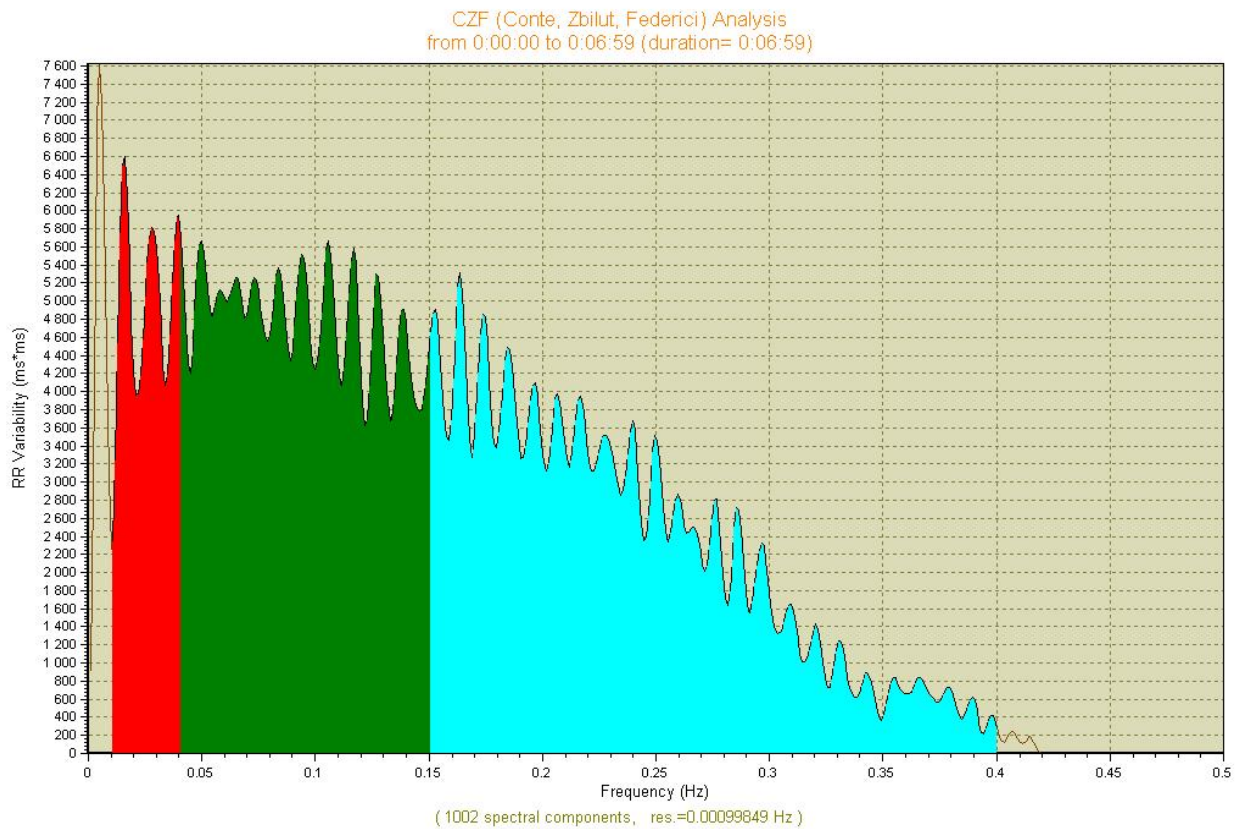


GM : CZF - controlled respiration

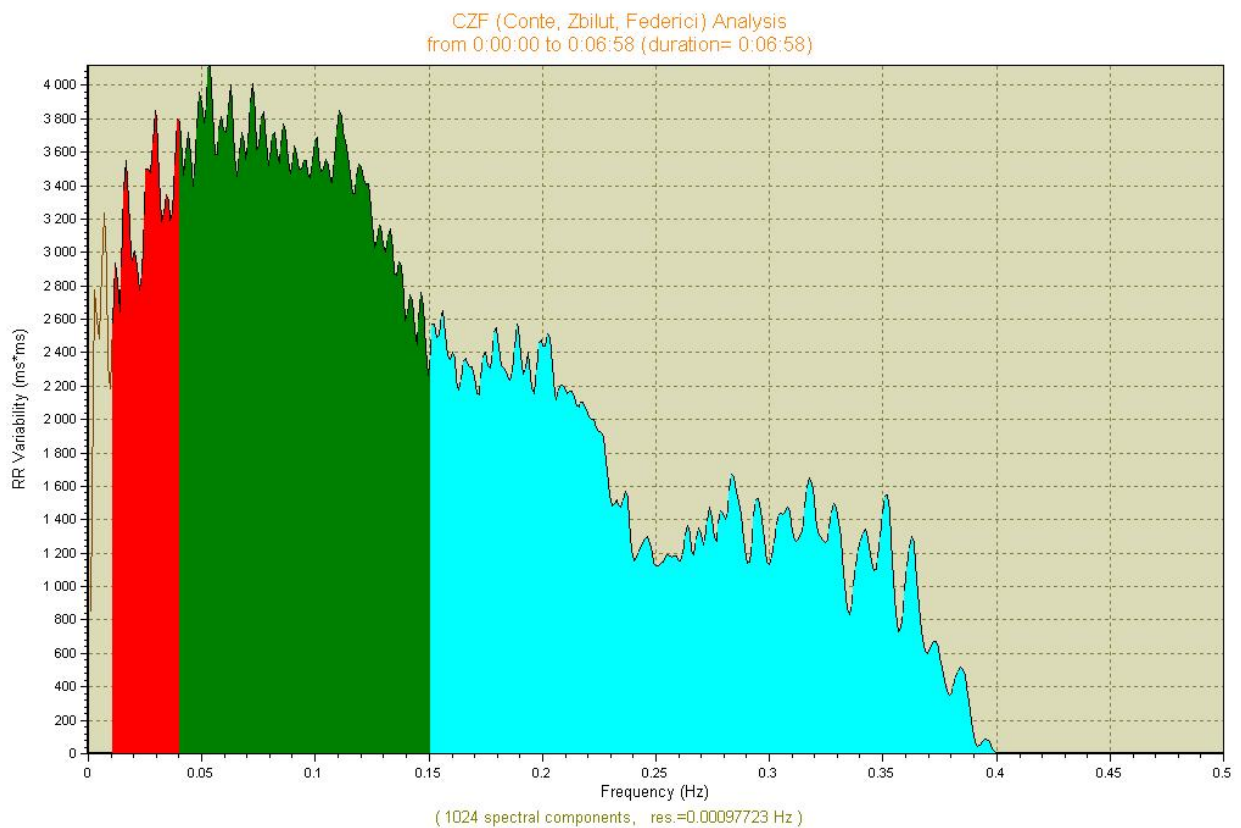
CZF (Conte, Zbilut, Federici) Analysis
from 0:00:00 to 0:06:59 (duration= 0:06:59)



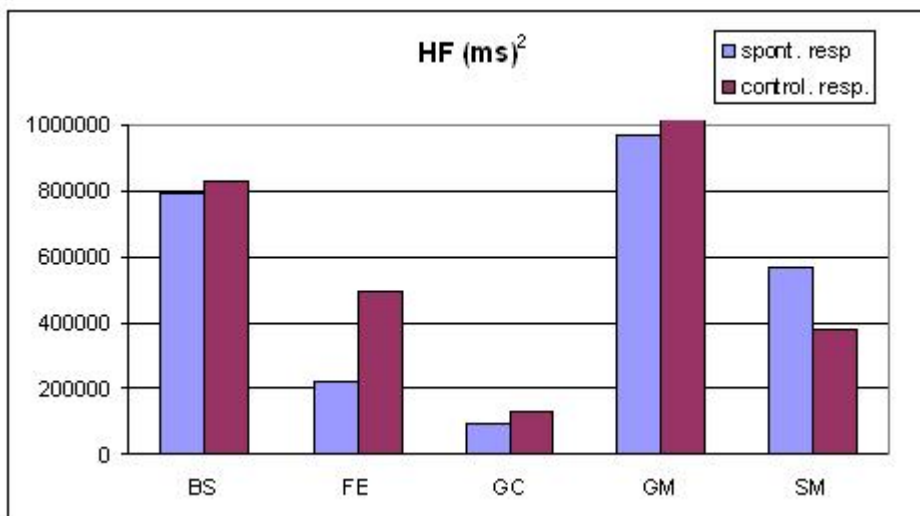
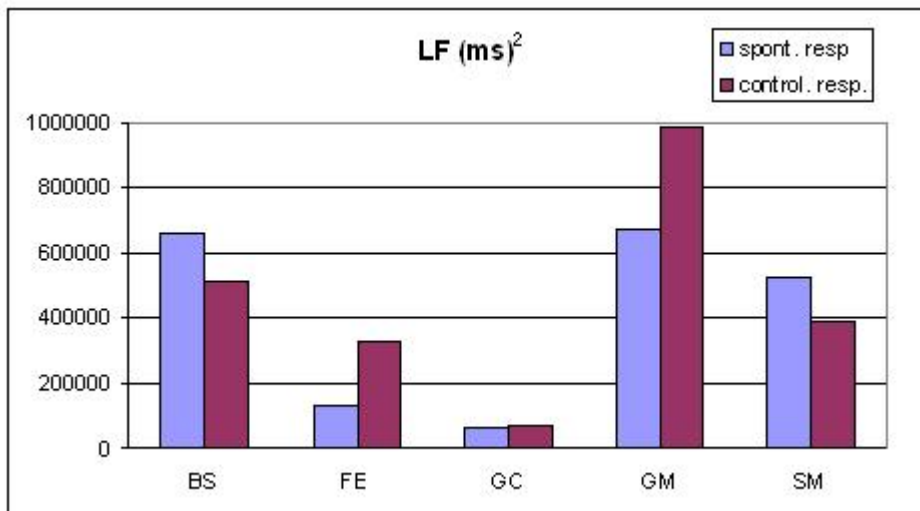
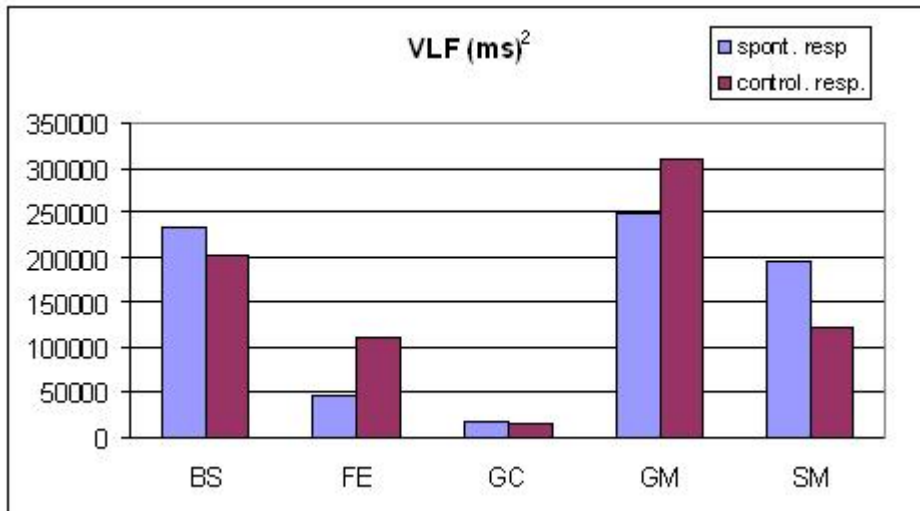
SM : CZF - spontaneous respiration

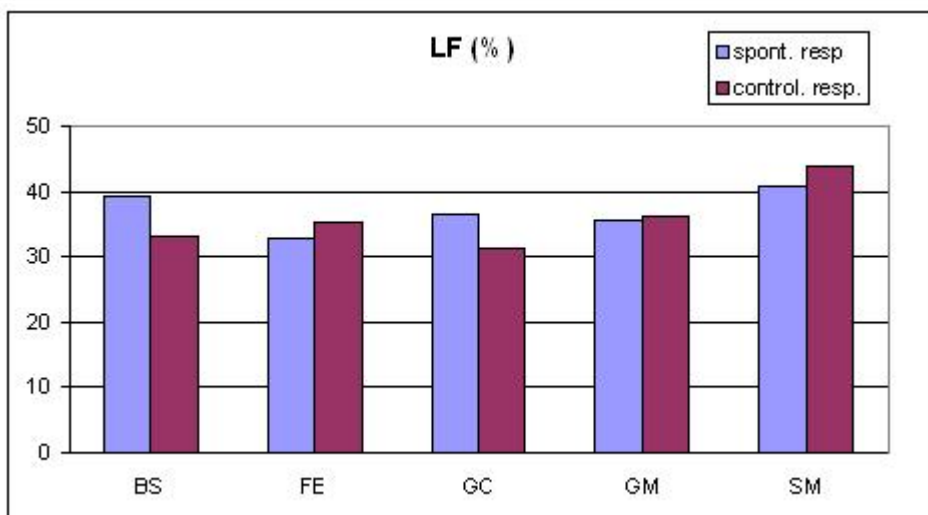
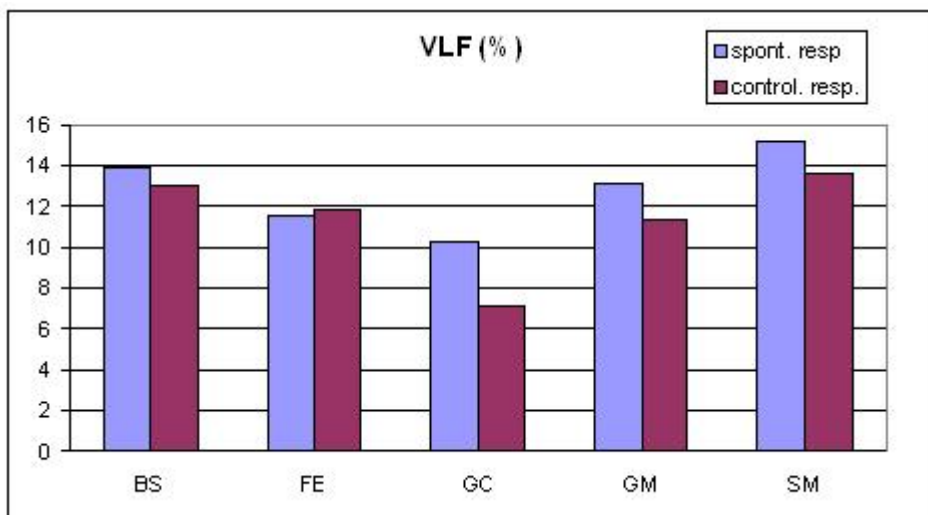
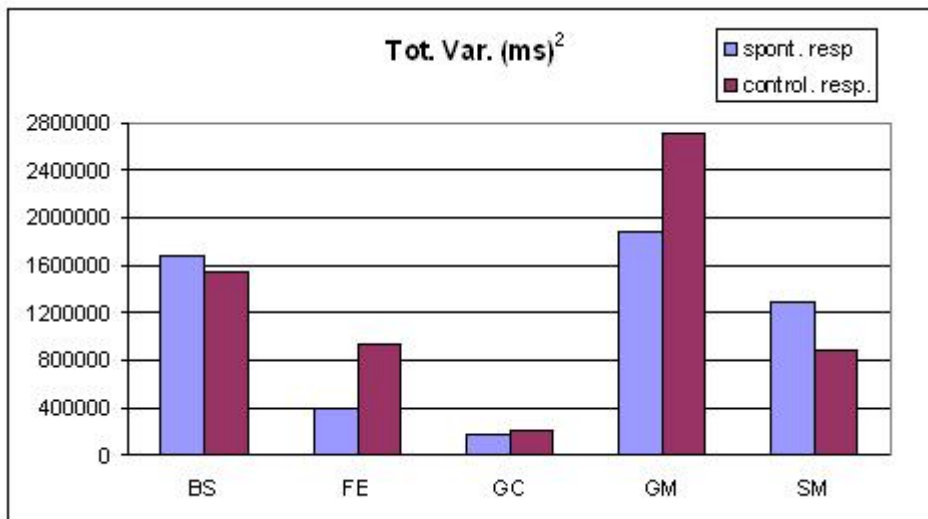


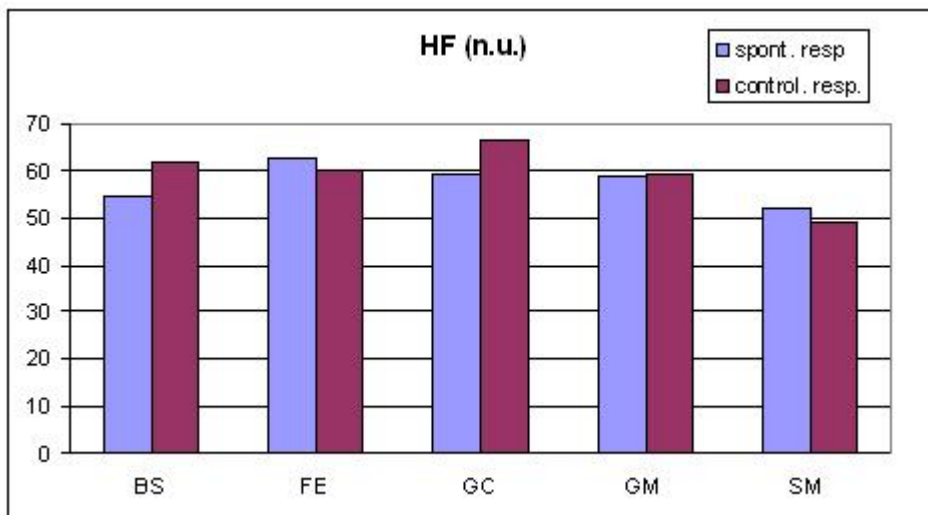
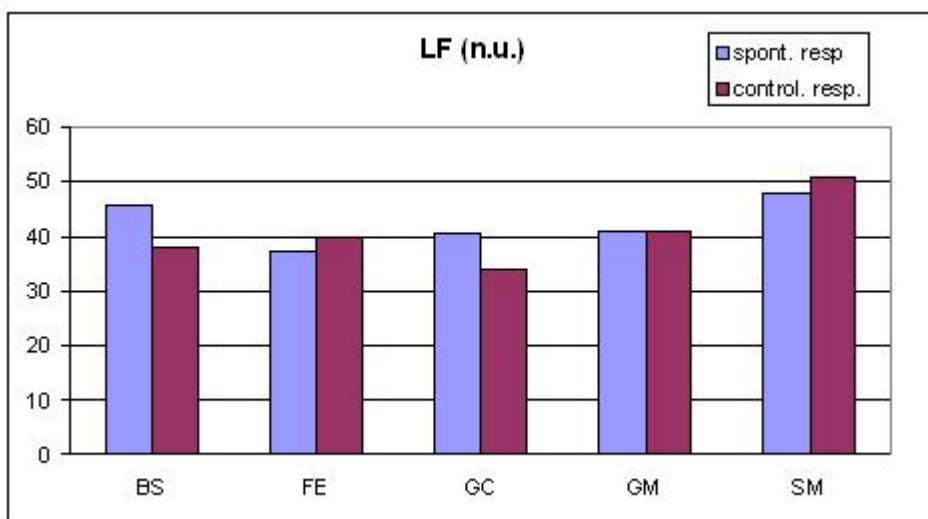
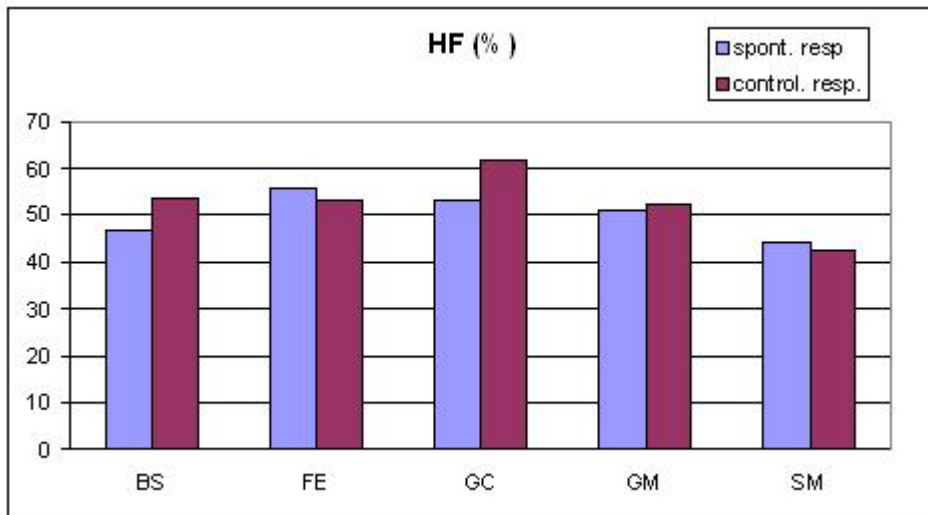
SM : CZF - controlled respiration

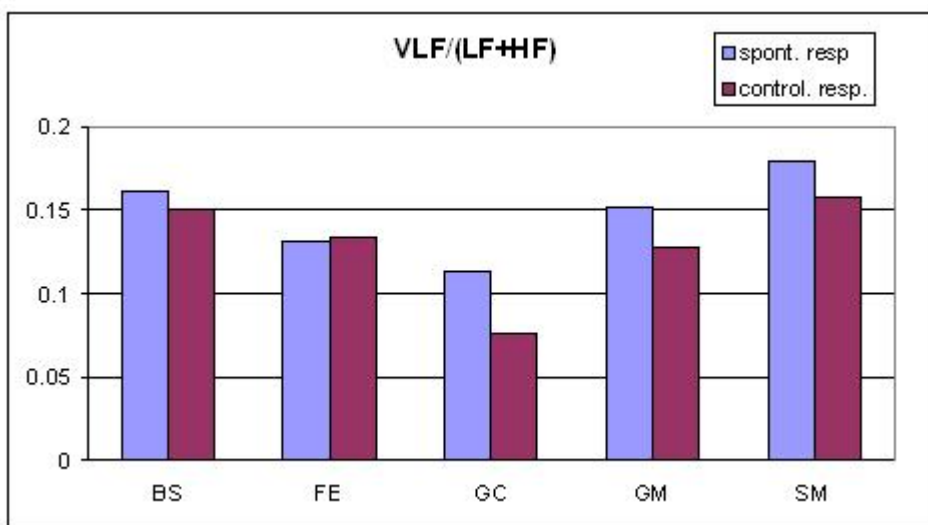
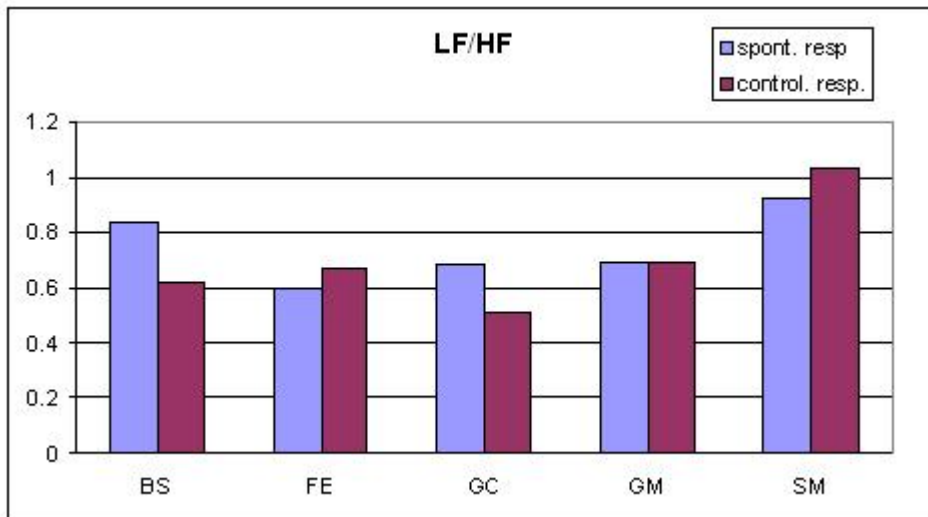


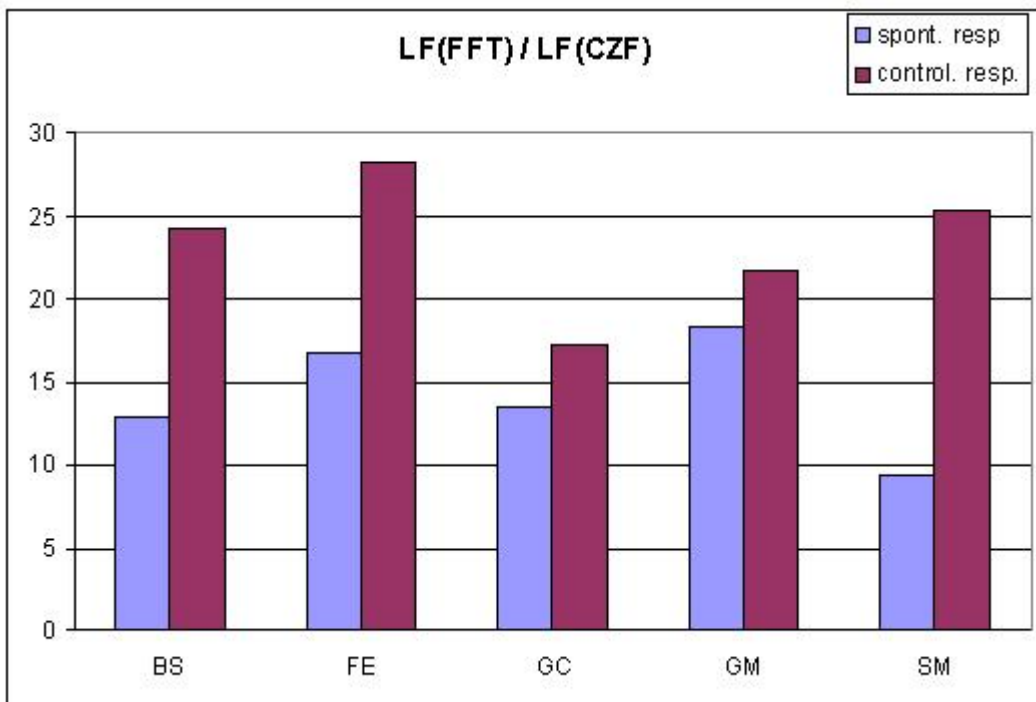
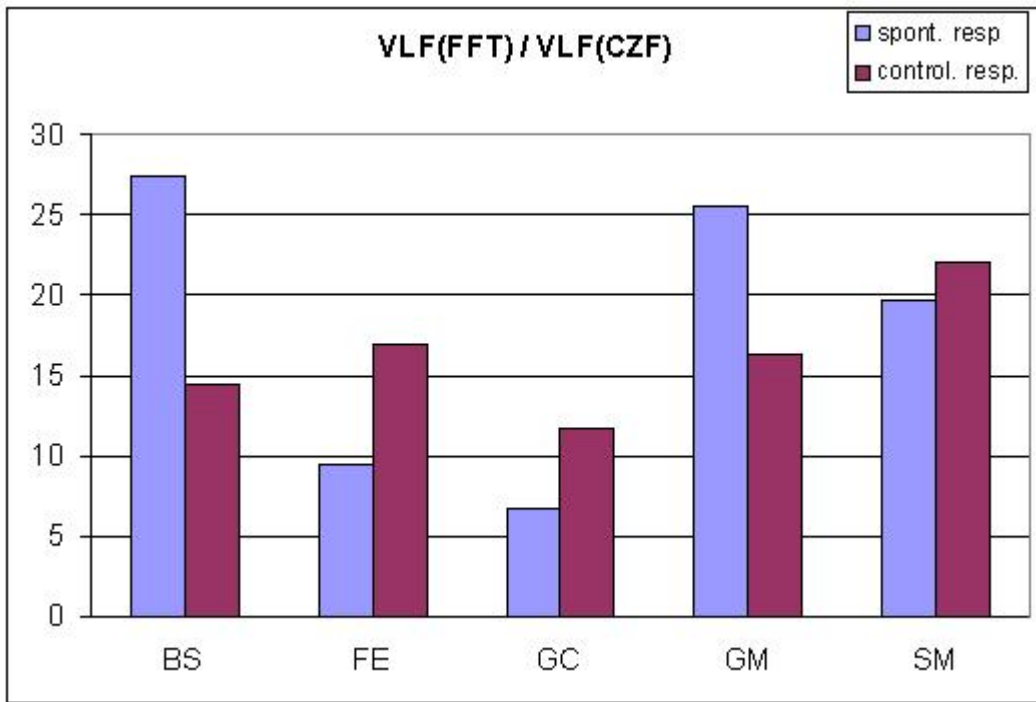
Figures 30

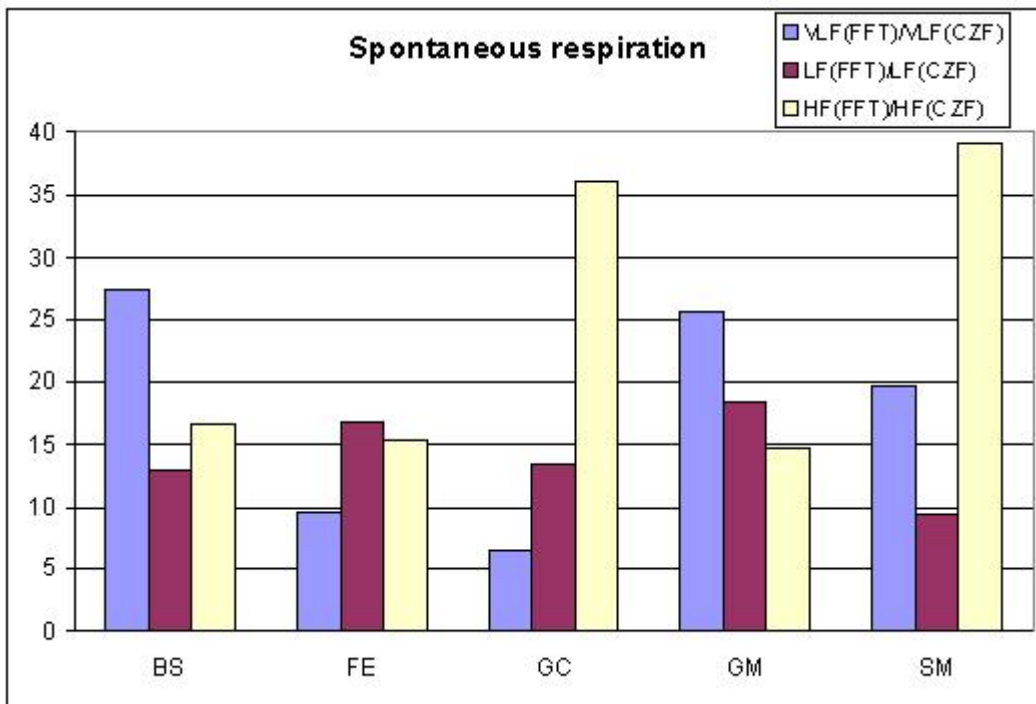
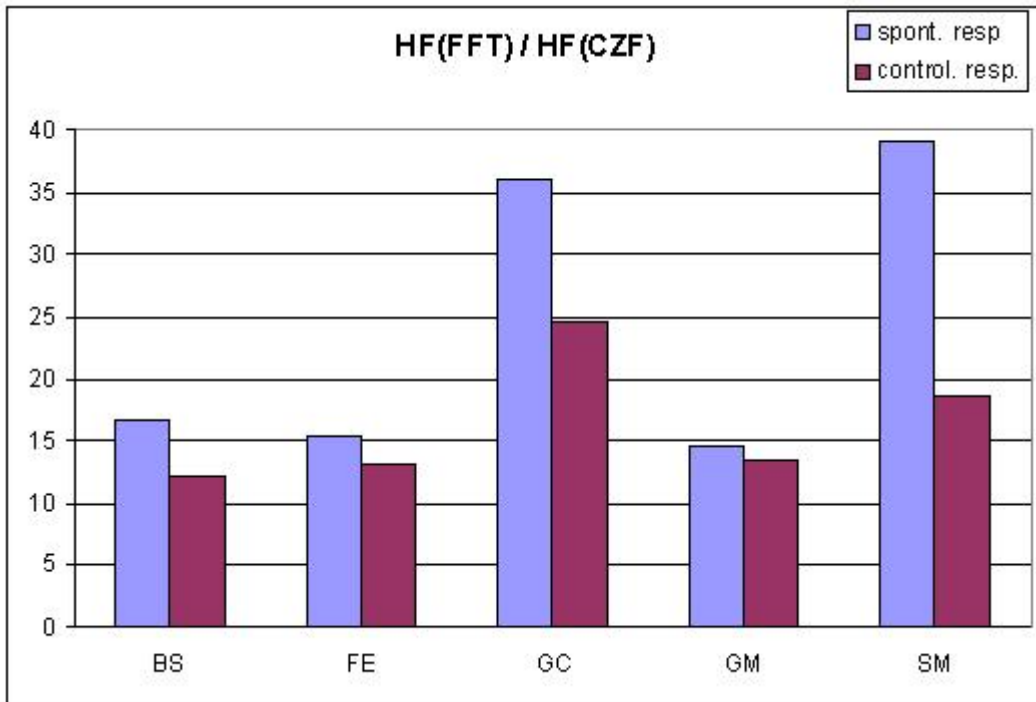


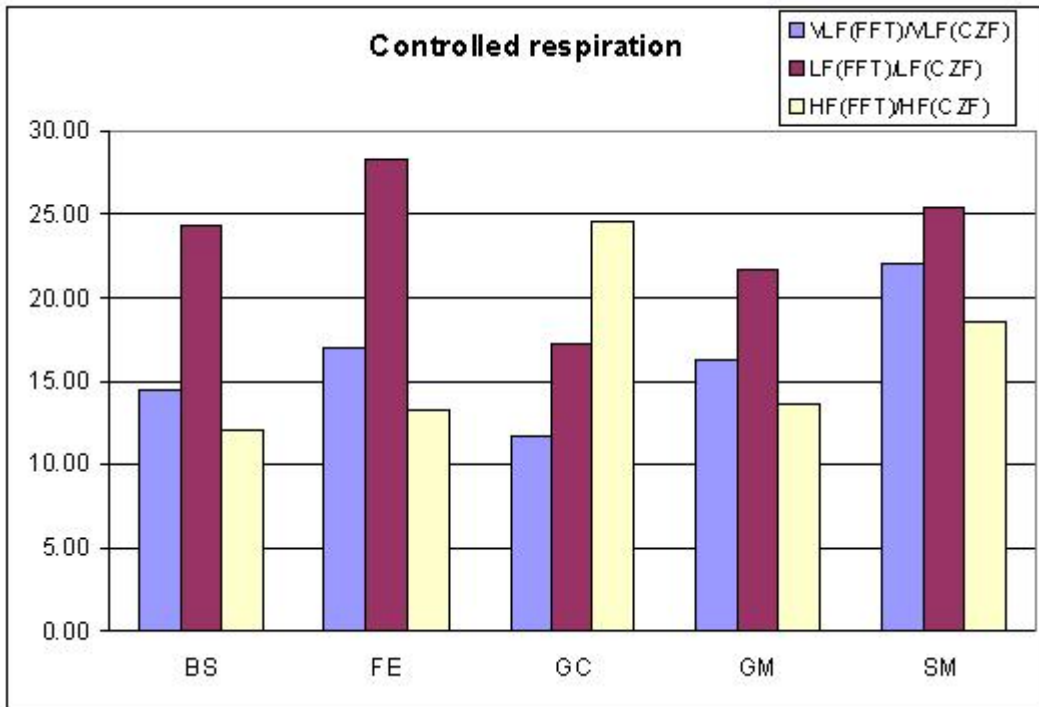






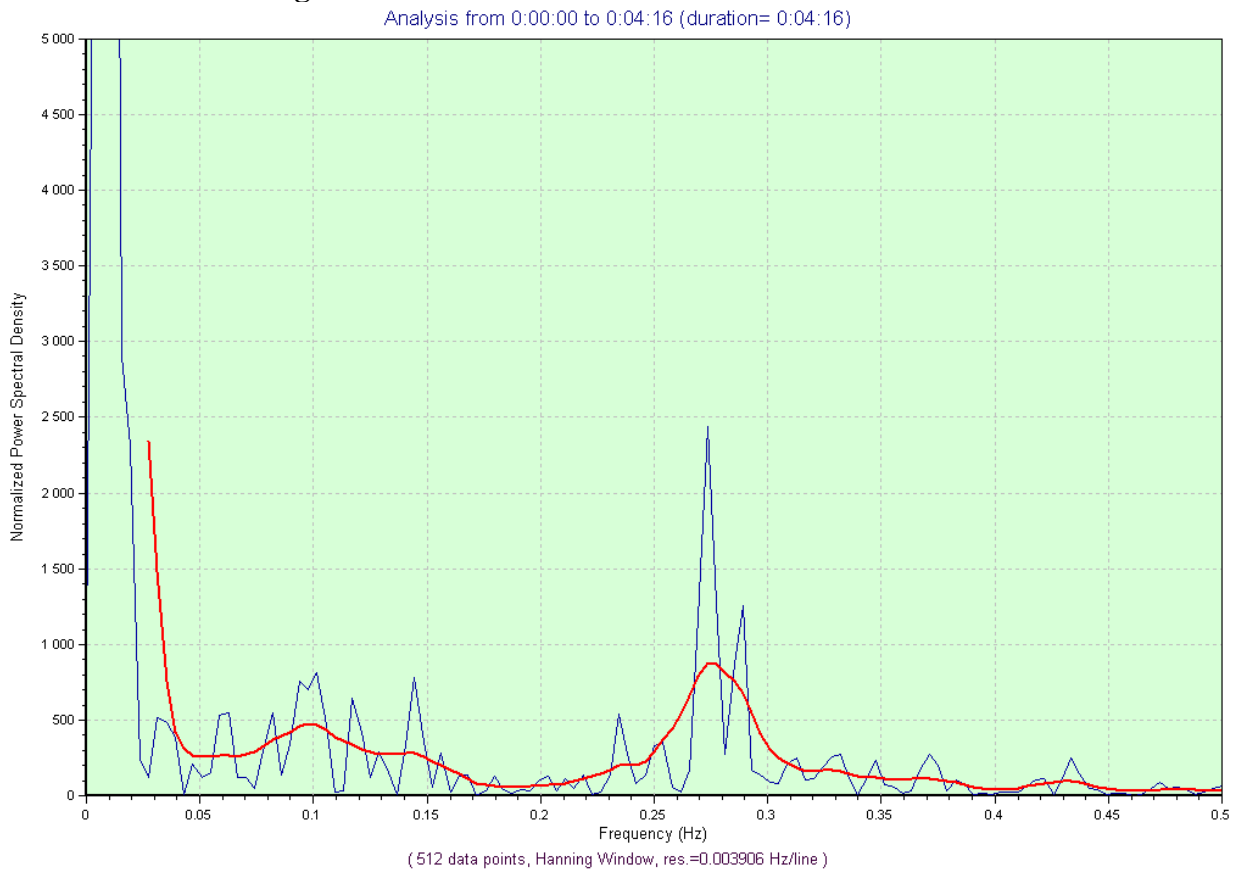




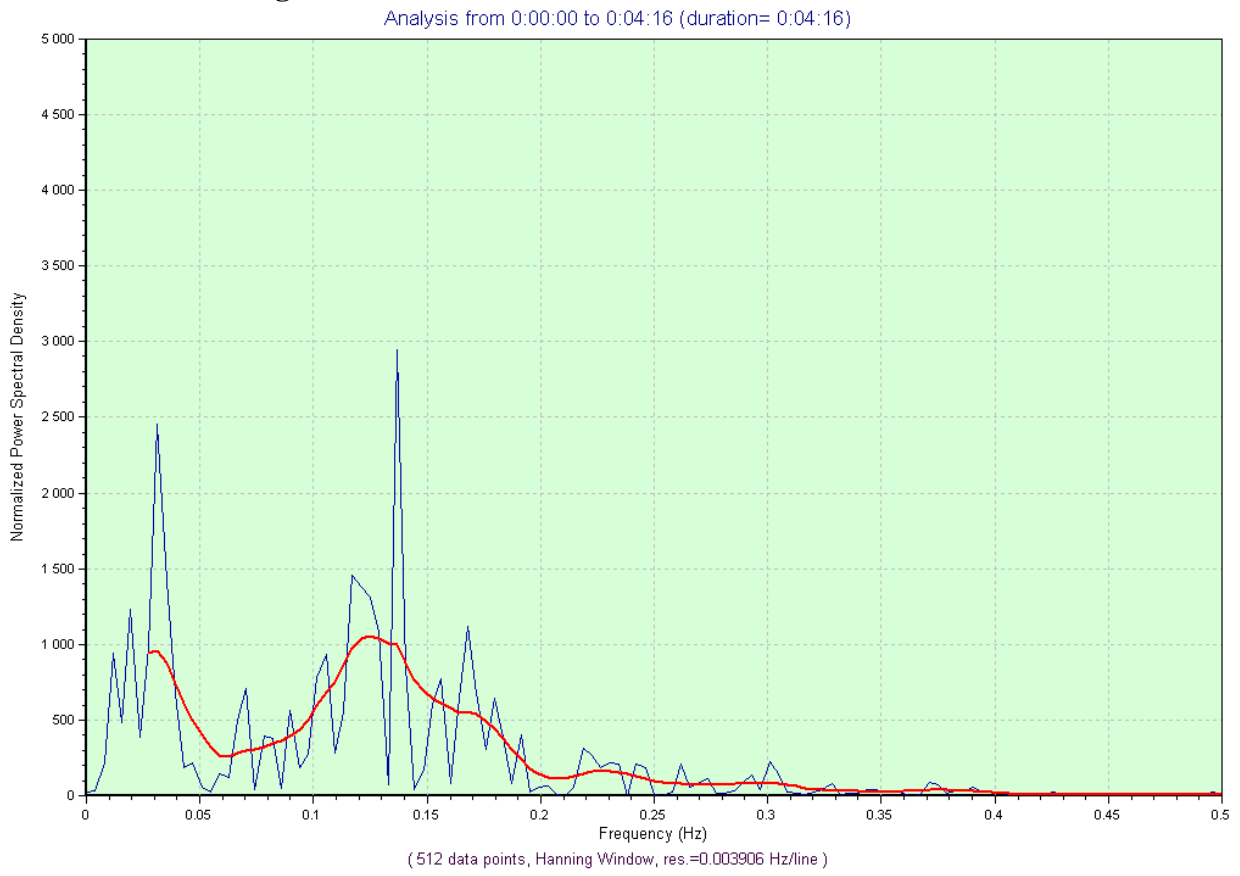


Figures 31

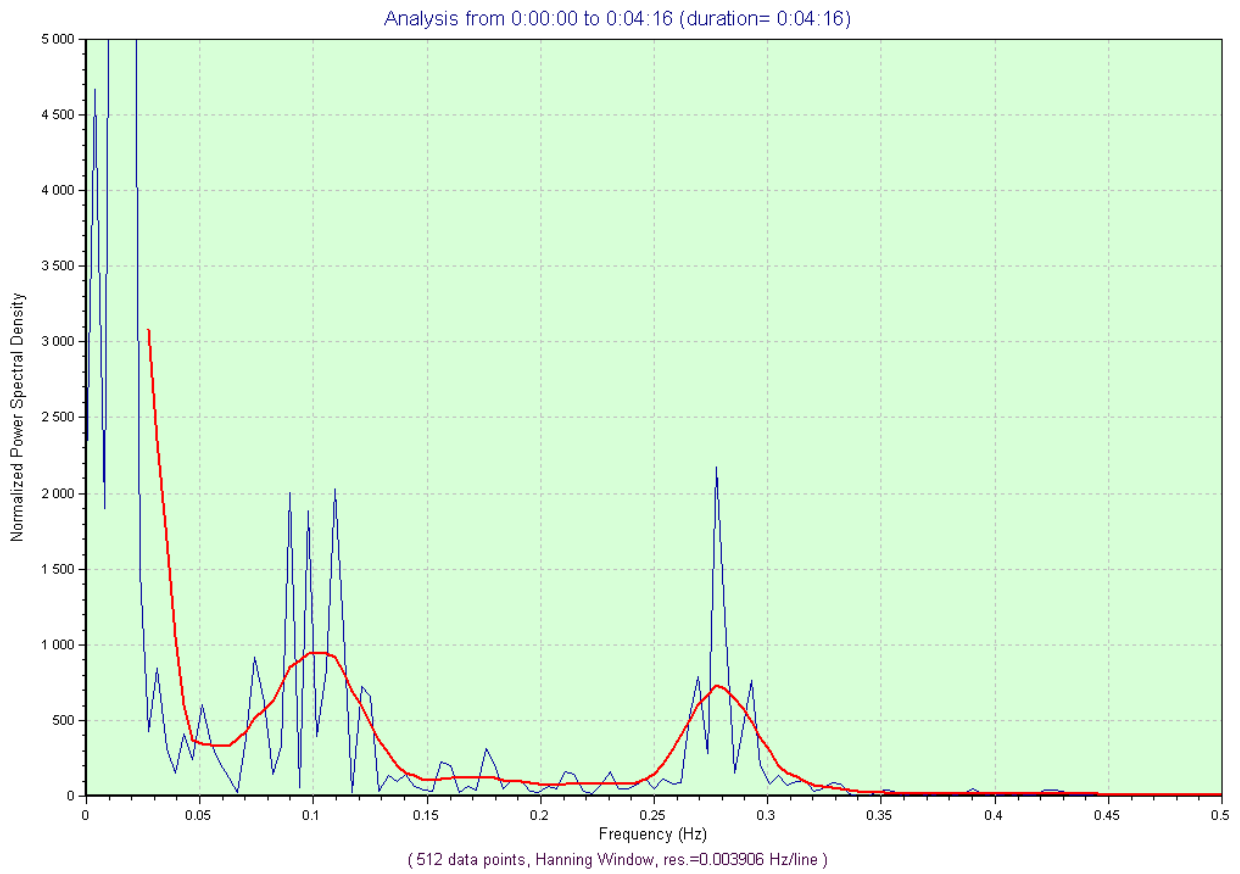
BMG Fourier - Hanning



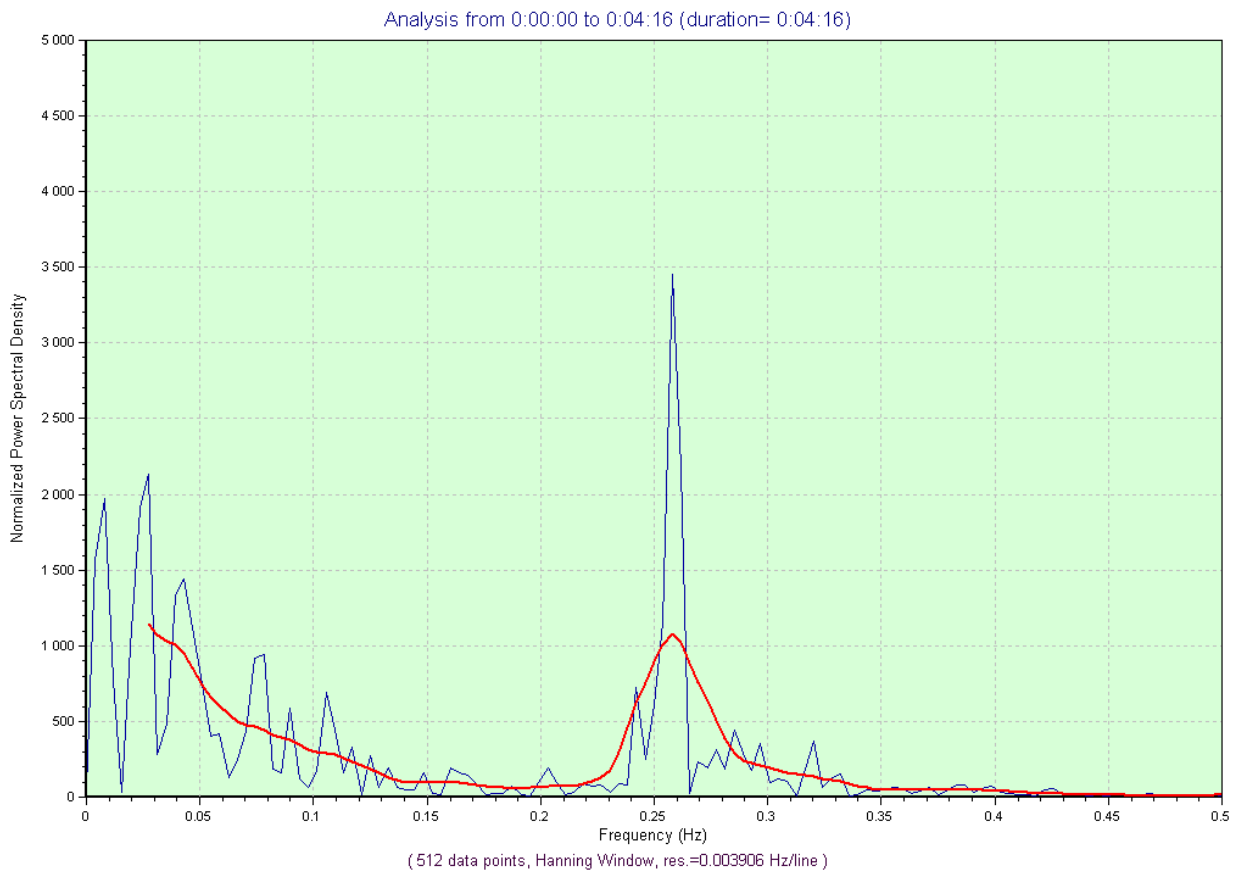
C-A Fourier - Hanning



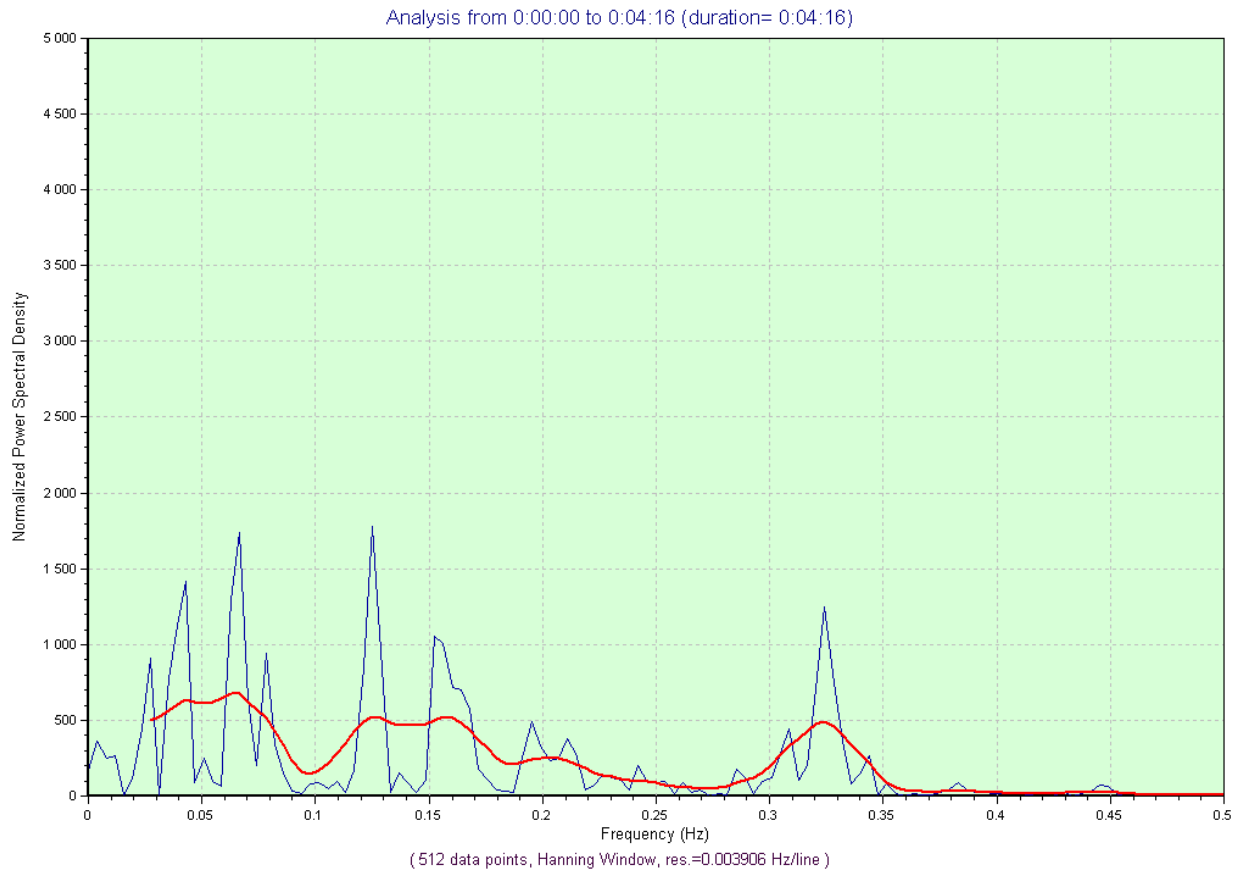
CO-A Fourier - Hanning



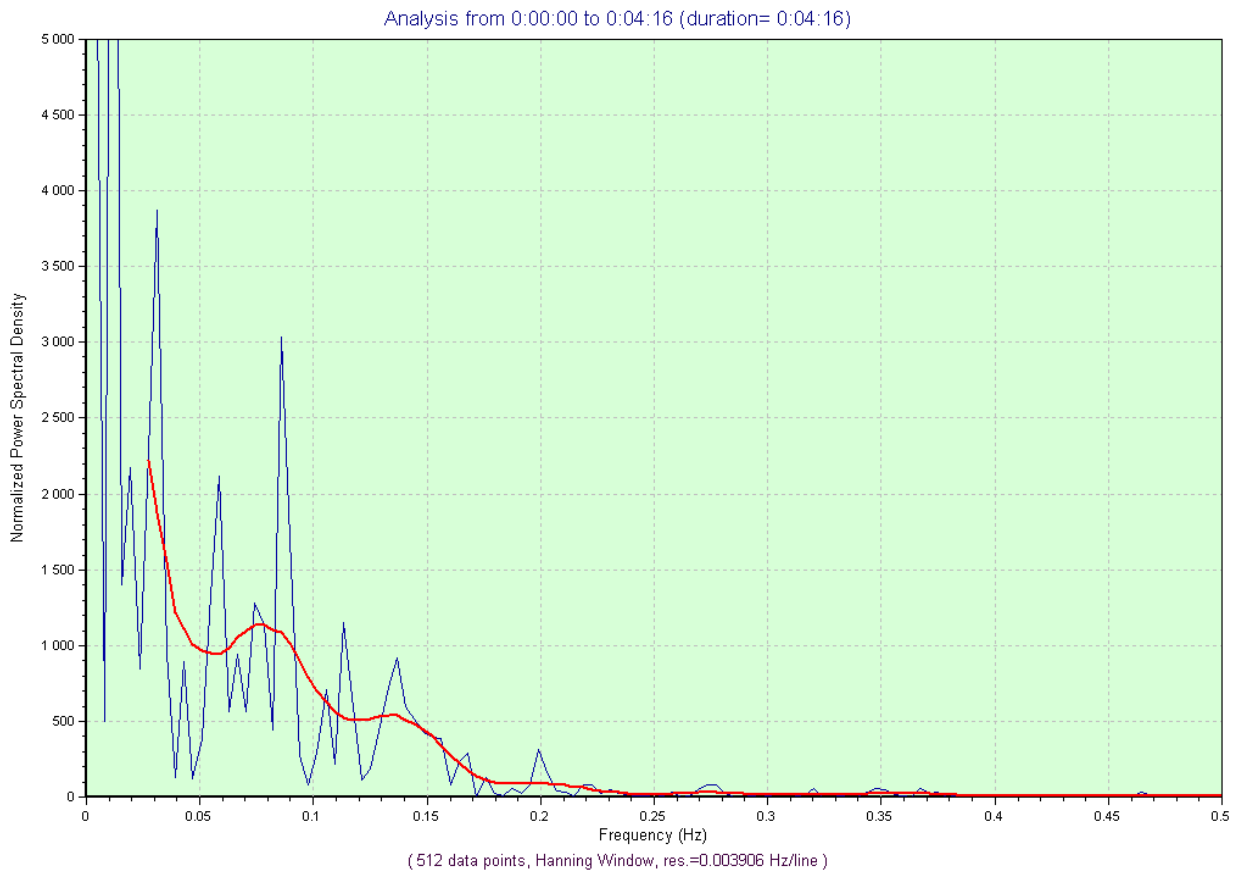
DM-S Fourier - Hanning



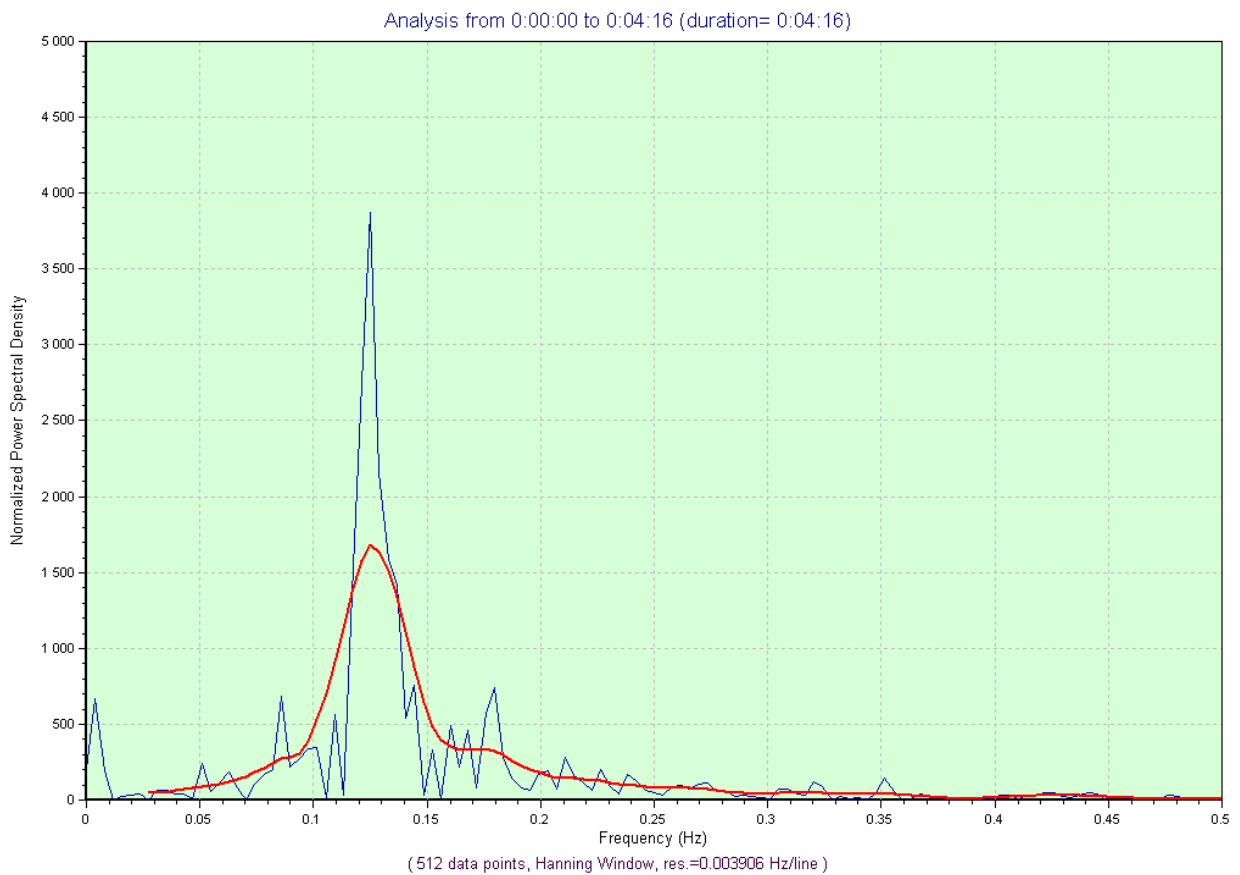
GV Fourier - Hanning



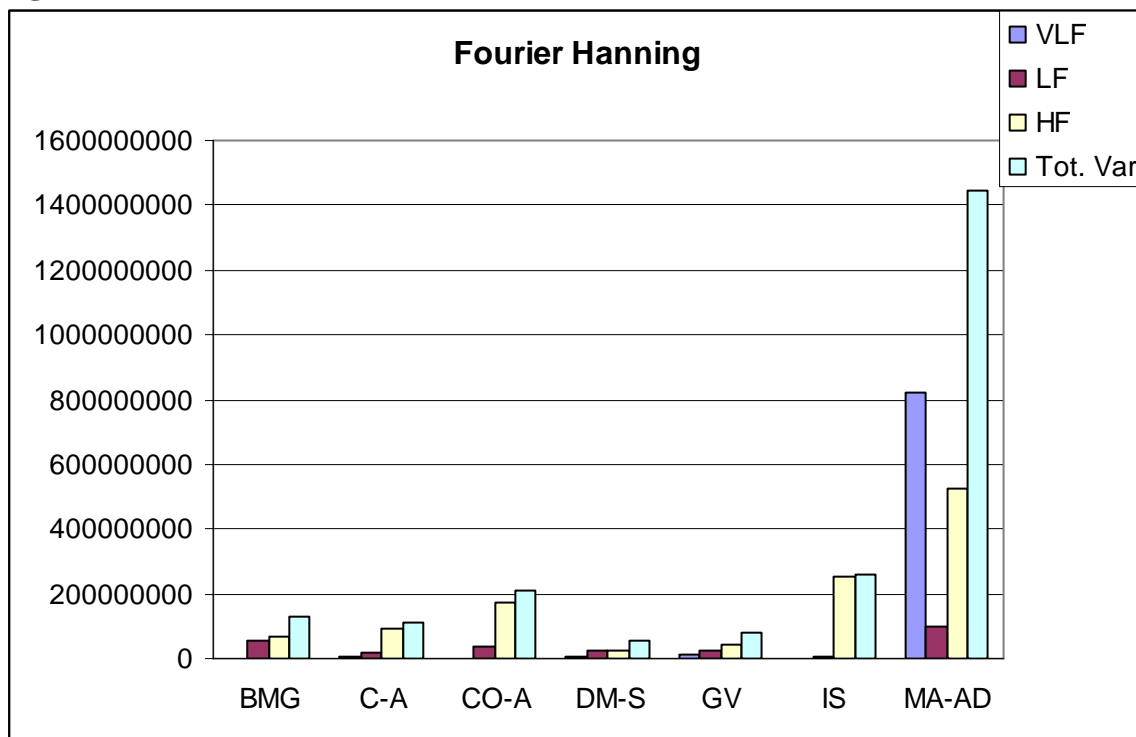
IS Fourier - Hanning



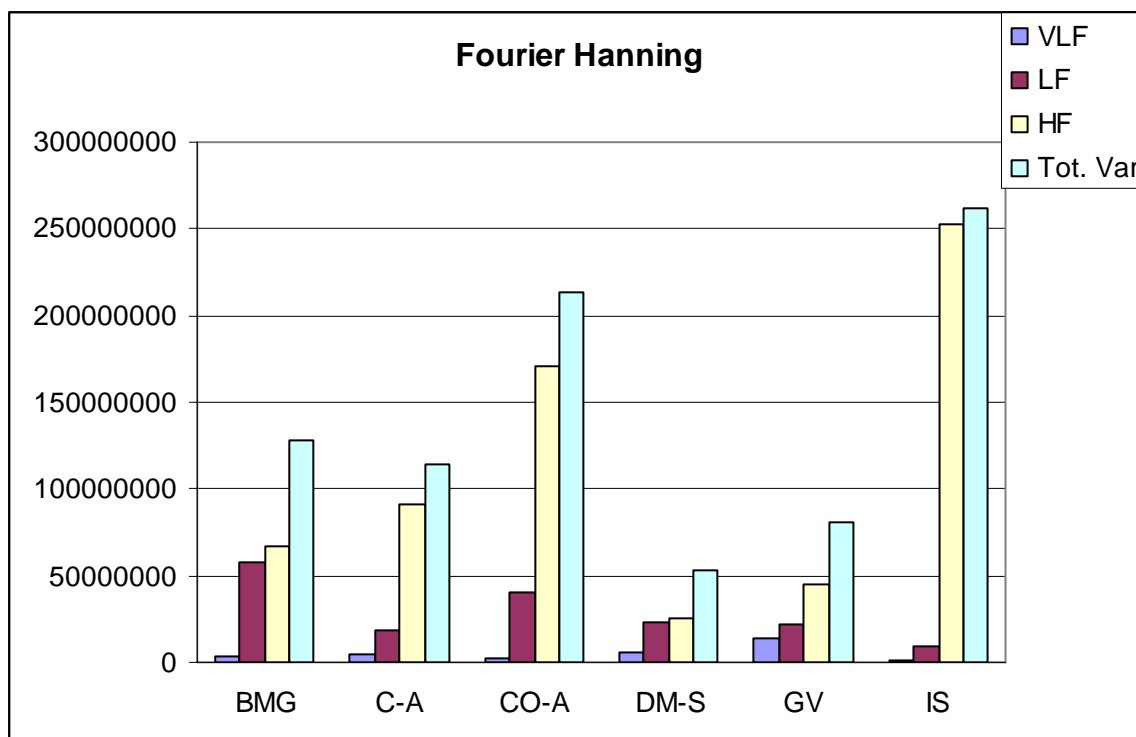
MA-AD Fourier - Hanning

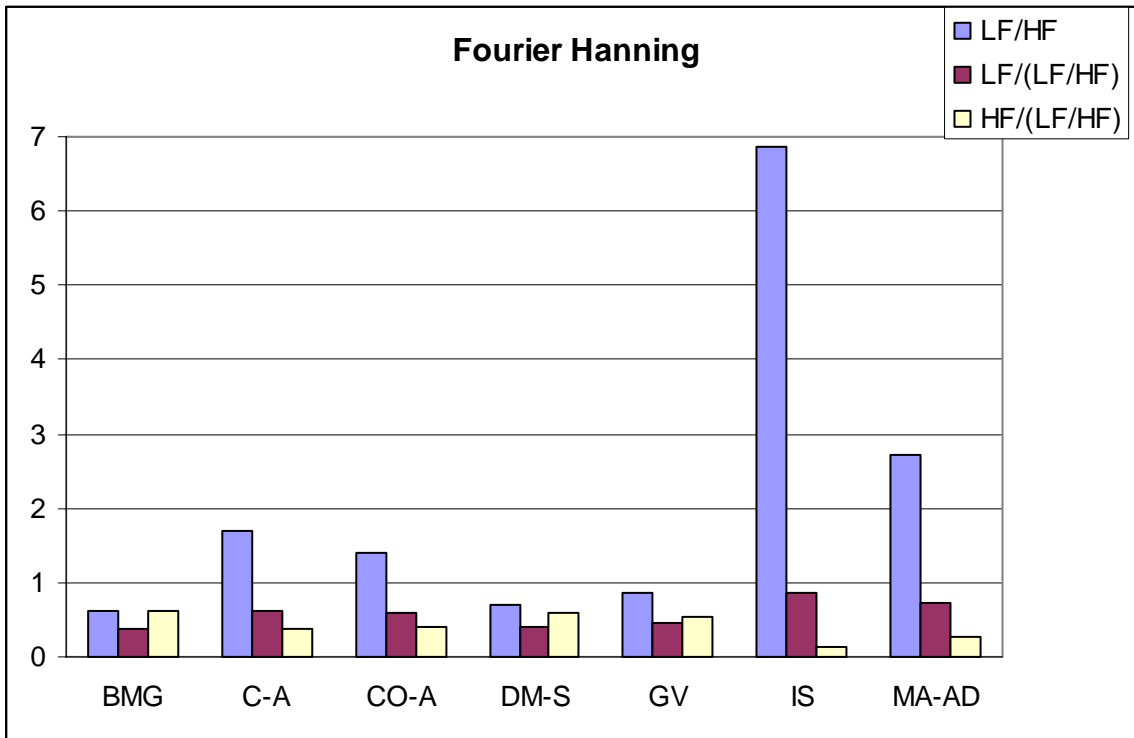


Figures 32



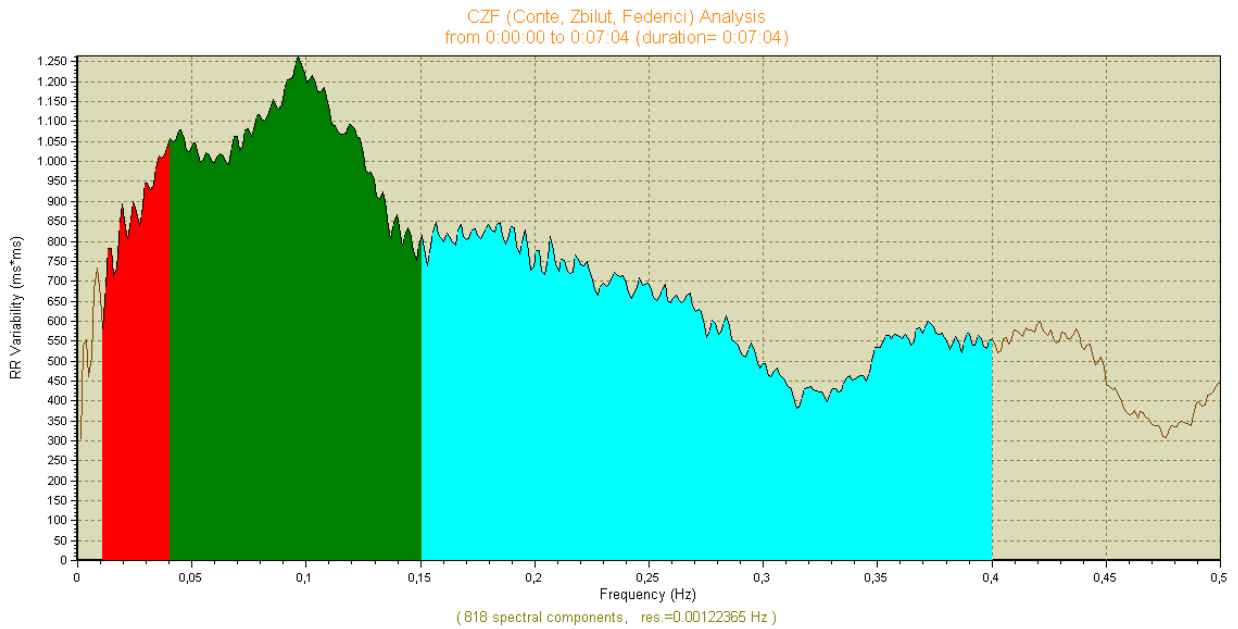
The previous one without the subject-MA-AD



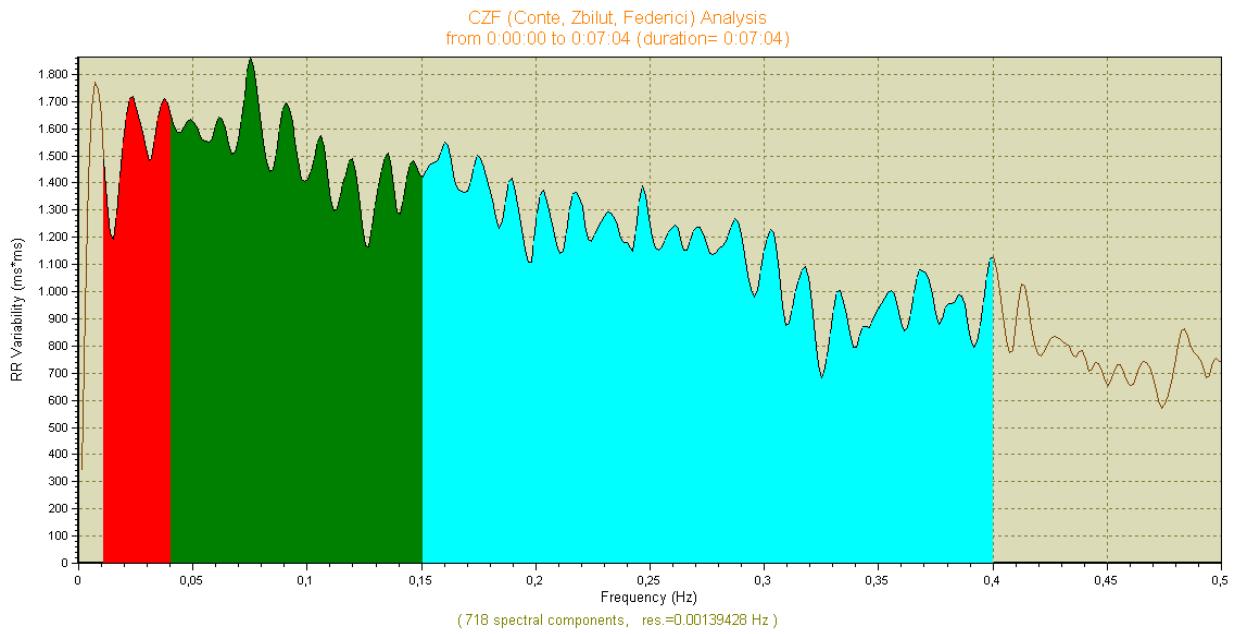


Figures 33

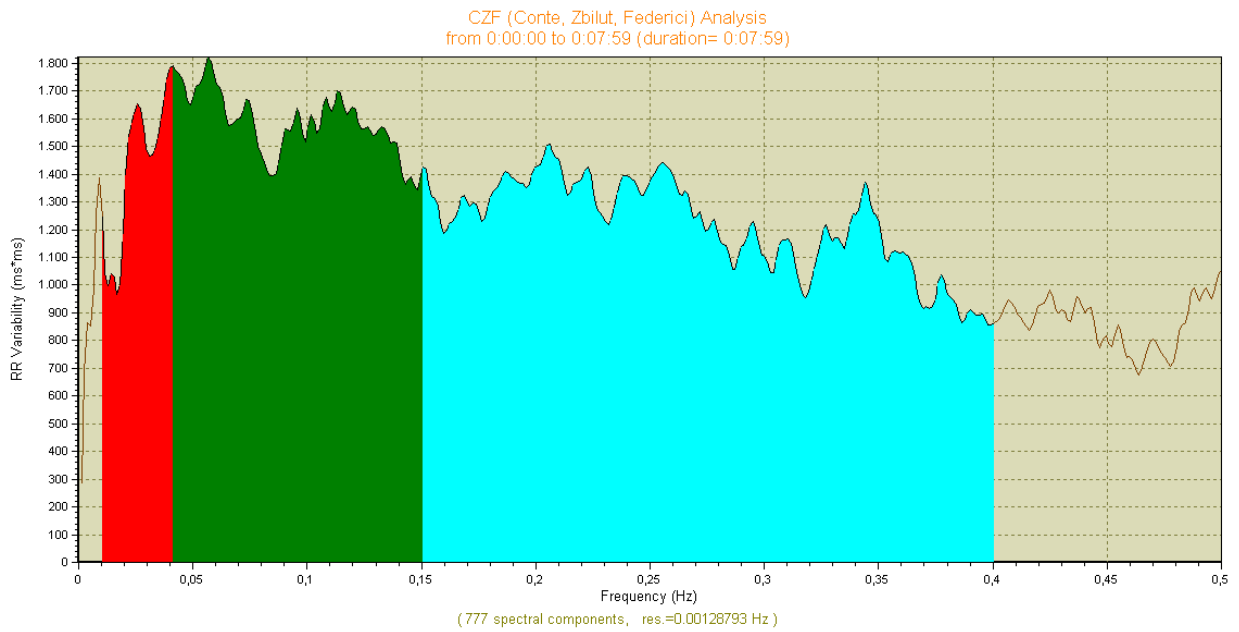
BMG



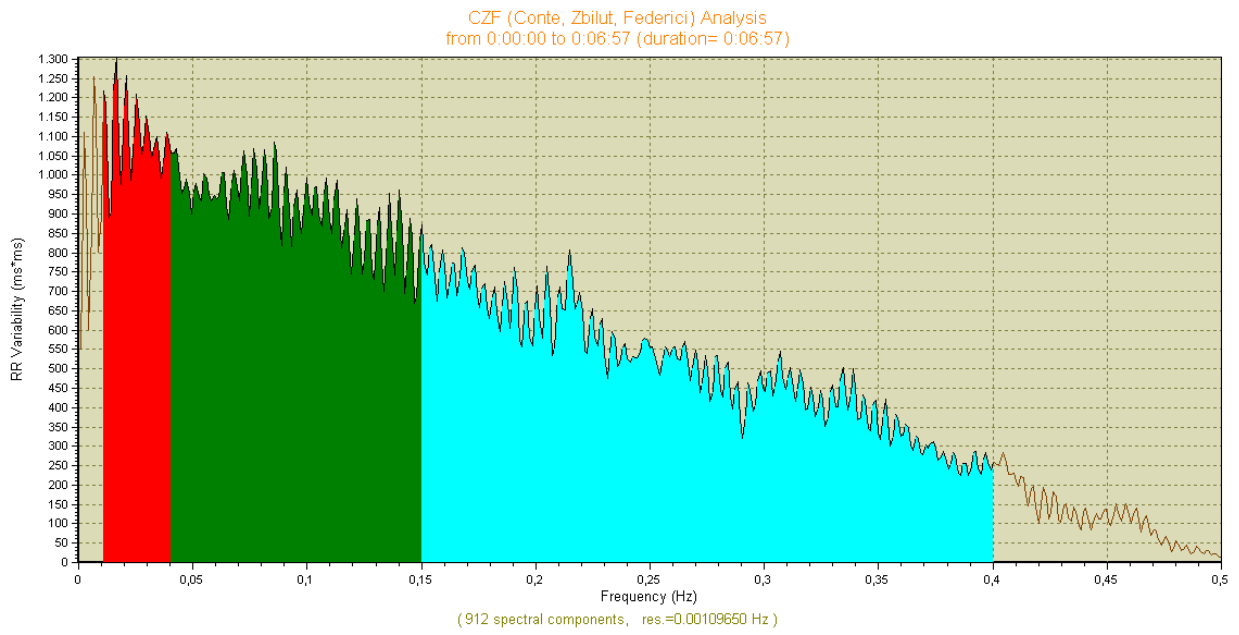
C-A



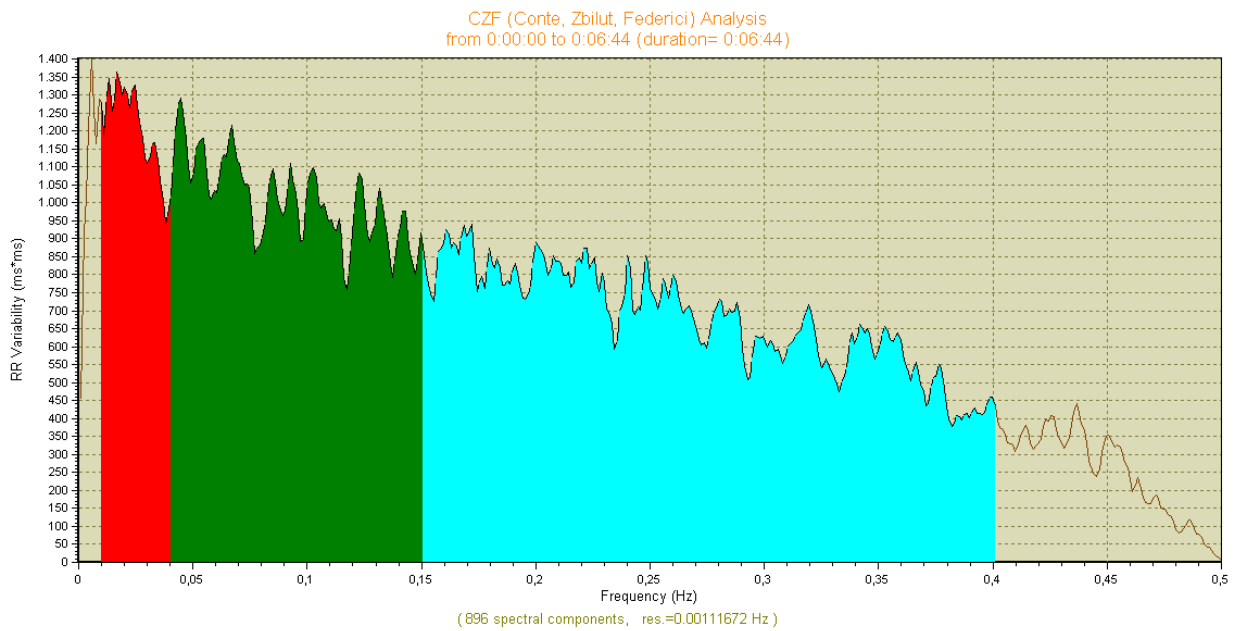
CO-A



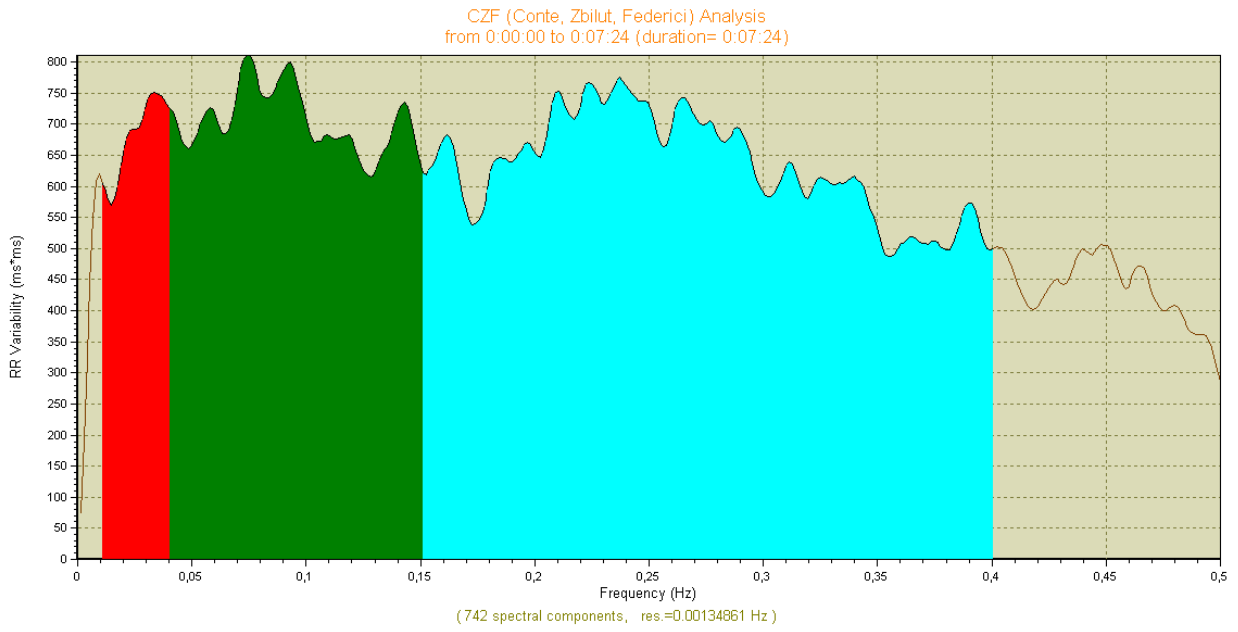
DM-S



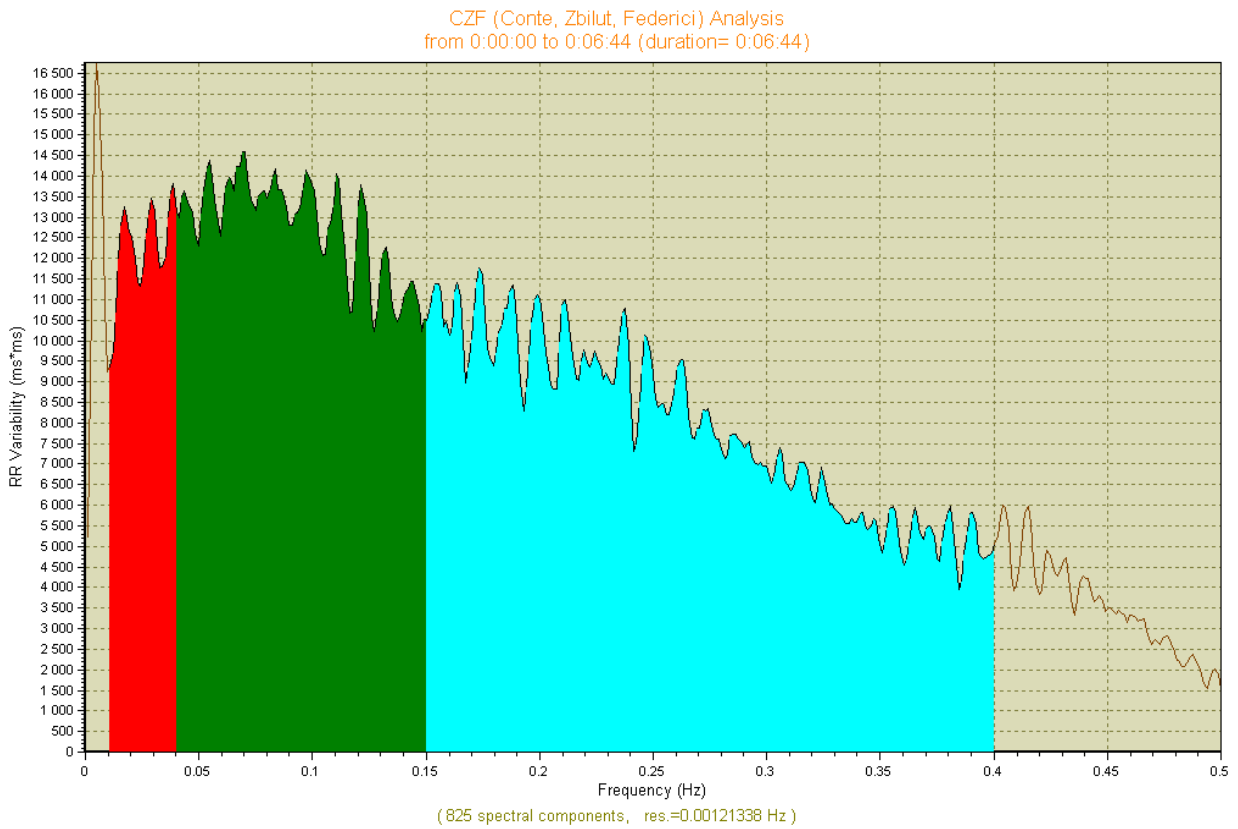
GV



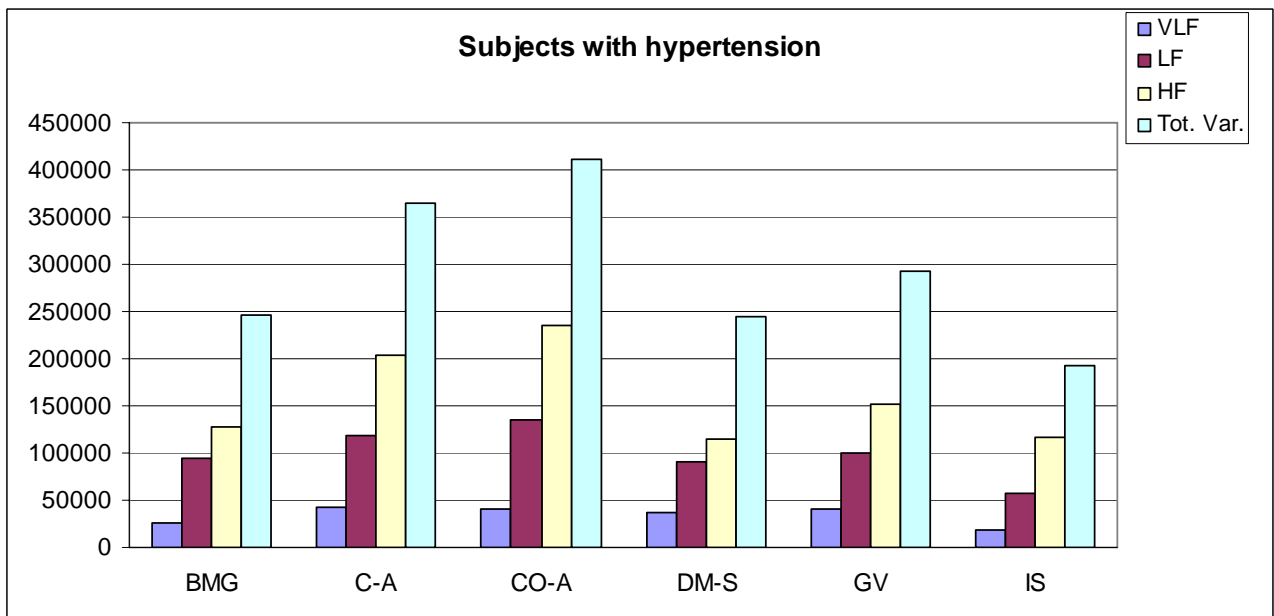
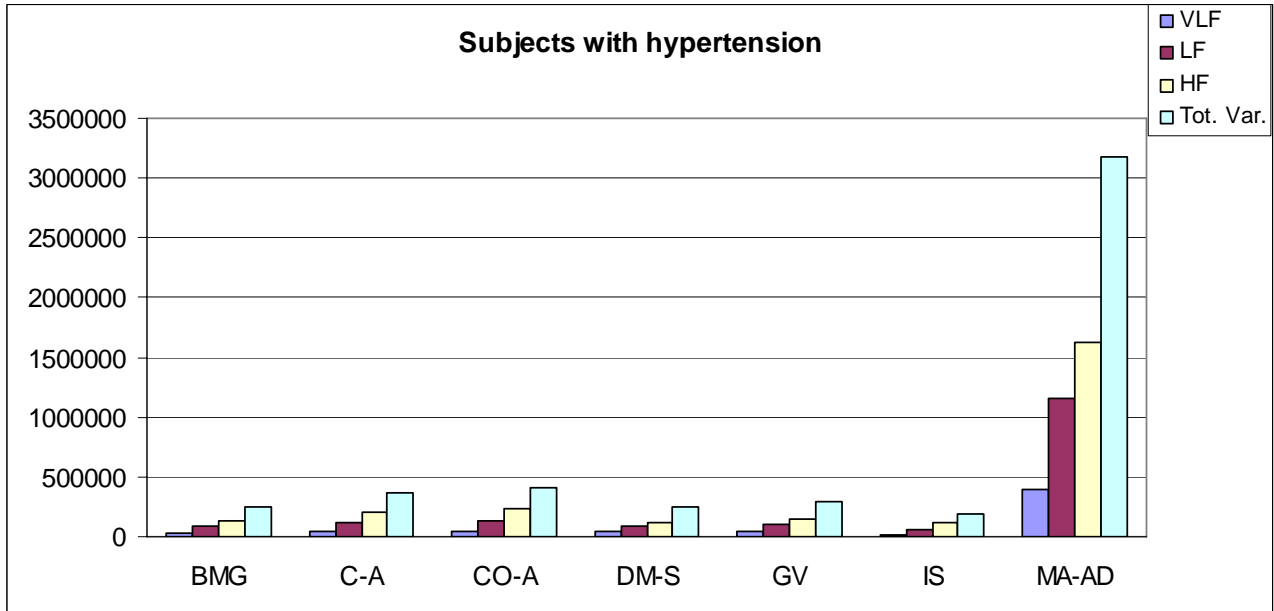
IS

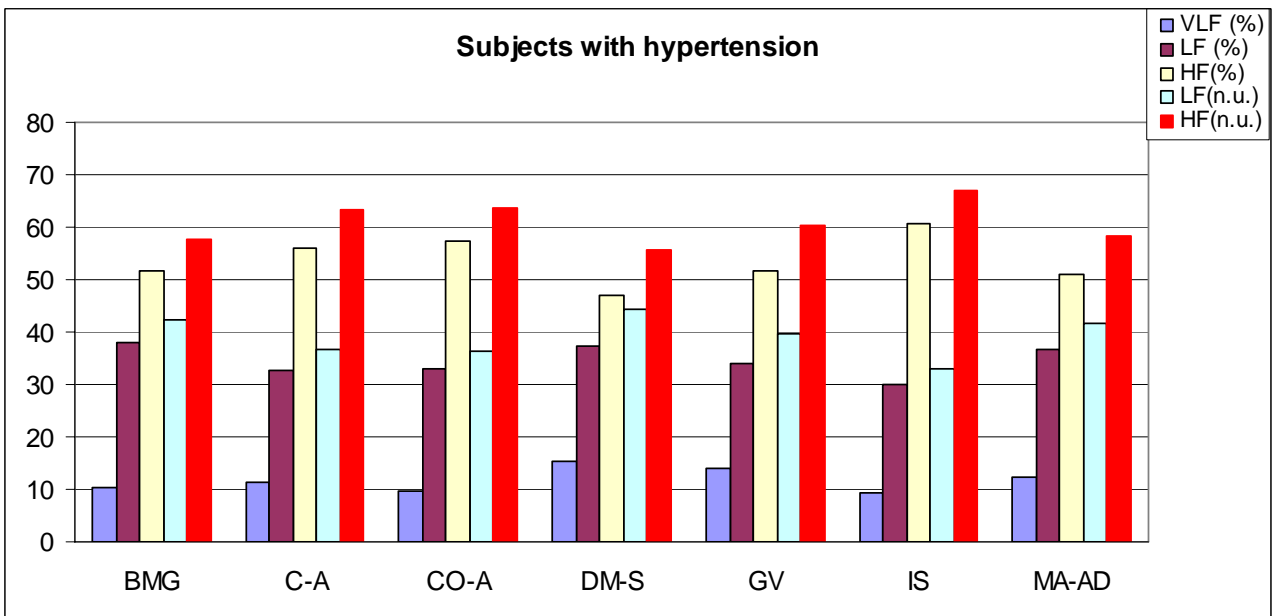
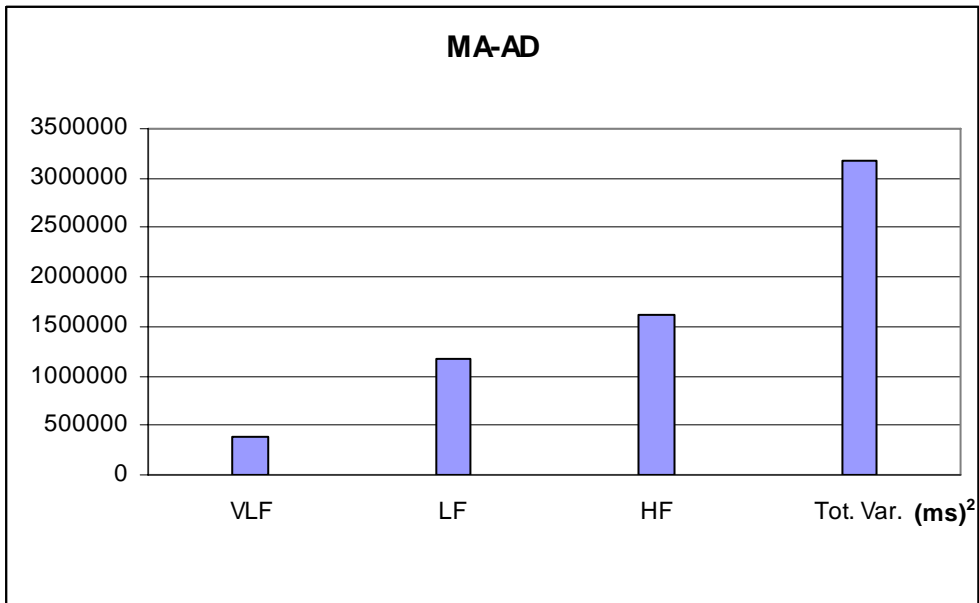


MA-AD



Figures 34





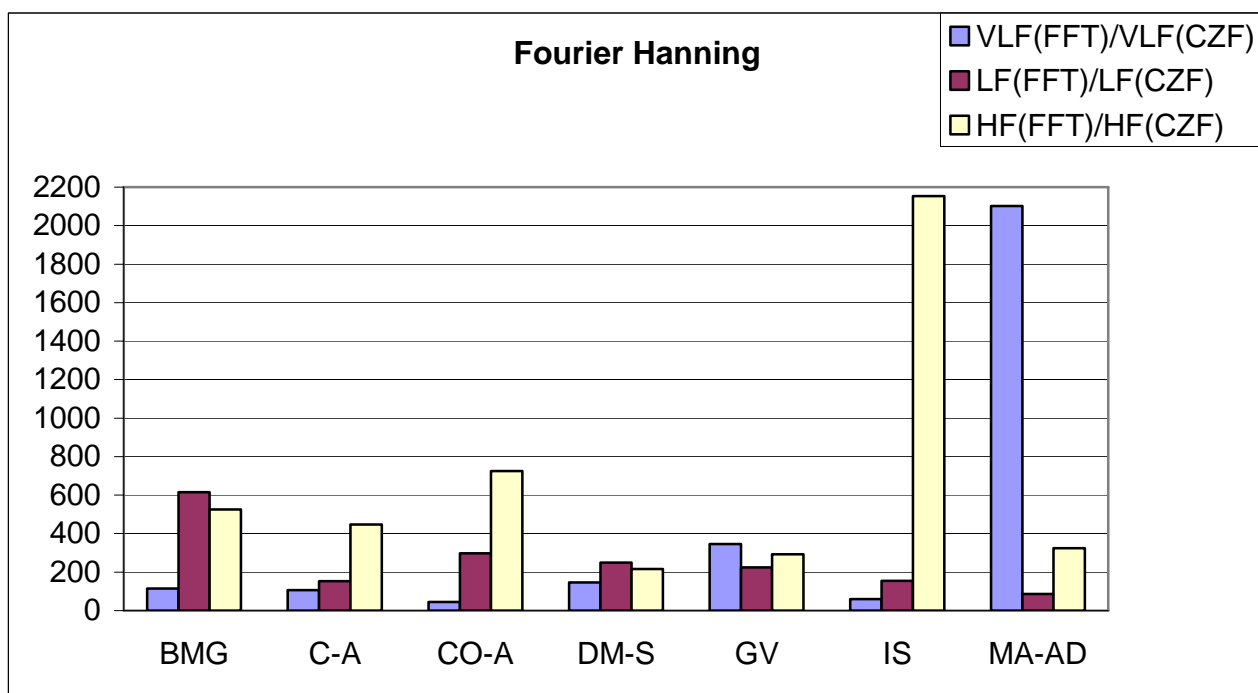
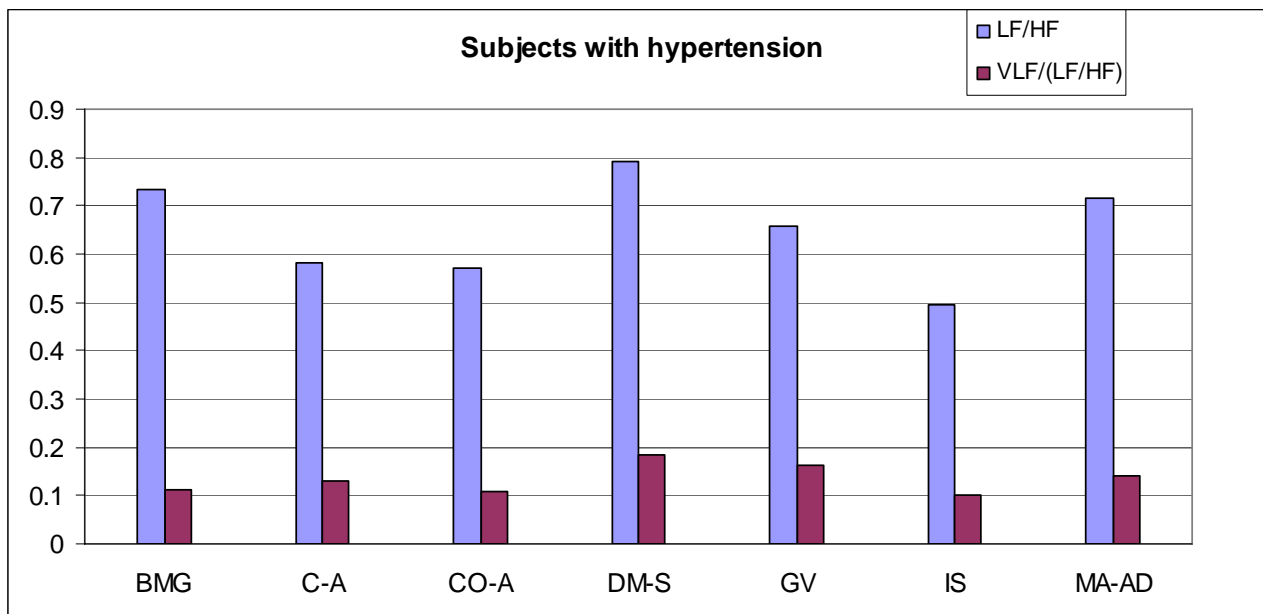


Table 2

	Fourier Hamming /CZF		
	VLF(FFT)/VLF(CZF)	LF(FFT)/LF(CZF)	HF(FFT)/HF(CZF)
BMG	125.84	660.26	572.52
C-A	118.43	163.48	490.88
CO-A	49.92	312.40	792.87
DM-S	162.75	276.63	236.18
GV	373.02	246.61	327.57
IS	62.58	167.84	2333.27
MA-AD	2064.23	95.12	353.85

	Fourier Hamming /CZF		
	VLF(FFT)/VLF(CZF)	LF(FFT)/LF(CZF)	HF(FFT)/HF(CZF)
BMG	11.22	25.70	23.93
C-A	10.88	12.79	22.16
CO-A	7.07	17.67	28.16
DM-S	12.76	16.63	15.37
GV	19.31	15.70	18.10
IS	7.91	12.96	48.30
MA-AD	45.43	9.75	18.81